Multi-element Stable Isotope Analysis of Alkylpyrazines and Pyridine from Roast Coffee

Dissertation zur Erlangung des
naturwissenschaftlichen Doktorgrades
der Julius-Maximilians-Universität Würzburg

vorgelegt von
Christina Preston
aus Aalen

Würzburg 2008

Eingereicht am: 26. September 2008
bei der Fakultät für Chemie und Pharmazie

1. Gutachter: Prof. Dr. P. Schreier
2. Gutachter: Prof. Dr. H.-U. Humpf
der Dissertation

1. Prüfer: Prof. Dr. P. Schreier
2. Prüfer: Prof. Dr. H.-U. Humpf
3. Prüfer: Prof. Dr. C. Sotriffer
des öffentlichen Promotionskolloquiums

Tag des öffentlichen Promotionskolloquiums: 21. Januar 2009

Doktorurkunde ausgehändigt am: ……

Acknowledgements

The following research was conducted at the chair of food chemistry, University of Würzburg, from January 2004 to May 2007, under the guidance of Professor Dr. Peter Schreier.

Professor Dr. Peter Schreier I thank for the isotopic-topic, the scientific support, the interesting discussions, not always strictly work-related, and the freedom of researching independently.

Furthermore, I thank Dr. Thorsten König, from Givaudan (formerly Quest International), for providing samples and Dr. Elke Richling, Dr. Dominique Kavvadias, as well as the student workers Christopher Heppel and Silvia Hummel, for the pre-work conducted on this research topic.

Special thanks go to the 'F-Praktikanten' Kathrin Kahle, Helena Bader, Stefanie Kohlhepp, Ina Kleinsteuber, Magdalena Müller, Karin Thomas, Christof Madinger and Tanja Welsch as well as to the 'C-Praktikanten' Daniela Trost and Fabian Oberle, who all supported me courageously during their advanced practical courses. They all contributed substantially to the success of this work, with their never-tiring energy, their good ideas and friendly relationships.

Dr. Frank Heckel and Dr. Sandra Elß divulged their GC-MS knowledge to me and taught me all they could about these machines. I thank them and Michael Kempf, both for the good working relationship between us in the GC-MS department and for their willingness to help out with the 'special' problems of the IRMS.

Eva-Maria Rumpel successfully gave me a three-month crash course in IRMS measurement, whilst Dr. Markus Appel contributed his extensive knowledge on the IRMS. With Dr. Sandra Elß's assistance the work with the machine was highly productive and always exciting. I thank the IRMS team for their help in the often eventful and seemingly never-ending work, and without whom stable isotopes would still be a mystery to us all.

A very special thank you goes to Theresia Feuerbach, who took loads of work off my shoulders, by conducting the practical work for other projects and helping out, whenever she could.

I thank my laboratory colleagues, Dr. Markus Appel, Theresia Feuerbach and Michael Kempf, for sharing rooms and laboratory benches with me, even if it was sometimes hard to find space for working.

For interpreting NMR results I had help from Dr. Markus Appel and Sanja Locher and for the work on the HPLC's I thank the 'cellar kids' Kathrin Kahle, Wolfgang Hümmer and Matthias Ackermann.

Of the non Food Chemists, Doris Moret gave invaluable pharmaceutical technical help and the workshop crew Matthias, Karl and especially Schorsch, were indispensable for all kinds of repairs and constructions. I will, furthermore, miss the 'Technischer Betrieb' with Andi, Pierre, Thomas and of course 'Herr Fritz' and thank them, particularly, for the lovely midday breaks we girls were invited to.

Otherwise, my never-ending thanks go to our working group, for all the good times, excursions, feasts and friendships we enjoyed together. Here, I would especially like to thank Dr. Sandra Elß and Kathrin Kahle for their friendship and our 'girls - pizza - ice cream - evenings', as well as Matthias Ackermann and Wolfgang Hümmer, who both participated in the friendship and sometimes in the evenings, if not always voluntarily for Wolfgang. Thank you also to everyone, who had to endure my questions and corrections to this piece of work, especially my father, who is now probably proficient enough to referate on stable isotope analysis off-by-heart.

My thanks also go to the F.R.U.I.T. Foundation, Heidelberg, Unibund and the program 'Chancengleichheit für Frauen in Forschung und Lehre' from the University of Würzburg for their financial support.

My main thanks go to my parents and my sister, who always let me do what I thought best, and supported me on my way with all means, as well as to my friend, Kathrin Diegelmann, whose friendship always meant a lot to me, and without whom, studying would have only been half as much fun and not as successful.

‘Theory is, when one knows everything, but nothing works,
Praxis is, when everything works, but no-one knows why.
For us theory and praxis are combined:
Nothing works and no-one knows why!’

- Unknown

Index

Publications

Elss, Sandra; Preston, Christina; Hertzig, Christine; Richling, Elke; Schreier, Peter. Über das Aromaprofil der Ananas (*Ananas comosus* [L.] Merr.) Eine Nachernte-Studie, *Flüssiges Obst*, **2003**, *70*, 734-737.

Preston, Christina; Richling, Elke; Elss, Sandra; Appel, Markus; Heckel, Frank; Hartlieb, Ariane; Schreier, Peter. On-line gas chromatography combustion/ pyrolysis isotope ratio mass spectrometry (HRGC-C/P-IRMS) of pineapple (*Ananas comosus*) volatiles, *J. Agric. Food Chem*., **2003**, *51*, 8027-8031.

Preston, Christina; Richling, Elke; Kahle, Kathrin; Kraus, Michael; Hümmer, Wolfgang; Appel, Markus; Heckel, Frank; Schreier, Peter. Ester Synthesis: Authenticity assessment by stable isotope analysis, In: Hofmann, Thomas; Rothe, Manfred; Schieberle, Peter (Editors) *State-of-the-Art in Flavour Chemistry and Biology*, Proceedings of the 7th Wartburg Symposium, **2004**, 358-362.

Kahle, Kathrin; Preston, Christina; Richling, Elke; Heckel, Frank; Schreier, Peter. On-line gas chromatography combustion/pyrolysis isotope ratio mass spectrometry (HRGC-C/P-IRMS) of major volatiles from pear fruit (*Pyrus communis*) and pear products, *Food Chem.*, **2005,** *91*, 449-455.

Elss, Sandra; Preston, Christina; Hertzig, Christine; Heckel, Frank; Richling, Elke; Schreier, Peter. Aroma profiles of pineapple fruit (Ananas comosus [L.] Merr.) and pineapple products, *LWT-Food Sci. Tech.*, **2005**, *38*, 263-274.

Richling, Elke; Preston, Christina; Kavvadias, Dominique; Kahle, Kathrin; Heppel, Christopher; Hummel, Silvia; König, Thorsten; Schreier, Peter. Determination of the $^{2}H/^{1}H$ and $^{15}N/^{14}N$ ratios of alkylpyrazines from coffee beans (*Coffea arabica* L. and *Coffea robusta* L.) by isotope ratio mass spectrometry, *J. Agric. Food Chem.*, **2005,** *53*, 7925-7930.

Elss, Sandra; Preston, Christina; Appel, Markus; Heckel, Frank; Schreier, Peter. Influence of technological processing on apple aroma analysed by high resolution gas chromatography mass spectrometry (HRGC-MS) and on-line gas chromatography combustion/pyrolysis isotope ratio mass spectrometry (HRGC-C/P-IRMS), *Food Chem.*, **2006**, *98* (2), 269-276.

Herbach, Kirsten M.; Stintzing, Florian C.; Elss, Sandra; Preston, Christina; Schreier, Peter and Carle, Reinhold. Isotope ratio mass spectrometrical analysis

of betanin and isobetanin isolates for authenticity evaluation of purple pitaya-based products, *Food Chem.*, **2006,** *99*, 204-209.

Richling, Elke; Appel, Markus; Heckel, Frank; Kahle, Kathrin; Preston, Christina; Schreier, Peter. Flavor authenticity studies, In: Ebeler, Susan; Takeoka, Gary; Winterhalter, Peter (Editors) *Perspectives and limits in Authentication of Food and Wine*, Oxford University Press, **2007**, Chapter 5.

Caja, María del Mar; Preston, Christina; Kempf, Michael; Schreier, Peter. Flavor authentication studies of α-ionone, β-ionone and α-ionol from various sources. *J. Agric. Food Chem.*, **2007**, *55*, 6700-6704.

Posters

Elss, Sandra; Richling, Elke; Preston, Christina; Appel, Markus; Heckel, Frank; Schreier, Peter. Ananas-Aromastoffe: Aromaprofil und Stabilisotopen-Analytik. 32. Deutscher Lebensmittelchemikertag, Munich, 08.-11. October **2003.**

Preston, Christina; Richling, Elke; Appel, Markus; Kahle, Kathrin; Heckel, Frank; Schreier, Peter. Ester Synthesis: Authenticity assessment by stable isotope analysis. 7th Wartburg Symposium on Flavour Chemistry & Biology, Eisenach, 21.-23 April **2004**.

Kahle, Kathrin; Preston, Christina; Richling, Elke; Schreier, Peter. Birnen-Aromastoffe: Aromaprofil und Stabilisotopen-Analytik. 33. Deutscher Lebens-mittelchemikertag, Bonn, 13.-15, September **2004**.

Elss, Sandra; Preston, Christina; Appel, Markus; Heckel, Frank; Schreier, Peter. Technologiebedingter Einfluss auf das Apfelaromaprofil: HRGC-MS- und HRGC-C/P-IRMS-Studien. 34. Deutscher Lebensmittelchemikertag, Hamburg, 19.-21, September **2005**.

Preston, Christina; Elss, Sandra; Kohlhepp, Stefanie; Appel, Markus; Heckel, Frank; Schreier, Peter. Stabilisotopenanalytik: Erfassung und Bewertung von technologiebedingten Isotopeneffekten von Aromastoffen. 34. Deutscher Lebensmittelchemikertag, Hamburg, 19.-21, September **2005**.

Herbach, K.M.; Stinzing. F. C.; Elss, S.; Preston, C; Schreier, P; Carle, R. Authentizitätskontrolle von Lebensmitteln aus violetter Pitaya mit Hilfe des

Stabilisotopenverhältnisses von Betanin- und Isobetaninisolaten. 34. Deutscher Lebensmittelchemikertag, Hamburg, 19.-21, September **2005**.

Preston, Christina; Richling, Elke; Kavvadias, Dominique; Kahle, Kathrin; Heppel, Christopher; Hummel, Silvia; König, Thorsten und Schreier, Peter. Alkylpyrazine aus Röstkaffee: Bestimmung der 2H/1H- und 15N/14N- Verhältnisse mittels Isotopenverhältnis-Massenspektrometrie. 35. Deutscher Lebensmittelchemikertag, Dresden, 18.-20, September **2006**.

Lectures

Preston, Christina; Kahle, Kathrin; Schreier, Peter. On-line gas chromatography combustion/pyrolysis isotope ratio mass spectrometry (HRGC-C/P-IRMS) of major volatiles from pear fruit (Pyrus communis) and pear products. Doktoranden-Seminar in Kloster Banz , 8.-11. January, **2005**.

Preston, Christina; Schreier, Peter. Frucht- und Fruchtsaftaromen: Kriterien zur Authentizitätsbewertung. GDCh Fruchtsäfte, fruchtsafthaltige Getränke: Technologie, Untersuchung und Beurteilung, Hameln, 7.-9. September **2005.**

Preston, Christina; Richling, Elke; Kavvadias, Dominique; Kahle Kathrin; Heppel, Christopher; Hummel, Silvia; König, Thorsten und Schreier, Peter. Bestimmung der $^{2}H/^{1}H$- und $^{15}N/^{14}N$- Verhältnisse von Alkylpyrazinen aus Kaffeebohnen (*Coffea arabica* L. und *Coffea canephora* var. *robusta*) mittels Isotopenverhältnis-Massenspektrometrie. GDCh-Regionaltagung Bayern, 13. March, **2006**.

Explanations and Abbreviations

Explanations:

- Green coffee beans are raw coffee beans which have been fermented and dried and are in their storage state before roasting.
- All aroma components from the roasted coffee bean are numbered chronologically, with bold Arabic numbers, in order of the retention time in the chromatograms. The structure matrix in the appendix summarises the components as an overview.
- Singly referred to substances, i.e. reagents of syntheses, are not numbered.
- All shown chromatograms and spectra were generated by using original data.
- Literature quotations are indicated by (maximal) the first two named authors and year of publication in brackets; the complete quotation is found in the bibliography.
- Registered trademarks are marked with a „®".

Abbreviations:

abbr.	abbreviation
AF	Anionic Fraction
AIR	international standard: nitrogen from air
approx.	approximately
CAM	Crassulacean Acid Metabolism
CF	Cationic Fraction
df	film strength of the stationary phase (GC)
EA	Elemental Analyser
EA-IRMS	Elemental Analyser – Isotope Ratio Mass Spectrometry
EA-C/P-IRMS	Elemental Analyser – Combustion/Pyrolysis - Isotope Ratio Mass Spectrometry
EI	Electronic Ionisation
EIF	Ethanol/Water Insoluble Fraction
ESF	Ethanol/Water Soluble Fraction
eV	electron Volt
GC	Gas Chromatography
GC-C/P-IRMS	Gas Chromatography – Combustion/Pyrolysis - Isotope Ratio Mass Spectrometry
GC-IRMS	Gas Chromatography - Isotope Ratio Mass Spectrometry
GC-MS	Gas Chromatography – Mass Spectrometry
GCP	Green Coffee Bean (Powder)
GISP	Greenland Ice Sheet Precipitation
HIF	n-Hexane Insoluble Fraction
HPLC	High Performance Liquid Chromatography
HRGC	High Resolution Gas Chromatography
HRGC-MS	High Resolution Gas Chromatography - Mass Spectrometry
HRGC-C/P-IRMS	High Resolution Gas Chromatography - Combustion/Pyrolysis - Isotope Ratio Mass Spectrometry
HSF	n-Hexane Soluble Fraction
IAEA	International Atomic Energy Agency
i.d.	inner diameter
IRMS	Isotope Ratio Mass Spectrometry
LC-MS	Liquid Chromatography – Mass Spectrometry
MS	Mass Spectrometry
m/z	mass - charge – ratio
n.m.	not measurable
NBS	National Bureau of Standards
NF	Neutral Fraction
NMR	Nuclear Magnetic Resonance

o.d.	outer diameter
PDB	Pee Dee Belemnite
PPF	Precipitated Polysaccharide Fraction
RT	Retention Time
SD	Standard Deviation
SDE	Simultaneous Distillation-Extraction
SLAP	Standard Light Antarctic Precipitation
SMOW	Standard Mean Ocean Water
SNIF-NMR®	Site-specific Natural Isotope Fractionation – Nuclear Magnetic Resonance Spectroscopy
SPF	Soluble Protein Fraction
TCD	Thermal Conduction Detector
TLC	Thin Layer Chromatography
V	Volt
Vs	Volt seconds (Peak Area)
V-PDB	Vienna Pee Dee Belemnite
V-SMOW	Vienna Standard Mean Ocean Water
WICF	Water Insoluble Cellulose Fraction
WIF	Water Insoluble Fraction
WIPF	Water Insoluble Pectin Fraction
WSF	Water Soluble Fraction

Summary

Gas chromatography – isotope ratio mass spectrometry (HRGC-IRMS) is an established technology for the authenticity assessment of achiral aroma compounds. For this technique, authentic reference data for both 'natural' and 'synthetic' origins of the aroma compounds is needed to define the limits and possibilities of authenticity assessments. For different fruit aroma compounds databases have been accumulated and have been used successfully. But this simplicity in the procedure of accumulating samples and filling the database fails, when the generation of aroma compounds are dependant on, not only the fruit itself, but also on a technological process as in the case of roasting coffee beans. In such a case, it is not enough simply to analyse samples from different origins for the database, but an examination of the influence of the technological process of roasting on the aroma is also needed. Furthermore, the generation process of the aroma compounds from their precursors during roasting should be analysed and determined.

The aim of this study was, therefore, to build up a database for alkylpyrazines (and pyridine) from roasted coffee, and to elucidate the questions determining the alkylpyrazine and pyridine generation in coffee beans in all aspects. For this purpose arabica and robusta green coffees from different regions of the world were roasted, and the stable isotope ratios, $^{15}N/^{14}N$ and $^{2}H/^{1}H$, of the produced alkylpyrazines and pyridine were compared to those of references, commercially available roast coffees, unspecified roast coffees, coffee products and coffee aromas. Additionally, the $\delta^{2}H_{V\text{-}SMOW}$ isotopic stability of alkylpyrazines in different solvents was determined to exclude isotopic effects in coffee products and coffee aromas. To elucidate the question as to how the stable isotope values, $^{15}N/^{14}N$, $^{2}H/^{1}H$ and $^{13}C/^{12}C$, of alkylpyrazine references were obtained and if these could be influenced somehow, different alkylpyrazines were synthesised. The generation process of alkylpyrazines during the roasting of coffee was analysed, by both roasting experiments and the fractionation of green coffee beans, into compound classes with subsequent roastings. In summary, the following results were acquired:

- Alkylpyrazines were found to be isotopically stable in both ethanol and water solutions during storage. The stable isotope values of coffee products, such as coffee drinks or aroma formulations, can be, therefore, analysed without doubts.

- For the first time, a database of various alkylpyrazines and pyridine from roast coffee, commercially available references and roast coffee products was constructed. Neither the $\delta^2H_{V\text{-}SMOW}$ nor the $\delta^{15}N_{AIR}$ values of these compounds were known before.

- The alkylpyrazine database demonstrates that an analytical differentiation between synthetic references, mostly ranging in the area of ± 0 ‰ for $\delta^{15}N_{AIR}$, and coffee bean derived alkylpyrazines, is possible. The $\delta^2H_{V\text{-}SMOW}$ values of most alkylpyrazines from roast coffee and products, ranging from -10 ‰ to -140 ‰, and the $\delta^{15}N_{AIR}$ values, ranging from -10 ‰ to 10 ‰, show their origin of amino acids and carbohydrates.

- A distinction between robusta and arabica self-roasted samples was seen in the $\delta^{15}N_{AIR}$ values for 2-ethyl-5/6-methylpyrazine (2 ‰ difference), 2,3,5-trimethylpyrazine (over 3 ‰ difference) and 2,3-dimethylpyrazine.

- Coffee aromas showed similar values to the synthetic references, in the correlation of $\delta^2H_{V\text{-}SMOW}$ and $\delta^{15}N_{AIR}$ values, for both 2-ethyl-3,5/6-di-methylpyrazine and 2-ethyl-3-methylpyrazine.

- In the roasting studies, the contents of pyridine, 3-methylpyridine and 3-ethylpyridine increased from the 'light' to 'dark' roast. This increase, in the amount of these compounds, being dependant on the length of time, can be contributed to thermal degradation of nitrogenous precursors, additional to Strecker degredation.

- The stable isotope ratios of the generated alkylpyrazines and pyridine in the roasting studies differed dependant on the compound and roasting duration. $^{15}N/^{14}N$ ratios of the alkylpyrazines were generally enriched, the more an alkylpyrazine was substituted. $^{13}C/^{12}C$ and $^{2}H/^{1}H$ ratios were the most enriched in the 'dark' roast, and the most depleted in the 'light' roast. Different N-, H-, and C-pools must contribute to the alkylpyrazine formation over the length of the roasting times, and, consequently, contribute to different $\delta^{15}N_{AIR}$, $\delta^{13}C_{V\text{-}PDB}$ and $\delta^2H_{V\text{-}SMOW}$ values.

- The syntheses of of various alkylpyrazines for comparison with synthetic references showed that the stable isotope values of the product alkylpyrazine are dependant on the stable isotope values of the educts.

- Alkylpyrazines generated by thermal degradation of amino acids, namely L-serine, L-threonine and a mixture thereof, as well as of diethylen-triamine displayed chromatogram compositions, found also in literary references. $\delta^2H_{V\text{-}SMOW}$ values of alkylpyrazines generated with L-serine did

not display the educt value but took on a value close to that of the employed water. Otherwise stable isotope values of generated alkylpyrazines took on similar values to the educts.

- The studies of pyridine formation, by roasting caffeine, amino acids and trigonelline, with and without citric acid, led to the observation that, the only pyridine formation using this method, derived from the roasting of trigonelline with citric acid.

- The fractionation of green coffee into compound classes was successful for most fractions regarding $\delta^{13}C_{V\text{-}PDB}$ and $\delta^{15}N_{AIR}$ values. $\delta^{2}H_{V\text{-}SMOW}$ values were affected, when water was used, and therefore not reliable for EA-P-IRMS analysis. The separation of polysaccharides and proteins was not performed with any satisfactory results. Bulk values of green coffee with $\delta^{2}H_{V\text{-}SMOW}$ = -30 ‰, $\delta^{13}C_{V\text{-}PDB}$ = -26.7 ‰ and $\delta^{15}N_{AIR}$ =8.5 ‰ concurred with literary references.

- Roasted ground green coffee bean (GCP) showed strong differences compared to roasted whole green beans in aroma profile and stable isotope values. The main differences were more pyridine and less alkylpyrazines, as well as more enriched $\delta^{15}N_{AIR}$, $\delta^{2}H_{V\text{-}SMOW}$ and $\delta^{13}C_{V\text{-}PDB}$ values.

- The roasting of green coffee fractions showed that the formation of pyridine in roast coffee aroma was found to derive from trigonelline and/or other low molecular substance degradation whilst the formation of alkylpyrazines was found to derive from polysaccharides and proteins.

- In all the roasted green coffee fractions, the alkylpyrazines with ethylrests had the most consistent stable isotope values. The amount of alkylpyrazines found, after roasting the fractions, decreased from the whole coffee beans over GCP, HIF to EIF.

Zusammenfassung

Die Gaschromatographie-Isotopenverhältnis-Massenspektrometrie (HRGC-IRMS) gehört zu den etablierten Verfahren zur Authentizitätsbewertung von achiralen Aromastoffen. Für diese Technik sind Datenbanken mit authentischen natürlichen und synthetischen Referenzproben notwendig, um die Grenzen und Möglichkeiten der Authentizitätsbewertung festzulegen. Bisher wurden für verschiedene Fruchtaromen solche Datenbanken erstellt und diese auch erfolgreich bei Fragen zur Authentizität genutzt. Diese Art des Vorgehens scheitert jedoch, wenn die Herkunft der Aromastoffe nicht nur von der Frucht abhängig ist, sondern auch von einem technologischen Prozess, wie z.B. im Falle der Kaffeebohnenröstung. In einem solchen Fall genügt es nicht, nur Proben verschiedener Art/Herkunft zu analysieren; auch der Einfluss des technologischen Prozesses auf das Aroma, d.h. die Entstehungsprozesse der Aromastoffe aus ihren Vorstufen müssen erforscht werden.

Ziel der vorliegenden Arbeit war es, eine Datensammlung für Alkylpyrazine (und Pyridin) von Röstkaffee zu erstellen und der Fragestellung bezüglich der Alkylpyrazin- (und Pyridin-)bildung nachzugehen. Zu diesem Zweck wurden die Stabilisotopenverhältnisse $^{15}N/^{14}N$ und $^{2}H/^{1}H$ der Alkylpyrazine von gerösteten Arabica- und Robusta-Kaffeebohnen mit denen von Referenzverbindungen, kommerziell erhältlichen Röstkaffees, Röstkaffees unbekannter Herkunft, Kaffeeprodukten und Kaffeearomen verglichen. Zusätzlich wurde die $\delta^{2}H_{V\text{-}SMOW}$-Stabilität der Alkylpyrazine in verschiedenen Lösemitteln bestimmt, um mögliche Austauscheffekte in Kaffeeprodukten und Kaffeearomen auszuschließen. Des weiteren wurde anhand von Synthesen verschiedener Alkylpyrazine überprüft, inwieweit deren Stabilisotopenwerte bei der Herstellung beeinflusst werden. Die Alkylpyrazinbildung während des Kaffeeröstens wurde auf verschiedene Weise untersucht, zum einen durch Röstexperimente unterschiedlicher Dauer und zum anderen durch Fraktionierung von grünem Kaffee in seine Komponenten mit anschließender Röstung dieser Fraktionen. Zusammenfassend lassen sich die folgenden Ergebnisse festhalten:

- Alkylpyrazine waren sowohl in Ethanol als auch in Wasser bezüglich ihrer $\delta^{2}H_{V\text{-}SMOW}$-Werte während der Lagerung stabil. Die Stabilisotopenwerte von Kaffeeprodukten, wie Kaffeegetränken oder Aromakonzentraten konnten daher ohne Bedenken analysiert werden.

- Zum ersten Mal wurde eine Datenbank aus verschiedenen Alkylpyrazinen und Pyridinen von Röstkaffee, kommerziell erhältlichen Referenzen und

Röstkaffeeprodukten erstellt. Weder $\delta^2H_{V\text{-}SMOW}$- noch $\delta^{15}N_{AIR}$-Werte dieser Verbindungen waren vorher bekannt.

- Die analytische Unterscheidung von synthetischen Referenzen, die meist in einem Bereich von ± 0 ‰ für $\delta^{15}N_{AIR}$ lagen, und Alkylpyrazinen aus Kaffeebohnen war möglich. Die $\delta^2H_{V\text{-}SMOW}$- und $\delta^{15}N_{AIR}$-Werte für die meisten Alkylpyrazine lagen im Bereich von -10 ‰ bis -140 ‰ bzw. -10 ‰ bis 10 ‰ und liessen damit auf ihre Herkunft aus Aminosäuren und Kohlenhydraten schließen.

- Bei selbstgerösteten Arabica- und Robusta-Proben wurden Unterschiede in den $\delta^{15}N_{AIR}$-Werten für 2-Ethyl-5/6-methylpyrazin (2 ‰ Unterschied), 2,3,5-Trimethylpyrazin (über 3 ‰ Unterschied) und 2,3-Dimethylpyrazin festgestellt.

- Kaffeearomen zeigten in der Korrelation von $\delta^2H_{V\text{-}SMOW}$- und $\delta^{15}N_{AIR}$-Werten für sowohl 2-Ethyl-3,5/6-dimethylpyrazin als auch 2-Ethyl-3-methyl-pyrazin ähnliche Werte wie die synthetischen Referenzen.

- Mit dem Grad der Röstung von grünen Bohnen stieg der Gehalt an Pyridin, 3-Methylpyridin und 3-Ethylpyridin von „leichter" zu „dunkler" Röstung an. Dieser Anstieg im Gehalt der Komponenten, verknüpft mit langer Röstdauer, ist auf thermische Abbaureaktionen von stickstoffhaltigen Vorstufen, zusätzlich zum Strecker-Abbau zurückzuführen.

- Die Stabilisotopenwerte der entstandenen Alkylpyrazine und Pyridin in den Röststudien waren von der Verbindung und Röstdauer abhängig. $^{15}N/^{14}N$-Verhältnisse waren angereicherter, je höher substituiert das Alkylpyrazin war. $^{13}C/^{12}C$- und $^{2}H/^{1}H$-Verhältnisse waren bei „leichter" Röstung am abgereichertsten und bei „dunkler" Röstung am angereichertsten. Die Röststudien zeigten, dass verschiedene N-, H-, und C-Quellen zu der Alkyl-pyrazin- und Pyridinentstehung beitragen müssen, um die verschiedenen $\delta^{15}N_{AIR}$-, $\delta^{13}C_{V\text{-}PDB}$- und $\delta^2H_{V\text{-}SMOW}$-Werte zu erklären.

- Die Synthese verschiedener Alkylpyrazine im Vergleich zu kommerziellen Referenzen zeigte, dass die Stabilisotopenwerte der Produkte von jenen der Edukte abhängig sind.

- Alkylpyrazine, die durch thermischen Abbau von Aminosäuren, wie L-Serin, L-Threonin (und einer Mischung hiervon) sowie Diethylentriamin gewonnen wurden, ergaben im Aromaprofil eine gute Übereinstimmung mit Literaturangaben. $\delta^2H_{V\text{-}SMOW}$-Werte von Alkylpyrazinen, die mit L-Serin erzeugt wurden, zeigten nicht die Isotopenverhältnisse des Eduktes,

sondern mit dem verwendeten Wasser vergleichbare Werte. Alle anderen Stabilisotopenwerte der Alkylpyrazine zeigten die Eduktwerte.

- Bei der Röstung von Koffein, Aminosäuren und Trigonellin (mit und ohne Zitronensäure) zeigte sich, dass Pyridin nur bei der Röstung von Trigonellin mit Zitronensäure gebildet wurde. Trigonellin kann als die Haupt-quelle von Pyridin in Röstkaffee angesehen werden.

- Die Fraktionierung von grünem Kaffee in seinen Komponenten war für die meisten Fraktionen hinsichtlich ihrer $\delta^{13}C_{V\text{-}PDB}$- und $\delta^{15}N_{AIR}$-Werte erfolgreich. Die $\delta^{2}H_{V\text{-}SMOW}$-Werte wurden häufig durch die Verwendung von Wasser als Extraktionslösung beeinflusst. Die Trennung von Polysacchariden und Proteinen führte dagegen nicht zum Erfolg. Globalwerte für grünen Kaffee von $\delta^{2}H_{V\text{-}SMOW}$ = -30 ‰, $\delta^{13}C_{V\text{-}PDB}$ = -26.7 ‰ und $\delta^{15}N_{AIR}$ = 8.5 ‰ waren in Übereinstimmung mit Literaturdaten.

- Gerösteter gemahlener grüner Kaffee (GCP) zeigte im Aromaprofil und den Stabilisotopenwerten Unterschiede zu im Ganzen gerösteten grünen Bohnen. Die Hauptunterschiede lagen im erhöhten Gehalt an Pyridin sowie angereicherten $\delta^{15}N_{AIR}$-, $\delta^{2}H_{V\text{-}SMOW}$- und $\delta^{13}C_{V\text{-}PDB}$-Werten für die gemahlenen Kaffeeproben.

- Das Rösten der einzelnen Fraktionen zeigte, dass die Pyridinbildung ausschließlich in der niedermolekularen, Trigonellin enthaltenden Fraktion stattfand, während die Alkylpyrazinentstehung ausschließlich in der Polysaccharid-/Proteinfraktion erfolgte.

- In allen gerösteten grünen Kaffeefraktionen zeigten die Alkylpyrazine mit Ethylresten die stabilsten Isotopenwerte. Der Gehalt an Alkylpyrazinen in den gerösteten Fraktionen verringerte sich mit zunehmender Fraktionierung von ganzen grünen Bohnen bis zur ethanollöslichen Fraktion.

1 Introduction

The sensual roasting aroma combined with the dry and bitter taste to the tongue is the main secret of the success of the coffee beverage. Germans drink an astounding 160 litres a year, so it is no wonder that coffee is the second most important world trading product, after oil, with a trading volume of US$ 12.3 billion. In particular, the aroma of coffee plays a strong role in the perception of the drink, determining its quality and success. Until recently, coffee aroma was only important for the brewed beverage as well as for a few further products, such as ice cream or chocolate, but in the past few years a whole range of new coffee-flavoured products has come onto the market, making coffee aroma a product of high value for confectionary, bakery, soft drinks and alcoholic drinks and bringing to the fore the question of the origin of the used aromas and their quality.

In a number of directives and regulations, the origin and authenticity of foodstuffs and food aromas have been regulated. Especially, the origin and the raw materials used, determine the price and, also, the market value of a foodstuff. Increasing food and health aspects and rising organic awareness lead to consumers wanting more ‘natural’ products or at least products with ‘natural’ ingredients. As the consumer is inclined to pay higher prices for products, which advertise such ‘natural’ ingredients, the danger arises for wrong statements concerning the quality of foodstuffs.

This applies to the aromatising of foodstuffs with aroma compounds and aroma formulas, where the last few years have shown that the consumer prefers products with ‘natural’ aromas compared to ‘nature-identical’ aromas. This buying behaviour has not only stimulated the industry into developing new methods of production of natural aroma compounds, but also given the rogue producers the possibility of cheating the consumer with false declarations, as the prices between ‘natural’ and ‘nature-identical’ aromas can vary up to 1000%. The consumer is protected by laws, stating that ‘natural’ aromas can only be gained via appropriate physical processes, such as distillation and extraction, or through enzymatic or microbial processes from educts of plant or animal origin.

It is important, therefore, to be able to control any declaration of the aroma in foodstuffs by chemical-analytical methods, in which adulterations can be determined. As ‘natural-identical’ compounds are chemically the same as ‘natural’ compounds, no determination can be performed using classical chemical-analytical methods but can only be performed using enantio-differentiation – in the case of chiral compounds – as well as stable isotope

analytical techniques. The latter rely on the fact that the stable isotope composition of aroma compounds is different, depending on their origin, i.e. synthetic or natural, so that the building of an aroma database, paired with statistical methods, gives assured statements about the authenticity of an aroma compound.

Concerning the authenticity assessment of achiral fruit aroma compounds, stable isotope analysis is a long established technique, but at present no roast aroma compounds and only few nitrogen-containing aroma compounds have been determined by this process. For roast aroma stable isotope determination, not only a database for these aroma compounds is needed but also, studies into their precursors and roast aroma formation thereof, concerning their isotope composition.

The research objective of this work was, therefore, to form a database for the stable isotope analysis of roast aroma compounds of coffee, alkylpyrazines (and pyridine), and to expand this, with basic knowledge on the isotopic influence of precursors, in the formation of these compounds. For this reason commercial and self-prepared roast coffee samples and products were analysed, via IRMS, to form a database, to which further products could be evaluated in the future. Following this, and to expand the database to include ‘synthetic’ references, certain alkylpyrazines were self-synthesised and their isotopic signature examined. The alkylpyrazines were, additionally, analysed for their stable isotope stability in certain solvents, which was important for determining the aroma formulations and extraction techniques employed. For expanding the knowledge on the stable isotope values in the formation of alkylpyrazines (and pyridine), the precursors of these compounds in green coffee were closely looked into, and their influence on derived roast aroma examined.

2 State of Knowledge

2.1 Sources, Distribution and Fractionation of Isotopes

Atoms of single chemical elements do not occur homogeneously in nature but always as a group of different nuclides with the same order number (= number of protons) and different mass (= number of protons + neutrons). For these elements the Nobel Prize winner, Frederick Soddy, first introduced the term 'isotope' during a speech delivered to the British Royal Society in the year 1913. Since then, this term has gained preference over a rival term 'pleiad' (Greek: sisters), the name of a group of stars. The word 'isotope' comes from within the periodic table of the elements, meaning that all isotopes of an element occupy the same (*iso*) place (*topos*) in this table. Isotopes are, therefore, all atoms of an element, which differ only in the quantity of neutrons inside the atom core. Up to now about 120 elements have been recognised, which have 3100 accompanying isotopes. Most of these isotopes are short-living radionuclides with only 283 isotopes belonging to the stable isotope category, undergoing no radioactive decay at all. Usually, every natural element has one or more stable isotope(s), whilst other isotopes undergo radioactive decay. Some elements, such as fluorine (F) and phosphorus (P), have only one single stable isotope, whereas others, such as tin (Sn), have 10 stable isotopes.

The 'relative isotope abundance' is determined as the percentage of an isotope relative to its element. This is declared in atom-%. When for each stable isotope, the relative isotope abundance is multiplied by the mass of the nuclide, and these are added together, the atom mass in 'Dalton' is achieved, as given in the periodic table of the elements. With most elements the lightest stable isotopes account for more than 95 % of all isotopes, such as with hydrogen (H), carbon (C) and nitrogen (N), but the opposite holds true for some elements such as boron (B) and lithium (Li), where heavy stable isotopes are abundant. Other elements, such as bromine (Br), silver (Ag) and europium (Eu), have, approximately, an equal distribution of both light and heavy stable isotopes. In the following work only some of the more relevant stable isotopes used in food chemistry, so-called 'bio-elements' (C, H, O, N, S), are discussed, particularly the stable isotopes of carbon (C), nitrogen (N) and hydrogen (H). Table 2-1 gives a generalised overview.

Table 2-1: Stable isotopes of the bio-elements hydrogen, carbon and nitrogen with their characteristics (after Schmidt et al., 2007).

Element	Symbol	Relative Natural Abundance [Atom- %]	Isotope Ratio R[a]
Hydrogen	^{1}H	99.9855	
	^{2}H	0.0145	0.000145
Carbon	^{12}C	98.892	
	^{13}C	1.108	0.0112041
Nitrogen	^{14}N	99.6337	
	^{15}N	0.3663	0.0036765

[a] R = [heavy isotope]/[light isotope] see equation (1)

The first machine built to detect isotopes was a double-focusing mass spectrometer from Francis Aston in 1919. With this machine Aston proved that neon was an isotope triplet (Fry, 2007). Nowadays, the well-established method for measuring isotope compositions is the isotope ratio mass spectrometer, in which the material to be measured is converted into simple measurement gases and the relative deviation of the isotope ratio is measured in comparison to a suitable standard. Table 2-2 gives an insight into the different standards and measurement gases used. The standards are essential as the difference in the analysed isotope composition is very small, being in the range of a few atom-%. The internationally recognised unit for isotope ratio measurement is δ, whose value is expressed in ‰ as seen in equation (2-1) (McKinney et al., 1950).

Table 2-2: Internationally used isotope standards with isotope ratio R as well as measurement gases (after Schmidt et al., 2007).

Isotope Ratio R[a]	International Standard	Isotope Ratio R[a]	Gas Type for IRMS Analysis
$^{2}H/^{1}H$	V-SMOW[b]	0.00015576	
	SLAP[c]	0.00008902	H_2
	GISP[d]	0.00012618	
$^{13}C/^{12}C$	V-PDB[e]	0.0112372	CO_2
$^{15}N/^{14}N$	AIR[f]	0.0036765	N_2

[a] R = [heavy isotope]/[light isotope], [b] Vienna Standard Mean Ocean Water, [c] Standard Light Antarctic Precipitation, [d] Greenland Ice Sheet Precipitation, [e] Vienna Pee Dee Belemnite, [f] Air Nitrogen

The δ value is expressed as

$$\delta\,[‰] = \frac{R_{(sample)} - R_{(standard)}}{R_{(standard)}} \times 1000 \qquad (2\text{-}1)$$

where R = isotope ratio $\frac{c_{(heavy\ isotope)}}{c_{(light\ isotope)}}$

So, for a low δ value, the sample to be analysed will be depleted in heavy isotopes.

Although isotopes have the same number of protons in the atom core and, therefore, also the same number of electrons in the atom hull, they do not behave exactly alike during chemical and physical actions. The different neutron quantity leads to different masses, which result into the characteristic 'isotope effects'. Light isotope bonds have more potential energy than heavy isotope bonds, which is why, when the same energy is applied to the bond, the light isotope bond needs less energy to be broken. Simply said, heavy isotopes make chemical bonds that are harder to make and to break, leading to quicker reactions with lighter isotopes (Bigeleisen, 1965). These 'kinetic isotope effects' are stronger the greater the mass difference of the isotope effects. For this reason the greatest effects are seen with the hydrogen isotopes protium (^{1}H), deuterium (^{2}H) and tritium (^{3}H), where the relative mass differences between 1, 2 and 3 are largest. Such kinetic isotope effects occur in enzyme-catalysed reactions, which are explained further in chapters 2.2.2, 2.3.2 and 2.4.2. A further type of isotope effect is based on the physical-chemical properties of compounds with different isotopes. This isotope effect influences are, for instance, the mol-volume, density, melting and boiling points, vapour pressure, chromatographic properties and spin-dependant spectroscopic technologies. In these cases the effects are called 'thermodynamic isotope effects'; a well known use is the separation of heavy uranium ^{238}U from lightweight uranium ^{235}U by centrifugation to achieve nuclear-usable uranium. Further effects, which can change isotope distribution, are so-called 'exchange reactions', where in one molecule single atoms, or even whole functional groups, are substituted, i.e. the proton transfer in enolising compounds. For analytical measurements, thermodynamic isotope effects and exchange reactions have to be taken into consideration to avoid possible isotope fractionation during sample preparation.

The shown isotope effects lead to marginal but significant aberrations of the relative abundance of single isotopes in the biosphere; these being climatic factors such as weather patterns or geographic locations, further thermodynamic effects during plant assimilation and transpiration, as well as kinetic isotope

effects during (bio-) chemical metabolism reactions. In the next chapters some relevant thermodynamic and kinetic isotope effects are briefly discussed.

2.2 Isotope Fractionation of Hydrogen

2.2.1 Thermodynamic Isotope Fractionation

Although, hydrogen is the most abundant element in the universe, on earth it represents only ca. 0.74 % by weight of the lithosphere, hydrosphere and atmosphere combined. In its natural state, hydrogen can only be found in volcanic gases and trapped in minute quantities in minerals and rocks (Römpp, 2006). The largest amounts of hydrogen are found together with oxygen as water, as well as bound to carbon in nearly all organic compounds.

The main reservoir of water in the biosphere is found in the oceans and, because of its constant isotope composition regarding ^{2}H and ^{18}O, it also represents the standard reference material (standard mean ocean water or 'SMOW'). Nevertheless, meteorological water originating from the oceans, which is part of the hydrological cycle, undergoes significant isotope fractionation, due mostly to thermodynamic isotope effects during evaporation, condensation and precipitation. Consequently, the hydrological cycle is, in the main, responsible for the global thermodynamic isotope fractionation of hydrogen, bearing in mind that the isotope fractionation of the hydrogen isotopes always correlates with that of oxygen (Friedmann, 1953). This linear correlation is reflected in the equation $\delta^{2}H = 8 \times \delta^{18}O + 10$ (Craig, 1961). The occurring isotope signatures of meteorological water are dependant on both geographic and climatic factors of each location on earth, and reflect the situation of geographical position (longitude, latitude and altitude), temperature, precipitation volume as well as moisture in the air at those locations (Epstein and Mayeda, 1953; Martin and Martin, 2003).

During cloud formation over the oceans, the lighter isotopes of water, i.e. those water isotopes depleted in ^{2}H and ^{18}O, in particular undergo evaporation as they have a higher vapour pressure and, through the insolation, they can go into the vapour phase more easily (Hoefs, 1973).

Most cloud formation occurs in equatorial parts of the world, which combined with the rotation of the earth causes further isotope fractionation to occur, leading to deuterium-depleted precipitations increasing with latitude. During the cloud passage over the continents, the enriched isotopomeric water molecules

are first to rain down in coastal regions, leaving the more depleted water molecules to condense at higher elevations, as seen in figure 2-1. Low temperatures promote even stronger fractionations of water vapour in clouds, so that extremely depleted values can be found in high-altitude glaciers or in Polar Regions.

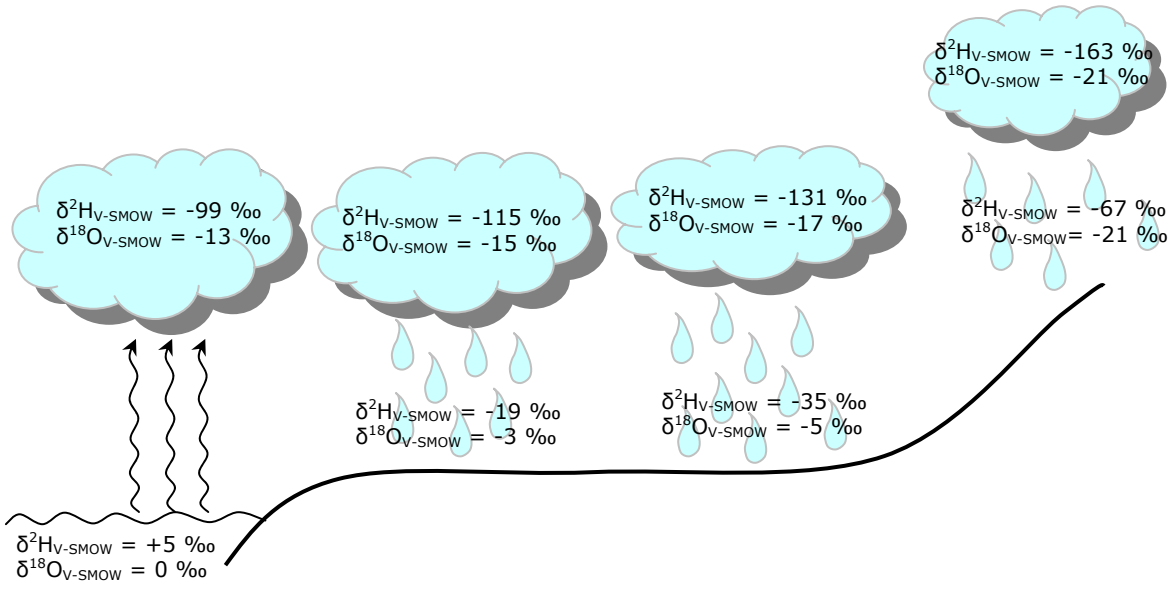

Figure 2-1: δ^2H and $\delta^{18}O$ distribution from the ocean to land, with the influence of altitude shown. Figure modified from Hoefs, 1973.

Inland air moisture influences the isotope fractionation of water, as well. In months rich in rainfall the precipitate is more depleted, whereas in months with lower amounts of rain the precipitate in enriched (Dansgaard, 1964). The geographic and climatic conditions in all places have defined influences on the isotopic composition of meteorological water, as mentioned above, which is how an isotope signature is formed, exhibiting a characteristic for each place on the globe. Analyses by Kluge et al. (1995) with orchids and succulents, from different habitats (forest and desert) in Madagascar, have shown that for the global $\delta^2H_{V\text{-}SMOW}$ values of plant biomass the deuterium concentrations of the meteorological water has less effect than other factors.

When the meteorological water has at last reached the plants, it is transported from the roots to the leaves through the xylem, where further isotope fractionations occur through transpiration processes. Leaf water in plants is enriched in ^2H and ^{18}O in comparison to the water taken up by the roots (Bricout, 1978). This is again due to the different vapour pressure of isotopomeric water. In comparison to meteorological water the enrichment of ^2H in leaf water is ~ 30 ‰ (Schmidt et al. 2003). Water in fruit is also enriched, but not as much

as in leaf water (Lesaint et al. 1974). Further important fractionation systems occur in kinetic processes during biochemical metabolism. Figure 2-2 shows an overview of $\delta^2H_{V\text{-}SMOW}$ values in nature of inorganic and organic hydrogen compounds with the expected fluctuation ranges.

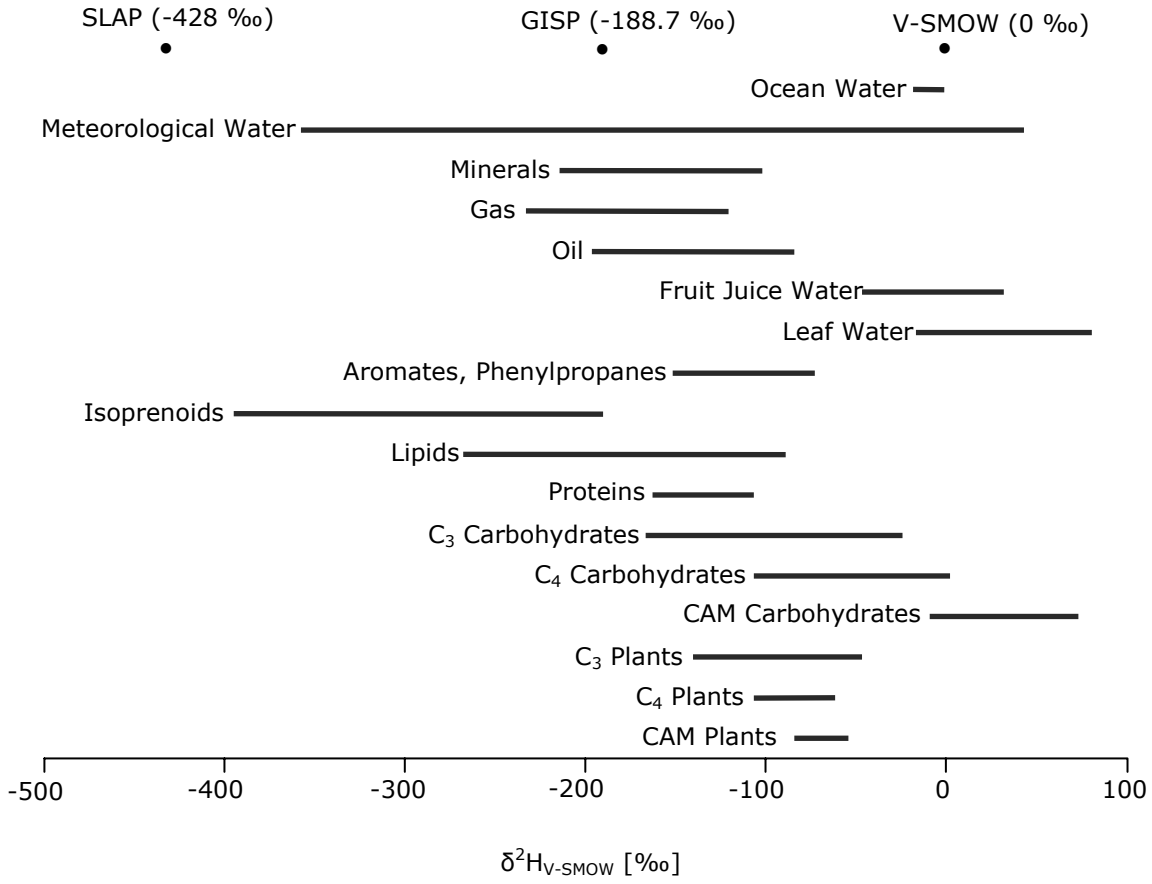

Figure 2-2: Overview of $\delta^2H_{V\text{-}SMOW}$ values in nature of inorganic and organic hydrogen compounds with the expected fluctuation ranges (Winkler, 1984; Sternberg et al., 1984 a; Naraoka and Chikaraishi, 2001; Schmidt et al., 2003; Schmidt et al., 2007).

2.2.2 Isotope Fractionation in Plants

For plants the only hydrogen source is from the water they take up from the ground. The $\delta^2H_{V\text{-}SMOW}$ value of the ground water is dependant on the value of the rain water (Gat, 1971), which, as already described, is dependant on geographic and climatic factors (see figure 2-1 and chapter 2.2.1). After being transported to the photosynthetically active leaves, a significant enrichment of heavy isotopic water molecules occurs up to $\delta^2H_{V\text{-}SMOW}$ = ~ 30 ‰, through gas exchange, in the stomata (Bricout, 1978). Although this enrichment is independent of the plant photosynthesis type (Flanagan et al., 1991), CAM plants growing in the wild

normally show higher deuterium enrichments than C_3 and C_4 plants. As CAM plants only enrich deuterium when subjected to water stress, and only transpire at night, this enrichment cannot only come only from different transpiration techniques, but also from the higher deuterium contents of the ground water at the usually dry growing locations of CAM plants (Ziegler et al., 1976; Sternberg et al. 1986).

During photosynthesis the hydrogen atoms of water are photochemically reduced into NAD(P)H, where they can be converted into organic material through biosynthesis. Until now, for this primary step, only Luo et al. (1991) have found a deuterium depletion of ~ -600 ‰ in hydrogen gas, produced by cyano-bacteria, when compared to source water. Further studies on photosynthetically produced cellulose show an isotope fractionation of Δ = 171 ‰ versus source water. As the cellulose, dependent on the growth conditions, exchanges 40 % to 100 % of its primarily fixed hydrogen atoms with water (secondary hydrogen exchange), Hayes (2001) deduces that, in plants, the primary reductant (H^- of NADPH) also has a very strong depletion, when compared to source water (Yakir and DeNiro, 1990). During the anabolic and catabolic metabolism processes in the plant the exchange reactions with water lead to an enrichment of $\delta^2H_{V\text{-}SMOW}$ values when compared to leaf water. For organic C_3 plant material the order of depletion of the $\delta^2H_{V\text{-}SMOW}$ values, relative to leaf water, can be observed as following a pattern as seen below (Schmidt et al., 2003):

Leaf water (0 ‰) > amino acids and organic acids (-50 ‰) > phenylpropanoids (-90 ‰) > carbohydrates (-110 ‰) > homogenisised plant material (-120 ‰) > proteins (-130 ‰) > hydrocarbons (-140 ‰) > lipids (-180 ‰) > sterine (-250 ‰) > phytol, sesquiterpenes (-330 ‰)

Following the model from Schmidt (2003), these values mirror the distance in the metabolism of each group of secondary plant compounds from that of the primarily fixed hydrogen of the photosynthesis. The deuterium depletion of each compound compared to leaf water is, therefore, due to the available reduction equivalents, metabolic product fluxes and kinetic isotope effects of participating enzymes. These enzymes show an isotope effect only if, during a biochemical reaction, the product flow is branched. A similar model explains the observed differences in the deuterium content of C_3 and C_4 plants (Fogel and Cifuentes, 1993): In C_4 plants two different kinds of photosynthetically active cells are found stapled around the vascular bundle of the leaf. The CO_2 is primarily fixed in the mesophyll cells as malate, and is transported into the bundle sheet cells together with the NADPH reduction equivalents, where CO_2 is released again and assimilated via the Calvin cycle. In C_3 plants CO_2 joins the Calvin cycle in the

stroma of the chloroplasts without an intermediate fixation or transportation. The pool of reduction equivalents found in the bundle sheet cells of C_4 cells is, therefore, consequently different to those found in C_3 plants, because in C_3 plants the photosynthesis takes place in a single cell in comparison to C_4 plants, where two types of cells and transportation processes play a large role. The comparatively higher deuterium concentration in C_4 plants seems to be a result of this different and more effective CO_2 fixation method (Smith and Ziegler, 1990).

A speciality is found in CAM plants, namely the strongly enriched deuterium content in cellulose nitrate (Sternberg and DeNiro, 1983). It was shown that this enrichment is independent of the $^2H/^1H$ ratios in lipids (Sternberg et al., 1984 a) and $^{18}O/^{16}O$ ratios in cellulose (Sternberg et al., 1984 b), which is why the authors rejected a transpiration-dependant cause and favoured different biochemical compartmenting, as well as favouring an enrichment during gluconeogenesis and carbohydrate metabolism in the cytoplasma (Sternberg et al. 1984 a). This model was confirmed by Luo and Sternberg (1991) by analysing the differences in the deuterium concentrations of starch and cellulose nitrate in C_3 and CAM plants. They found that, independent of the photosynthesis type, the cellulose was more enriched with deuterium compared to that of starch. As a rule, the lower the deuterium content in the starch, the larger the difference to the deuterium content of the plant's cellulose. Generally, the CAM plants had the highest enrichment in deuterium in its starch.

2.3 Isotope Fractionation of Carbon

2.3.1 Thermodynamic Isotope Fractionation

Primary carbon sources for all biological material are atmospherical CO_2 and hydrospherical HCO_3^-. Gaseous carbon dioxide has a global mean value of $\delta^{13}C_{V\text{-}PDB}$= ~ -7 ‰ to -10 ‰. This homogeneous $^{13}C/^{12}C$ isotope ratio is achieved by equilibration processes in the atmosphere (Hoefs, 1973). This ratio can be influenced locally due to natural (Freyer, 1979; Martin and Sutherland, 1990) and anthropogenic (Keeling et al., 1979; Penuelas and Azcon-Bieto, 1992) emissions. In water, dissolved HCO_3^- shows a $\delta^{13}C_{V\text{-}PDB}$ value of ~ ± 0 ‰, with the difference to gaseous carbon dioxide being explained by isotope fractionation during the following equilibration reactions, (Deuser and Degens, 1967; Mook et al., 1974; Marlier and O´Leary, 1984), which lead on to $^{13}C_{V\text{-}PDB}$ enrichment (Δ = ~ 8 ‰) of the hydrogen carbonate during global atmospheric gas exchanges with the hydrosphere:

(2-2) $CO_{2\ (gaseous)} \leftrightarrow CO_{2\ (dissolved)}$

(2-3) $CO_2 + H_2O \leftrightarrow HCO_3^- + H^+$ and

(2-4) $^{13}CO_2 + H^{12}CO_3^- \leftrightarrow {}^{12}CO_2 + H^{13}CO_3^-$

Land plants, which assimilate atmospherical CO_2, are, therefore, more depleted in ^{13}C than aqueous plants and organisms (Schmidt et al., 2007). Further significant influences on the $\delta^{13}C_{V\text{-}PDB}$ values of plant material are caused by light irradiation (Ehleringer et al., 1986; Evans et al., 1986), transpiration rates (Farquhar et al., 1982) and salt content (Downton et al., 1985). Figure 2-3 shows the $\delta^{13}C$ distribution in the ecosystem including the above mentioned influences.

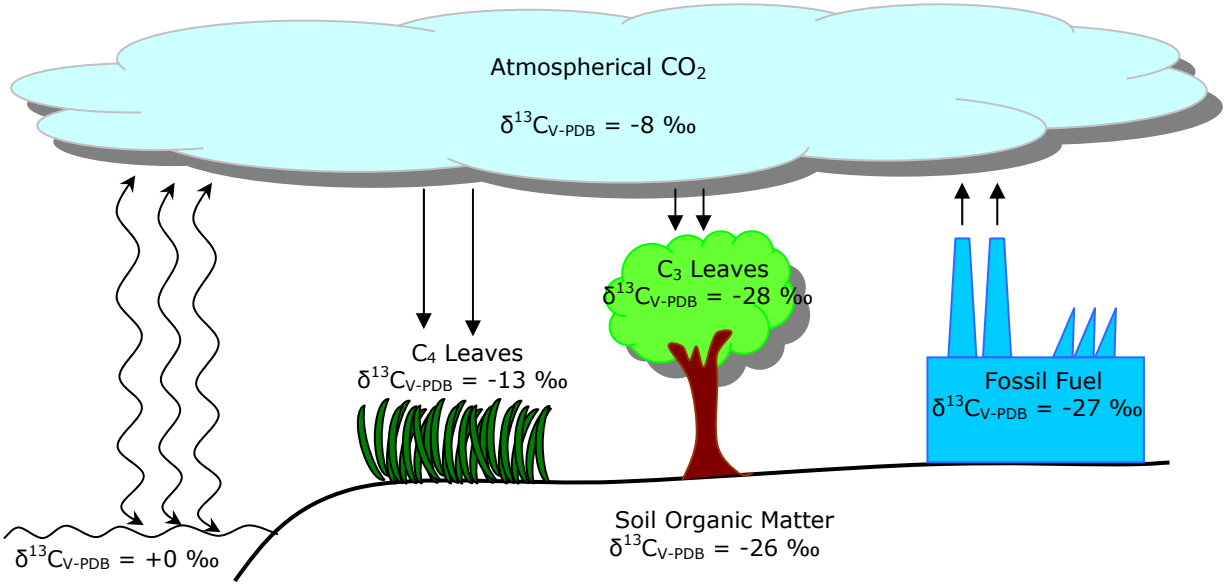

Figure 2-3: $\delta^{13}C$ distribution in the ecosystem, with arrows indicating CO_2 fluxes. Figure modified from Peterson and Fry, 1987.

2.3.2 Isotope Fractionation in Plants

The isotope fractionation of carbon is understood far better than that of hydrogen. Dependent on the type of photosynthesis, the assimilation of CO_2 leads, at the beginning of the biogenesis of plant biomass and single compounds, to significant differences in $^{13}C/^{12}C$ ratios. In figure 2-4 an overview of $\delta^{13}C_{V\text{-}PDB}$ values in nature of inorganic and organic hydrogen compounds with the expected fluctuation ranges is presented.

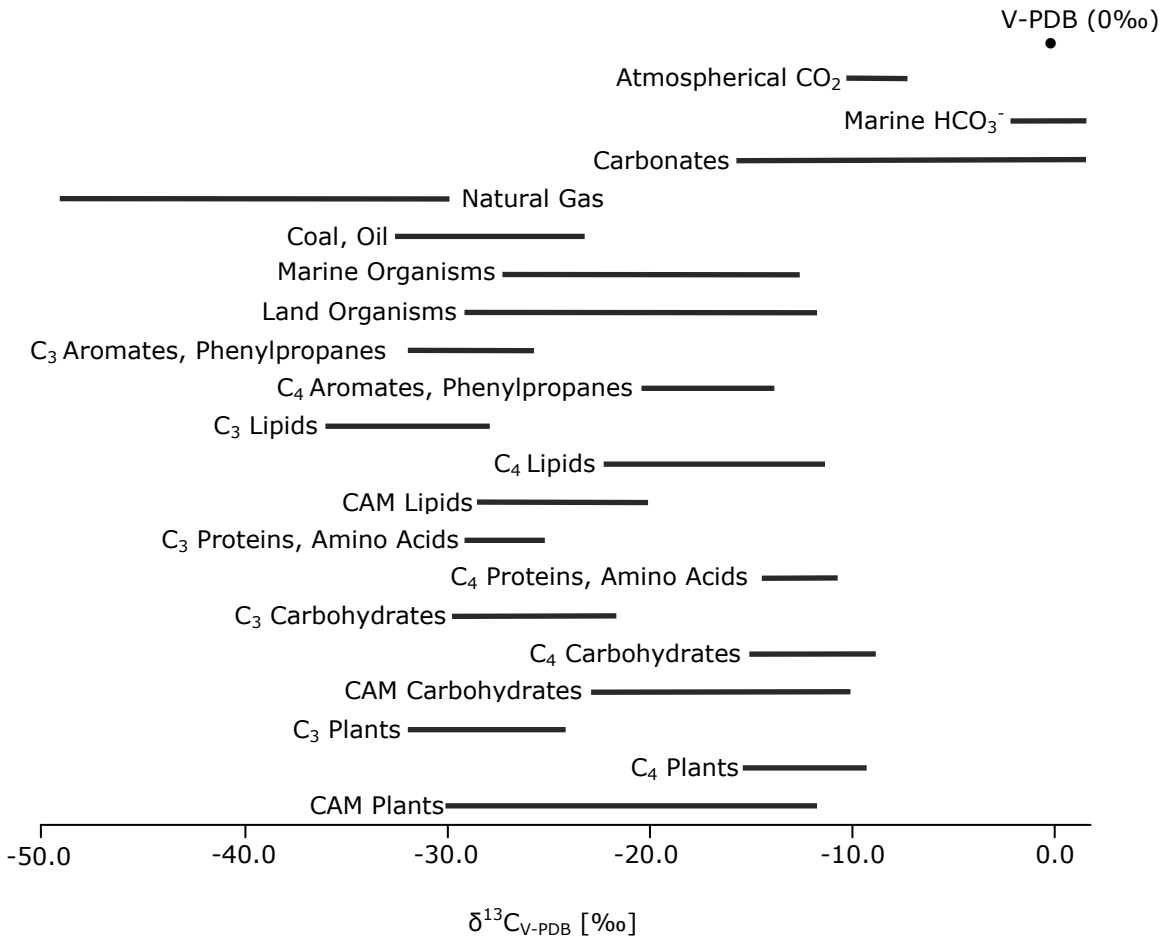

Figure 2-4: Overview of $\delta^{13}C_{V\text{-}PDB}$ values in nature of inorganic and organic carbon compounds with the expected fluctuation ranges (Hoefs, 1973; Winkler, 1984; Sternberg et al., 1984 a-c; Naraoka and Chikaraishi, 2001; Schmidt et al., 2007).

In C_3 plants the incorporation of CO_2 goes through the Calvin cycle into the stroma of the chloroplasts. The atmospheric CO_2 is joined to D-ribulose-1,5-biphosphate by the enzyme ribulosebiphosphate-carboxylase to form two molecules of the C_3 compound 3-phospho-D-glycerate, as first photosynthesis products. This enzymatic reaction of the CO_2 fixation has a large kinetic isotope effect (Park and Epstein, 1960; Christeller et al., 1976), which leads to a favourised incorporation of the lighter $^{12}CO_2$. The exact value of the depletion, in comparison to that of CO_2, can only be given with caution, as the experimentally found values in literature vary, depending on the origin of the enzyme and the experimental design (O'Leary, 1981; Winkler et al., 1982). The *in vitro* found isotope fractionation seems to be generally far larger than the *in vivo* observed effects (O'Leary, 1981; Ivlev, 2001). The values of ~ -18 ‰ for the enzymes from spinach and corn, as found by Schmidt at al. (1978), mark a depletion minimum, although depletion values of up to ~ -30 ‰ and more have been found (Estep et al., 1978). O'Leary (1981) gives, therefore, an average value of

$\delta^{13}C_{V\text{-}PDB}$ = ~ -30 ‰ ± 10 ‰ for this ^{13}C depletion level, which has remained unchanged until today (~ -29 ‰, Hobbie and Werner, 2004).

In C_4 plants the CO_2 is integrated into organic material over the Hatch-Slack cycle. The absorbed CO_2 in the mesophyll cells is dissolved and converted into HCO_3^-, which is then, together with phosphoenolpyruvate, transformed by phosphoenolpyruvate carboxylase (Cooper et al., 1971) into the compound oxaloacetate, which in turn is then converted into malate and transported to the bundle sheet cells for CO_2 fixation. This fixation is conducted, as with the C_3 plants, in the Calvin cycle, after the transported CO_2 is freed from malate and converted with ribulosebisphosphate carboxylase. The difference in the C_4 metabolism, in comparison to the C_3 plants, lies in the fact that the CO_2 comes from a ^{13}C enriched substrate pool in the form of HCO_3^- , which discriminates, via equations (2) and (3), towards the heavier isotope (see chapter 2.3.1). The observed $\delta^{13}C_{V\text{-}PDB}$ values of ~ -10 ‰ to -16 ‰ in C_4 plant biomass (Whelan et al., 1970) are, furthermore, an expression of the kinetic depletion of only -2 ‰ to -2.5 ‰ compared to $^{13}CO_2$ during the phosphoenolpyruvate carboxylase fixation (Whelan et al., 1973; Reibach and Benedict, 1977; Schmidt et al., 1978) and the nearly complete transformation of the transported CO_2 in the bundle sheet cells. The differences in the $\delta^{13}C_{V\text{-}PDB}$ values of C_3 and C_4 plants show the effectiveness of the CO_2 assimilation (O'Leary, 1981).

CAM plants have, similar to the C_4 plants, a prefixation of CO_2 as C_4 compound in the Crassulacean Acid Metabolism. A difference is found though, as the CO_2 assimilation is not spaciously but temporally divided in the Calvin cycle. CAM plants show a diurnally acid rhythm, expressed through a change in pH value of the cell fluid in a day-night-shift. With the CO_2 uptake occurring at night, the CO_2 is first fixed, via phophoenolpyruvate carboxylase, as malate and stored in the cell vacuole. During the daytime, the stomata are closed and the stored acids are transported to the chloroplasts and enzymatically decarboxylated. In this way the CO_2 is brought into the Calvin cycle via the ribulosebisphosphate carboxylase. This adaptation, especially in dry places, enables CAM plants to conduct photosynthesis in the daytime with closed stomata and to uptake CO_2 at night when the water loss is the smallest (Sayed, 2001). Many CAM plants do not strictly adhere to this CAM photosynthesis method, but additionally uptake CO_2 in the daytime, transforming it directly over the ribulosebisphosphate carboxylase into the Calvin cycle. Intermediate values, between those of C_3 and C_4 plants, have been observed for CAM biomass, dependent on the extent of the day fixation (Ziegler et al., 1976; Ziegler, 1996; Winter and Holtum, 2002).

The type of photosynthesis in C_3, C_4 or CAM plants is, as can be seen, the basis for the $\delta^{13}C_{V\text{-}PDB}$ values of plant biomass. For further non-statistical isotope distribution of $^{13}C/^{12}C$ ratios of individual compounds in plants, a whole range of enzymes have been found (Hobbie and Werner, 2004). The best-known, and best analysed, isotope fractionation in biochemical secondary metabolism is, probably, the pyruvate-dehydrogenase catalysed decarboxylation of pyruvate with the genesis of acetyl-CoA (DeNiro and Epstein, 1977). This leads to a ^{13}C depletion of ~ -7 ‰ ± 3 ‰ in lipids when compared to primary metabolised carbohydrates (Naraoka and Chikaraishi, 2001) and a ^{13}C depletion of ~ -2.4 ‰ to 9.9 ‰ when compared to leaf biomass (Chikaraishi and Naraoka, 2004). Lipids from C_3 plants normally show smaller differences towards their carbohydrates (4 ‰ to 6 ‰) than the lipids from C_4 plants (8 ‰ – 10 ‰). It is presently under discussion as to whether this phenomenon derives from different concentrations of lipids in the plants (Collister et al., 1994; Naraoka and Chikaraishi, 2001; Conte et al., 2003). This enzymatic isotope fractionation leads to a ^{13}C depletion in the carbonyl function of the acetyl-CoA and, therefore, to a ^{13}C depletion of fatty acids and isoprenoides (DeNiro and Epstein, 1977; Melzer and Schmidt, 1987). A similar effect is found with the pyruvate decarboxylase, which is responsible for the ^{13}C depletion in the carbonyl function of acetaldehyde (Alvarez et al., 1991; Sun et al., 1995). Fructose-1,6-bisphosphate aldolase leads to a ^{13}C enrichment in the positions C-3 and C-4 of carbohydrates during glycolysis and gluconeogenesis (Gleixner and Schmidt, 1997).

2.4 Isotope Fractionation of Nitrogen

2.4.1 Thermodynamic Isotope Fractionation

Atmospheric N_2 gas is the most abundant form of nitrogen in the biosphere, with a constant $\delta^{15}N_{AIR}$ value of 0 ‰ (Mariotti, 1983). Other forms of nitrogen in the biosphere have $\delta^{15}N_{AIR}$ values ranging from -10 ‰ to 10 ‰, close to the N_2 gas value. This is due to the fact that nitrogen is often the limiting factor in plant growth and bacterial mineralization and, therefore, kinetic isotope fractionation does not play such a strong role, as all available nitrogen is consumed. Isotope fractionation occurs during decomposition, where the loss of ^{14}N is faster than ^{15}N, which leads to an enrichment of heavier isotopes with increasing depth in both soils and in the ocean, of the order of 5 ‰ to 10 ‰ (Mariotti et al., 1981). Nitrification and denitrification in the sea promote substantial isotope effects of Δ = 10 ‰ to 40 ‰ and, where nitrate is not limiting growth, phytoplankton assimilate nitrate with small isotope effects (Δ = 4 ‰ to 8 ‰) (Altabet and Francois, 1994; Hobbie et al., 1998; Liu and Kaplan, 1989). Nitrogen isotope

values of ammonium and nitrate in rainfall lie in the range of $\delta^{15}N_{AIR}$ = -18 ‰ to 8 ‰, where the negative values are related to soil and anthropogenic emissions in highly industrialised areas (Heaton, 1987). These negative values have been helpful in tracing anthropogenic influences in natural systems. For an overview, figure 2-5 shows the $\delta^{15}N$ distribution in the ecosystem.

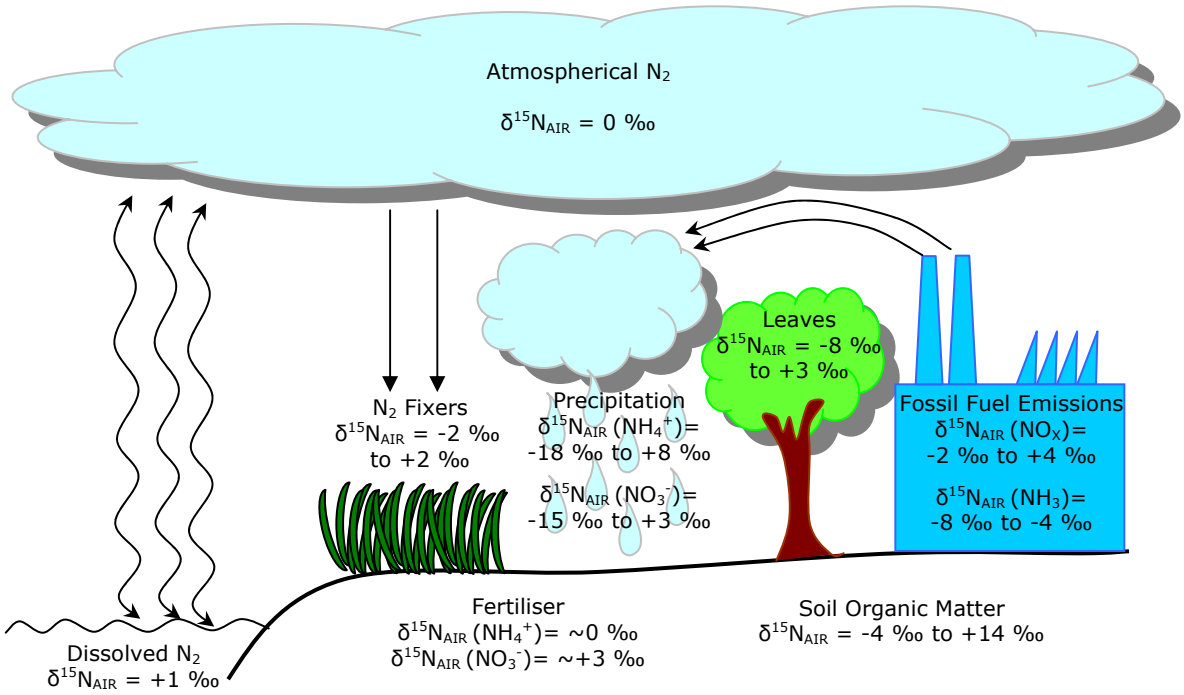

Figure 2-5: $\delta^{15}N$ distribution in the ecosystem, with arrows indicating fluxes. Figure modified from Peterson and Fry (1987).

In plants the relative amount of nitrogen is less than 1 % of dry biomass, in contrast to its functional importance. To be available for plants N_2, NH_3 and NO_X have to be converted into NO_3^-, NH_4^+ or other metabolites mostly by micro-organisms. As the global $\delta^{15}N$ value of plant biomass is primarily determined by the value of the nitrogen source, it is difficult to compare $\delta^{15}N$ values of compounds from different origins. To compare the observed relative ^{15}N depletion of the final product with its source an isotope discrimination factor is used as follows:

$$\alpha = 1 + \frac{\delta^{15}N_{(source)} - \delta^{15}N_{(product)}}{1000} \qquad (2\text{-}5)$$

2.4.2 Isotope Fractionation in Plants

$\delta^{15}N_{AIR}$ values of nitrogen in plants are mainly determined by the primary sources, namely fertilisers, ammonium and nitrate, and N_2 from nitrogen assimilation. An overview over different $\delta^{15}N_{AIR}$ values is shown is figure 2-6. Normally, plant material is slightly depleted in ^{15}N compared to its nitrogen source (Faulhaber et al., 1997). Uptake, transport, accumulation and excretion of nitrogen depend on individual conditions and mechanisms of the plants and can vary strongly from plant to plant (Wirén et al., 1997; Evans, 2001). The intake of nitrogen into the plants progresses via nitrate and ammonium.

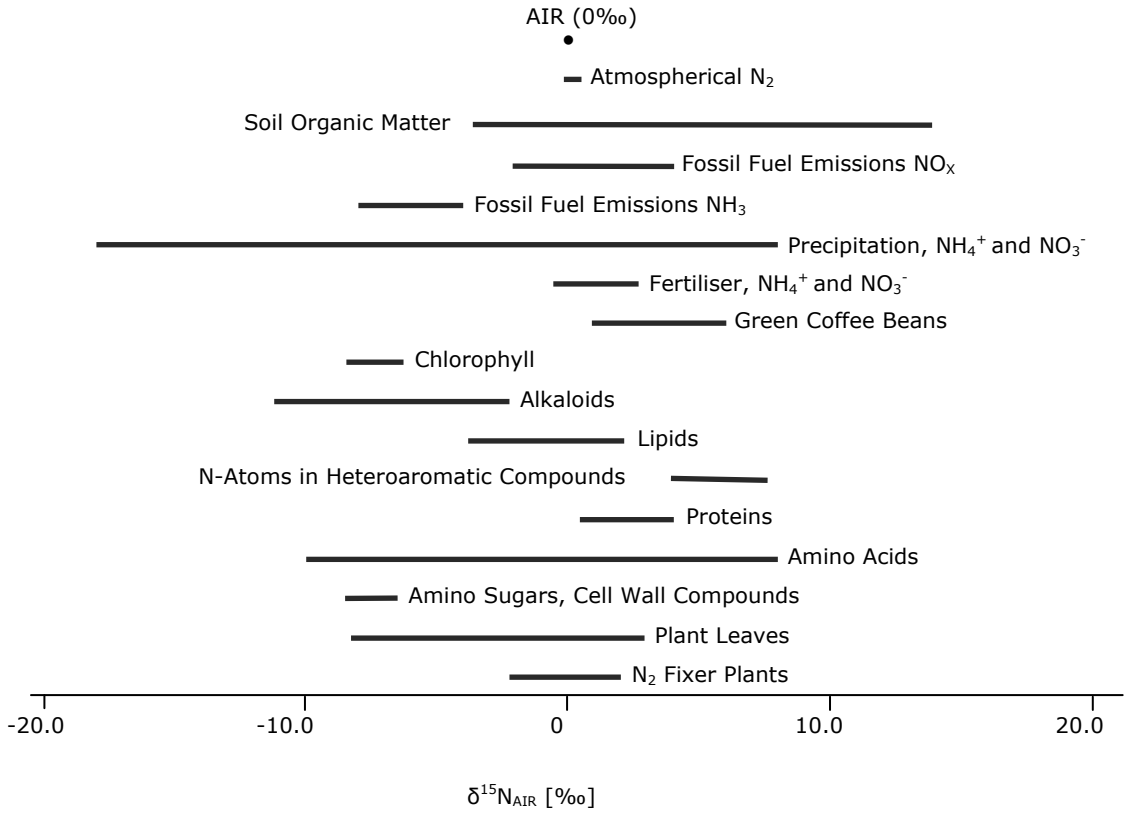

Figure 2-6: Overview of $\delta^{15}N_{AIR}$ values in nature of inorganic and organic nitrogen compounds with the expected fluctuation ranges (Peterson and Fry, 1987; Werner and Schmidt, 2002; Serra et al., 2005).

In vivo analyses of isotope fractionation during nitrate assimilation often measure the isotopic shift between the nitrate pool and the total bound nitrogen in organic biomass. For this uptake α-factors between 1.003 and 1.03 have been found (Handley and Raven, 1992; Fogel and Cifuentes, 1993). The observed *in vivo* isotope discrimination measurements are unfortunately often overlapped by kinetic isotope effects, so that finally the intake of nitrate by higher plants does proceed without notable nitrogen isotope discrimination (Yoneyama et al.,

1998 a; 2001). The found enrichment of ^{15}N in the biomass is mainly caused by the nitrogen isotope effect on the assimilatory nitrate reductase reaction. Nitrate is transported to the chloroplasts, where it is reduced by nitrate reductase and nitrite reductase into ammonia/ammonium; in C_4 plants this step probably only occurs in the mesophyll cells (Richter, 1996). The ammonia is converted as explained below into the α-amino group of glutamate. The large differences in the extent of the ^{15}N discrimination found is due to further influences, such as external nitrate concentration (Yoneyama, 1991), nitrate transfers between different compartments and different excretion of the non-reduced ^{15}N enriched nitrate, which corresponds to between 5 % and 80 % of the nitrate uptake (Medina and Schmidt, 1982; Handley and Raven, 1992; Yoneyama, 1995). This effect is similar to the CO_2 fixation in plants, where the CO_2 binding reactions overlap with the diffusion of CO_2 in and out of the plants stomata and therefore cause a variation of $\delta^{13}C$ values in organic plant material (see chapter 2.3.2).

Ammonium, on the other hand, is accumulated and transported by special carrier systems. The ammonia is rapidly distributed to different organelles and converted by the glutamine synthetase reaction and 2-oxoglutarate amino-transferase-(GOGAT)-reaction into the α-amino group of glutamates. The uptake of ammonium itself has a ^{15}N depletion of up to ~ -29 ‰ (Hoch et al., 1992; Yoneyama et al., 2001), depending on the external ammonium concentration. There is evidence of an isotope effect on the glutamine synthetase reaction, leading to a relative depletion of ^{15}N in the amide group.

Symbiotic mycorrhiza binds nitrogen from NO_3^- and NH_4^+ into organic forms, i.e. glutamine, and gives it to the plant in exchange for glutamic acid (Smith and Read, 1997). The nitrogen in the glutamine is ^{15}N enriched, as is the mycorrhiza itself, compared to soil nitrogen and plant nitrogen (Högberg et al., 1999; Hobbie et al., 1999 a; Kozhu et al., 2000; Tjepkema et al., 2000).

N_2 gas, which has been assimilated by symbiotic nitrogen fixating rhizobia, is either transported as ammonium into the plant (Tyerman et al., 1995) or in the form as alanine (Waters et al., 1998; Allaway et al., 2000). Isotope fractionation rarely occurs during any of these steps, nor during the immediate transformation to glutamine via the glutamate synthetase reaction (Evans et al., 1996; Yoneyama et al., 1998 a). This is confirmed through observations that the global ^{15}N values of biomass from N-assimilation belong to the lowest of all known $\delta^{15}N$ values. It has, however, been observed that nodules of symbiotic plants are enriched in ^{15}N towards the host plant, which can be explained by losses of NH_3 into the atmosphere.

Nearly all nitrogen, indifferent of its assimilation pathway, is found in its main organic form as glutamine, which is available, through transamination reactions, for other amino acids (Richter, 1996), and nitrogen compounds, i.e. heteroaromates (Yoneyama, 1995). From the compound glutamine onwards, nitrogen isotope fractionation occurs as in an enclosed system, except for losses of NH_3 into the atmosphere (Harper and Sharpe, 1998) or sometimes losses of organic N as root exudates (Jones at al., 1994). Kinetic isotope effects on enzyme catalysed reactions in the enclosed system occur during transaminations (Macko et al., 1986; Rishavy and Cleland, 2000), lyase reactions (Hermes et al., 1985; Kim and Raushel, 1986; Abell and O'Leary, 1988; Gani et al., 1999) and hydrolyse reactions (O'Leary et al., 1974; Medina et al., 1982; Parkin et al., 1991; Merkler et al., 1993). They lead to branching in the isotope values of the different product pools.

As mentioned earlier, the $\delta^{15}N_{AIR}$ values depend significantly on individual conditions of the plants so that isotope values are hard to compare. To try to 'normalise' $\delta^{15}N_{AIR}$ values of nitrogen containing compounds from different sources, their $\delta^{15}N_{AIR}$ values are correlated to the $\delta^{15}N_{AIR}$ value of the proteins from the same source, as these normally represent the largest nitrogen pool in plants. In the proteins themselves the amide-N is relatively enriched in ^{15}N compared to that of α-amino-N. Alkaloids on the other hand are relatively depleted in ^{15}N compared to the corresponding proteins (Gaebler et al., 1963). A further way to compare values is by correlating them with bulk $\delta^{15}N_{AIR}$ values, which are for the most part proteins. Studies with labelled nitrate sources have shown that amino acids, nucleotides, ureides and chlorophyll fractions are enriched in ^{15}N, whilst hexosamine and amide show depleted values of ^{15}N, compared to the bulk value (Gonzáles-Prieto et al., 1995). Relative to the bulk $\delta^{15}N$ value of the plant cell, compounds that receive N atoms directly from the amide-N of glutamine, i.e. amino acids and proteins, are generally ^{15}N enriched; secondary products such as chlorophyll, lipids, amino sugars and alkaloids are ^{15}N depleted (Macko et al., 1990; Kennicutt et al., 1992; Taylor et al., 1997; Schimmelmann et al., 1998). The branching points for these isotope discrimina-tions are between the glutamine and glutamate pools, with a probable kinetic nitrogen isotope effect on the GOGAT reaction combined with an unknown reaction, in which serine is involved.

Values for amino acids vary from $\delta^{15}N_{AIR}$ = -10 ‰ to 8 ‰ (Werner and Schmidt, 2002), with the ^{15}N enrichment showing the following pattern: aspartic acid/asparagine > glutamic acid/glutamine > threonine, proline, valine > glycine + alanine + serine, γ-aminobutyric acid and phenylalanine (Yoneyama and Tanaka, 1999). The high enrichment of asparagine and glutamine might derive

from their function as transport and storage metabolites, whilst the other amino acids are more depleted in ^{15}N, depending on their further functions in the plant metabolism. The relative ^{15}N depletion of serine and glycine in proteins of C_3 plants and their relative ^{15}N enrichment in C_4 plants may be due to the role they play in the respiratory nitrogen cycle. In conclusion, the nitrogen isotope ratios of amino acids differ due to their biosyntheses, turnover rates, metabolic functions and branching points in plant metabolism (Macko et al., 1987; Werner and Schmidt, 2002). But even strong branching points are found between amino acid precursors and their secondary metabolites, as in the case of nicotine and its precursor aspartic acid. Aspartic acid has a $\delta^{15}N$ value of 8.5 ‰ and donates its nitrogen atom to the pyridine ring of nicotine; this on the other hand has a $\delta^{15}N$ value of -5.2 ‰. It seems as if such secondary products are not immediately isotopically connected to the large pools of aspartic acid, but maybe they originate from an independent secondary metabolic pool, which is even in individual cells and their compartments (Jamin et al., 1997; Richards and Schuster, 1998).

2.5 Methods and Applications of Stable Isotope Analysis in Food Chemistry

2.5.1 Site-Specific Natural Isotope Fractionation – Nuclear Magnetic Resonance (SNIF – NMR®)

For both authenticity assessment of aroma compounds and state control of wine, deuterium nuclear magnetic resonance spectroscopy is an effective technique to detect adulterations. As with other non-symmetrical atoms, with an uneven number of protons and/or neutrons, the deuterium core has a spin and a magnetic moment which can be analysed, therefore, using nuclear magnetic resonance spectroscopy. In a magnetic field of 9.4 Tesla, the deuterium core provides a resonance frequency of 61,402 MHz, with the proton on the other hand showing a resonance frequency of 400 MHz. This fact can be used and the natural deuterium occurrence site-specifically analysed (Martin and Martin, 1981; Schmidt et al., 2007). However, as elegant as this technique is, it can only be used in special circumstances. As deuterium has only a relative natural abundance of 0.0145 atom-%, high amounts of substance, and/or long measurement times, are needed for substance analyses. With a minimal substance requirement of 500 mg a signal accumulation of 20 h is needed, although measurement time and substance amount can be lessened through stronger magnetic fields (Hanneguelle, 1991). Schmidt et al. (2005 a) considers 150 mg of substance and 10 h measurement time as state-of-the-art. For normal routine measurements, with manifold measurements of the same substance,

amounts of 1 g to 1.5 g are needed, whereas with other techniques, such as isotope ratio mass spectrometry, only a few mg are required. However, not only global isotope values are obtained, but also, with improved resolution, detailed information about the intra-molecular deuterium distribution of a molecule, i.e. the 'fingerprint' of the origin, and synthesis history of a compound (Schmidt et al., 2005 a), can be determined. A further problem with SNIF-NMR® is that only pure substances can be measured.

SNIF-NMR® spectra are evaluated by giving an internal standard (normally tetramethylurea, TMU) to the sample, with known deuterium content, and the received signals then evaluated in comparison to this standard. Although, there are certified standards, other standards can be equally used, after following validation by separate IRMS analyses. The resulting signals are single peaks with no further splitting, as the relative natural abundance of deuterium, at only 0.0145 atom-%, prevents, more or less, any two neighbouring C atoms in one molecule having two deuterium atoms (Schmidt et al., 2007). The assignment of the signals to various positions in the molecule is carried out by means of proton spectra, with the chemical shift being the same. Routinely SNIF-NMR® is used in state controls of wine, see chapter 2.5.3.2 (Schmidt et al., 2007).

2.5.2 Isotope Ratio Mass Spectrometry (IRMS)

Mass spectrometric methods are, by far, the most used analytical method for natural isotope abundance measurement, as the instruments can cover a large area of challenges. The sample to be measured must be converted, quantitatively and without isotope fractionation, with an elemental analytic decomposition method, into appropriate measurement gases. After ionisation, the isotopomeric gas molecules are separated, within the magnet field of a sector mass spectrometer, according to their mass/charge ratio and are detected in different Faraday collectors. The comparisons, to certified international standards, allow the determination of the isotope ratios of the sample (Schmidt et al., 2007).

Until a few years ago, it was only possible to measure larger amounts of sample, with elemental analysers, in the pyrolysis (EA-P-IRMS) and combustion (EA-C-IRMS) modes, and $^{13}C/^{12}C$- and $^{15}N/^{14}N$- isotope ratios, via coupling with gas chromatographs and special interfaces, in the combustion mode. In recent years, commercial pyrolysis systems have been able to determine the gas chromatographic of $^{18}O/^{16}O$ and $^{2}H/^{1}H$ isotope ratios. Aroma analyses of single compounds belong now to the established determinations in food chemistry

(Schmidt et al., 2007; Richling et al., 2007), especially the gas chromatographic determination of $^{13}C/^{12}C$ ratios, and, when the dynamic linearity range is considered, also $^{2}H/^{1}H$ isotope ratios. Even the state food-control organ has used this technique increasingly in recent years. The gas chromatographic analysis of $^{18}O/^{16}O$ isotope ratios is still complicated, due to the pyrolysis technique of converting the sample into CO, but it is still a helpful tool for making assured statements concerning the authenticity of an aroma component (Schmidt et al., 2005 a; Richling et al., 2007). The configuration of an IRMS system for isotope ratio measurement of aroma compounds, as used in our laboratory, is shown as follows (figure 2-7):

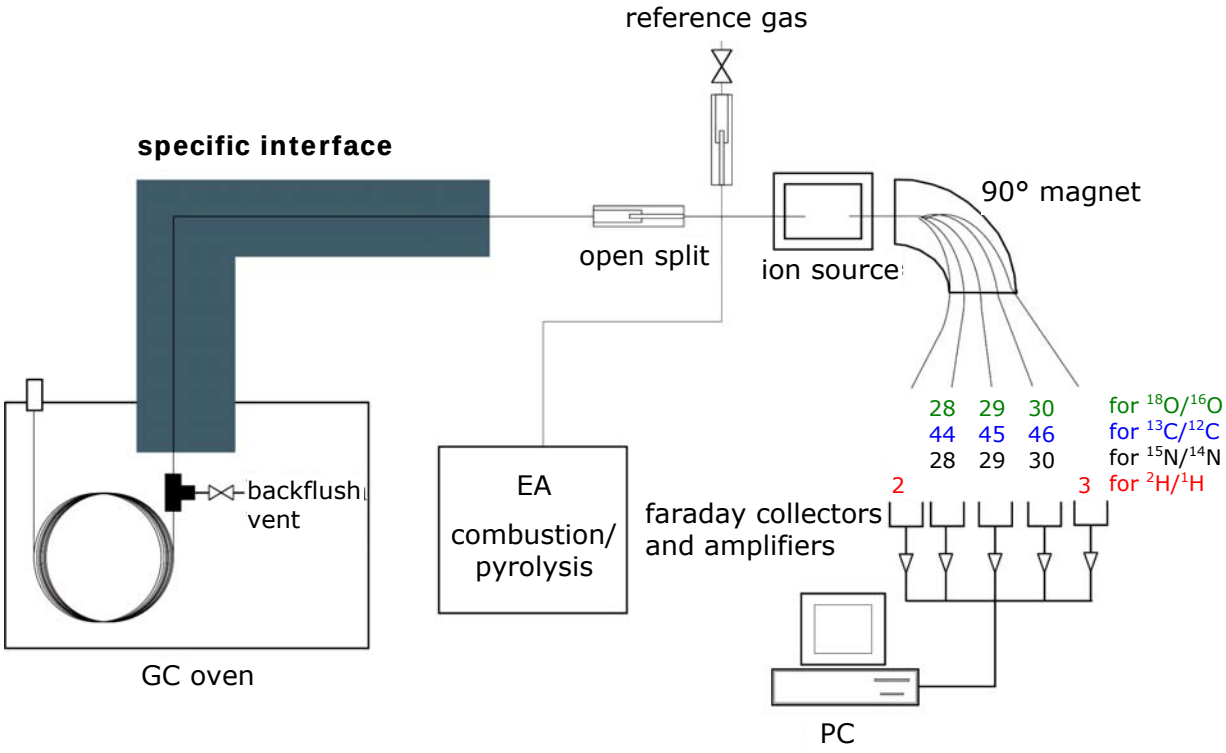

Figure 2-7: Schematic configuration of the EA/HRGC-C/P-IRMS system used in this work. The main components are a sector field mass spectrometer, an elemental analyser for both combustion and pyrolysis as well as a gas chromatograph with special interfaces for combustion and pyrolysis (chapter 2.5.2.2). For more detailed descriptions of the system see chapter 2.5.2 to 2.5.2.2.2.

2.5.2.1 Elemental Analyser – Isotope Ratio Mass Spectrometer (EA-IRMS)

When using the elemental analysers for isotope ratio determination, only pure substances in mg amounts can be analysed. The advantages are the use of international primary and secondary standards for the measurements, which are released by the IAEA in Vienna and the quick sample turnover. However, isotope ratio measurements of authentic aroma compounds, i.e. from fruit or plant extracts, are not suitable with this method because of the substance mixture and the small concentration of the analyte in the sample. Only elaborately isolated or commercially available pure substances can be analysed. If, however, bulk values of materials or non-volatile compounds are of interest, then the elemental analysers are indispensable. As there are no international standards for gas chromatographic analyses of single compounds, despite many research projects (Serra et al., 2007), elemental analysers are needed to calibrate tertiary standards, as 'working standards', for daily laboratory use. These standards are usually the pure form of the substances to be analysed, which are first measured via EA-C/P-IRMS with the IAEA standards. Then these working standards are analysed via GC-C/P-IRMS, and only when the δ values of elemental analysers and gas chromatograph are identical, with negligible deviations, is the isotope ratio determination of the analyte in the aroma extract, via the validated working standard, accepted (Ruff, 2001; Hör, 2001).

The used elemental analysers in this research project consisted of two machines, one each for pyrolysis and combustion, which were coupled, in parallel to the gas chromatograph via a needle valve, to the mass spectrometer. During the EA measurements the parallel coupled gas chromatograph was decoupled through an 'open split', and a helium 'backflush' used to eliminate measurement falsification by background noise.

2.5.2.1.1 Elemental Analyser – Combustion – Isotope Ratio Mass Spectrometry (EA–C–IRMS)

The elemental analytical isotope ratio measurement of carbon occurs in a quartz tube, which is filled with tungsten oxide, quartz wool and copper, then heated to 1000 °C. An oxygen pulse lasting a few seconds, the time being dependent on the amount of substance being analysed, oxidises some of the copper producing copper oxide. Tin capsules are filled with a few milligrams of sample and introduced into the system via an autosampler. After the introduction of the sample into the elemental analyser, the tin capsule is oxidised exothermally and instantaneously into tin oxide, which leads, together with the catalysers, to a

complete combustion of the carbon to $^{13}CO_2/^{12}CO_2$ (M_r = 44 and 45), but also of the other organic compounds into water, nitrogen and nitrogen oxides. A constant helium flow transfers the reaction gases over elemental copper to reduce nitrogen oxide (M_r (N_2O) = 44) into N_2, which then flows over a water separator. The water separator absorbs water, which is formed during combustion of the organic compounds, with help from an appropriate chemical, i.e. magnesium perchlorate. After passing over the water separator the reaction gases are transferred to a temperated Porapak® column, where they are separated and then conveyed to the isotope ratio mass spectrometer. At the beginning and in between a measurement series, a certified reference CO_2 gas, with a known isotope content and validated via IAEA standards, i.e. NBS 22, IAEA-CH-7, is introduced, which enables $\delta^{13}C_{V\text{-}PDB}$ values of the sample to be determined (see chapter 2.1) (Ruff, 2001).

The measurement of nitrogen isotope values is conducted in the same way, as above, with one small difference: after the combustion of the nitrogen in the sample into $^{28}N_2/^{29}N_2$ (M_r = 28 and 29), the reaction gases pass over the water separator, filled to two thirds with carbosorb®, which separates the CO_2 from the measurement gases. This step is essential, as CO_2 interferes with the N_2 measurement by partly forming CO gas (M_r (CO_2) = 28) in the mass spectrometer, which overlaps with the N_2 peak, and due to the large size of this CO peak, consequently falsifies the values. This can be seen as a double peak in the chromatogram. Otherwise, the gases pass, as with carbon, through the Porapak® column, where they are separated and then conveyed to the isotope ratio mass spectrometer. As with carbon, at the beginning and in between a measurement series, a reference N_2 gas, with a known isotope content and validated via IAEA standards, i.e. IAEA-N1, IAEA-N2, is introduced which enables $\delta^{15}N_{AIR}$ values of the sample to be determined (see chapter 2.1)(Ruff, 2001). As there is no commercially certified N_2 gas in amounts for routine measurements available, the mass spectrometer is calibrated against a reference certified N_2 gas with a defined $\delta^{15}N_{AIR}$ value. For routine measurement, laboratory N_2 gas is calibrated to IAEA-N-1 and IAEA-N-2 standards.

2.5.2.1.2 Elemental Analyser – Pyrolysis – Isotope Ratio Mass Spectrometry (EA–P–IRMS)

The elemental analytical isotope ratio measurement of hydrogen occurs in a quartz glass carbon tube filled with nickel wool, glass carbon slivers and nickel-coated carbon, then heated to 1440 °C. Silver capsules are filled with a few milligrams of sample and introduced into the system via an autosampler. In the

high temperature oven the pyrolysis products of the sample $^{2}H_2/^{3}H_2$ and $^{28}CO/^{30}CO$ (for oxygen measurement) are generated and, via a constant helium flow, the reaction gases are transferred over a water separator, where they are dried with magnesium perchlorate, and CO_2 is absorbed via carbosorb®. Subsequently, the gases are transferred to a temperated molecular sieve column, where they are separated and then conveyed to the isotope ratio mass spectrometer. Analogous to the measurements of carbon and nitrogen, at the beginning and in between a measurement series, a certified reference H_2 gas with a known isotope content and validated via IAEA standards, i.e. V-SMOW, IAEA-CH-7, is introduced, which enables $\delta^{13}C_{V\text{-}PDB}$ values of the sample to be determined (see chapter 2.1).

For the isotope ratio measurement of H_2 further criteria must be considered to ensure the accuracy of the measurements. First of all, after calibration of the mass spectrometer, but before the beginning of a measurement series and dependent on the amount of water in the ion source of the mass spectrometer, the so-called *H_3*-factor has to be determined. The necessity for this correction factor results from the fact that, during the hydrogen isotope ratio measurements, linearity problems arise through ion molecule reactions in the ionisation volume. In the ion source of the mass spectrometer during the (incomplete) ionisation of H_2 gas, not only the wanted HH^+ (m/z = 2) and HD^+ (m/z = 3) ions occur, but also the electron deficient compound H_3^+ (equations 2-6 and 2-7), which also being detected in the collector with the m/z = 3, consequently, simulates a higher deuterium content.

(2-6) $H_2 + e^- \rightarrow H_2^+ + 2e^-$

(2-7) $H_2^+ + H_2 \rightarrow H_3^+ + H\bullet$

The formation tendency of the H_3^+ ion is dependent both on the partial pressure and the concentration of the hydrogen gas in the ion source. Whilst the concentration of the di-atomic ions (H_2^+, HD^+, D_2^+) grows linearly with the partial pressure of the gas in the ion source, the concentration of the tri-atomic ions (H_3^+, H_2D^+, HD_2^+, D_3^+) grows by the square of the pressure and, therefore, by the square of the quantity of H_2^+ ions (Schmidt, 1974; Habfast, 1997). This occurs via the ratios of the ion currents (*i*), which are measured as m/z = 2 and 3 at different partial pressures, and is determined by the equation (2-8) below (Habfast, 1997):

(2-8) $$\frac{i(3)}{i(2)} = \frac{HD^+ + H_3^+}{H_2^+} = \frac{HD^+}{H_2^+} + \frac{k[H_2^+]}{H_2^+} \rightarrow \frac{HD^+}{H_2^+} = \frac{i(3)}{i(2)} + ki(2)$$

The momentary H_3 factor (k) has to be known for each measurement of deuterium. The determination of the factor occurs through the measurement of D/H ratios in H_2 gas pulses of differing intensity (Hilkert et al., 1999). The variation of the H_2 gas pulses into the ion source of the mass spectrometer is controlled via a needle valve.

The importance of the linear measurement area for the determination of D/H ratios is discussed in chapter 2.5.2.2.2, as this is especially important for the gas chromatographic determination of D/H ratios.

2.5.2.2 Gas Chromatography – Isotope Ratio Mass Spectrometry (GC-IRMS)

For HRGC-IRMS measurements a commercially available gas chromatograph is used, which has a suitably attached interface appliance, for the conversion of the analyte into the corresponding measurement gases. Samples of aroma extracts, or (diluted) reference solutions, are always introduced in the 'splitless' mode onto the capillary column, via the autosampler, to ensure the quantity of substance is sufficient for isotope ratio measurements. The used capillary columns have a length of 60 m, to compensate for the loss of separation, through uncoated transfer capillaries, during the transfer of the measurement gases into the mass spectrometer. Temperature programs can be adjusted for each separation problem, whilst preserving the usual quality control features.

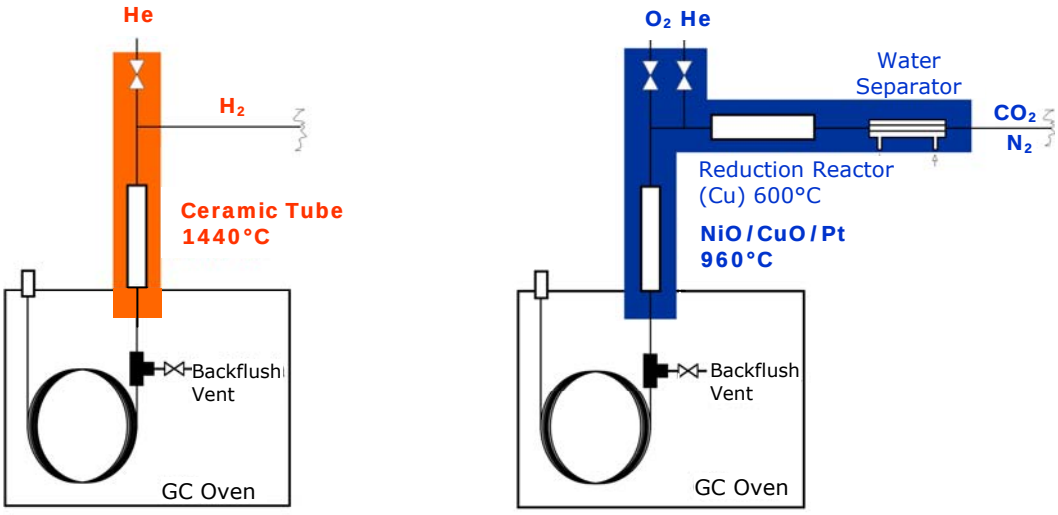

Figure 2-8: Schematic setup of the interface types used in this project for HRGC-C/P-IRMS analytics.

In particular, the quantitative integration of peak areas is important as significant isotope discrimination can occur during the gas chromatographic separation of analytes (Barrie et al., 1984; Shepard et al., 1976; Matthews and Hayes, 1978). Figure 2-8 shows the schematic setup of the used combustion and pyrolysis interfaces.

2.5.2.2.1 Gas Chromatography – Combustion – Isotope Ratio Mass Spectrometry (GC – C – IRMS)

The gas chromatographic isotope ratio measurement of carbon is conducted with the aid of a combustion interface, which oxidises the eluating molecules of the capillary column into CO_2. The transfer from the capillary column into this combustion oven is realised via a T-fitting with a flow splitter ('backflush' valve), which allows a selective transfer of chosen substances, by turning a constant helium flow on or off, at specific times. The construction of the combustion interface corresponds to that of the elemental analyser but is slightly different as it has to cope with the smaller substance quantity. This combustion oven consists of a heating element which holds a thin ceramic tube (Al_2O_3, length = 320 mm, 0.5 mm i.d., 1.5 mm o.d.) with three small wires consisting of copper, nickel and platinum, respectively. By floating the combustion oven with oxygen at 960 °C at constant intervals, normally once a day, the metals are partially oxidised and in this form are the real catalysator for the quantitative combustion of the eluents. The need for reoxidation is influenced by the number of samples and/or the sample application and is shown by the incomplete oxidation of the eluents (seen by significantly changed $\delta^{13}C_{V\text{-}PDB}$ values and $\delta^{15}N_{AIR}$ values of the working standards). After this oxidation reactor the measurement gases flow through a reduction oven to reduce nitrogen oxides to nitrogen. The construction is similar to the combustion oven, but with only 620 °C and a ceramic tube with three thin copper wires integrated. The reduction oven eliminates, furthermore, formed oxygen and extends the life-span of the ion source. Combustion water is eventually removed via a Nafion® membrane (perfluorated ion exchanger), which is flushed with helium gas. The cleaned measurement gases are transferred on-line via an 'open-split' into the mass spectrometer. Reference gas pulses, as described in chapter 2.5.2.1.1, allow the determination of the $\delta^{13}C_{V\text{-}PDB}$ and $\delta^{15}N_{AIR}$ values of the analytes. Carbon and nitrogen measurements differ only in two areas: the reoxidation time is far shorter for ^{15}N measurements to reduce the quantity of nitrogen oxides and carbon dioxide is removed by freezing in a transfer capillary using liquid nitrogen.

2.5.2.2.2 Gas Chromatography – Pyrolysis – Isotope Ratio Mass Spectrometry (GC – P – IRMS)

The gas chromatographic isotope ratio measurement of hydrogen is conducted with the help of a pyrolysis interface, which converts the analytes into hydrogen gas. The transfer from the capillary column to the pyrolysis reactor is realised, analogous to gas chromatographic carbon measurements, via a T-fitting with a flow splitter ('backflush' valve). The construction of the pyrolysis interface consists of a heating element, which holds a thin ceramic tube (Al_2O_3, length = 320 mm, 0.5 mm i.d., 1.5 mm o.d.) without any additional catalysator. At a temperature of 1440 °C organically bound hydrogen in the analyte is converted quantitatively into hydrogen gas (Burgoyne and Hayes, 1998; Hilkert et al., 1999). The reaction gas is not cleaned further, in contrast to carbon and nitrogen measurements. A control of the pyrolysis quality can be conducted by detection of methyl fragments with a m/z = 15. The obtained measurement gas is transferred to the mass spectrometer via an 'open split' connection. Reference gas pulses, as described in chapter 2.5.2.1.1, allow the determination of the $\delta^2H_{V\text{-}SMOW}$ values of the analytes.

A further criterion for the determination of D/H ratios after the H_3^+ factor (see chapter 2.5.2.1.2) is the linear measurement range of organic substances, especially for gas chromatographic measurements (Hör, 2001). This can be different for each compound, because the various quantities of hydrogen atoms in the molecule result in different numbers of hydrogen molecules after pyrolysis. Research work by Burgoyne and Hayes (1998) indicates that the time in the reactor plays a role: the authors showed that the hydrogen pyrolysis produced quantitative results when the temperature was between 1430 °C and 1460 °C without catalyst, and the eluent was longer than 300 ms in the reactor. In practice this means that working standards and reference standards of the analyte are analysed in different concentrations over the complete measurement range via HRGC-P-IRMS. The determined $\delta^2H_{V\text{-}SMOW}$ values are compared to those of EA-P-IRMS, where such dynamic measurement ranges are far less pronounced or even non-existent. In the linear measurement range the $\delta^2H_{V\text{-}SMOW}$ values of the standards, measured via GC-P-IRMS, correspond to those measured by EA-P-IRMS.

2.5.3 Application of Stable Isotope Analysis

In food chemistry IRMS and SNIF-NMR® are a part of the analytical methods that can be used, but their application is limited to only a few fields, which are

illustrated in the next sections. As it can be seen analytical fields cover questions for which there are either no answers or no answers provided by classical analytics. Examples are particularly found in fruit juice, sugar and wine analytics, where the consumer should to be kept from additives in food and/or stretched foodstuffs, and in the multi-element isotope analysis for origin assessment of wine, meat, cheese and butter (see chapter 2.5.3.2). A further large usage is the authenticity assessment of aroma compounds, explained in chapter 2.5.3.1. Current research is inspecting the strength of statements concerning food chains and the linked feeding types of livestock and the differentiation possibilities of conventional-to-organic products (recommendation of the AG Isotopes, 2007).

2.5.3.1 Authenticity Assessment of Aroma Compounds

The use of aroma compounds for producing foodstuff is clearly defined by German and European regulations. In the EWG directive, 88/388/EWG, the use of aroma compounds is controlled, with regulation (EC) 2232/96 defining the building of a European index for aroma compounds, which is up and running and will be later applied to food. The present state of this 'positive list' is included in the commission's aroma compound index E 1999/217/EWG and will have approx. 2000 substances, when activated. Independent of this, the German aroma regulation, BGBl. I S.1127 dated 15.05.2006, defines the market ability and labelling of commercial aroma products. Appendix 1 of the aroma regulation lists the definition for aroma and differentiates between 'natural', 'nature-identical' and 'synthetic' aroma compounds. It is clearly regulated as to which aroma is allowed to be named 'natural' and which not. Following on from this regulation, only those aroma compounds or aroma extracts are permitted to be called 'natural', which have been gained via appropriate physical processes, such as distillation and extraction, or through enzymatic or microbial processes from educts of plant or animal origin. 'Nature-identical' aroma compounds, on the other hand, are aroma compounds which are produced chemically, but are also found in nature, with the same molecular structure. Here, therefore, lies the potential for adulteration, as the structure of the compound is the same, but the price difference between 'natural' and 'nature-identical' can vary by the order of 1000 % (Serra et al., 2005). 'Synthetic' aroma compounds have no natural role model in nature and are produced only by synthetic means. At present the aroma regulation lists 17 'synthetic' aroma substances, which are permitted for use in certain product groups.

A classical method for differentiating between 'natural' and 'nature-identical' aroma compounds is by the determination of *ee* values (*enantiomeric excess*) of

chiral compounds. This technique utilises the fact that, in a biological system, normally one enantiomer is favoured, or even exclusively formed, during biosynthesis. The surplus of a specific enantiomer, also named ee value, is known today for many plants, with the natural abundance serving as a criterion for authenticity assessment. Chemically produced compounds, on the other hand, show a racematic distribution of enantiomers (Mosandl, 2004). This type of authenticity assessment is, unfortunately, limited to chiral compounds, which are only one small group of the total aroma compounds, but enantioselective synthesis methods and/or selective purification steps can impair the full potential of this method. Since the beginning of the 1990's GC-C-IRMS has been more frequently used for authenticity assessment, but this technique can only be used for certain compounds, as the $\delta^{13}C_{V\text{-}PDB}$ values of 'natural' aroma compounds normally only show the isotope signature of C_3 plants. These C_3 values often coincide with those of 'synthetic' molecules, so that this method is used for the authenticity assessment of C_4 aroma compounds (Ruff, 2001). The use of genuine internal isotope standards, as well as intermolecular isotope correlations, for $\delta^{13}C$ 'finger printing' of essential oils can make full use of this single element method in the future (Braunsdorf et al., 1993; Mosandl et al., 1994; Mosandl, 1995).

The commercial availability of systems, with the ability to determine $\delta^{18}O_{V\text{-}SMOW}$ and $\delta^{2}H_{V\text{-}SMOW}$ values at the end of the 1990's (Werner et al., 1996; Hener et al., 1998; Hilkert et al., 1999), opened up the possibility for multi-element isotope ratio analyses. Until now vast empirical data banks have been built up to answer authenticity questions. The possibility for discriminating between 'naturally' and 'synthetically', and sometimes 'biotechnologically' produced aroma compounds, is made easier through the fact that isotope values of single compounds are dependent on their origin, i.e. petrochemical or natural origin (see figure 2-2, 2-4 and 2-6), and eventually on the preparation procedure. For data acquisition, a large number of authentic reference samples are needed, to be able to make assured statements when analysing single compounds. Because of their continued importance even today 'key compounds' are continually being re-analysed, such as vanillin (Kaunzinger et al., 1997; Hör, 2001; Scharrer and Mosandl, 2002), benzaldehyde (Culp and Noakes, 1990; Ruff et al., 2000), linalool and linalyl acetate (Hör et al., 2001 a; Jung et al., 2005), citral (Hör et al., 2001 b; Bilke and Mosandl, 2002; Nhu-Trang et al., 2006), α- and β-ionone (Sewenig et al., 2005; Mar Caja, 2007), γ- and δ-decalactone (Tamura et al., 2005), cinnamon aldehyde (Culp and Noakes, 1990; Sewenig et al. 2003), cinnamic acid and derivates (Fink et al., 2004; Schmidt et al., 2007), aliphatic and fruit ester (Preston et al., 2003 and 2004; Kahle et al., 2005; Schmidt et al., 2007), C_6 alkenales and alkenoles (Bréas et al., 1994; Hör et al., 2001 a; Elss et

al., 2006), anthranilates and derivatives (Faulhaber et al., 1997) and alkylpyrazines (Richling et al., 2005).

2.5.3.2 Further Applications

Nowadays, in food chemistry analytics, techniques and methods for stable isotope ratio determination occupy a fixed place, concentrating mostly on a few applications. Besides the authenticity assessment of aroma compounds, stable isotope analyses are used especially where adulteration of food by illegal addition of endogenically existing components is a possibility, or where statements concerning the origin of foodstuffs are needed. In wine analytics the site-specific deuterium content of the methyl group of the fermentatively won ethanol (D/H_1 value) is determined via SNIF-NMR®. This is correlated to the fermented sugar and allows a determination of non-allowed sugaring of the wine (Bauer-Christoph et al., 1997). A control on the addition of water in wine is obtained by the determination of the $\delta^{18}O$ content of the water after equilibration with CO_2; this can also be used together with the data from the European wine data base (regulation (EG) 2729/2000; Joint Research Centre, Ispra) or the third country data base (BfR, Berlin) for origin determination (see chapter 2.2.1) (Schmidt et al., 2005 a).

In fruit juice analytics, the proof of an illegal addition of citric acid is determined by the $\delta^2H_{V\text{-}SMOW}$ value of calcium citrate, as citric acid from fruit has higher deuterium values than that from biotechnological sugar fermentation (Jamin et al., 2005). The proof of sugaring can also be performed on ethanol after fermentation of the sugar. Honey authenticity assessment is performed by comparison of the $\delta^{13}C_{V\text{-}PDB}$ values of the sample and proteins therein, and can indicate adulteration with C_3 sugars, as the difference is not permitted to be greater than 1 % (Schmidt et al., 2005 a). Even more exact results are performed via HPLC-IRMS, through the correlation of the $\delta^{13}C_{V\text{-}PDB}$ values of the single sugars (Cabañero et al., 2006). In maple syrup the malic acid is precipitated quantitatively as Pb-salt and used as an intrinsic $\delta^{13}C$ standard to define illegal sugaring (Tremblay and Paquin, 2007). A differentiation of natural and synthetic caffeine is possible via EA-P-IRMS using the $\delta^{18}O$ value (Richling et al., 2003).

A further large scope for stable isotope application is the determination of the geographic origin, often only with the combination of multi-element isotope data, and sometimes paired with further chemical parameters and statistical methods, for an assured classification. In cheese, for instance, the determination of $\delta^{13}C$,

$\delta^{15}N$ and $\delta^{34}S$ of casein paired with the $\delta^{13}C$ and $\delta^{18}O$ values of glycerine leads to the differentiation between French, Italian and Spanish cheese types (Camin et al., 2004). Further origin assessments with $\delta^{15}N$ values are possible for milk and wine (Kornexl et al., 1997) as well as caffeine (Danho et al., 1992; Richling et al., 2003). Analyses for the differentiation between organically and conventionally produced products exist but, unfortunately, without any clear statements (Schmidt et al., 2005 b; Georgi et al., 2005). With eggs, $\delta^{13}C$ values smaller than -24 ‰ and $\delta^{15}N$ values larger than 10 ‰ are an indication, if not a proof, of free-range eggs (Schmidt et al., 2005 a).

2.6 Coffee and Coffee Aroma

2.6.1 History and Importance of Coffee

Coffee is one of the most loved and consumed beverages in the world. Its fascination can be explained by its sensual roasting aroma combined with the dry and bitter taste to the tongue. Nowadays, coffee-drinking is an established custom in many cultures. This explains the success the coffee plant has experienced throughout the world. One of the many legends as to how coffee was discovered tells how nomads noticed that their goats and camels were livelier after eating red berries from a certain bush. In Ethiopia these fruits were crushed, together with fat, and eaten as balls. These 'energy balls' were used by the nomads for keeping awake during long walking periods and whilst tending their animals. Around 1000 A.D. a brew made from green coffee beans was tried and named *qahwa*, meaning brewed drink from plants. Slave traders transported the coffee from Ethiopia to Arabia in the 14th century, but it was not until the 15th century that the green coffee beans were roasted prior to brewing as a coffee drink. Arabia grew to be a monopolist in coffee cultivating and their most important trading post was the port of Mocha, also named Mokka, in Yemen. The popularity of coffee increased during the Ottoman Empire and soon the first cafés opened in Constantinople, albeit against opposition from religious groups. For two centuries the Yemenis held the monopoly on coffee by ensuring that the seeds were roasted or steamed before exporting. But from the 17th century onwards, the Arabs lost their coffee monopoly to the Dutch, who commenced exporting coffee plants to their colonies - first Ceylon, then Java and Surinam and finally to Cayenne in Middle America, from where it was exported to Brazil, consequently starting a worldwide cultivation of coffee (Flament, 2002).

Today coffee is one of the most important trading products, after oil, with the value of exports exceeding US$ 12.3 billion. In the crop year 2006/07, the world

production of coffee reached 125 million bags (1 bag = 60 kg), with Brazil's 43 million bags making it the world's largest producer. Further large coffee producing countries are Vietnam, Columbia, Indonesia, Ivory Coast, Mexico and India. The world production of coffee has stagnated in recent years, just exceeding demand except in years of significant crop losses, such as those in Brazil in the years 1995/96 and 1999, when frost and drought led to production drops and, subsequently, higher coffee prices (Rehm et al., 1996).

2.6.2 Botanic and Production Types

The coffee plant *Coffea* belongs to the family *Rubiaceae* and consists of 70 different *Coffea* types. Only two of these, *Coffea arabica* and *Coffea robusta*, have relevance for the market, with ca. 65 % and 35 % of the world production, respectively. A further type, which only plays a regional role, is *Coffea liberica*, with ca. 1 % of the market (Belitz et al., 2001). Coffee needs certain conditions for growing, with *Coffea robusta* being more robust than *Coffea arabica*. The plants are not frost resistant and prefer altitudes of 600m – 1200m in the tropics and subtropics between the 23 latitude above and the 25 latitude below the equator. The 'coffee berries', which are used for coffee making, are cherry-type stone fruits each with two seeds, i.e. the 'coffee beans'. These are flattened on the insides and consist of an endocarp, with the embryo in the inside of the endosperm. Around this bean the so-called 'silverskin', or episperm, is found. If only one bean exists in a coffee cherry, then it generally has a round form. In plantations the coffee plants are maintained to bush height to simplify harvesting, although the plants can reach heights of 3 to 8 m. The coffee plants build cherries from the 3rd year onwards and can continue producing for ca. 30 years. These cherries need 8 to 12 months to ripen to a dark red colour before being harvested, either manually, or using stripping machines.

Two main procedures are used for further processing the coffee fruits - the 'dry process' and the 'wet process'. In the so called 'dry process', which is particularly popular in Brazil for robusta type coffees, the coffee cherries are dried in the sun, immediately after harvesting. Afterwards, the dried husks are removed by husking, to reveal only the bean with its silverskin. After this process the coffee beans are sorted unwashed and packed into sacks. The 'wet process' is a far more complex and expensive method being normally reserved for high-quality coffee, i.e. arabica. The harvested fruits are washed, and the fruit flesh is separated from the beans by pulping, without damaging the coffee beans. The beans and fruit flesh, which still adheres to the beans, are placed in tubs for 1 to 3 days, where they are flushed with water, following which a fermentation occurs

of microorganisms and coffee-own enzymes with pektinolytic activities, resulting in the rest of the fruit flesh being loosened sufficiently to allow it to be washed away. After this step the beans are either sun-dried or air-dried at 65 °C to 85 °C. This 'parchment coffee' still has its parchment, which is removed by hulling. Top-quality coffee is then polished to remove the silverskin and smooth the surface. The obtained raw coffee is submitted to size grading and sorting, packed into sacks and shipped to the roasteries (Rehm and Epsig, 1996; Belitz et al., 2001).

The roasteries, with different roasting methods, are found mainly in the importing countries. The direct contact roasting method is almost obsolete these days, as roasting times take up to half an hour, but can still be found in small coffee shops which have their own roasteries. With maximum roasting times of 15 minutes, a combined contact-convection roasting method is far more practicable. Modern short-time roasting procedures shorten the roasting time to 2 - 5 minutes. After roasting, the coffee beans are packed, either as ground or as whole beans, in an air-free environment and stored cool.

2.6.3 Composition of Green Coffee Beans

The composition of green coffee beans is not very easily determined as a wide variability is to be expected depending on age, origin, type and treatment of the coffee beans. Even though analytical methods were earlier imprecise, Wolfrom in 1960 and Navellier in 1961 gave a mean composition of green coffee as follows: glucides (58 %), lignine (2 %), lipids (13 %), proteins (13 %), ash (4 %), non-volatile acids (8 %), trigonelline (1 %) and caffeine (1 %). Since then many further studies have been performed to determine the composition of green coffee beans (Derbesy et al., 1969; Roffi et al., 1973; Clifford, 1975 a and b; Clifford and Kazi, 1987; Guyot et al., 1988 a; De Maria et al., 1995, 1996 b; Martin et al., 1998). Smith (1963 a) and Feldman et al. (1969) first showed the importance of the non-volatile compounds for coffee flavouring, noticing a decrease in the content of proteins, chlorogenic acid and sucrose on roasting. Russwurm (1970) postulated that, additional to the above mentioned precursors, also carbohydrates, free amino acids, polyamines and tryptamines, lipids, phenolic acids, trigonelline and various acids play a role in flavour formation. Soon afterwards Merrit et al. (1970) showed a relationship between volatile compounds and their precursors in the green coffee bean. Since then much research has centred on the relationship between single aroma compounds and their precursors, the effect of roasting and the contribution of single non-volatile

compounds to certain volatile substances (Baltes 1976, 1979; Clifford and Kazi, 1987; De Maria et al., 1995, 1996 b and references within all mentioned).

The green bean composition is, as in all plants, complex and not easily describable in detail. Four important groups of compounds associated with coffee beans are (1) nitrogenous components, (2) carbohydrates, (3) lipids and (4) chlorogenic acids, and are described in following. A compilation of the constituents of green coffee and their changes during roasting is summarised in table 2-3.

Table 2-3: Content of constituents in green coffee beans (after Wolfrom et al., 1960; Clifford, 1985 b; Souci, 2000; Fischer et al., 2000).

Compound		Content in Green Coffee Bean
water		6 % - 10 %
carbohydrates	polysaccharides (PS)	50 % - 60 %
	• mannan, galactomannan	• 50 % of polysaccharides
	• arabinogalactan	• 22 % of polysaccharides
	• cellulose	• 20 % of polysaccharides
	sucrose	6 % - 8 %
lipids	total	10 % - 17 %
	• triglycerides	• 75 % of lipids
	• free fatty acids	• 0.5 % to 1.9 % of lipids
	• diterpenes	• 20 % of lipids
	• sterols	• 2 % of lipids
	• tryptamides	• 0.2 %-0.3 % of lipids
protein	polyamides	10 % - 14 %
	free amino acids	0.1 % - 1 %
caffeine		1 % - 2.5 %
trigonelline		0.8 % - 3.0 %
volatiles		>300 compounds

(1) One of the well known nitrogenous components, and recognised as being responsible for the stimulating effect, is caffeine, a purine ring system, which was first isolated by Friedlieb Runge, in 1820, from green coffee. Other caffeine metabolites, such as theophylline, theobromine, paraxanthine, theacrine, libertine and methylliberine, have been found in small quantities (Kappeler and Baumann, 1986), although theacrine and methylliberine have not been detected in arabica. The caffeine content in green coffee varies between 1 % - 2.5 % of

dry matter and is slightly lower in arabica than in robusta (Roffi et al., 1973; Clifford and Kazi, 1987). The loss of caffeine during roasting is moderate being only a few percent, but when the weight loss of the beans is also taken into account, the relative content of caffeine can actually increase by up to 10 % (Macrae, 1985). The stability of the purine ring, following heat treatment, is underlined by the fact that only a few pyrimidines or imidazoles have been found in roasted coffee volatiles. The determination of the geographic origin of coffee, using isotope ratios $^{15}N/^{14}N$, $^{13}C/^{12}C$ and $^{2}H/^{1}H$ in samples of caffeine extracted from green arabicas and robustas from 16 countries, has already been tried by Prodolliet et al. (1998), but without success. Richling et al. (2003) were successful, however, in differentiating between caffeine from different plant types, i.e. guarana and coffee, as well as synthetic origins using the isotope ratios $^{15}N/^{14}N$, $^{13}C/^{12}C$ and $^{2}H/^{1}H$ and were thus able to determine the caffeine origin in food products.

A further nitrogenous compound, which was first isolated from green coffee by Polstorff in 1909, is trigonelline (pyridinium, 3-carboxy-1-methyl-), belonging to the betaines. This nicotinate derivate amounts to 0.8 % - 3.0 % in green coffee (Hughes and Smith, 1946; Mazzafera, 1991) but decreases strongly during roasting to 0.25 % - 0.63 %. This decomposition leads to nicotinic acid, methyl nicotinate, pyridines and pyrroles. As pyridine is a characteristic of highly roasted coffees, with its stringent and slightly pungent odour, a mechanism of pyridine formation from trigonelline, under coffee roasting conditions, via a decarboxylation over 1-methylpyridinium hydroxide leading to pyridine, has been proposed by Rizzi and Sanders (1996). The non-decarboxylative mechanism leads to the ester methyl nicotinate by a methyl migration and, subsequently, to nicotinic acid, see figure 2-9. Trigonelline cannot be the only contributor to pyridine formation, concludes De Maria et al. (1996 a), but protein pyrolysis, reactions of glucose and amino acids and the reaction of ammonia on 2,4-pentadienal have been shown to produce pyridine (Kato et al., 1973; Baltes and Bochmann, 1987 d; Mottram, 1991).

For determining the degree of roast, the ratios of trigonelline content to caffeine content have been proposed (Nakabayashi and Masano, 1986), in which this ratio decreases from 0.86 in green beans to 0.15 for dark roasts. Furthermore, Stennert and Maier (1996) have, alternatively, proposed a trigonelline/nicotinic acid ratio.

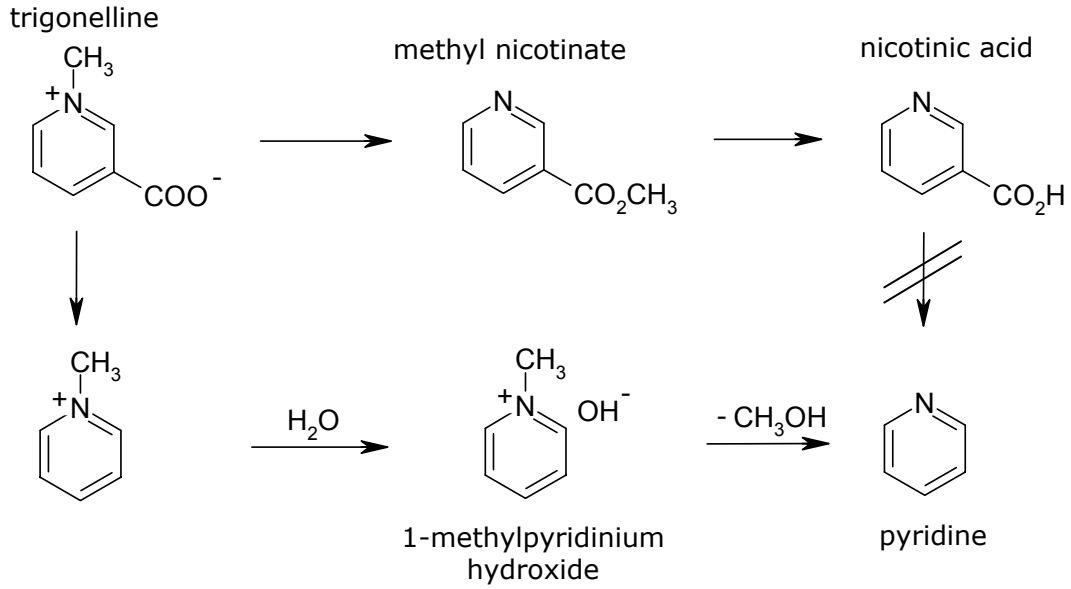

Figure 2-9: Formation mechanism of pyridine from trigonelline as proposed by Rizzi and Sanders (1996).

Proteins and free amino acids were not analysed extensively in the past, as the methods were too difficult and complex with most of the proteins having molecular weights above 150000 Dalton. The protein content in green coffee is approx. 10 % in both arabica and robusta. The major amino acid constituents of the proteins are glutamic acid (19 % of total protein), aspartic acid (10 %) and leucine (9 %) (Feldman et al., 1969; Roffi et al., 1973). The albumin, a water-soluble protein, has a similar amino acid composition to that of the insoluble protein (Thaler and Gaigl, 1962). Similarities have been found between the total amino acid content in proteins of both arabica and robusta coffees, with differences, on the other hand, found in the content of alanine, phenylalanine and tryptophan (Macdonald and Macrae, 1986). Although the free amino acid content in green coffee varies only between 0.1 % and 1 %, it probably contributes significantly to the final flavour of roasted coffee (Walter et al., 1970; Maier, 1981; Tressl et al., 1983; Macdonald and Macrae, 1986). The quantity of free amino acids is higher in robusta than in arabica. This free amino acid content decreases strongly during roasting, leaving only traces in the final roasted bean. Many different quantities of single free amino acids have been analysed (Tressl et al., 1983; Arnold et al., 1994; Arnold and Ludwig, 1996), with the investigations often concentrating on the differences between arabica and robusta (Tressl et al., 1983; Macdonald and Macrae, 1986) and changes in ripening processes (Guyot et al., 1988 a), post-harvest treatments (Arnold and Ludwig, 1996), decaffeination (Tressl, 1981) and steam-treatment (Steinhart and Luger, 1995). The main components of the free amino acids are glutamic acid, aspartic acid, asparagine and glutamine, proline, alanine, arginine and

serine. The differences between arabica and robusta are slight, but robusta does produce higher quantities of minor amino acids (Arnold et al., 1994). The role that certain amino acids play in volatile aroma compound formation is described later in chapter 2.6.4 and 2.7.2.

(2) Carbohydrates are the second main group in the green coffee bean and are split into polysaccharides and lower molecular sugars. The polysaccharides represent 50 % to 60 % of dry matter in the beans, consisting of mannans, arabinogalactans and cellulose (Wolfrom et al., 1960, 1961, Wolfrom and Patin, 1964, 1965; De Maria et al., 1996 a), with further constituents of the polysaccharides being glucoglactomannans, xylans, pectins and glucans (Oosterveld et al., 2003). As to whether the content and properties of polysaccharides differ between arabica and robusta has not been established sufficiently (Thaler, 1976; Clifford, 1985 b; Fischer et al., 2001). For arabica coffee beans 50 % of the polysaccharides consist of mannan and galactomannan, 22 % of arabinogalactan and 20 % of cellulose (Fischer et al., 2000). The analysis of these polysaccharides is not easy, with the extraction being mostly non-quantitative and the different types of polysaccharides being hard to separate from one another. Polysaccharides are lost in part by roasting via condensation with proteins, protein fragments and chlorogenic acids.

Of the lower molecular saccharides, sucrose is the most abundant sugar with a content of 6 % - 7 % in green coffee and only traces after roasting (Wolfrom et al., 1960). A higher quantity of sucrose was found in arabica compared to robusta (Trugo and Macrae, 1983; Tressl et al., 1983) with maturity of the beans leading to rising levels of sucrose (Guyot et al., 1988 a).

(3) The lipid fraction extracted by a non-polar solvent consists of triglycerides of fatty acids (75 %), free fatty acids (0.5 % - 1.9 %), diterpenes (20 %), sterols (2 %), and 5-hydroxytryptamine amides from the wax coating of the bean (0.2 % - 0.3 %) and may include non-lipid substances such as caffeine (Clifford 1985 b; Folstar 1985; Kaufmann and Hamsagar 1962; Carisano and Gariboldi 1964). The main fatty acids in the triglycerides are linoleic acid (30 % - 47 %), palmitic acid (25 % - 35 %), oleic acid (9 % - 17 %) and stearic acid (6.5 % - 11 %), with a similar distribution being found in the free fatty acids of the oil. On roasting there is a slight decrease in the content of the lipids but the profiles remain similar. The thermal oxidative degeneration of the lipids leads to aldehydes, which contribute to the formation of heterocycles, as explained further in chapter 2.7.2. Cafestol as the main constituent of the diterpenes, is followed by kahweol as the second constituent, with other diterpenes being metabolites of the first two. The diterpenes occur as esters of fatty acids, with

saturated esters being more abundant than unsaturated (Folstar et al., 1975). The determination of 16-*O*-methylcafestol, which is found in green robustas only (Speer, 1989), is used as a method for characterising coffee blends. Speer et al. (1992 a) succeeded in detecting 2 % robusta in mixtures of coffee blends with this characterisation. During roasting dehydration products of cafestol and kahweol are formed (Speer et al. 1992 b). Sterols can be found in free and esterified forms (Folstar, 1985), with the three main sterols being sitosterol (53 % - 54 % of the sterolic fration), stigmasterol (20 % - 22 %) and campesterol (18 % - 19 %).

(4) Chlorogenic acids (CGA) were first identified in coffee by Payen (1846 a), who deduced the crystallised compound to be a mixed salt, which he named 'chloroginate de potasse et de caffeine' (Chlorogensaures Kali-Kaffeïn, Payen, 1846 b). Gorter (1908 a) found, upon hydrolysis, that the chlorogenic acid was split into caffeic and quinic acids. They belong to a family of esters, which consist of quinic acid with several hydroxycinnamic acids, particularly caffeic, ferulic and *p*-coumaric acids, either as mono- or as di-ester. The content of chlorogenic acids was estimated to be 4.3 % in roasted coffee. In green coffee the content of CGAs varies from 6.5 % for arabica to 9 % for robusta (Clifford, 1985 a). Due to roasting, the content of CGA drops to 1.75 % - 3 % (Trugo and Macrae, 1984). CGAs play a great role, contributing to the taste of coffee with their astringent taste.

Green coffee has a faint but characteristic odour, which was consequently studied to detect quality impairments before roasting, as off-flavours corresponded to defective beans. As early as 1957, the first volatiles of green coffee beans were detected, being acetic, propanoic, butanoic, pentanoic, malic, citric and quinic acids (Clements and Deatherage, 1957; Lentner and Deatherage, 1959). In the following years further compounds were identified, so that the total number now exceeds 300 compounds. Of these compounds, the most abundant groups belong to the hydrocarbons, alcohols, aldehydes, esters and acids. Belonging to the most important compounds of green coffee aroma are pentanal, acetaldehyde, dimethyl sulphide, acetone, isobutyraldehyde and methoxypyrazines (Zlatkis and Sivetz, 1960; Rodriguez et al., 1969; Vitzhum et al., 1976). Of the methoxypyrazines, the predominant member is 2-isobutyl-3-methoxypyrazine, which is responsible for the typical flavour of green bell pepper *Capsicum annum*, green peas and the wine cabernet sauvignon. The methoxypyrazines are not formed by Maillard reaction, unlike the pyrazines found in roast coffee, but must be of biogenetic origin. Procida et al. (1997) have found methylpyrazine and pyridine in minor amounts in green coffee, along side methoxypyrazines.

2.6.4 Roast Coffee Aroma

The roasting process can be divided into 4 phases. In the drying phase at approx. 50 °C water starts to evaporate and proteins are denaturised. In the development phase at ca. 100 °C non-enzymatic browning reactions occur. At 150 °C gases develop in the bean, such as carbon monoxide and carbon dioxide and lead to a volume enlargement of the bean. In the decomposition phase between 180 °C and 250 °C the coffee bean groove springs open and the typical coffee aroma develops. This process is, though, far more complicated with different components contributing to the overall aroma impression, a simplified overview is shown in figure 2-10.

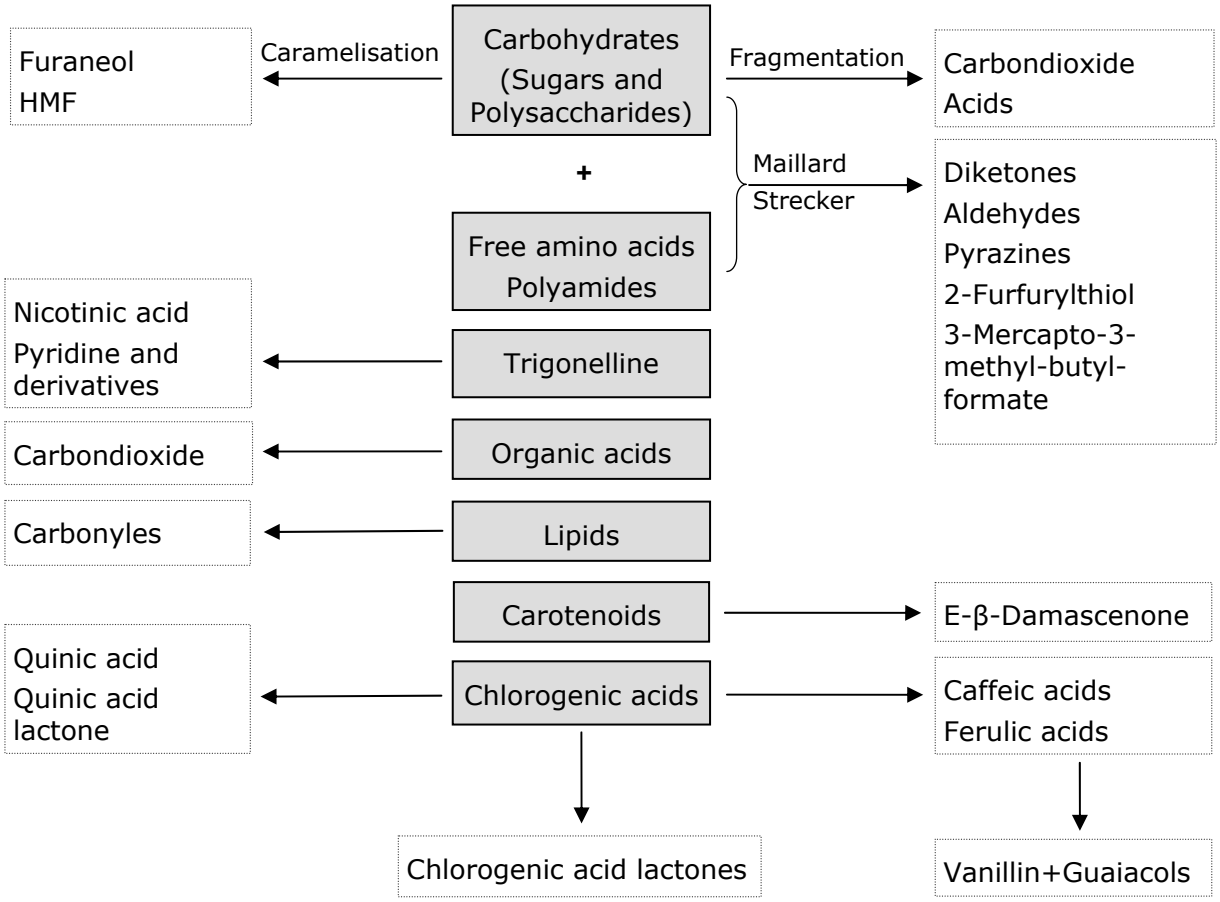

Figure 2-10: Main classes of volatile compounds in roast coffee and their non-volatile precursors in green coffee, simplified scheme from Yeretzian et al. (2002)

The aroma compounds of roasted coffee are formed, for the greater part, via Strecker/Maillard reactions (see chapter 2.7.2), thermal decomposition and fragmentation reactions. Many factors play a role, especially temperature, roast duration, bean type and pH value. The volatile aroma complex amounts to 0.1 %

of the roast coffee, most of it being in the aroma oil, which itself amounts to 10 % of the roast coffee. Already, over 850 aroma compounds have been identified in roast coffee aroma, since the first attempts of isolating and identifying constituents of coffee aroma began over 200 years ago. The history of coffee aroma research is very extensive and, consequently, will not be discussed in this work, an excellent review is given in Ivon Flaments book: Coffee Chemistry (2002). All kinds of constituents have been found in roast coffee aroma with different functions and structures. The main constituents of roast coffee aroma are furans and pyrans, pyrazines, ketones, phenols, pyrrols and hydrocarbons; additional aroma compound groups include alcohols, aldehydes, acids and anhydrides, esters, lactones, thiophenes, oxazoles, thiazoles, pyridines with further compounds containing nitrogen and sulphur. As can be seen, the aroma groups are widespread with each group contributing to the flavour of coffee in its own way. As pyrazines are a large group of the coffee flavour compounds, the research in this work concentrated on these interesting constituents, particulary the alkylpyrazines, and to a lesser extent on pyridine, belonging to the pyridines.

2.7 Alkylpyrazines

2.7.1 Characteristics of Alkylpyrazines

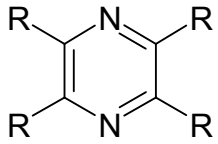

Figure 2-11: General structure of alkylpyrazines with R = hydrogen or alkylrest.

Alkylpyrazines belong to the heterocyclic organic compounds, with a 1,4-diazin structure and alkyl side chains, as shown in figure 2-11. Many volatile alkylpyrazines are formed during the heating of foodstuffs, i.e. cooking of meat, bread baking or roasting of cocoa and coffee beans. Since the 1920s, when Reichstein and Staudinger (1926) reported alkylpyrazines for the first time, altogether 70 different alkylpyrazines have been identified, of which approx. 35 have been identified in roast coffee. Not all of these alkylpyrazines contribute to the aroma of roast coffee, as they have different concentrations and odour thresholds, but they constitute to about 14 % of the overall volatile content of roast coffee (Buffo and Cardelli-Freire, 2004). These odour thresholds depend on the structure of the alkylpyrazines, with their different chain lengths and substitution patterns (Wagner et al., 1999). Gas chromatographic - olfactometric

analyses have shown, for 2-ethyl-3,5-dimethylpyrazine, one of the lowest odour thresholds of all alkylpyrazines, with a value in water of 0.04 ppb, given by Buttery and Ling (1997), and in air of 0.011 µg/m^3 air, by Czerny et al. (1996). Further values of other alkylpyrazines are found in table 2-4. A further interesting fact is that the odour quality changes, due to the substitution pattern of the alkylpyrazines, as in dimethylpyrazine to trimethylpyrazine, where a change is noticed from nutty to earth/roasty; these flavour impressions being predominantly for alkylpyrazines. Alkylpyrazines are thermostable, water vapour soluble and very soluble in water, ether and ethanol.

Table 2-4: Alkylpyrazines found in roast coffee and their characteristics (Moran et al., 1980; Wagner et al., 1999; Belitz et al., 2001; Merck Catalogue).

Compound	Formula	M_R	bp [°C]	Odour threshold [pmol/l air]	LD_{50} [mg/kg]
Pyrazine	$C_4H_4N_2$	80,09	115-118	-	2730 (Mouse, i.p.)
2-Methylpyrazine	$C_5H_6N_2$	94,12	136	>21000	1800 (Rat oral)
2,3-Dimethylpyrazine	$C_6H_8N_2$	108,14	156	8150	613 (Rat oral)
2,5-/2,6-Dimethylpyrazine	$C_6H_8N_2$	108,14	152-155	16850/15925	1020/880 (Rat oral)
2,3,5-Trimethylpyrazine	$C_7H_{10}N_2$	122,17	173	410	806 (Rat oral)
2-Ethylpyrazine	$C_6H_8N_2$	108,14	152	18536	-
2-Ethyl-3-methylpyrazine	$C_7H_{10}N_2$	122,17	174	286	600 (Rat oral)
2-Ethyl-5-/6-methylpyrazine	$C_7H_{10}N_2$	122,17	171	-	900 (Rat oral)
2-Ethyl-3,5-/3,6-dimethylpyrazine	$C_8H_{12}N_2$	136,20	181	0,07/18	456 (Rat oral)

M_R molecular mass; bp boiling point; LD_{50} lethal dosis for 50 % of the tested animals; - no information; i.p.=intraperitoneal

2.7.2 Chemistry of Formation

The large distribution of alkylpyrazines is formed only at high temperatures in food, with different pathways being discussed. A formation, via the Maillard

reaction, is one of the pathways that contribute to pyrazine formation. This reaction has not been proved in detail for each pyrazine, as so many factors and fragments play a role, but partial steps have been explained by model reactions and labelled model reactions.

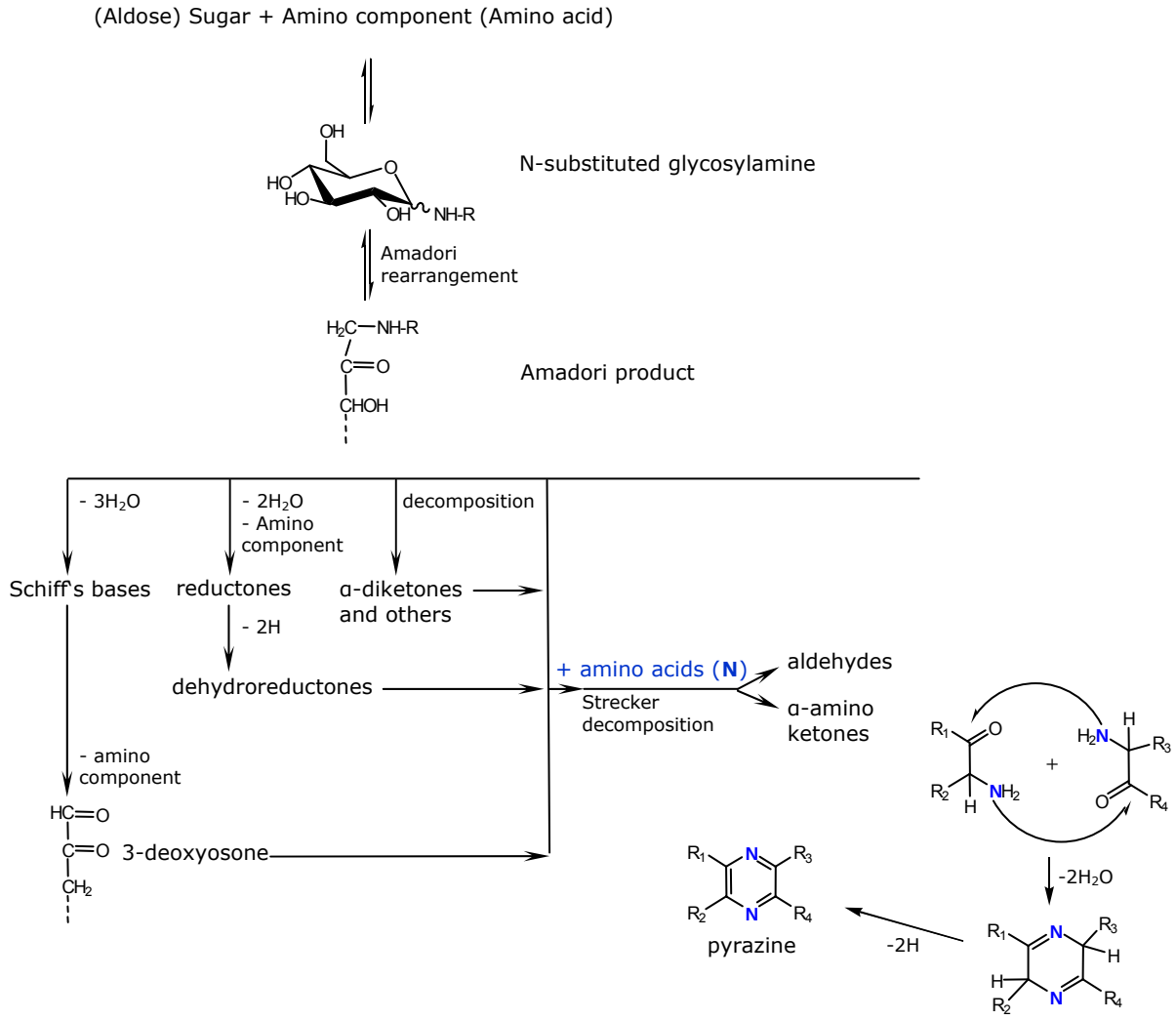

Figure 2-12: Alkylpyrazine formation via Maillard reaction (modified scheme from Vitzthum et al., 1976).

The first steps of the Maillard reaction have been known for nearly one hundred years, when Camille Maillard first observed that free amino acids, when heated, interact with reducing sugars to form nitrogenous heterocycles and melanoidins by non-enzymatic reaction. First N-substituted glycosylamines, the instable Amadori and Heyns components, are formed from reducing sugars and amino components. These Amadori and Heyns components are dehydrated to deoxyosones and dehydroreductones, which decompose, via retroaldolisation, to fragments, such as glyoxal, pyruvaldehyde, glyceraldehyde, 2,3-butanedione, 2-oxopropanal, acetaldehyde, 1-hydroxy-2-propanone and acetoin. These products can now perform the Strecker degradation with amino acids, so that α-amino

ketones, amino aldehydes and Strecker aldehydes are formed. α-Amino ketones and aldehydes condense rapidly to instable 2,5-dihydropyrazines, which dehydrate further to pyrazines. Figure 2-12 shows an overview of the proposed pyrazine formation via the Maillard reaction. This reaction leads, with other degradation products of the Amadori and Heyns components, to further aroma components and melanoidins.

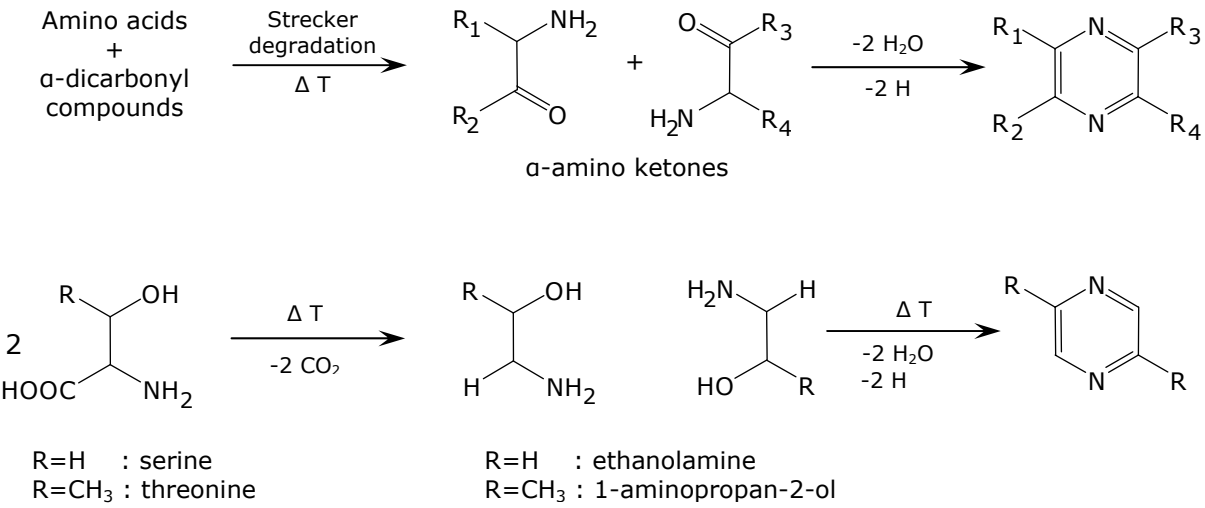

Figure 2-13: Formation of pyrazines via Strecker degradation of hydroxyamino acids (modified from Baltes und Bochmann, 1987 c).

A further possibility for alkylpyrazine formation is the cyclocondensation of 3-hydroxyamino acids after decarboxylation (Odell, 1973; Baltes and Bochmann, 1986), as shown in figure 2-13. Of these compounds, serine and threonine are found in green coffee and are decomposed strongly during roasting, so that only traces are found in roast coffee. In model reactions involving these two amino acids, with or without sucrose and other sugars, a row of different alkylpyrazines were identified (Kato et al., 1970; Wang and Odell, 1973; Baltes and Bochmann, 1986, 1987 c, 1987 e; Ho and Chen, 1999; Yaylayan and Keyhani, 2001 a and b).

The type of alkylpyrazine, which is formed, and its yield are dependent on pH and temperature, as these factors influence the Maillard reaction and Strecker degradation (Bristow and Isaacs, 1999; Farouk, 2000; Ames, 2001 a and b). Koehler et al. (1969) and Coleman III and Lawson (2000) found in model experiments with labelled educts that, of the pyrazine structure, only nitrogen originates from the amino acids, with the ring being built up from sugar material. In the above explained reactions, the α-amino group of amino acids was built

into the pyrazine ring structure, whereas Ho et al. (1993) found that ammonia from the deamidation of asparagine and glutamine can take part in the pyrazine formation.

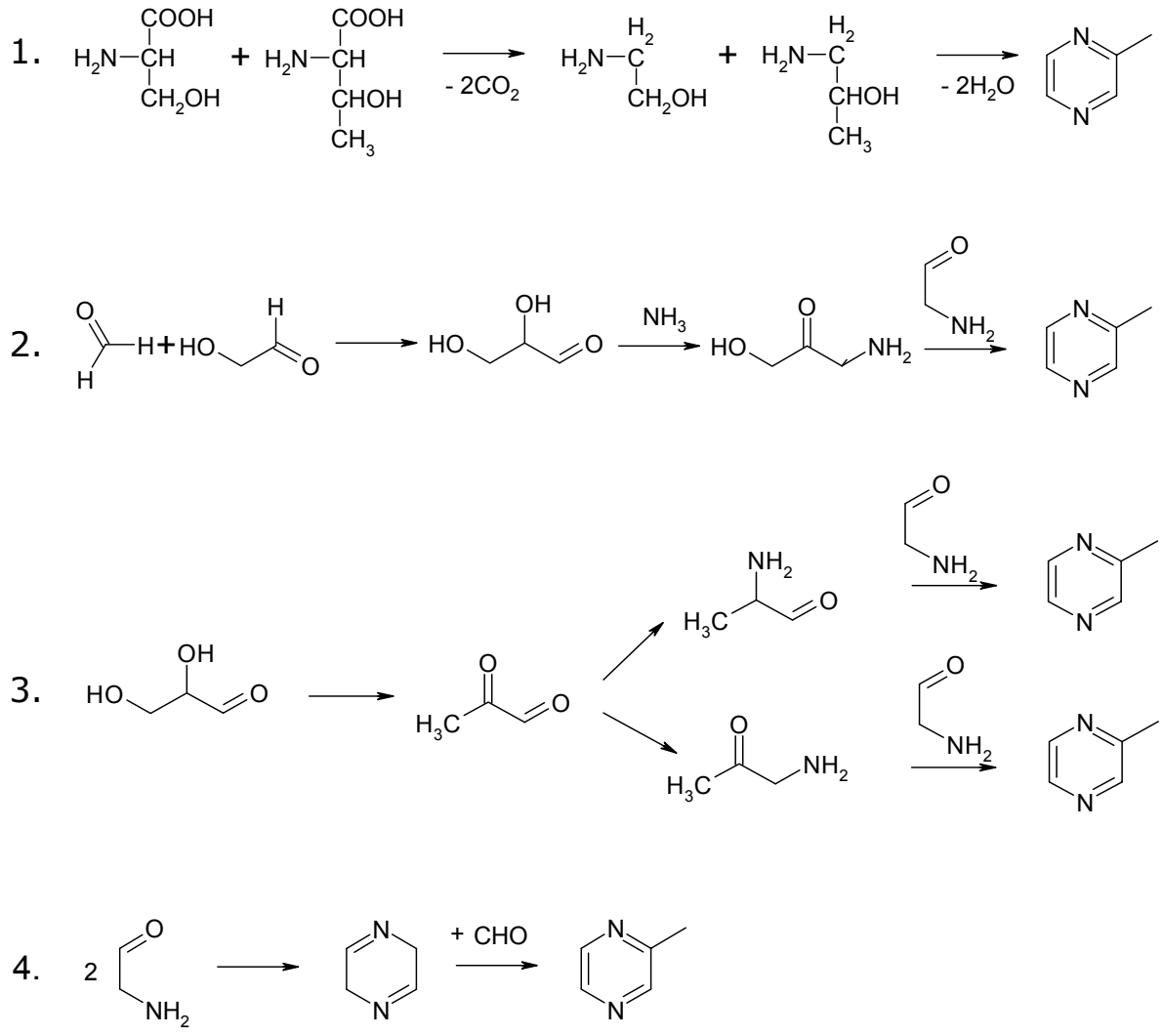

Figure 2-14: Different formation pathways for methylpyrazine; 1. Strecker degradation of serine and threonine and condensation to methylpyrazine; 2. Maillard decomposition products react with ammonium and amino aldehydes to methylpyrazine; 3. Different condensation products of ammonium with Maillard decomposition products lead to methylpyrazine; 4. Formaldehyde condensates with the intermediate dihydropyrazine (Baltes, 1986; Hwang et al., 1995; Chen and Ho, 1998; Yaylayan and Keyhani, 2001 a and b).

Not only monomeric and dimeric components play a role in alkylpyrazine formation, but also peptides, proteins and starch can participate in the generation of flavour compounds (Rizzi, 1989; Ludwig, 2000). The alkyl chains of

pyrazines also have different formation pathways. They are either incorporated in the amino ketones, which react with dihydropyrazines and then pyrazines, or they can condensate as aldehydes on the intermediate dihydropyrazines. As the explanations above have shown, the formation of alkylpyrazines is not a straightforward process with more than one pathway and different educts for each pyrazine possible (Hwang et al., 1995). The vast pyrazine formation possibilities are shown in figure 2-14 on the compound methylpyrazine.

2.8 Research Objective

In the past numerous research groups have dedicated their work to coffee authentication regarding origin or botany. Different compounds of the coffee beans were analysed for these studies including the distribution of tocopherols and triglycerides (González et al., 2000), over 50 different elements by ICP-MS (Prodolliet et al., 2001), amino acid contents and peptides (Arnold et al., 1994, 1996; Casal et al., 2003, 2005; Ludwig et al., 2000; Macdonald and Macrae, 1986) and polysaccharides (Fischer et al., 2000, 2001). Concerning stable isotope analysis of coffee compounds, caffeine was explored extensively (Dunbar and Wilson, 1982; Danho et al., 1992; Prodolliet et al., 1998; Richling et al., 2003) and recently bulk carbon, nitrogen and boron values of green coffee beans have been assessed (Serra et al., 2005).

The authenticity assessment of achiral aroma compounds, via stable isotope analysis of carbon, hydrogen and oxygen is de facto established. However, regarding the differentiation between natural and synthetic origin (see chapter 2.5.2.2 and 2.5.3.1), the nitrogen containing aroma compounds and nitrogen measurements have been so far neglected, with only anthranilates and derivatives presently being investigated (Faulhaber et al., 1997). As for all authenticity questions regarding stable isotope analysis of aroma compounds, to be able to make assured statements a vast database of values is needed. For this database, authentic references and samples are required, as only with these can other samples be classified. This is insufficient, however, when the formation pathways of the aroma compounds are not exactly known and other influences play a role in the stable isotope values, other than geographic, soil and plant-innate features (see chapter 2.2, 2.3 and 2.4). This is the case with alkylpyrazines from coffee. How these alkylpyrazines derive from the many possible precursors, is until now not known exactly, as so many reaction pathways are possible. Consequently, it is not known how the stable isotope values of these pyrazines react to differing formation conditions, as pH value, temperature and duration of the roast, or how much the isotope values reflect

the biogenetic origin of the alkylpyrazines. So many questions arise, when forming a database for alkylpyrazines from roasted coffee, many of which were addressed in this research project, for instance: What influence does the geographic origin have? Is there a difference between robusta and arabica coffees? How do roasting conditions influence isotope values? Concerning the alkylpyrazines as a chemical compound, further problems have to be analysed first such as: Is there an influence on isotope values during sample preparation? How can it be avoided and are the compounds isotopically stable when stored in different solvents, as used for aroma extracts? For authenticity assessment of aroma compounds, synthetic and natural references are needed, although the origin of these is not always clear. For this reason alkylpyrazine references and a pyridine precursor were synthesised to determine isotope values for comparison with coffee samples, and to see, if these could be influenced, by changing synthesis conditions. To try to clarify the formation of alkylpyrazines and pyridine, green coffee beans were fractioned into compound classes, which were measured via EA-C/P-IRMS and subsequently roasted. The isotope values of the alkylpyrazines of each compound class were compared to monitor the changes. All these questions were addressed, enabling the compilation of a database of roast coffee alkylpyrazines, with the future ability of conducting authenticity assessments on roast coffees and products, using coffee aroma.

3 Results and Discussion

3.1 Stable Isotope Stability of Alkylpyrazines in Ethanol and Water

For aroma compounds in solvents the most important questions, regarding isotopic influences concern their stability in different solvents. Water and ethanol have protic properties, and are often in contact with the aroma compounds during sample preparation, as well as frequently being used in aroma formulations for commercial aroma extracts. Water is, furthermore, the solvent for the production of coffee products, i.e. coffee drinks. Preliminary studies on the influence of solvents on aroma compounds had shown, that acids, i.e. 2-methylpropionic acid, were affected isotopically by water (Preston et al., 2005), and García-Martin et al. (2001) had proved that an isotope exchange with surrounding water was possible, so an examination of alkylpyrazines was needed.

For the examinations of isotope stability the same procedure was employed. The studies were performed using chemically pure reference compounds of known isotopic values, with the relevant stable isotope values of these compounds being measured both before and after the storage time. Comparisons between the isotope values confirmed whether a significant isotope fractionation had occurred during the storage.

3.1.1 Stability of Alkylpyrazines in Ethanol

The stability of alkylpyrazines in ethanol at 25°C was investigated, using the compounds **2**, **3**, **6**, **11**, **12**/**13** and **14**. In the following figure 3-1, the results for 2-ethyl-3,5-dimethylpyrazine are shown as an example, with all other results, exhibiting similar tendencies, being located in tables A-13 to A-18 of the appendix.

Ethanol is a weak protonating solvent, which can theoretically exchange hydrogen atoms with other compounds, as well as being a popular solvent for aroma extraction formulations. To be able to make accurate and assured statements for aroma compounds stored in ethanol, their $\delta^2H_{V\text{-}SMOW}$ stability was checked over a period of 20 days. As can be seen in figure 3-1, the reference, here represented by 2-ethyl-3,5/6-dimethylpyrazine, exhibited a value of $\delta^2H_{V\text{-}SMOW}$ = -105 ‰ before storage, whilst the solvent ethanol showed, dependant upon the pH value, a $\delta^2H_{V\text{-}SMOW}$ value varying between -204 ‰ and -224 ‰. During the storage of 2-ethyl-3,5/6-dimethylpyrazine in ethanol the

$\delta^2H_{V\text{-}SMOW}$ values varied between -98 ‰ and -109 ‰, thus showing no significant changes in its isotope values towards the isotope value of the solvent, as was expected. The slight fluctuations in the isotope values of the stored reference were within accepted measurement tolerances.

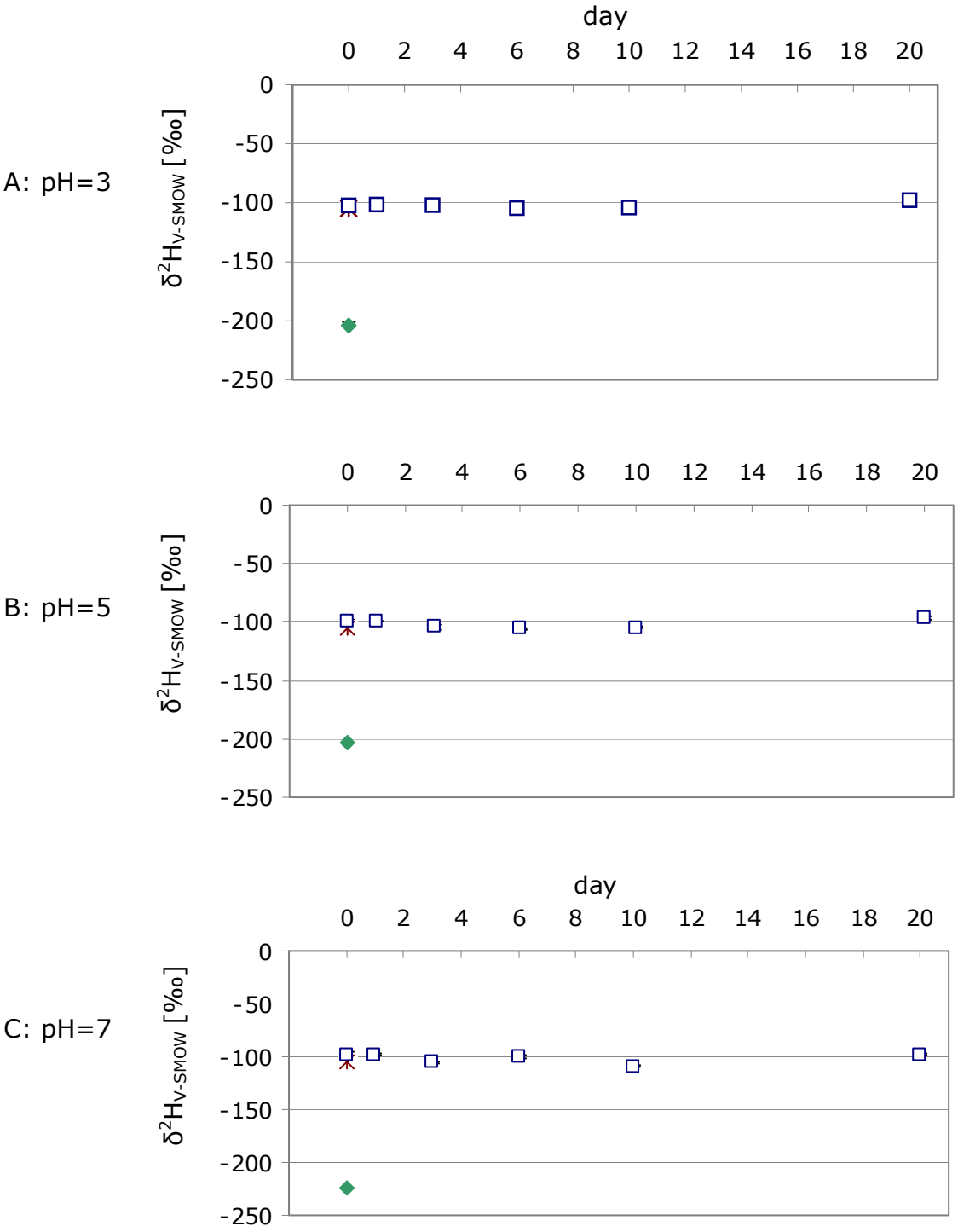

Figure 3-1: Stability diagrams for 2-ethyl-3,5/6-dimethylpyrazine in ethanol at 25°C with A: pH value 3, B: pH value 5 and C: pH value 7; with ◆ = solvent, ✳ = reference and □ = stored reference.

3.1.2 Stability of Alkylpyrazines in Water

The stability of alkylpyrazines in water at 25°C was investigated, using the compounds **2**, **3**, **6**, **11**, **12**/**13** and **14**. In the following figure 3-2, the results for 2-ethyl-3,5-dimethylpyrazine are shown as an example, with all other results, exhibiting similar tendencies, being located in Tables A-13 to A-18 of the appendix.

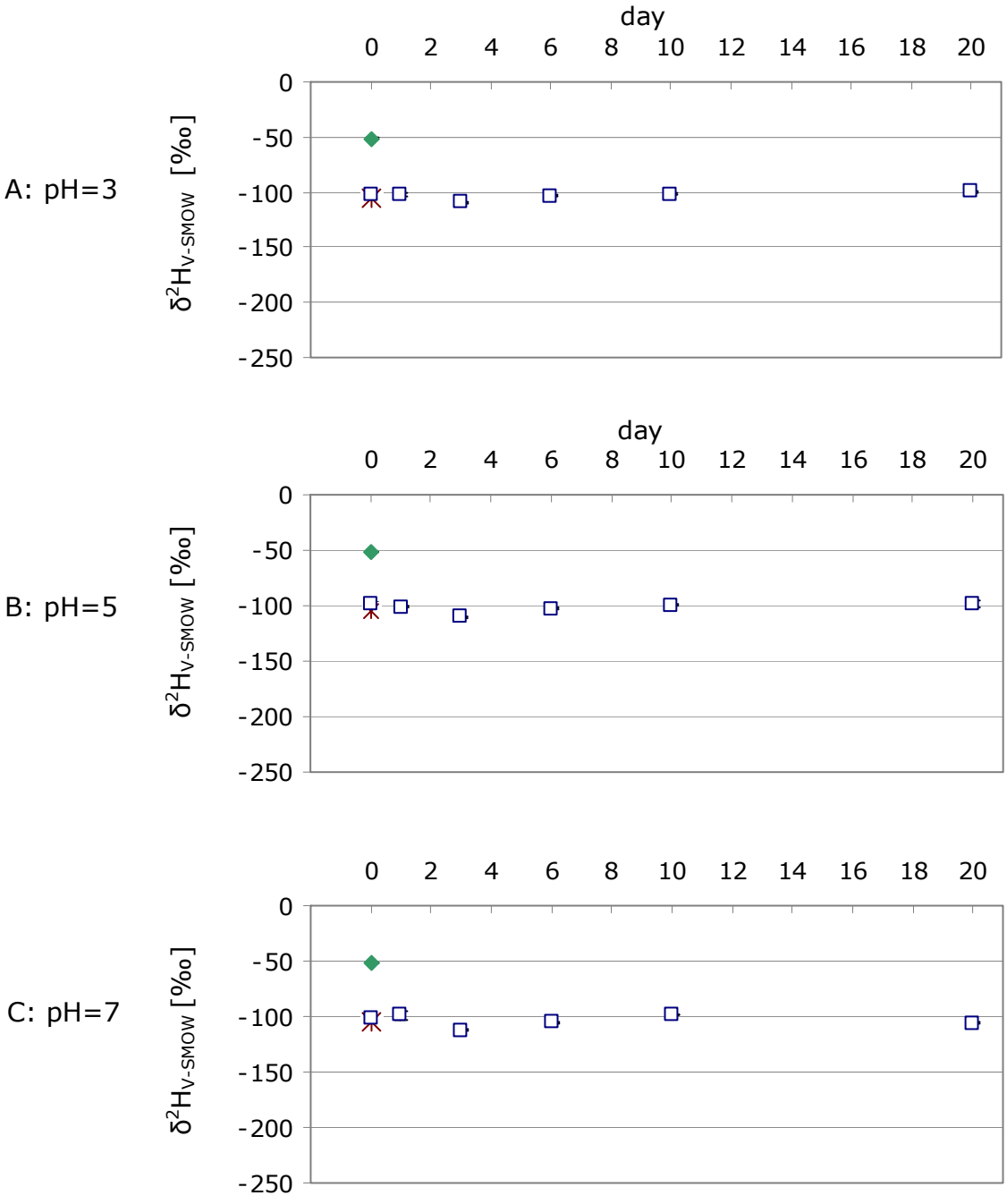

Figure 3-2: Stability diagrams for 2-ethyl-3,5/6-dimethylpyrazine in water at 25°C with A: pH value 3, B: pH value 5 and C: pH value 7; with ◆ = solvent ✳ = reference and □ = stored reference.

Water is a stronger protonating solvent than ethanol and is often used during sample preparation. It is known that water can exchange protons with acids and polyoles and, therefore, change their original $\delta^2H_{V\text{-}SMOW}$ value considerably towards that of the isotope value of water (Preston et al., 2005). For this reason, the protonating properties of water, with alkylpyrazines, were checked by measuring their $\delta^2H_{V\text{-}SMOW}$ stability over a period of 20 days. As can be seen in figure 3-2, the stored reference, here represented by 2-ethyl-3,5/6-dimethylpyrazine, exhibited an initial $\delta^2H_{V\text{-}SMOW}$ value of -105 ‰, but showed no significant changes in its isotope values towards the isotope value of the solvent over this 20 day period, with the $\delta^2H_{V\text{-}SMOW}$ values varying between -98 ‰ and -112 ‰. These variations were within accepted measurement tolerances.

3.2 Stable Isotope Analyses, $^{15}N/^{14}N$ and $^{2}H/^{1}H$, of Alkylpyrazines and Pyridine from Roast Coffee Aroma

3.2.1 Roast Coffee Aroma Profile and Sample Preparation

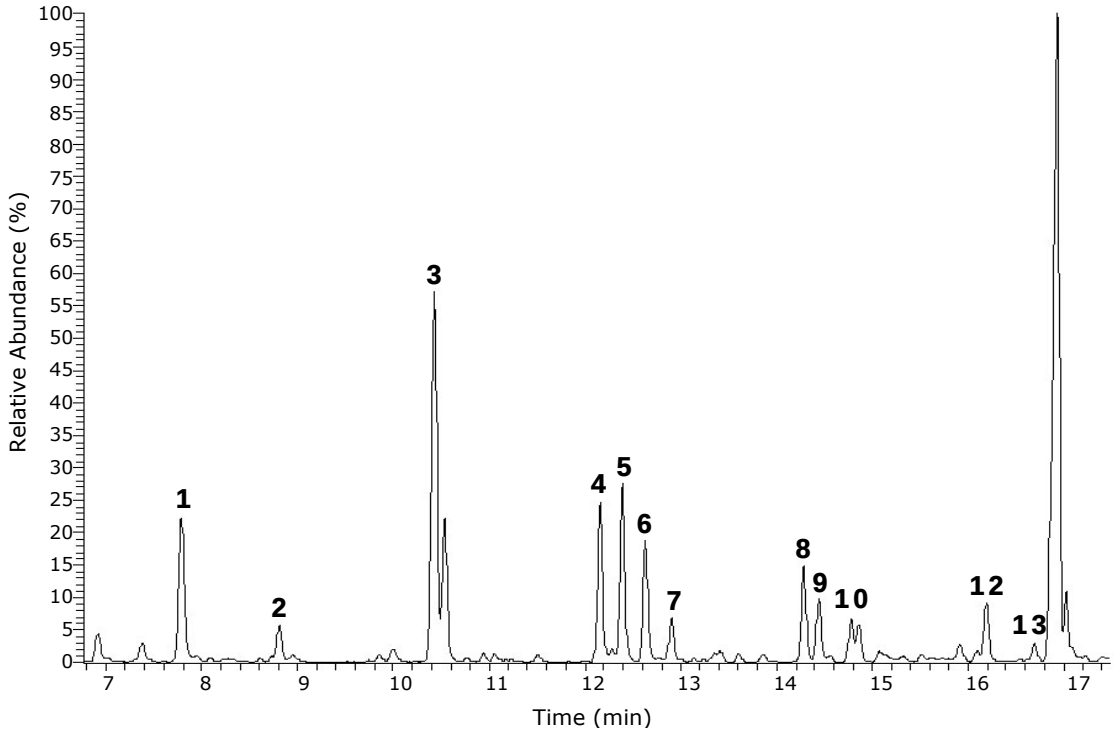

Figure 3-3: Representative HRGC-MS total ion chromatogram (sector) of roasted coffee bean (*Coffea arabica* L.) volatiles. The peak numbers indicate the compounds under IRMS study, **1** pyridine, **2** pyrazine, **3** 2-methylpyrazine, **4** 2,5-dimethylpyrazine, **5** 2,6-dimethylpyrazine, **6** 2-ethylpyrazine, **7** 2,3-dimethylpyrazine, **8** 2-ethyl-5-methylpyrazine, **9** 2-ethyl-6-methylpyrazine, **10** 2-ethyl-3-methylpyrazine, **12** 2-ethyl-3,5-dimethylpyrazine, **13** 2-ethyl-3,6-dimethylpyrazine.

Although many studies have been conducted towards the volatile constituents of roast coffee and many reviews have been published (Clarke, 1986; Grosch, 1998; Flament, 2002 and references within), none have examined the stable isotope composition of any compound, with our study being the first (Richling et al., 2005). Because of their high impact on roast coffee quality, their sensory importance and their typical nutty and earth/roasty impression, alkylpyrazines and pyridine were the central focus of interest in this work. Figure 3-3 shows a section from a roast coffee aroma profile for *Coffea arabica* L., with the characteristic alkylpyrazines and pyridine. Some roast coffee samples showed, furthermore, the compound 2,3,5-trimethylpyrazine (**11**), with a near-identical retention time as for (**10**). 2,3,5,6-Tetramethylpyrazine (**14**) was found in roast cocoa samples, and later analysed as a further origin of alkylpyrazines. The chromatogram shows the difficulty to be expected for the HRGC-C/P-IRMS analysis, as the compounds partly co-eluate with other roast coffee aroma components and are, as such, non-measurable. An elaborate procedure was, therefore, needed to separate alkylpyrazines and pyridine from other compounds. This was conducted as shown in figure 3-4.

According to figure 3-4, green coffee beans were roasted for 6 min at 210 °C and then ground to powder. Commercially roasted coffee beans were also ground and the resulting ground coffees, including other commercial coffee products, were subjected to simultaneous distillation and extraction. The resulting crude aroma extracts were analysed via GC-MS to define the aroma composition of the samples and the measurable volatiles, then a silica gel fractionation, with pentane/diethyl ether concentrations varying from 100 % pentane to 100 % diethyl ether in 20 % steps, was performed. In the resulting fractions, the 60 % diethyl ether fraction contained 2-ethylpyrazine (**6**), 2-ethyl-5/6-methylpyrazine (**8**/**9**), 2-ethyl-3-methylpyrazine (**10**) and 2-ethyl-3,5/6-methylpyrazine (**12**/**13**). 2-Methylpyrazine (**3**), 2,5/6-dimethylpyrazine (**4**/**5**), 2,3-dimethylpyrazine (**7**), and 2,3,5-trimethylpyrazine (**11**) were recovered in the 80 % diethyl ether fraction. Pyridine (**1**) and pyrazine (**2**) were eluted in the 100 % diethyl ether fraction. Because of insufficient separation of components **4** and **5**, **8** and **9,** as well as **12** and **13,** during HRGC-C/P-IRMS analysis, the isotope ratios were measured for the mixtures of **4**/**5**, **8**/**9** and **12**/**13**, respectively.

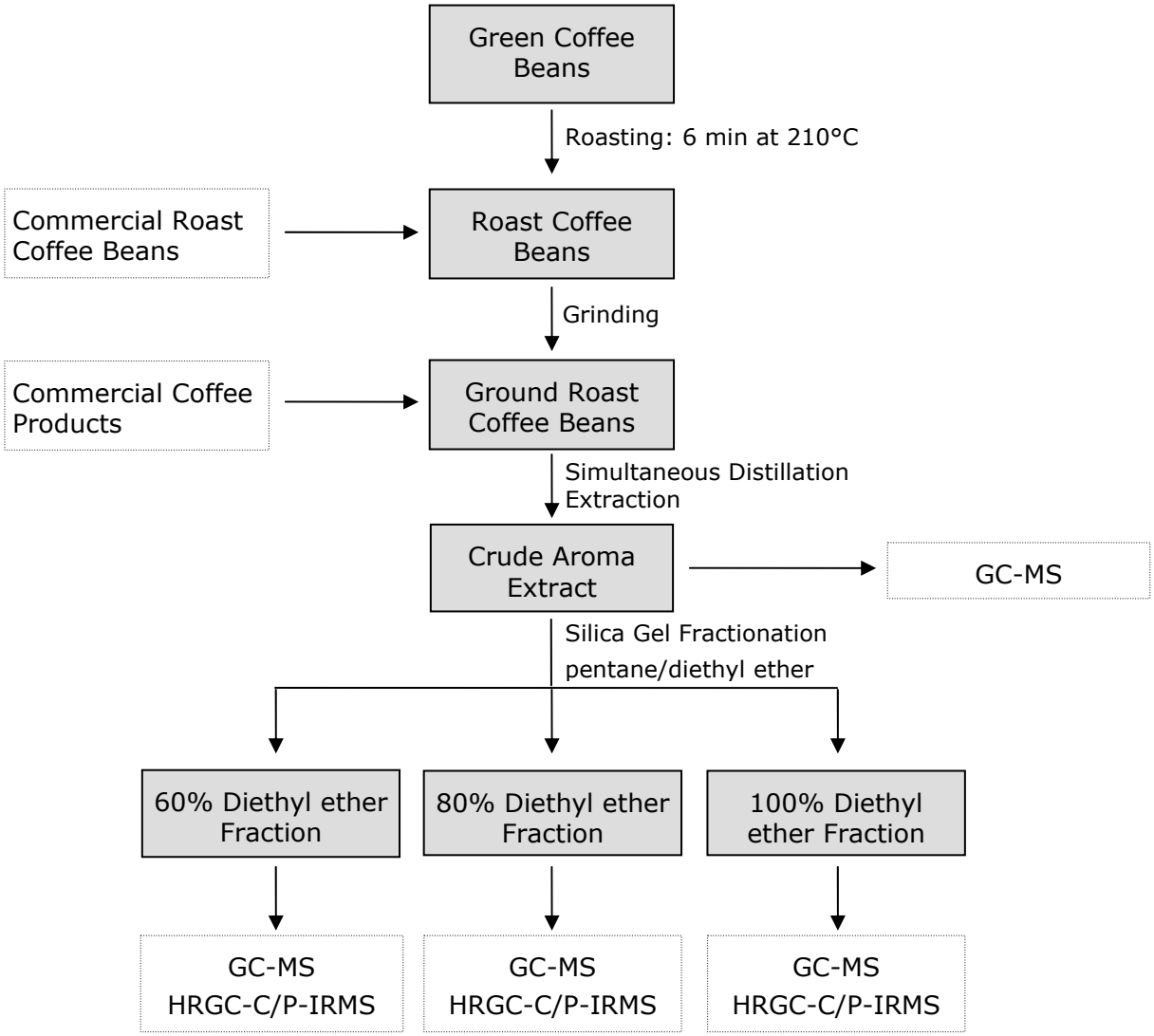

Figure 3-4: Scheme for the work-up procedure of coffee samples.

3.2.2 $^{15}N/^{14}N$ and $^{2}H/^{1}H$ Analyses of Volatiles of Self-Roasted Coffee Beans

For preliminary analyses of coffee alkylpyrazines and pyridine as well as for an overview of $\delta^{15}N_{AIR}$ and $\delta^{2}H_{V\text{-}SMOW}$ values of this compound group, self-roasted arabica (**A**) and robusta (**R**) coffee beans, as well as synthetic (■) and declared to be 'natural' (■) references, were analysed and correlated in figures 3-5 to 3-14. The results of compounds **1** to **13** are presented singly in the following chapter.

The correlation of $\delta^{15}N_{AIR}$ and $\delta^{2}H_{V\text{-}SMOW}$ data of pyridine (**1**) from various origins is outlined in figure 3-5. The graph shows synthetic references with $\delta^{15}N_{AIR}$ values from 0.0 ‰ to -0.4 ‰ and $\delta^{2}H_{V\text{-}SMOW}$ values from -10 ‰ to -21 ‰, with

no references 'declared to be natural' being obtainable. More depletion is found in the data of **1** from self-roasted arabica and robusta coffees (n=9). They range from -1.7 ‰ to -22.1 ‰ for $\delta^{15}N_{AIR}$ values and from -43 ‰ to -83 ‰ for $\delta^{2}H_{V\text{-}SMOW}$ values, respectively. A clear differentiation of samples and synthetic references is promising with this data. Such a strong depletion in the $^{15}N/^{14}N$ values is unusual, with only 2,3-dimethylpyrazine showing two samples with a depletion greater than -10 ‰, both these being robusta samples. The formation of pyridine in the roast coffee bean remains unclear, with the strong depletion in the $\delta^{15}N_{AIR}$ values indicating a difference from the alkylpyrazines formation. The stable isotope values of pyridine are a point of interest in the following chapters 3.2.4 and 3.4, where they are discussed further.

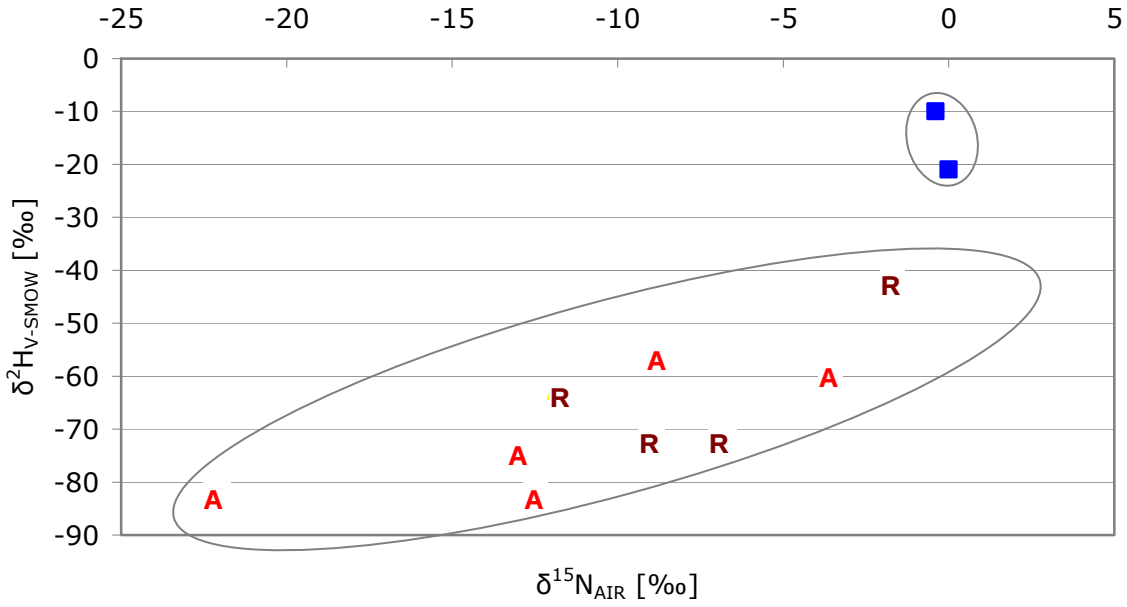

Figure 3-5: Correlation of $\delta^{15}N_{AIR}$ and $\delta^{2}H_{V\text{-}SMOW}$ values [‰] of pyridine **1** from self-roasted arabica coffee (**A**), self-roasted robusta coffee (**R**) and synthetic references (■).

For pyrazine (**2**), only arabica self-roasted coffee (n = 2) and one synthetic reference were available for measurement, as displayed in figure 3-6. The $\delta^{15}N_{AIR}$ values for the arabica self-roasted coffees varied from -1.8 ‰ to -3.7 ‰, with the $\delta^{2}H_{V\text{-}SMOW}$ results being determined to be in the range from -4 ‰ to -59 ‰. The only synthetic reference showed $\delta^{15}N_{AIR}$ and $\delta^{2}H_{V\text{-}SMOW}$ values of -1.5 ‰ and -112 ‰, respectively. A difference, particularly in the $^{2}H/^{1}H$ ratios, is seen between the reference and coffee samples, but with the sample amounts being so small, and with the robusta samples not being analysed, a clear-cut distinction is not possible.

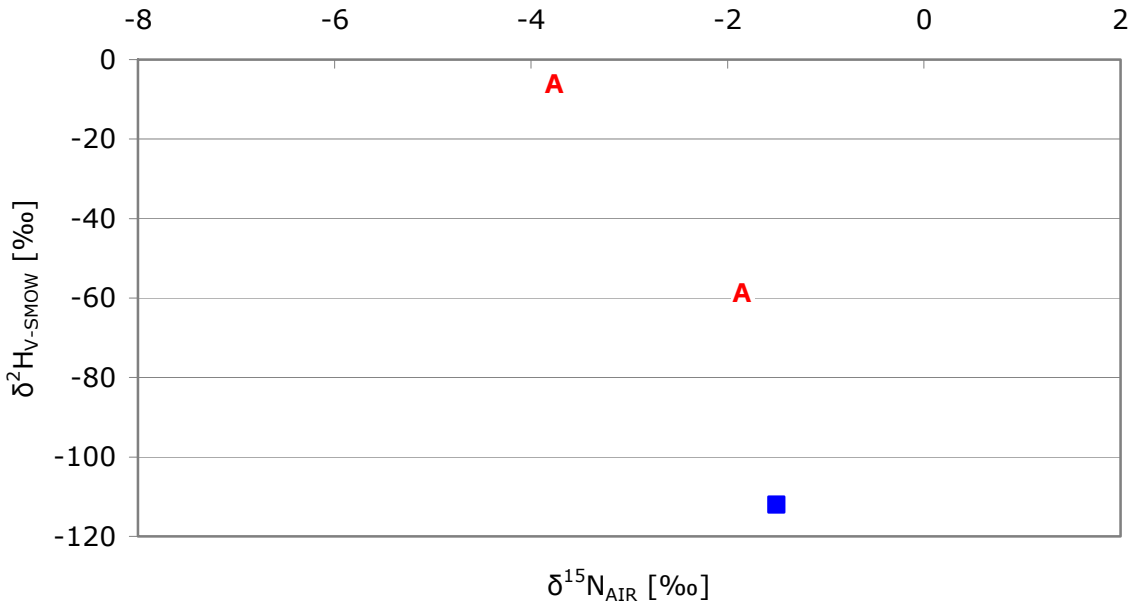

Figure 3-6: Correlation of $\delta^{15}N_{AIR}$ and $\delta^{2}H_{V\text{-}SMOW}$ values [‰] of pyrazine **2** from self-roasted arabica coffee (**A**) and synthetic references (■).

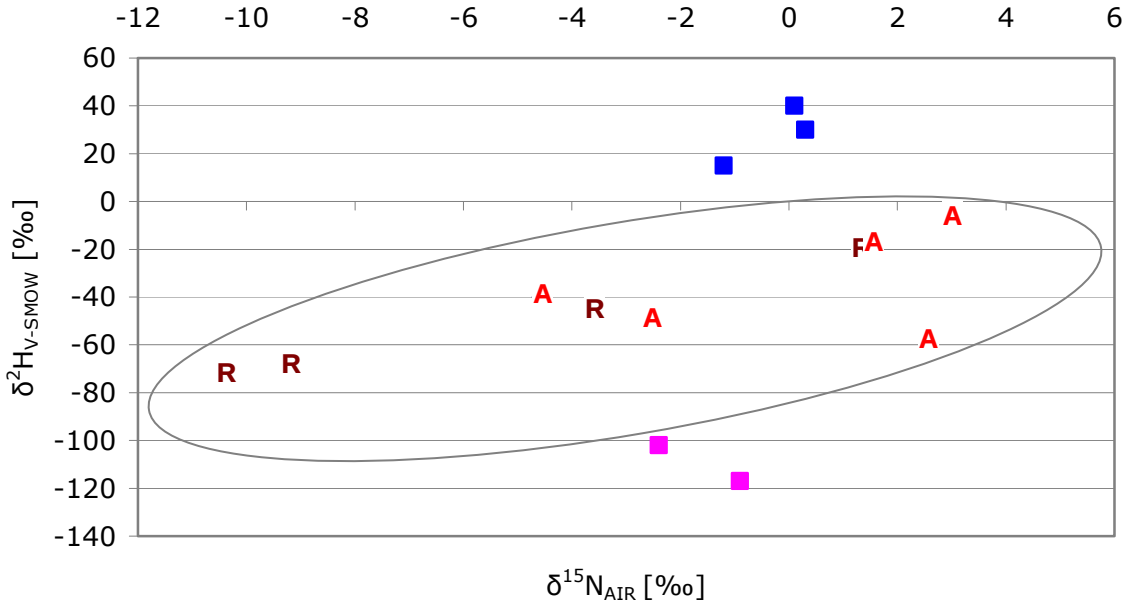

Figure 3-7: Correlation of $\delta^{15}N_{AIR}$ and $\delta^{2}H_{V\text{-}SMOW}$ values [‰] of 2-methylpyrazine **3** from self-roasted arabica coffee (**A**), self-roasted robusta coffee (**R**), synthetic references (■) and references 'declared to be natural' (■).

The correlation of $\delta^{15}N_{AIR}$ and $\delta^{2}H_{V\text{-}SMOW}$ data of 2-methylpyrazine (**3**) from various origins is outlined in figure 3-7. The graph shows differences between synthetic references ($\delta^{15}N_{AIR}$ from 0.3 ‰ to -1.2 ‰ and $\delta^{2}H_{V\text{-}SMOW}$ from 15 ‰ to 40 ‰) and references 'declared to be natural' ($\delta^{15}N_{AIR}$ from -0.9 ‰ to -2.4 ‰ and $\delta^{2}H_{VSMOW}$ from -102 ‰ to -117 ‰). Especially, the $\delta^{2}H_{V\text{-}SMOW}$ values

of the synthetic references, with their positive values, were surprising and found by no other component. Located between these two groups is data of 2-methyl-pyrazine from self-roasted arabica and robusta coffees (n=9). They range from 3.0 ‰ to -10.2 ‰ for $\delta^{15}N_{AIR}$ values and from -5 ‰ to -77 ‰ for $\delta^{2}H_{VSMOW}$, respectively. Two robusta samples from India, however, showed a stronger depletion in the $\delta^{15}N_{AIR}$ values compared to the rest of the investigated coffee samples.

It was not possible to separate 2,5/6-dimethylpyrazine (**4**/**5**) by HRGC-IRMS analysis. Thus, combined parameters (**4 / 5**) were measured instead. The correlation data of $\delta^{15}N_{AIR}$ and $\delta^{2}H_{V\text{-}SMOW}$ for **4 / 5** is displayed in figure 3-8. The references were found to be pure samples of **4** and **5**, so these values are singly presented. The $\delta^{15}N_{AIR}$ and $\delta^{2}H_{V\text{-}SMOW}$ values of the synthetic reference **4** (n = 4) showed values ranging from -1.6 ‰ to -5.5 ‰ and from -59 ‰ to -80 ‰, respectively. The three strongly depleted references in $\delta^{15}N_{AIR}$ are, therefore, compound **4**. The 'declared to be natural' references (n = 2) showed a $^{15}N/^{14}N$ ratio of -0.5 ‰ to 0.5 ‰ as well as a $^{2}H/^{1}H$ ratio of -50 ‰ to -149 ‰, respectively. For the synthetic references **5** (n = 2), $\delta^{15}N_{AIR}$ data of -0.6 ‰ to -1.0 ‰ was measured and $\delta^{2}H_{V\text{-}SMOW}$ data of -86 ‰ to -133 ‰. The 'declared to be natural' reference displayed a $\delta^{15}N_{AIR}$ value of -0.1 ‰ and a $\delta^{2}H_{V\text{-}SMOW}$ value of -151 ‰. Self-roasted arabica coffees (n = 2) ranged from 3.1 ‰ to 3.4 ‰ ($\delta^{15}N_{AIR}$) and -40 ‰ to -75 ‰ ($\delta^{2}H_{V\text{-}SMOW}$), distinctly outside the values for the references.

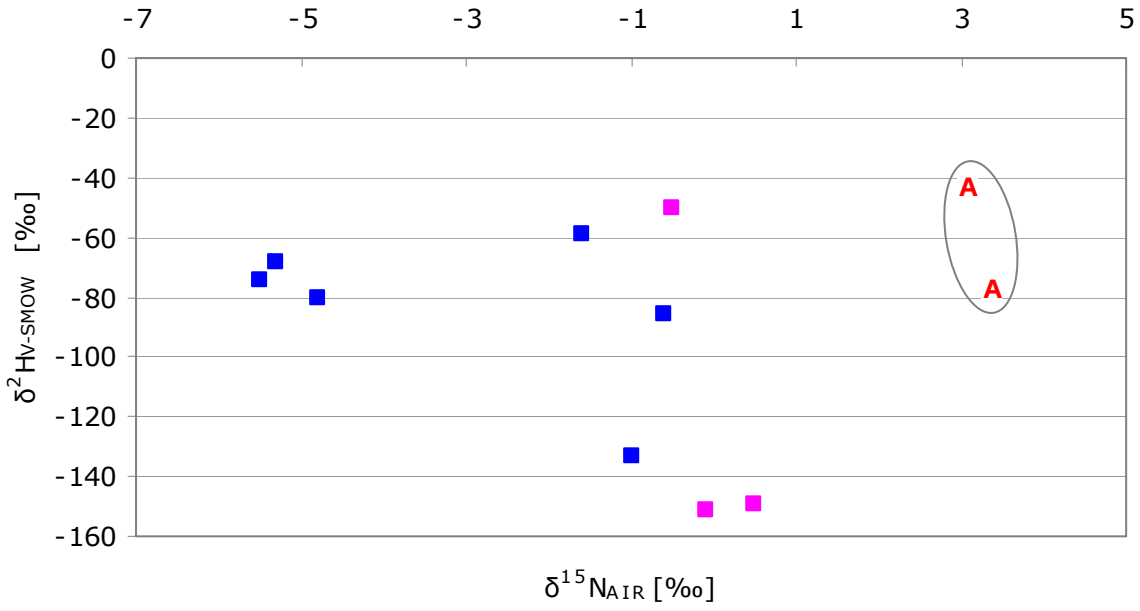

Figure 3-8: Correlation of $\delta^{15}N_{AIR}$ and $\delta^{2}H_{V\text{-}SMOW}$ values [‰] of 2,5/6-dimethyl-pyrazine **4**/**5** from self-roasted arabica coffee (**A**), synthetic references (■) and references 'declared to be natural' (■).

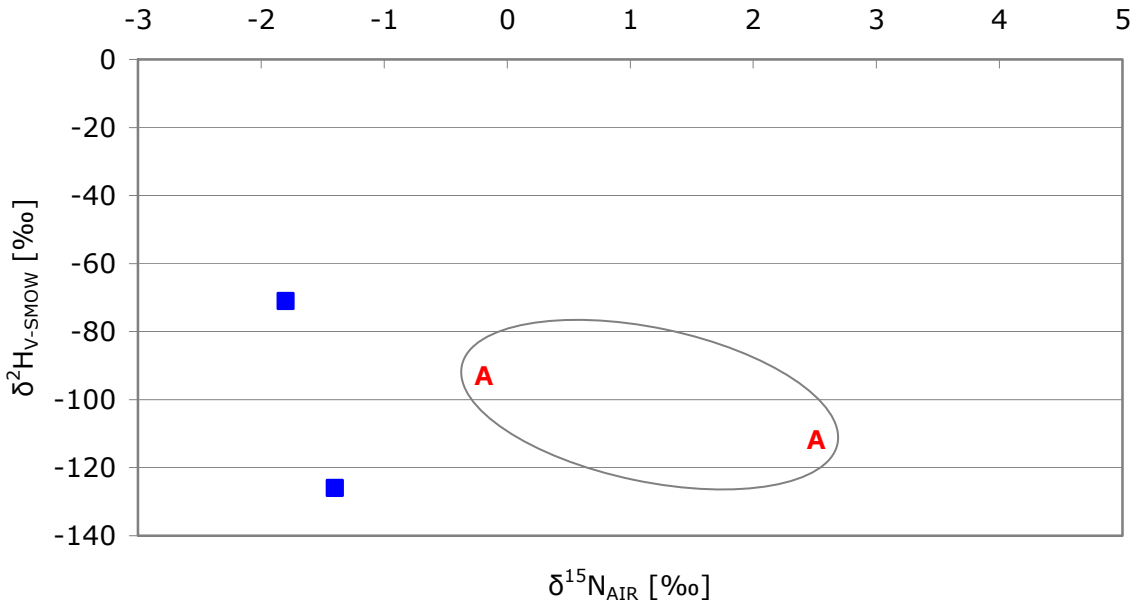

Figure 3-9: Correlation of $\delta^{15}N_{AIR}$ and $\delta^{2}H_{V\text{-}SMOW}$ values [‰] of 2-ethylpyrazine **6** from self-roasted arabica coffee (**A**) and synthetic references (■).

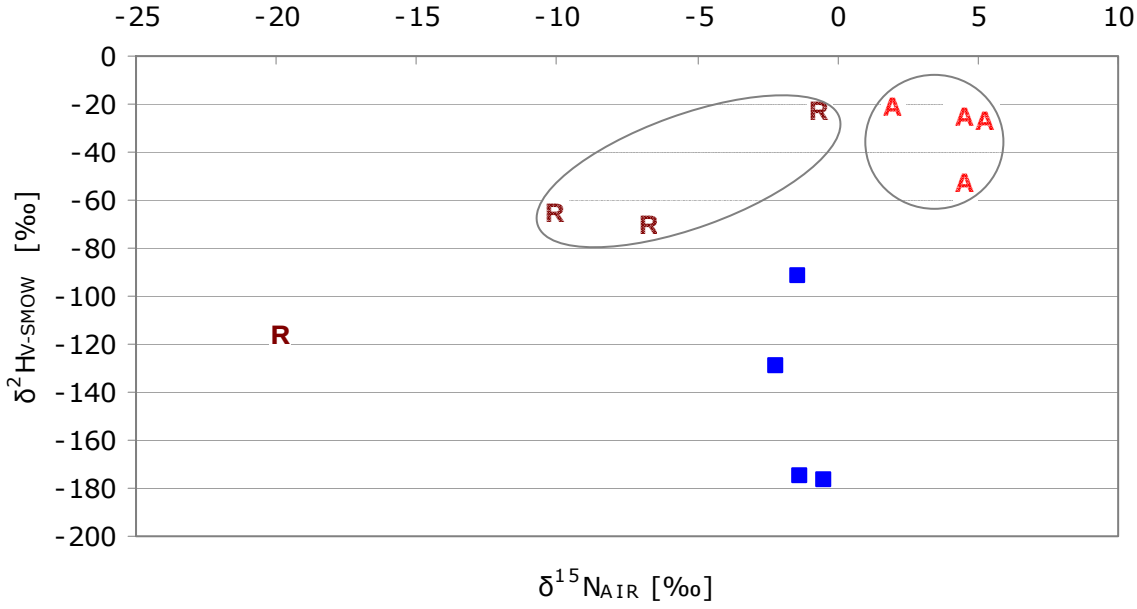

Figure 3-10: Correlation of $\delta^{15}N_{AIR}$ and $\delta^{2}H_{V\text{-}SMOW}$ values [‰] of 2,3-dimethylpyrazine **7** from self-roasted arabica coffee (**A**), self-roasted robusta coffee (**R**) and synthetic references (■).

The results obtained for 2-ethylpyrazine (**6**) are displayed in figure 3-9. Only two synthetic references, with $\delta^{15}N_{AIR}$ values of -1.4 ‰ to -1.6 ‰ and $\delta^{2}H_{V\text{-}SMOW}$ values of -59 ‰ to -126 ‰, were available. Of self-roasted samples, only two

arabica coffees were measurable, these ranging from -0.2 ‰ to 2.5 ‰ ($\delta^{15}N_{AIR}$) and from -93 ‰ to -111 ‰ ($\delta^{2}H_{v\text{-}SMOW}$). This data may be promising for synthetic and coffee sample differentiation, but additional data is required.

The correlation of $\delta^{15}N_{AIR}$ and $\delta^{2}H_{V\text{-}SMOW}$ values of 2,3-dimethylpyrazine (**7**), from different sources, is outlined in Figure 3-10. The $\delta^{15}N_{AIR}$ values for **7** from self-roasted coffees (n=8) varied from 5.2 ‰ to -10.2 ‰, with the $\delta^{2}H_{V\text{-}SMOW}$ results ranging from -21 ‰ to -69 ‰. One strongly depleted robusta sample from Malabar displayed values of -20.0 ‰ and -114 ‰ for $\delta^{15}N_{AIR}$ and $\delta^{2}H_{V\text{-}SMOW}$, respectively. The other two strongly depleted values were also robusta samples from India and Indonesia. Measurements of the references resulted in a range from -92 ‰ to -177 ‰ for $\delta^{2}H_{V\text{-}SMOW}$ and for $\delta^{15}N_{AIR,}$ in a very narrow range, between -0.5 ‰ and -2.2 ‰. A grouping of robusta and arabica samples is evident, as well as a differentiation with the synthetic references. This seems to be promising for authenticity assessment, provided that extended data information will be available in the future.

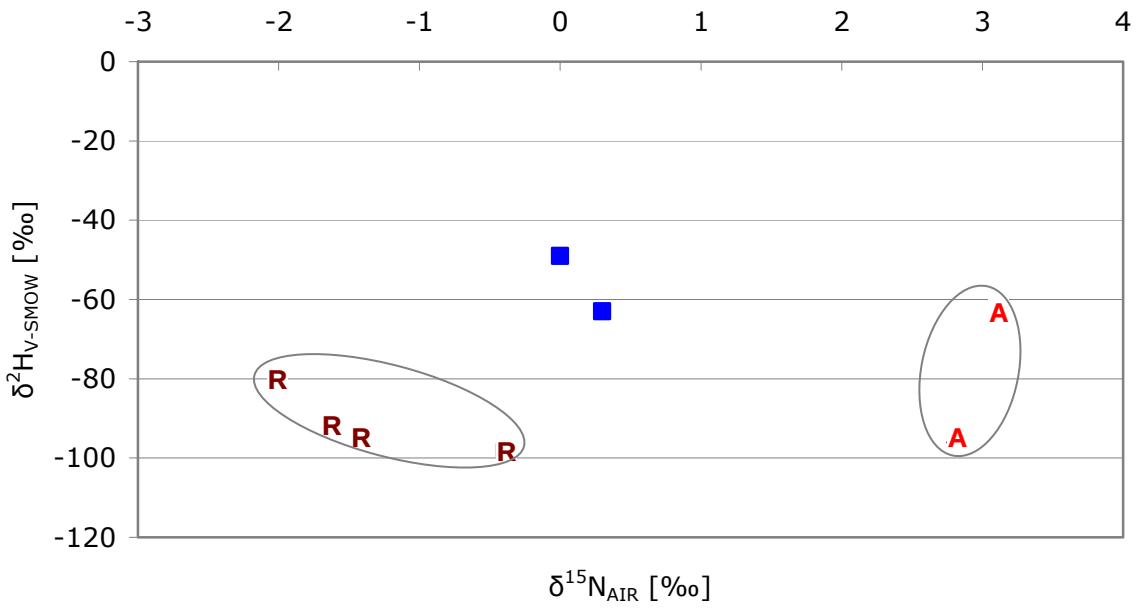

Figure 3-11: Correlation of $\delta^{15}N_{AIR}$ and $\delta^{2}H_{V\text{-}SMOW}$ values [‰] of 2-ethyl-5/6-methylpyrazine **8**/**9** from self-roasted arabica coffee (**A**), self-roasted robusta coffee (**R**) and synthetic references (■).

Because of their chromatographic co-elution, 2-ethyl-5/6-methylpyrazine (**8**/**9**) could not be measured separately by HRGC-IRMS. The $\delta^{15}N_{AIR}$ and $\delta^{2}H_{V\text{-}SMOW}$ data of self-roasted arabica and robusta coffees, as well as synthetic references of both substances **8 / 9,** are shown in Figure 3-11. Unfortunately, no 'declared to

be natural' reference was available. The synthetic samples **8**/**9** revealed $^{15}N/^{14}N$ ratios of 0.0 ‰ to 0.3 ‰ and $^{2}H/^{1}H$ ratios of -49 ‰ to -63 ‰, respectively. For **8**/**9**, from self-roasted Arabica and Robusta samples (n = 6), $\delta^{15}N_{AIR}$ and $\delta^{2}H_{VSMOW}$ values were measured from 3.1 ‰ to -2.0 ‰ and, from -64 ‰ to -98 ‰ in a relatively compact region, respectively. As for nitrogen isotope values, a difference of ca. 3 ‰ was observed between the arabica and robusta varieties, but the number of samples needs to be increased before making assured authenticity statements.

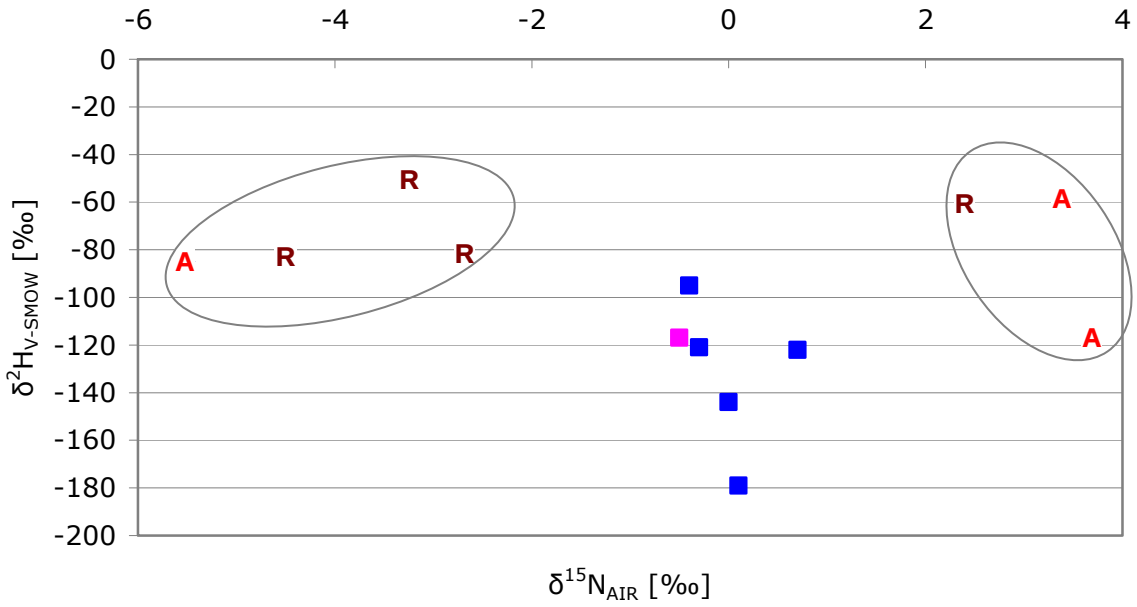

Figure 3-12: Correlation of $\delta^{15}N_{AIR}$ and $\delta^{2}H_{V\text{-}SMOW}$ values [‰] of 2-ethyl-3-methylpyrazine **10** from self-roasted arabica coffee (**A**), self-roasted robusta coffee (**R**), synthetic references (■) and 'declared to be natural' references (■).

All references of 2-ethyl-3-methylpyrazine (**10**), including a reference 'declared to be natural', showed a markedly narrow range for $\delta^{15}N_{AIR}$ values between 0.7 ‰ and -0.5 ‰ (Figure 3-12). The $\delta^{2}H_{V\text{-}SMOW}$ data differed between -95 ‰ and -179 ‰. This data is distinctly different from that observed for the robusta and arabica coffee samples under study. They ranged, in two separate groups, from 3.7 ‰ to -5.5 ‰ for $\delta^{15}N_{AIR}$ and from -49 ‰ to -119 ‰ for $\delta^{2}H_{V\text{-}SMOW}$. As **10** is an organoleptically attractive coffee constituent, this clear-cut distinction could be of interest in assessing its authenticity in coffee-flavoured products (see section 3.2.3).

2,3,5-Trimethypyrazine (**11**) was not detectable in sufficient amounts in each coffee sample for the HRGC-IRMS analysis. The correlation of $\delta^{15}N_{AIR}$ and $\delta^{2}H_{V\text{-}SMOW}$ data of **11** is outlined in Figure 3-13. The $\delta^{15}N_{AIR}$ and $\delta^{2}H_{V\text{-}SMOW}$ values from self-roasted coffees (two arabica and one robusta coffee varieties) varied

from 4.3 ‰ to 0.3 ‰ and from -42 ‰ to -98 ‰, respectively. A difference exceeding 3 ‰ between arabica and robusta was noticed, but the number of samples needs to be increased to be able to make assured statements on authenticity assessments. Measurements of synthetic references resulted in a more depleted range varying from -0.8 ‰ to -1.4 ‰ for $\delta^{15}N_{AIR}$ and from -113 ‰ to -182 ‰ for $\delta^{2}H_{V\text{-}SMOW}$. Two references 'declared to be natural' showed values of 0.6 ‰ and 0.2 ‰ for $\delta^{15}N_{AIR}$ as well as -109 ‰ and -143 ‰ for $\delta^{2}H_{V\text{-}SMOW}$, respectively.

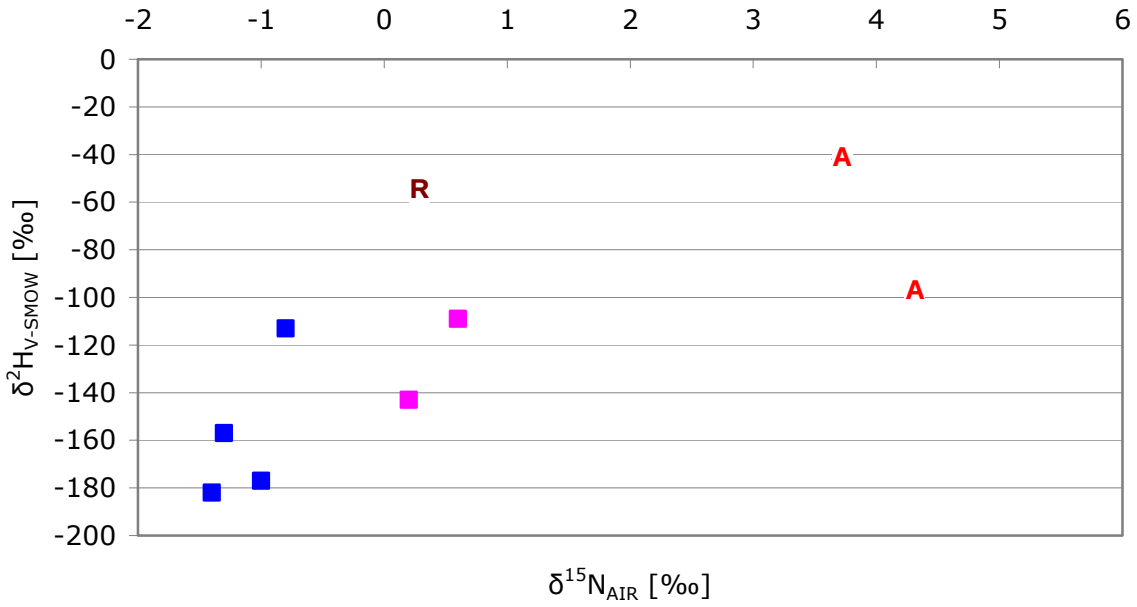

Figure 3-13: Correlation of $\delta^{15}N_{AIR}$ and $\delta^{2}H_{V\text{-}SMOW}$ values [‰] of 2,3,5-trimethylpyrazine **11** from self-roasted arabica coffee (**A**), self-roasted robusta coffee (**R**), synthetic references (■) and 'declared to be natural' references (■).

For 2-ethyl-3,5/6-dimethylpyrazine (**12**/**13**) only synthetic references (n=3) and self-roasted arabica samples (n=2) were available, as displayed in figure 3-14. The two arabica sample results were in a narrow range with $\delta^{15}N_{AIR}$ and $\delta^{2}H_{V\text{-}SMOW}$ values of 4.3 ‰ to 4.4 ‰ and -57 ‰ to -66 ‰, respectively. The references were found to have $\delta^{15}N_{AIR}$ values of -1.3 ‰ to 3.2 ‰ and $\delta^{2}H_{V\text{-}SMOW}$ values of -105 ‰ to -144 ‰.

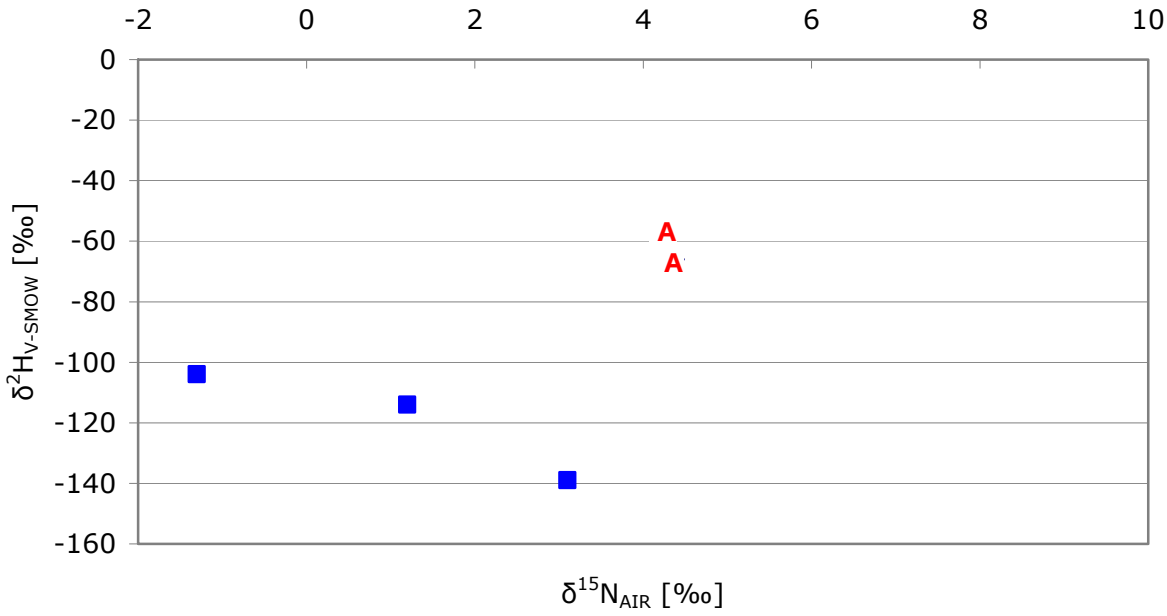

Figure 3-14: Correlation of $\delta^{15}N_{AIR}$ and $\delta^{2}H_{V\text{-}SMOW}$ values [‰] of 2-ethyl-3,5/6-dimethylpyrazine **12**/**13** from self-roasted arabica coffee (**A**) and synthetic references (■).

To extend these first insights into the authenticity assessment of selected coffee volatiles, further commercial products were analysed and compared to the already tested data. These results can be found in chapter 3.2.3.

3.2.3 $^{15}N/^{14}N$ and $^{2}H/^{1}H$ Analyses of Volatiles of Commercial Coffee Products

Different commercial products were analysed to extend the database of alkylpyrazines and pyridine, these being commercially available roast coffee bought in a local supermarket (▲), roast coffee from unspecified origins (◆), different types of coffee products, such as instant coffee or coffee drinks (●), coffee aromas (●) and one cocoa sample (✳).For comparison purposes, the values for self-roasted coffees, determined in chapter 3.2.1, are presented as shaded ellipses in the figures. The $\delta^{15}N_{AIR}$ and $\delta^{2}H_{V\text{-}SMOW}$ values of compound **1** to **14** are correlated in the following figures 3-15 to 3-25.

The correlation of $\delta^{15}N_{AIR}$ and $\delta^{2}H_{V\text{-}SMOW}$ values of pyridine (**1**) from different sources is outlined in figure 3-15. Commercially available roast coffee (n = 7), as well as roast coffee from unspecified origins (n = 4), provided the widest data range with $\delta^{15}N_{AIR}$ values of -1.6 ‰ to -35.7 ‰ and $\delta^{2}H_{V\text{-}SMOW}$ values of -53 ‰ to -117 ‰. The coffee products (n = 9) showed a less depleted region in its

data, similar to the self-roasted coffees, with $\delta^{15}N_{AIR}$ and $\delta^{2}H_{V\text{-}SMOW}$ values of -1.7 ‰ to -27.4 ‰ and -56 ‰ to -93 ‰, respectively. Two main points can be observed in this figure; firstly, the more depleted the $\delta^{15}N_{AIR}$ value of the sample, the more depleted the $\delta^{2}H_{V\text{-}SMOW}$ value is, and secondly, the synthetic references are clearly separated from the coffee samples in both the $^{15}N/^{14}N$ and $^{2}H/^{1}H$ data.

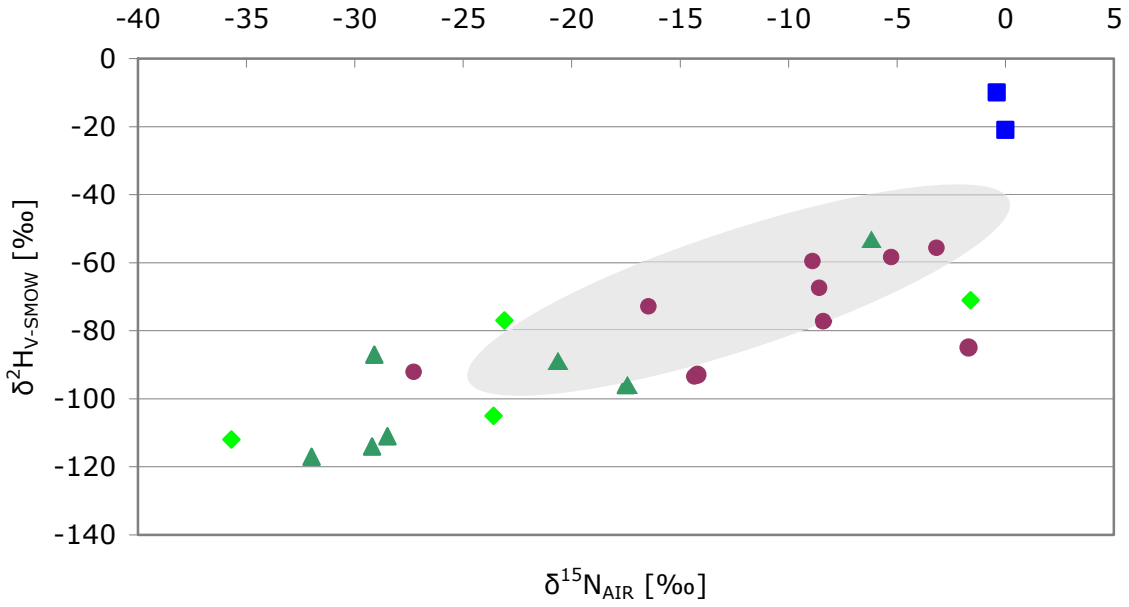

Figure 3-15: Correlation of $\delta^{15}N_{AIR}$ and $\delta^{2}H_{V\text{-}SMOW}$ values [‰] of pyridine **1** from commercially available roast coffee (▲), roast coffee from unspecified origins (◆), coffee products (●) and synthetic references (■). The shaded ellipse marks the region of arabica and robusta self-roasted coffees, already shown in figure 3-5.

As with the self-roasted coffee samples, pyrazine (**2**) was not available in sufficient amounts for analysis in all samples - these results are presented in figure 3-16. The commercially available roast coffees (n = 2) displayed $\delta^{15}N_{AIR}$ values of 0.2 ‰ to -7.5 ‰ and $\delta^{2}H_{V\text{-}SMOW}$ values of -34 ‰ to -72 ‰. For one roast coffee, of unspecified origin, a positive $^{2}H/^{1}H$ value was recorded as 3 ‰ ($^{15}N/^{14}N$ value = 0.9 ‰) and one coffee product was measured with $\delta^{15}N_{AIR}$ and $\delta^{2}H_{V\text{-}SMOW}$ values of -0.5 ‰ and -25 ‰, respectively. The synthetic reference again clearly differs from the coffee samples, but more data is again needed before an authenticity assessment can be performed.

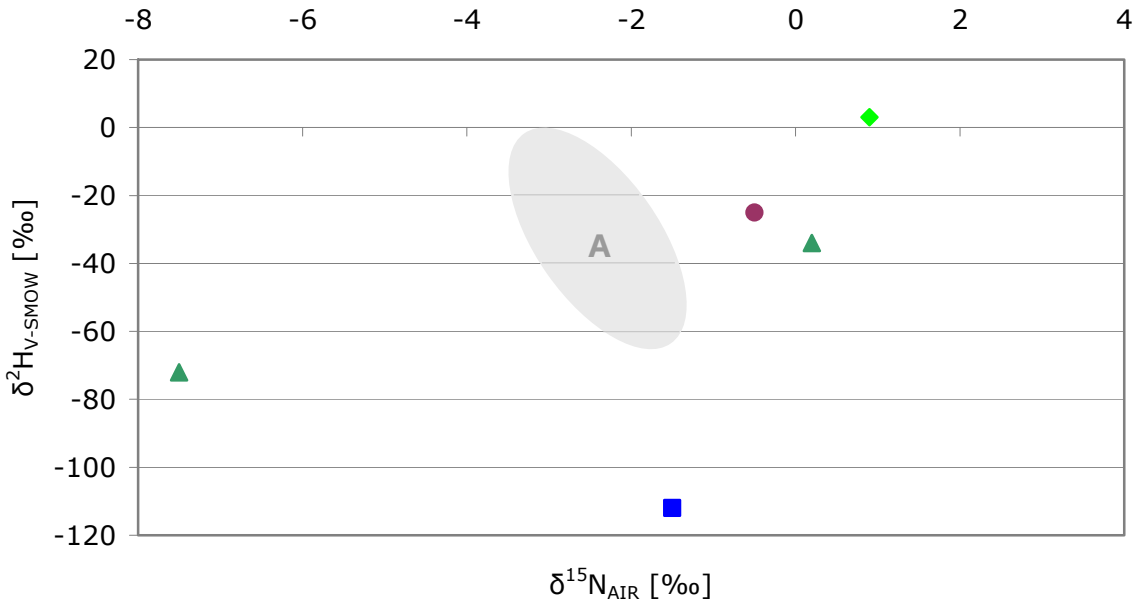

Figure 3-16: Correlation of $\delta^{15}N_{AIR}$ and $\delta^{2}H_{V\text{-}SMOW}$ values [‰] of pyrazine **2** from commercially available roast coffee (▲), roast coffee from unspecified origins (◆), coffee products (●) and synthetic references (■). The shaded ellipse marks the region of arabica self-roasted compounds (A), already shown in figure 3-6.

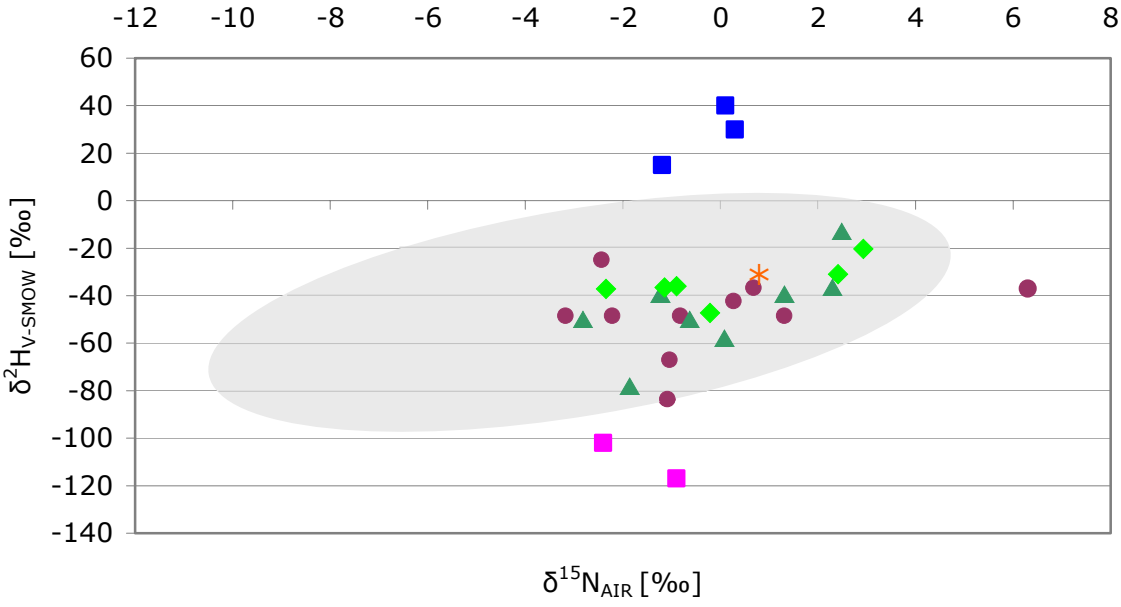

Figure 3-17: Correlation of $\delta^{15}N_{AIR}$ and $\delta^{2}H_{V\text{-}SMOW}$ values [‰] of 2-methylpyrazine **3** from commercially available roast coffee (▲), roast coffee from unspecified origins (◆), coffee products (●), cocoa sample (✳), synthetic references (■) and 'declared to be natural' references (■). The shaded ellipse marks the region of arabica and robusta self-roasted compounds, already shown in figure 3-7.

The $\delta^{15}N_{AIR}$ and $\delta^{2}H_{V\text{-}SMOW}$ values of 2-methylpyrazine (**3**) from commercially available roast coffee (n = 8), unspecified roast coffee samples (n = 6) and coffee products (n = 10), displayed in figure 3-18, are located in the region from 2.9 ‰ to -3.1 ‰ for $\delta^{15}N_{AIR}$ and from -13 ‰ to -83 ‰ for $\delta^{2}H_{V\text{-}SMOW}$, except for one coffee product which displayed values of 6.3 ‰ and -37 ‰, respectively. These values are in a far closer region than for self-roasted coffee samples. A clear-cut differentiation is found, from all coffee samples, between the synthetic references with strongly enriched $^{2}H/^{1}H$ values and the 'declared to be natural' references with depleted $^{2}H/^{1}H$ values of below -100 ‰. One roast cocoa sample with values of 0.8 ‰ ($\delta^{15}N_{AIR}$) and -30 ‰ ($\delta^{2}H_{V\text{-}SMOW}$) had similar values to the coffee samples.

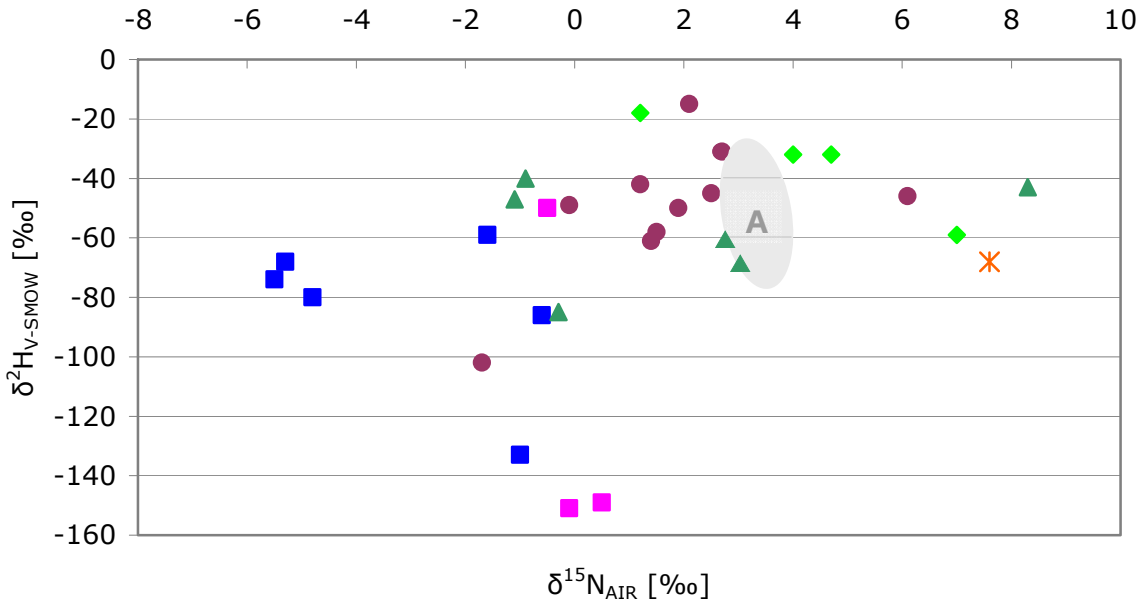

Figure 3-18: Correlation of $\delta^{15}N_{AIR}$ and $\delta^{2}H_{V\text{-}SMOW}$ values [‰] of 2,5/6-dimethylpyrazine **4**/**5** from commercially available roast coffee (▲), roast coffee from unspecified origins (◆), coffee products (●), cocoa sample (✳), synthetic references (■) and 'declared to be natural' refences (■). The shaded ellipse marks the region of arabica self-roasted compounds, already shown in figure 3-8.

The compounds 2,5/6-dimethylpyrazine (**4**/**5**) were not separable chromatographically and were, therefore, measured together; the correlation of their $\delta^{15}N_{AIR}$ and $\delta^{2}H_{V\text{-}SMOW}$ values is displayed in figure 3-18. For these compounds **4**/**5**, commercially available roast coffee (n = 6), roast coffee from unspecified origins (n = 4), coffee products (n = 10) and one cocoa sample were analysed. The commercially available roast coffees showed widespread $\delta^{15}N_{AIR}$ values of -1.1 ‰ to 8.3 ‰ and $\delta^{2}H_{V\text{-}SMOW}$ values of -40 ‰ to -85 ‰. The roast coffee

from unspecified origins showed slightly more enriched values of 1.2 ‰ to 7.0 ‰ ($\delta^{15}N_{AIR}$) and -18 ‰ to -59 ‰ ($\delta^{2}H_{V\text{-}SMOW}$). The coffee products displayed values in between these last two groups ($\delta^{15}N_{AIR}$ = -1.7 ‰ to 6.1 ‰; $\delta^{2}H_{V\text{-}SMOW}$ = -15 ‰ to -102 ‰) and the single cocoa sample showed a strongly enriched $^{15}N/^{14}N$ value of 7.6 ‰ and a $^{2}H/^{1}H$ value of -68 ‰. The references showed generally more depleted values in $^{15}N/^{14}N$ and $^{2}H/^{1}H$ than the coffee samples, however a clear-cut distinction was not possible.

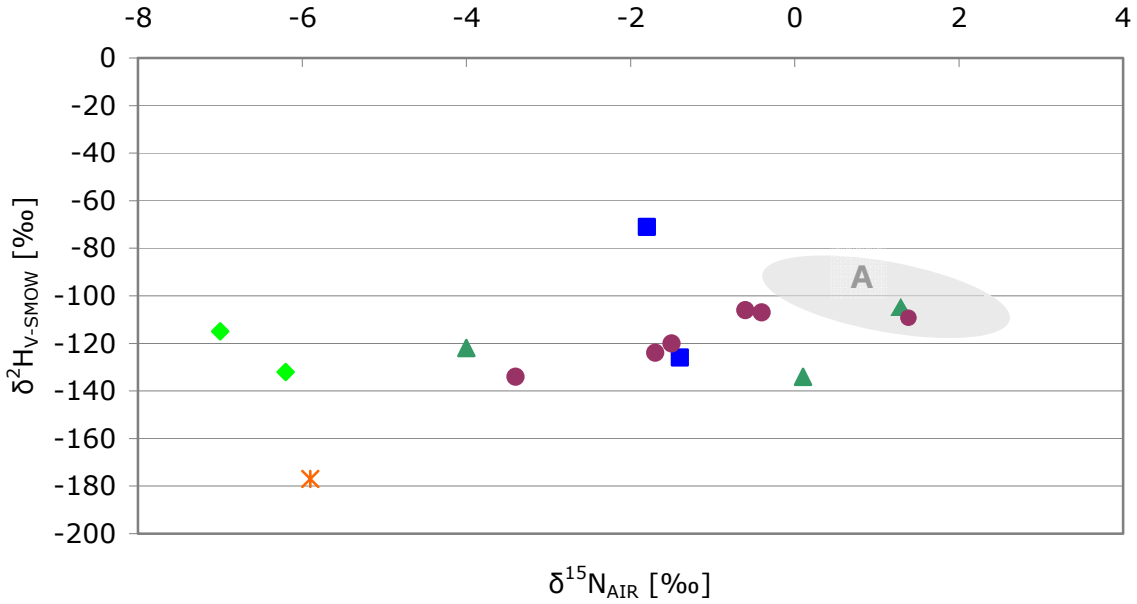

Figure 3-19: Correlation of $\delta^{15}N_{AIR}$ and $\delta^{2}H_{V\text{-}SMOW}$ values [‰] of 2-ethylpyrazine **6** from commercially available roast coffee (▲), roast coffee from unspecified origins (◆), coffee products (●), cocoa sample (✳) and synthetic references (■). The shaded ellipse marks the region of arabica self-roasted compounds, already shown in figure 3-9.

The correlation of $\delta^{15}N_{AIR}$ and $\delta^{2}H_{V\text{-}SMOW}$ data of 2-ethylpyrazine (**6**) from various origins is outlined in figure 3-19. Commercially available roast coffees (n = 3) ranged from 1.3 ‰ to -4.0 ‰ ($\delta^{15}N_{AIR}$); the $\delta^{2}H_{V\text{-}SMOW}$ data varied from -105 ‰ to -134 ‰. Other roast coffees (n = 2) showed more depleted $\delta^{15}N_{AIR}$ values of -6.2 ‰ to -7.0 ‰ and $\delta^{2}H_{V\text{-}SMOW}$ values of -115 ‰ to -132 ‰. The coffee products (n = 6) varied from 1.4 ‰ to -3.4 ‰ and -106 ‰ to -134 ‰ for $\delta^{15}N_{AIR}$ and $\delta^{2}H_{V\text{-}SMOW}$ values, respectively. The only cocoa sample was the most depleted in its $^{2}H/^{1}H$ ratio (-177 ‰) and displayed a $^{15}N/^{14}N$ ratio of -5.9 ‰. Most of the samples analysed here were more depleted in their $^{15}N/^{14}N$ ratios than the self-roasted samples. A differentiation with synthetic references was not possible.

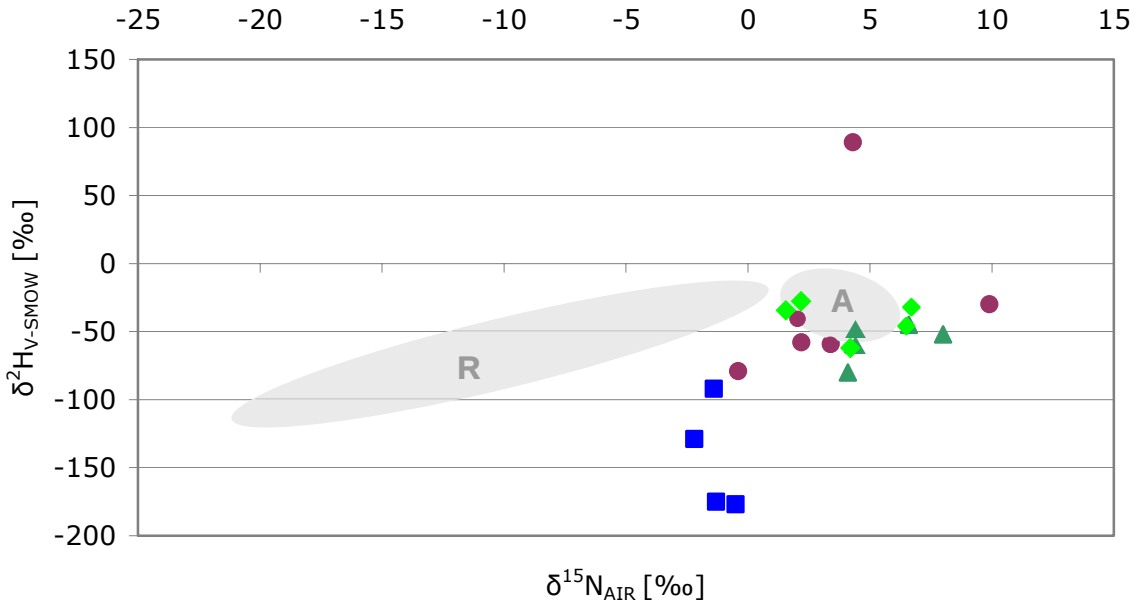

Figure 3-20: Correlation of $\delta^{15}N_{AIR}$ and $\delta^{2}H_{V\text{-}SMOW}$ values [‰] of 2,3-dimethylpyrazine **7** from commercially available roast coffee (▲), roast coffee from unspecified origins (◆), coffee products (●) and synthetic references (■). The shaded ellipse marks the regions of arabica (A) and robusta (R) self-roasted compounds, already shown in figure 3-10.

For 2,3-dimethylpyrazine (**7**) the results are displayed in figure 3-20. Commercially available coffees (n = 5) showed values concentrated in the region from 4.1 ‰ to 8.0 ‰ and -45 ‰ to -80 ‰ for $\delta^{15}N_{AIR}$ and $\delta^{2}H_{V\text{-}SMOW}$, respectively. Roast coffee from unspecified origins (n = 5) displayed similar values of $\delta^{15}N_{AIR}$ = 1.6 ‰ to 6.7 ‰ and $\delta^{2}H_{VSMOW}$ = -28 ‰ to -62 ‰. A wider range was found for coffee products with most being in the region of -0.4 ‰ to 9.9 ‰ ($\delta^{15}N_{AIR}$) and -30 ‰ to -79 ‰ ($\delta^{2}H_{VSMOW}$), with one product having a very enriched $^{2}H/^{1}H$ ratio of 89 ‰ ($\delta^{15}N_{AIR}$ = 4.3 ‰). Authenticity assessment seems to be promising for this compound, provided that extended data information will be available in the future, as most of the commercial coffees and products are in the range of arabica self-roasted coffees, providing significant differences to synthetic references.

With 2-ethyl-5/6-methylpyrazine (**8 / 9**) no chromatographic separation was possible. Thus, combined parameters **8 / 9** were measured with the correlation of $\delta^{15}N_{AIR}$ and $\delta^{2}H_{V\text{-}SMOW}$ data of commercial coffees and products being displayed in figure 3-21. With the exception of one commercial sample ($\delta^{15}N_{AIR}$ value of 6.5 ‰ and $\delta^{2}H_{V\text{-}SMOW}$ of -26 ‰), all other commercial coffees (n = 6) exhibited data in the same $\delta^{15}N_{AIR}$ range as self-roasted samples, but with more depleted $\delta^{2}H_{V\text{-}SMOW}$ values (from -101 ‰ to -127 ‰). The unspecified roast coffees (n =

7) varied from 0.0 ‰ to 4.7 ‰ and -75 ‰ to -110 ‰ for $\delta^{15}N_{AIR}$ and $\delta^{2}H_{V\text{-}SMOW}$, respectively. The coffee products (n = 8), again with the exception of one sample ($^{15}N/^{14}N$ ratio 9.5 ‰ and $^{2}H/^{1}H$ ratio -95 ‰), were once more found to be in the region of the self-roasted samples, with $\delta^{15}N_{AIR}$ values of -0.1 ‰ to 2.9 ‰ and $\delta^{2}H_{V\text{-}SMOW}$ values of -84 ‰ to -103 ‰. The single cocoa sample showed a relatively depleted $^{2}H/^{1}H$ ratio of -126 ‰ and a $^{15}N/^{14}N$ ratio of -0.3 ‰.

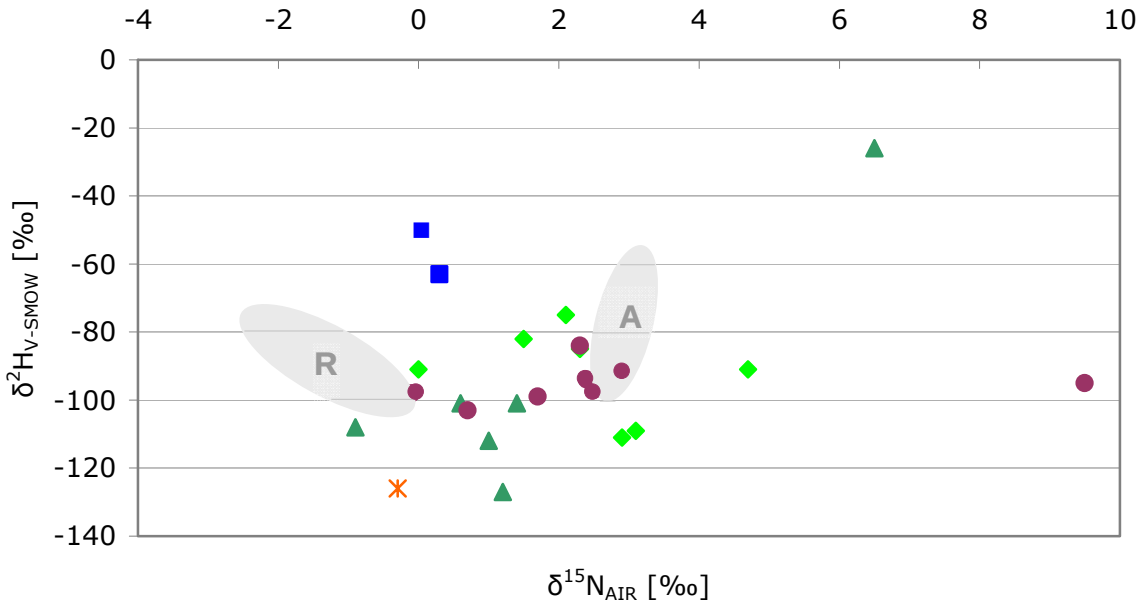

Figure 3-21: Correlation of $\delta^{15}N_{AIR}$ and $\delta^{2}H_{V\text{-}SMOW}$ values [‰] of 2-ethyl-5/6-methylpyrazine **8**/**9** from commercially available roast coffee (▲), roast coffee from unspecified origins (◆), coffee products (●), cocoa sample (✳) and synthetic reference (■). The shaded ellipse marks the regions of arabica (A) and robusta (R) self-roasted compounds, already shown in figure 3-11.

The data for 2-ethyl-3-methylpyrazine (**10**) from the self-roasted coffees in figure 3-12 was promising for the distinction between 'natural' and synthetic references. Commercially available roast coffees (n = 4), as shown in figure 3-22, varied between the two self-roasted groups with values of -4.7 ‰ to 1.0 ‰ for $\delta^{15}N_{AIR}$ and -62 ‰ to -92 ‰ for $\delta^{2}H_{V\text{-}SMOW}$. Unspecified roast coffees (n = 4) were spread even further with values for $\delta^{15}N_{AIR}$ and $\delta^{2}H_{V\text{-}SMOW}$ of -7.1 ‰ to 1.6 ‰ and -87 ‰ to -107 ‰, respectively. The $\delta^{15}N_{AIR}$ and $\delta^{2}H_{V\text{-}SMOW}$ data for coffee products (n = 10) ranged between -4.4 ‰ to 2.2 ‰ and -76 ‰ to -125 ‰, respectively, and for coffee aromas (n = 4) values of -1.5 ‰ to 0.9 ‰ ($\delta^{15}N_{AIR}$) and -138 ‰ to -105 ‰ ($\delta^{2}H_{V\text{-}SMOW}$) were recorded. A clear-cut distinction found between the self-roasted coffees and references was, unfortunately, not definitive when analysing the other coffee samples, as these were too close to the references in the $^{15}N/^{14}N$ ratios.

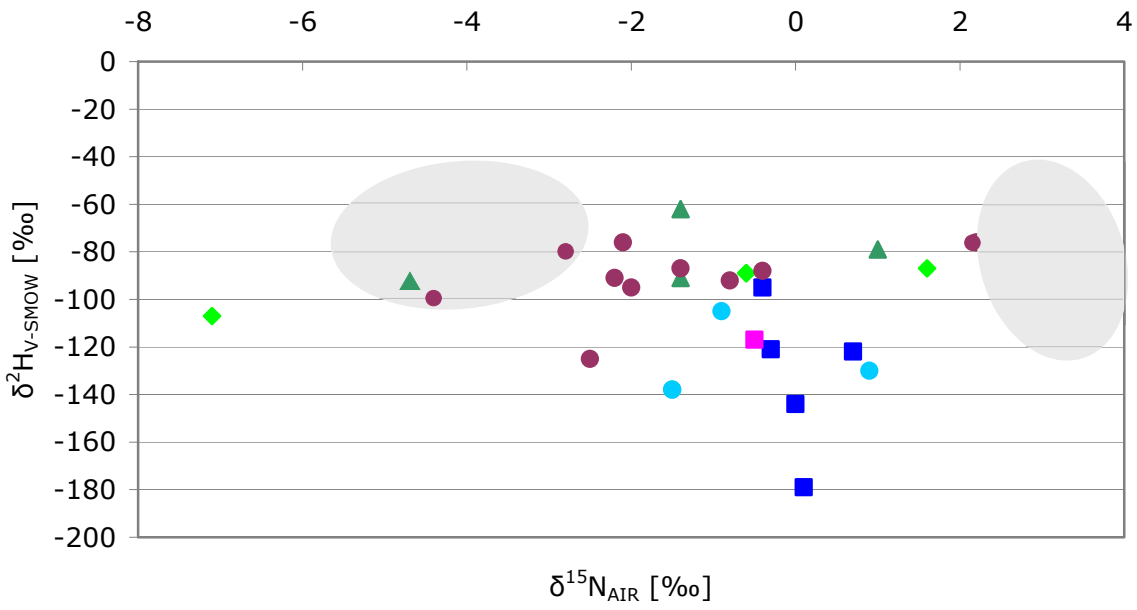

Figure 3-22: Correlation of $\delta^{15}N_{AIR}$ and $\delta^{2}H_{V\text{-}SMOW}$ values [‰] of 2-ethyl-3-methylpyrazine **10** from commercially available roast coffee (▲), roast coffee from unspecified origins (◆), coffee products (●), coffee aroma (●), synthetic references (■) and 'declared to be natural' references (■). The shaded ellipse marks the regions of arabica and robusta self-roasted compounds, already shown in figure 3-12.

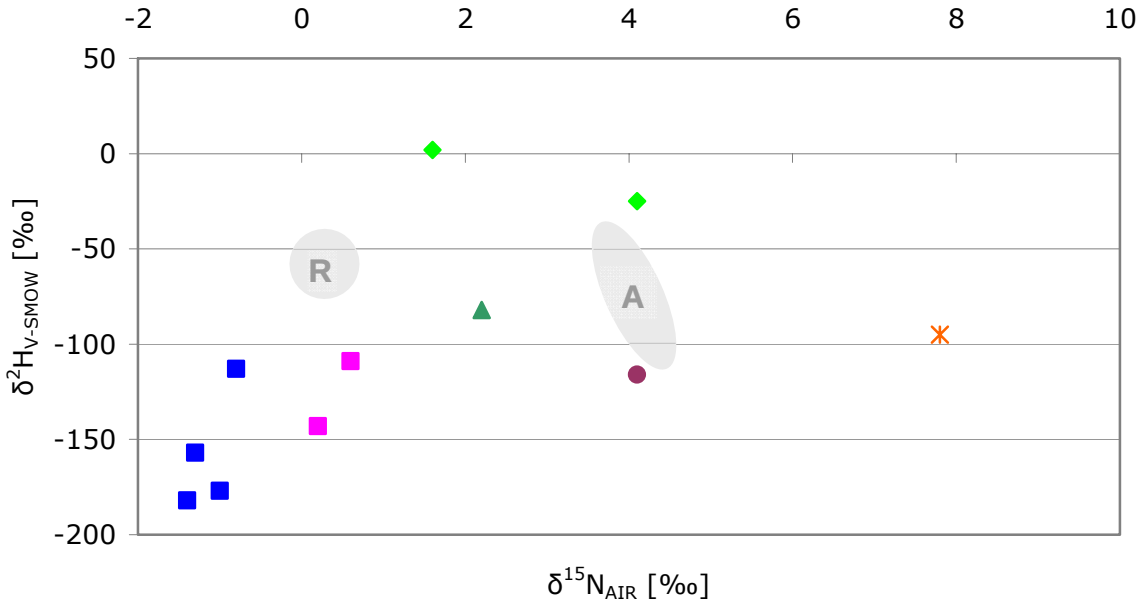

Figure 3-23: Correlation of $\delta^{15}N_{AIR}$ and $\delta^{2}H_{V\text{-}SMOW}$ values [‰] of 2,3,5-trimethylpyrazine **11** from commercially available roast coffee (▲), roast coffee from unspecified origins (◆), coffee products (●), cocoa sample (✳), synthetic references (■) and 'declared to be natural' references (■). The shaded ellipse marks the regions of arabica (A) and robusta (R) self-roasted compounds, already shown in figure 3-13.

2,3,5-Trimethylpyrazine (**11**) was not found in many roast coffees or products, with the results of the analyses being found in figure 3-23. One commercial roast coffee was located between the robusta and arabica samples based on its values of 2.2 ‰ for $\delta^{15}N_{AIR}$ and -82 ‰ for $\delta^{2}H_{V\text{-}SMOW}$. Two unspecified roast coffees displayed similar $^{15}N/^{14}N$ ratios as the self-roasted coffees with values of 1.6 ‰ to 4.1 ‰ but with more enriched $^{2}H/^{1}H$ ratios of 2 ‰ to -25 ‰. One coffee product displayed $\delta^{15}N_{AIR}$ and $\delta^{2}H_{V\text{-}SMOW}$ values of 4.1 ‰ and -116 ‰, respectively. One cocoa sample showed the most enriched $\delta^{15}N_{AIR}$ value of all samples (7.8 ‰) and a $\delta^{2}H_{V\text{-}SMOW}$ value of -95 ‰.

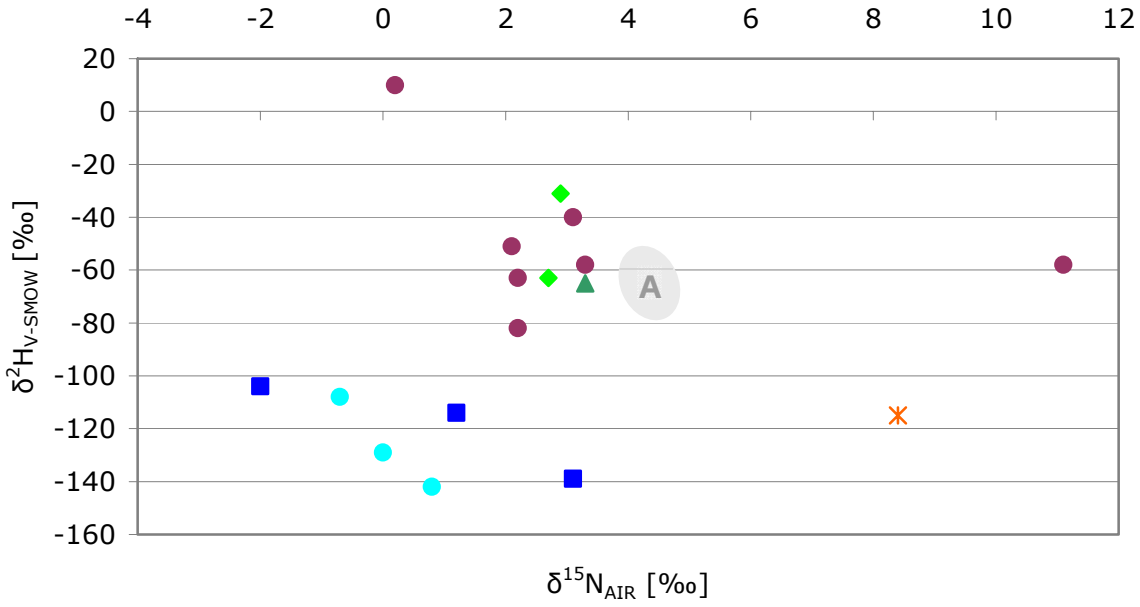

Figure 3-24: Correlation of $\delta^{15}N_{AIR}$ and $\delta^{2}H_{V\text{-}SMOW}$ values [‰] of 2-ethyl-3,5/6-dimethylpyrazine **12**/**13** from commercially available roast coffee (▲), roast coffee from unspecified origins (◆), coffee products (●), coffee aroma (●), cocoa sample (✳) and synthetic references (■). The shaded ellipse marks the regions of arabica (**A**) self-roasted compounds, already shown in figure 3-14.

For 2-ethyl-3,5/6-dimethylpyrazine (**12**/**13**) commercial roast coffee (n = 1), roast coffee from unspecified origins (n = 2), coffee products (n = 7), coffee aroma (n = 3) and one cocoa sample were measured and the results displayed in figure 3-24. All samples, except the cocoa sample ($\delta^{15}N_{AIR}$ = 8.4 ‰ and $\delta^{2}H_{V\text{-}SMOW}$ = -115 ‰) and one coffee product showed more depleted $^{15}N/^{14}N$ ratios than the analysed self-roasted arabicas. The roast coffees (commercial and unspecified) displayed $\delta^{15}N_{AIR}$ values of 2.7 ‰ to 3.3 ‰ and $\delta^{2}H_{V\text{-}SMOW}$ values of -31 ‰ to -65 ‰. The coffee products showed, except for two samples, similar data to the roast coffees with $^{15}N/^{14}N$ ratios of 0.2 ‰ to 11.1 ‰ and $^{2}H/^{1}H$ ratios of 10 ‰ to -82 ‰. The coffee aromas were placed between the synthetic references with $\delta^{15}N_{AIR}$ and $\delta^{2}H_{V\text{-}SMOW}$ values of 0.8 ‰ to -0.7 ‰ and -108 ‰ to

-142 ‰, respectively. With the correlation of $\delta^{15}N_{AIR}$ and $\delta^{2}H_{V\text{-}SMOW}$ data a slight distinction between roast coffees and synthetic references is possible.

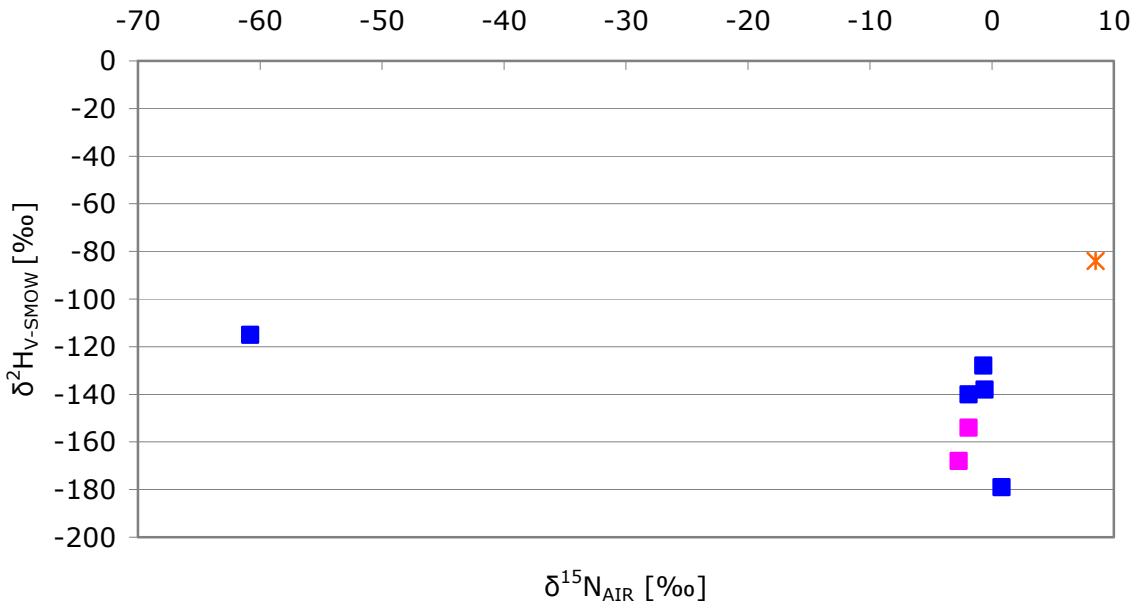

Figure 3-25: Correlation of $\delta^{15}N_{AIR}$ and $\delta^{2}H_{V\text{-}SMOW}$ values [‰] of 2,3,5,6-tetramethylpyrazine **14** from cocoa sample (✳), synthetic references (■) and 'declared to be natural' references (■).

2,3,5,6-Tetramethylpyrazine (**14**) was found only in roast cocoa, with the correlation for $\delta^{15}N_{AIR}$ and $\delta^{2}H_{V\text{-}SMOW}$ values of references and one cocoa sample being shown in figure 3-26. The synthetic (n = 5) and 'declared to be natural' (n = 2) references showed, except for one interesting synthetic reference ($\delta^{15}N_{AIR}$ = -60.8 ‰ and $\delta^{2}H_{V\text{-}SMOW}$ = -115 ‰) a narrow $\delta^{15}N_{AIR}$ region of -2.7 ‰ to 0.8 ‰ and a $\delta^{2}H_{V\text{-}SMOW}$ range of -128 ‰ to -179 ‰. The cocoa sample showed slightly enriched values in both the $^{15}N/^{14}N$ ratio (8.5 ‰) and the $^{2}H/^{1}H$ ratio (-84 ‰).

3.2.4 Aroma Profile and $^{15}N/^{14}N$, $^{2}H/^{1}H$ and $^{13}C/^{12}C$ Analyses of Roast Coffee Volatiles of Different Roasting Degrees

To extend these first insights into the authenticity assessment of selected coffee volatiles and to ascertain the influence of the degree of roasting on the $^{15}N/^{14}N$, $^{2}H/^{1}H$ and $^{13}C/^{12}C$ ratios, a green arabica coffee sample was roasted to three different grades - 'light', 'middle' and 'dark' - and the aroma profiles and isotope values compared with each other. This step was necessary to be able to evaluate the recently obtained data from the coffee samples, in the hope of explaining

some of the unclear data, such as the extreme values of pyridine (**1**) and 2,3-dimethylpyrazine (**7**).

Initially, the aroma profiles of the three roasts, 'light', 'medium' and 'dark' were obtained and the compounds **1** to **10**, therein, compared; the chromatograms are shown in figure 3-26.

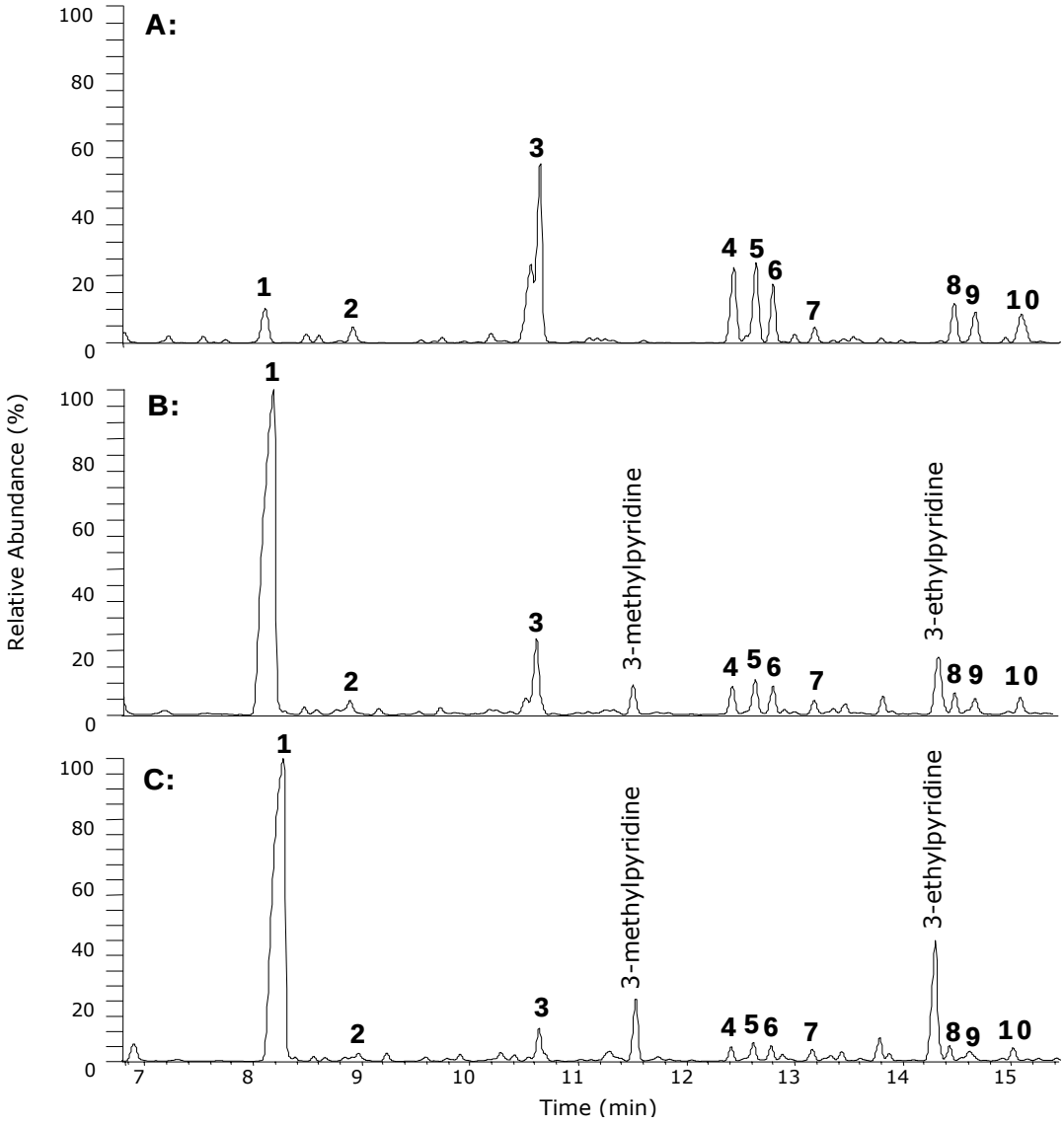

Figure 3-26: Representative HRGC-MS total ion chromatogram (sector) of roasted coffee bean (*Coffea arabica* L.) volatiles of A: 'light' roast, B: 'medium' roast and C: 'dark' roast. The peak numbers indicate the compounds under IRMS study, **1** pyridine, **2** pyrazine, **3** 2-methylpyrazine, **4** 2,5-dimethylpyrazine, **5** 2,6-dimethylpyrazine, **6** 2-ethylpyrazine, **7** 2,3-dimethylpyrazine, **8** 2-ethyl-5-methylpyrazine, **9** 2-ethyl-6-methylpyrazine, **10** 2-ethyl-3-methylpyrazine

The three roasting types varied only in their roasting time, with the roasting temperature, in all three cases, being the same. In each of the roasts all ten compounds were identified. For the 'light' roast the main component identified was 2-methylpyrazine (**3**), with only small amounts of pyridine (**1**) present. In the 'medium' roast, which had a slight burnt note to the nose, a different picture was noted. Compounds **3** to **10** displayed the same ratio amounts between each other, pyrazine (**2**) being slightly less and pyridine (**1**) being the dominant compound. Furthermore, two new compounds were detected - 3-methylpyridine and 3-ethylpyridine. The 'dark' roast, with a very dominant burnt odour, showed the pyridine compounds **1**, 3-methylpyridine and 3-ethylpyridine as the abundant volatiles in this sector of the aroma extract. The amounts of these components were higher than in the 'medium' roast, with pyrazine being almost non-detectable, whilst all the other compounds **3**-**10** maintained a similar range, as before.

The roasting studies have shown that the duration of roasting has an effect on the formation and the amount of aroma compounds. The darker the roast, the more pyridine and substituted pyridines were found, with the amounts increasing relative to the duration of the roast. On the other hand, most of the alkylpyrazines maintained stable quantities, aside from pyrazine, which decreased with increasing length of the roast. These results lead to a further question – 'How does this different formation behaviour influence the stable isotope values of the compounds'.

In figure 3-27 the $\delta^{15}N_{AIR}$ values of the compounds **1**, **2**, **3**, **4**/**5**/**6**, **7**, **8**/**9**, **10** of the three roasts were compared. Due to lacking chromatographic separation the two groups of compounds **4**, **5** and **6**, as well as **8** and **9**, were measured as combined parameters. Generally, it can be seen that the $\delta^{15}N_{AIR}$ values of all roasts rose from pyridine (**1**) ('medium' roast $^{15}N/^{14}N$ ratio = -7.5 ‰) to 2-ethyl-3-methylpyrazine (**10**) ('medium' roast $^{15}N/^{14}N$ ratio = 7.3 ‰), with only compound **8**/**9** not maintaining this trend. This means, therefore, that the more an alkylpyrazine is substituted, the more enriched is its $\delta^{15}N_{AIR}$ value. One further interesting behaviour was noted between the different roasts: compounds **2**, **3**, **4**/**5**/**6**, **7** and **10** showed no large differences between their $\delta^{15}N_{AIR}$ values for 'light', 'medium' or 'dark' roast, with the maximum difference being 1 ‰. Pyridine (**1**) displayed its maximal depletion in the 'medium' roast (-7.5 ‰), with longer roasting leading to its maximal enrichment (-1.0 ‰) in the 'dark' roast. Measurement errors for compound **1** can be excluded due to multiple measurement rows at different times. The enrichment of **1** in the 'dark' roast compared to the 'medium' roast must lie in the utilisation of other, more enriched amino-precursors during the length of the roast. Compound **8**/**9** showed

its strongest enrichment in the light roast, with the $^{15}N/^{14}N$ ratio being the highest measured of all compounds in all roasts (9.2 ‰). This value then dropped significantly in the 'medium' roast (0.7 ‰), and was further, but only slightly, depleted in the 'dark' roast (0.4 ‰). This tendency was unclear, however, as the isomeric compound **10** displayed constant values in all roasts.

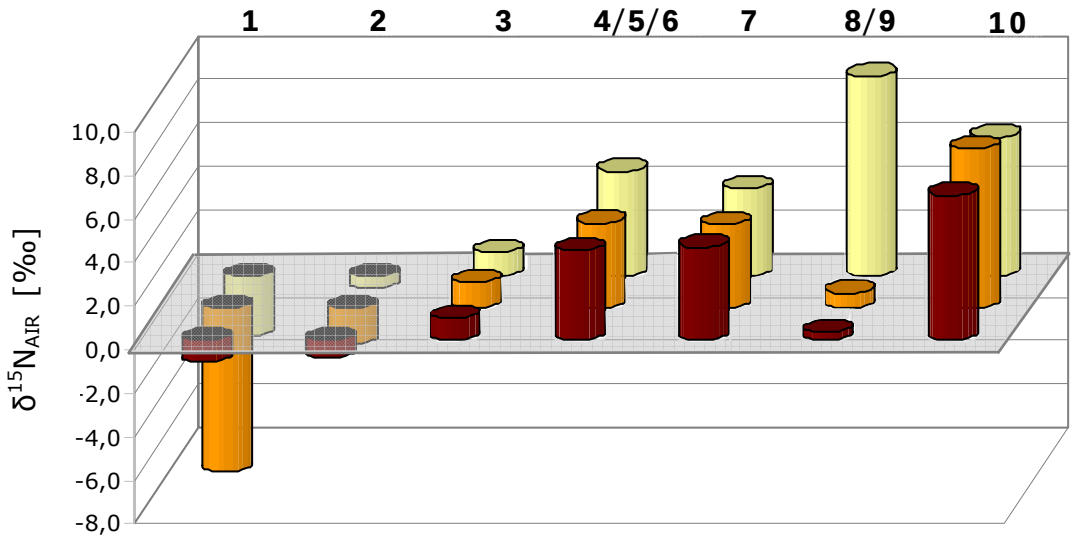

Figure 3-27: $\delta^{15}N_{AIR}$ values [‰] of □: 'light' roast, ■: 'medium' roast and ■: 'dark' roast coffee. The numbers indicate the compounds under IRMS study, **1** pyridine, **2** pyrazine, **3** 2-methylpyrazine, **4** 2,5-dimethylpyrazine, **5** 2,6-dimethylpyrazine, **6** 2-ethylpyrazine, **7** 2,3-dimethylpyrazine, **8** 2-ethyl-5-methylpyrazine, **9** 2-ethyl-6-methylpyrazine, **10** 2-ethyl-3-methylpyrazine

For $\delta^2H_{V\text{-}SMOW}$ values, a slightly different picture was observed, as displayed in figure 3-28. For the 'light' roast the most enriched compound was pyrazine (**2**, $^2H/^1H$ ratio = -75 ‰), with the 'light' roast generally showing the most stable $^2H/^1H$ ratios, varying from -75 ‰ to -109 ‰. The 'medium' roast provided its $^2H/^1H$ ratio maximum with pyrazine (**2**, $\delta^2H_{V\text{-}SMOW}$ = -3 ‰), once again the most enriched compound, and its minimum with 2,3-dimethylpyrazine (**7**, $\delta^2H_{V\text{-}SMOW}$ = -103 ‰). The 'dark' roast had its most enriched $\delta^2H_{V\text{-}SMOW}$ value of -6 ‰ with compound **3**, and its most depleted $\delta^2H_{V\text{-}SMOW}$ value of -88 ‰ with compound **7**. In general the $\delta^2H_{V\text{-}SMOW}$ values increased from the 'light' roast to the 'dark' roast. Concerning single compounds, only compound **7** displayed constant values over all three roasts. For compounds **1**, **3**, **4**/**5**/**6** and **8**/**9**, a strong tendency to enrichment was noticed from 'light' towards 'dark' roasts. Compounds **2** and **10** provided their most enriched values in the 'medium' roast.

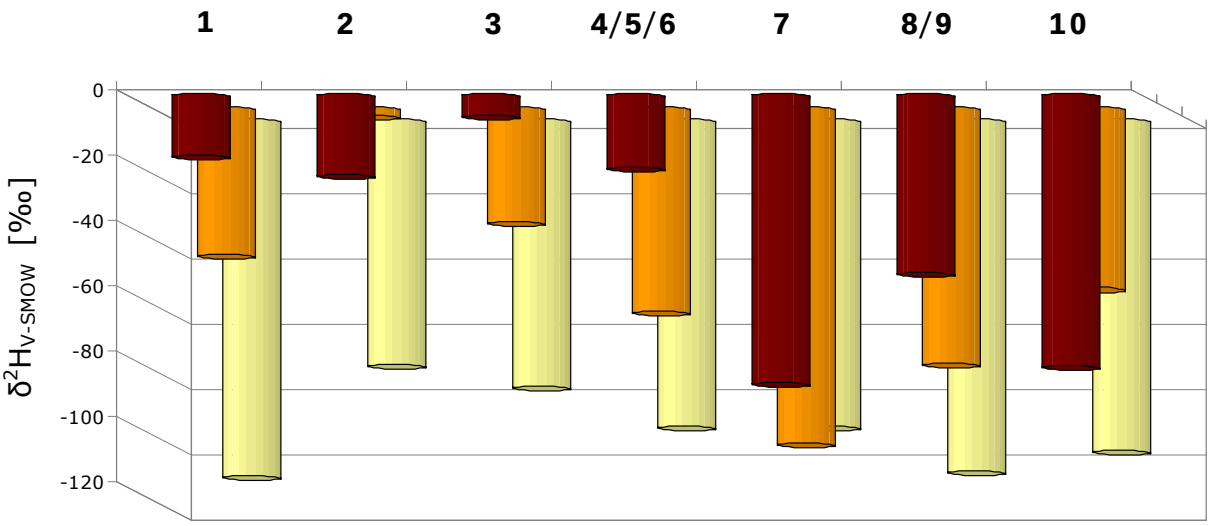

Figure 3-28: $\delta^2H_{V\text{-}SMOW}$ values [‰] of □: 'light' roast, ■: 'medium' roast and ■: 'dark' roast coffee. The numbers indicate the compounds under IRMS study, **1** pyridine, **2** pyrazine, **3** 2-methylpyrazine, **4** 2,5-dimethylpyrazine, **5** 2,6-dimethylpyrazine, **6** 2-ethylpyrazine, **7** 2,3-dimethylpyrazine, **8** 2-ethyl-5-methylpyrazine, **9** 2-ethyl-6-methylpyrazine, **10** 2-ethyl-3-methylpyrazine

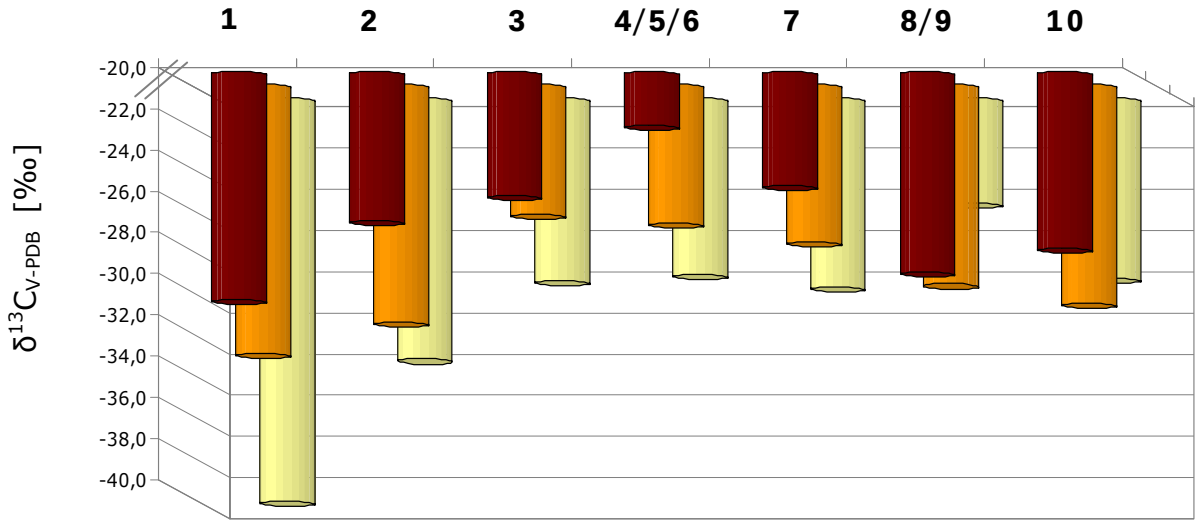

Figure 3-29: $\delta^{13}C_{V\text{-}PDB}$ values [‰] of □: 'light' roast, ■: 'medium' roast and ■: 'dark' roast coffee. The numbers indicate the compounds under IRMS study, **1** pyridine, **2** pyrazine, **3** 2-methylpyrazine, **4** 2,5-dimethylpyrazine, **5** 2,6-dimethylpyrazine, **6** 2-ethylpyrazine, **7** 2,3-dimethylpyrazine, **8** 2-ethyl-5-methylpyrazine, **9** 2-ethyl-6-methylpyrazine, **10** 2-ethyl-3-methylpyrazine

Figure 3-29 displays the $\delta^{13}C_{V\text{-}PDB}$ values of the compounds **1** to **10** in the 'light', 'medium' and 'dark' roasts. Large differences weren't expected between the

values, as the $^{13}C/^{12}C$ ratios were expected to derive from sugars, which should have very similar values. Surprisingly enough, the $\delta^{13}C_{V\text{-}PDB}$ values ranged from -39.6 ‰ to -22.6 ‰, with the most depleted, in all three roasts, being pyridine (**1**). For compounds **1** to **7** the 'dark' roast was the most enriched and the 'light' roast the most depleted, whereas compounds **8**/**9** had their most depleted $^{13}C/^{12}C$ ratio in the 'medium' and 'dark' roast ($\delta^{13}C_{V\text{-}PDB}$ = -29.7 ‰), with compound **10** having its most depleted $^{13}C/^{12}C$ ratio in the 'medium' roast ($\delta^{13}C_{V\text{-}PDB}$ = -30.6 ‰). In general the 'dark' roast was more enriched than the 'light' roast.

3.2.5 Conclusion

3.2.5.1 Conclusion to $^{15}N/^{14}N$ and $^{2}H/^{1}H$ Analyses of Roasted Coffee Beans and Products

For the alkylpyrazines **1**-**14** a database was constructed, for the first time, with many analyses performed, using roast coffee samples and coffee products. The stable isotope data for alkylpyrazines seems promising, as neither the $\delta^{2}H_{V\text{-}SMOW}$ nor the $\delta^{15}N_{AIR}$ values of these compounds were known before.

For compound **1** a distinction between synthetic references and roast coffee was evident, with many commercial coffees and products being in the same range as self-roasted coffees. Compound **2** also showed a distinction between those coming from synthetic references and those from roast coffee, but the number of samples proved insufficient for making a clear statement. For alkylpyrazine **3**, a distinction between synthetic references, natural references and roast coffee samples and products was noticed, with the $^{2}H/^{1}H$ ratios being enriched for synthetic references, depleted for 'declared to be natural' references with all roast coffee samples being located in between. The commercial samples and products exhibited an even tighter distribution in their isotope values than the self-roasted samples. A differentiation between coffee **3** and reference **3** was possible.

A promising differentiation was found for compounds **4**/**5** from self-roasted arabica coffees and the references, but this difference was, unfortunately, missing from other coffee samples, with a few of them showing very similar values to those of the references. The same case was found for compound **6,** with promising results regarding the values of the references and the self-roasted arabica beans, but the results from commercial coffees and coffee

products were interwoven with both self-roasted coffees and synthetic references.

Interesting results were obtained for alkylpyrazine **7**. A difference was seen for both self-roasted coffees and references, with robusta coffees having negative $\delta^{15}N_{AIR}$ values, arabica having positive values and references positioned in between, with slightly more depleted $\delta^{15}N_{AIR}$ values. Noticeable, also, was the similarity of range between the robusta self-roasted coffees of compound **7** and **1**. The commercial coffees and products displayed values mostly in a narrow range, around those of the values for arabica roast coffees.

Compound **8**/**9** showed a difference of arabica and robusta self-roasted coffees of 2 ‰, both differing also from the only synthetic reference. The other measured samples were found mostly in a region located between arabica and robusta coffees, with significant differences to the synthetic reference.

Compound **10** showed a clear-cut distinction between the self-roasted coffees and references, as well as a difference of 3 ‰ in the $\delta^{15}N_{AIR}$ values between the two self-roasted groups, whereas the other measured commercial samples and products showed values between those of arabica and robusta, slightly overlapping with those of the references. An explanation for the strongly depleted arabica sample and the enriched robusta sample, cannot be found, measurement mistakes can be excluded. Coffee aromas had isotope values around the values of the references.

Compound **11** was not measured in all samples, so that the data for this alkylpyrazines is scarce. A distinction was seen between arabica and robusta in a few samples and also a difference between these and the references. The few other coffee samples measured were found to be in the region of the self-roasted samples. Alkylpyrazines **12**/**13** were analysed and a difference found between arabica self-roasted coffees and the references. The commercial coffee samples and coffee products were found, mostly, to have similar values to the arabica coffees, with the coffee aromas having, as with compound **10**, similar values to those of the references. Compound **14** showed an extraordinarily depleted reference in the $^{15}N/^{14}N$ ratio, otherwise, only the cocoa sample contained this compound, which differed clearly from the references.

The findings of this study demonstrate that an analytical differentiation between synthetic references, most ranging in the area of ± 0 ‰ for $\delta^{15}N_{AIR}$, and coffee bean derived alkylpyrazines, is possible. Analytical differences between robusta and arabica were clearly noticeable in the case of one compound **8**/**9**, whereas

some compounds detected no differentiation at all, with yet again others requiring more samples for analysis. The differences in the $\delta^{15}N_{AIR}$ values of some of the alkylpyrazines between arabica and robusta samples remain unclear. The reasons might be found in the different amounts and different $\delta^{15}N_{AIR}$ values of participating amino acids in arabica and robusta coffees (Werner and Schmidt, 2002), with aspartic acid, glutamic acid and amide-N showing enriched $\delta^{15}N_{AIR}$ values, and serine and glycine having depleted $\delta^{15}N_{AIR}$ values (Medina and Schmidt, 1982). Furthermore, the reason for the strong depletion in the $\delta^{15}N_{AIR}$ values of compound **1** and **7** remains unclear.

The $\delta^{2}H_{V\text{-}SMOW}$ values of alkylpyrazines from roast coffee and products from -10 ‰ to -140 ‰ display their origin of amino acids ($\delta^{2}H_{V\text{-}SMOW}$ = -50 ‰) and carbohydrates ($\delta^{2}H_{V\text{-}SMOW}$ = -110 ‰) (Schmidt et al., 2003). It is widely accepted, that the amino acids only contribute their N-atom to the pyrazine molecule and that the carbon derives from the carbohydrate component (Koehler et al., 1969; Yaylayan and Keyhani, 2001 a; Totlani and Peterson, 2005), although, when no carbohydrates are present amino acids produce alkylpyrazines via thermal degradation (Wang and Odell, 1973; Yaylayan and Keyhani, 2001 b). In these carbohydrates the intramolecular deuterium and carbon distribution is different, with i.e. glucose showing the highest deuterium enrichment on the C-4 and C-5 atoms and the greatest depletion on C-6 (Martin et al., 1986; Schleucher at al., 1999; Zhang et al., 2002) and also the highest carbon enrichment on the C-3 and C-4 atoms and depletion on C-1 and C-6 atoms (Rossmann et al., 1991; Gleixner and Schmidt, 1997). Further research, with labelled carbohydrates, from Totlani and Peterson (2005) and Yaylayan and Keyhani (2001 a) showed that alkylpyrazines consisted of intact di-carbon and tri-carbon sugar fragmentation pieces, with these contributing different amounts to the alkylpyrazines. The large differences between the hydrogen and carbon values of certain compounds can derive, therefore, not only from different educts with different isotope values, but also from the fragments of these, displaying different isotope values. In the end the actual isotope pattern of compounds depends on the actual metabolic status of the plant and metabolic fluxes.

3.2.5.2 Conclusion to $^{15}N/^{14}N$, $^{2}H/^{1}H$ and $^{13}C/^{12}C$ Analyses of Roast Coffee Volatiles of Different Roasting Degrees

The most predominant observation in these roasting studies, concerning the alkylpyrazine and alkylpyridine distribution, was the large difference in content of pyridine (**1**) and the growing content of 3-methylpyridine and 3-ethylpyridine from ‘light’ to ‘dark’ roast. It is widely accepted that the formation of nitrogen

containing aroma compounds is, to some part, not only due to the Strecker degradation, but also due to a thermal degradation of compounds, which result in highly reactive aldehydes, ketones and amines, as do Strecker components. As the amount of alkylpyridines rise over time, and consequently, over heat induction, it is very likely therefore, that their main formation pathways lie, not so much in Strecker degradation, but in thermal degrading mechanisms.

The roasting studies with 'light', 'medium' and 'dark' roasts of an arabica green coffee showed isotopically interesting results. Generally, for the $^{15}N/^{14}N$ ratios it was observed, that the more an alykylpyrazine was substituted, the more enriched was its $\delta^{15}N_{AIR}$ value, with the only exception being compound **8**/**9**. Furthermore, the compounds **2**, **3**, **4**/**5**/**6**, **7** and **10** showed no large differences between their $\delta^{15}N_{AIR}$ values for 'light', 'medium' or 'dark' roast, with the maximal difference being 1 ‰. Pyridine (**1**) was the most depleted compound in all three roasting levels.

The $\delta^{2}H_{V\text{-}SMOW}$ values rose from the 'light' roast to the 'dark' roast. Only compound **7** displayed, relatively, constant values over all three roasts. For compounds **1**, **3**, **4**/**5**/**6** and **8**/**9**, a strong tendency to enrichment from 'light' to 'dark' roast was noticed. The 'light' roast compounds showed, in general, the most stable $^{2}H/^{1}H$ ratios, with values from -75 ‰ to -109 ‰.

Interesting, yet unexpected, differences were seen in the $\delta^{13}C_{V\text{-}PDB}$ values of 'light', 'medium' and 'dark' roasted arabica green coffee. The most depleted compound in all three roasts was pyridine (**1**), as it was with the $\delta^{15}N_{AIR}$ values. For compounds **1** to **7** the 'dark' roast was the most enriched, and the 'light' roast the most depleted, with the overall difference being 17 ‰, which is a huge value when taking into consideration that the carbon structure of alkylpyrazines is, theoretically, from carbohydrates, which have similar values even between plant types (see chapter 2.3.2). Pyridine (**1**) holds an exceptional position, as its formation (according to literary references), with carbohydrates, proteins and trigonelline playing a role, remains unclear as to which component plays a role, and to what degree.

Altogether, the differences found were surprising regarding the inhomogenity of isotope values for some compounds. It was seen that different N-, H-, and C-pools must contribute to the alkylpyrazine formation over the length of the roasting times, and, consequently, contribute to different $\delta^{15}N_{AIR}$, $\delta^{13}C_{V\text{-}PDB}$ and $\delta^{2}H_{V\text{-}SMOW}$ values. Further studies, concerning the influence of roasting time and also of temperature, need to be conducted to ensure that the stable isotope

values of the aroma components, measured in roast coffee and coffee products, are comparable and, most importantly, reproducible.

3.3 Stable Isotope Analyses, $^{15}N/^{14}N$, $^{2}H/^{1}H$ and $^{13}C/^{12}C$, of Synthesised Alkylpyrazines and Studies to Pyridine Formation

The formation of the roast coffee database and, particularly, the stable isotope analysis of the commercially available references, led to the question 'How are the commercially available references synthesised or obtained, and can their stable isotope values be influenced, i.e. in the choice of the educts or in the changing of the synthesis conditions?' The origin of the commercially available references was, unfortunately, not determinable, and neither was the synthesis methods of these products. A further question, which arose during the analysis of the roast coffee samples and during the analysis of green coffee fractions, was: 'What factors play a role in the formation of pyridine?' These questions are addressed in the following chapter.

3.3.1 Alkylpyrazine Syntheses via Condensation of α-Diketones and α-Diamines

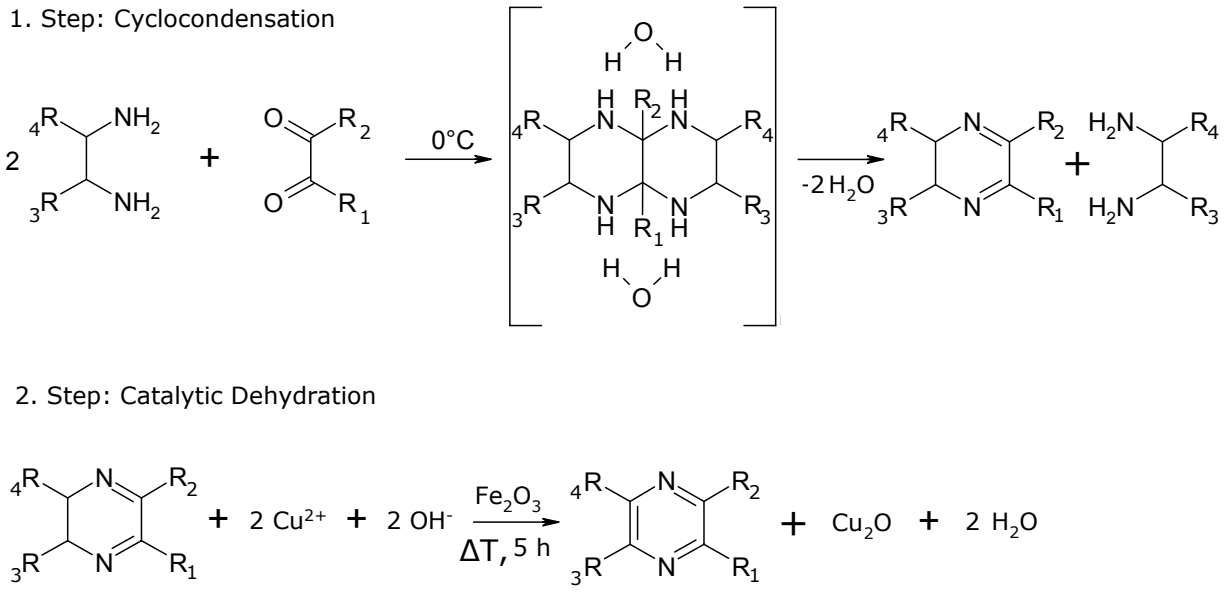

Figure 3-30: Postulated principle of the alkylpyrazine synthesis from α-diketones and α-diamines. First step from Stetter (1953) and Flament and Stoll (1967), second step from Jorré (1897).

The classic alkylpyrazine synthesis, via condensation of α-diketones and α-diamines, was developed by Jorré (1897) and further advanced by Stetter

(1953), Flament and Stoll (1967), Nakatani and Yanatori (1973) and Flament (2002). Depending on the available α-diketone and α-diamine educts, different alkylpyrazines can be synthesised using this method. The reaction mechanism for this synthesis involves the addition of 2 mol α-diamine on 1 mol α-diketone, to form naphthpiperazine-dihydrate. This compound precipitates as a white crystalline mass, which, via stirring or warming to 50 °C to 60 °C, decomposes under water elimination, to 1 mol dihydropyrazine and 1 mol α-diamine, resulting in 5,6-dihydropyrazine. The second step, the catalytic dehydration, was performed using Fehling's solution, under reflux, to form the wanted alkylpyrazine - see figure 3-30. The subsequent catalytic dehydration, using Fehling's solution, was conducted by Jorré (1897). As no exact amounts were published, Fehling's solution, which was known to react non-stoichiometrically as an oxidation reagent (Römpp-Lexikon, 2006), was, subsequently, added in excess, along with catalysts Fe_2O_3 and CuO in an ethanolic KOH solution, because dihydropyrazines are acid-labile and can form, under acidic conditions, other pyrazines (Odell, 1973; Shibamoto et al., 1977). The best results were obtained with hourly additions of Fehling's reagent.

The obtained solutions, after performing steps 1 and 2, were purified via SDE, with no further separation being conducted, as silica gel fractionation proved to be insufficient in separating the intermediate compounds and products. Both the intermediate product after step 1, and the end product after step 2, were analysed and verified via HRGC-MS, with the purified alkylpyrazine then being measured via HRGC-C/P-IRMS.

Using this method the alkylpyrazines 2,3-dimethylpyrazine (**7**), 2-ethyl-3-methylpyrazine (**10**), 2,3,5-trimethylpyrazine (**11**) and 2-ethyl-3,5/6-dimethylpyrazine (**12**/**13**) were synthesised and their $\delta^{15}N_{AIR}$, $\delta^{13}C_{V\text{-}PDB}$ and $\delta^{2}H_{V\text{-}SMOW}$ values compared to their educts and to commercially available references.

3.3.1.1 Synthesis and $^{15}N/^{14}N$, $^{2}H/^{1}H$ and $^{13}C/^{12}C$ Analyses of 2,3-Dimethylpyrazine

For the synthesis of 2,3-dimethylpyrazine (**7**), ethylendiamine and 2,3-butanedione were employed. They condensed, as planned, into 2,3-dimethyl-5,6-dihydropyrazine, which could be identified positively via the mass spectra database of our laboratory and the Beilstein database. This mass spectra is displayed in chapter 4.6.2.1, figure 4-4.

The catalytic dehydration led to 2,3-dimethylpyrazine (**7**) with a purity of 66 %, and further compounds found included the intermediate product 2,3-dimethyl-5,6-dihydropyrazine and 2,3,5,6-tetramethylpyrazine (**14**) - see figure 3-31. After this successful synthesis, the $\delta^{15}N_{AIR}$, $\delta^{2}H_{V\text{-}SMOW}$ and $\delta^{13}C_{V\text{-}PDB}$ values of both of the educts, ethylendiamine and 2,3-butanedione, plus the product 2,3-dimethylpyrazine (**7**) were analysed and compared, as shown in table 3-1.

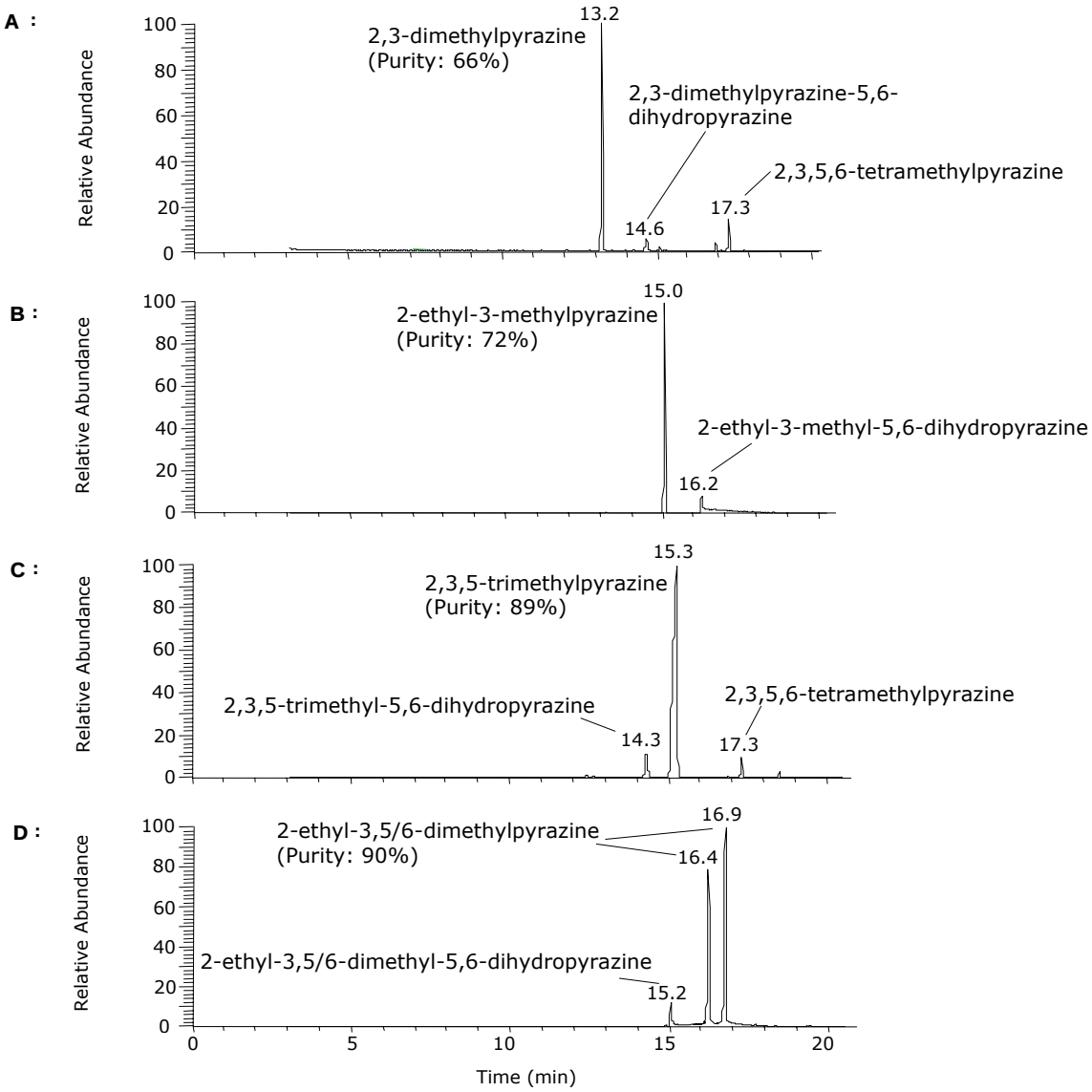

Figure 3-31: Total ion chromatograms of the synthesised alkylpyrazines A: 2,3-dimethylpyrazine (**7**), B: 2-ethyl-3-methylpyrazine (**10**), C: 2,3,5-trimethylpyrazine (**11**) and D: 2-ethyl-3,5/6-dimethylpyrazine (**12**/**13**)

For the alkylpyrazine syntheses, via condensation of α-diketones and α-diamines with subsequent oxidation, $\delta^{15}N_{AIR}$ values were expected to be in the region of the α-diamine, with $\delta^{13}C_{V\text{-}PDB}$ values expected between the educts and $\delta^{2}H_{V\text{-}SMOW}$ values also expected between the educts but with slight variations possible, due to oxidation.

Table 3-1: $\delta^{15}N_{AIR}$, $\delta^{2}H_{V\text{-}SMOW}$ and $\delta^{13}C_{V\text{-}PDB}$ values of educts, ethylendiamine and 2,3-butanedione, and the product 2,3-dimethylpyrazine (**7**).

Compound	$\delta^{15}N_{AIR}$ value [‰] ± SD	$\delta^{2}H_{V\text{-}SMOW}$ value [‰] ± SD	$\delta^{2}C_{V\text{-}PDB}$ value [‰] ± SD
ethylendiamine	-0.7 ± 0.3	-137 ± 2	-24.9 ± 0.2
2,3-butanedione	-	-179 ± 2	-29.4 ± 0.1
2,3-dimethylpyrazine (**7**)	-2.9 ± 0.1	-164 ± 1	-35.1 ± 0.1

Surprisingly, for the product 2,3-dimethylpyrazine (**7**), only the $\delta^{2}H_{V\text{-}SMOW}$ value of -164 ‰ was between the values of the educts. The $\delta^{15}N_{AIR}$ value of -2.9 ‰ was more depleted than the educt value of -0.7 ‰, as was the $\delta^{13}C_{V\text{-}PDB}$ value of -35.1 ‰. As the extraction and purification processes were exhaustive, and no fractionation took place during these steps, the depletion must have occurred, therefore, during the synthesis. As the yield was only 26 %, isotope fractionation could have occurred during either or both steps. For the synthesis of 2,3,5-trimethylpyrazine the influence of the second step was investigated - see chapter 3.3.1.3.

The comparison of the self-synthesised 2,3-dimethylpyrazine, with commercially available references, showed that the $^{15}N/^{14}N$ and $^{13}C/^{12}C$ ratios for the commercial products ranged between -0.5 ‰ to -2.2 ‰ and -23.0 ‰ to -30.4 ‰, respectively, with the $^{15}N/^{14}N$ and $^{13}C/^{12}C$ ratios for the self-synthesised products being more depleted with values of -2.9 ‰ and -35.1 ‰, respectively. The $^{2}H/^{1}H$ ratio for the self-synthesised product, with a value of -164 ‰, lay within the range of the commercial products, having values from -92 ‰ to -177 ‰. Had the synthesis expressed all the stable isotope values in the median of the educts, then the stable isotope values would be positioned in between those of the commercial products.

3.3.1.2 Synthesis and $^{15}N/^{14}N$, $^{2}H/^{1}H$ and $^{13}C/^{12}C$ Analyses of 2-Ethyl-3-methyl-pyrazine

For the synthesis of 2-ethyl-3-methylpyrazine (**10**), ethylendiamine and 2,3-pentanedione were employed. They condensed, as planned, into 2-ethyl-3-methyl-5,6-dihydropyrazine. For 2-ethyl-3-methyl-5,6-dihydropyrazine no literary references were found for the mass spectrum. As this intermediate compound could not be purified sufficiently for NMR-analysis, without leading to isotope discrimination, the fragmentation pattern of the mass spectrum was

analysed and the compound subsequently found was the required 2-ethyl-3-methyl-5,6-dihydropyrazine - see chapter 4.6.3.1, figure 4-7.

The catalytic dehydration led to 2-ethyl-3-methylpyrazine (**10**) showing a purity of 72 ‰, with one further compound found being, the intermediate product, 2-ethyl-3-methyl-5,6-dihydropyrazine - see figure 3-31. After this successful synthesis, the $\delta^{15}N_{AIR}$, $\delta^{2}H_{V\text{-}SMOW}$ and $\delta^{13}C_{V\text{-}PDB}$ values of both of the educts, ethylendiamine and 2,3-pentanedione, plus the product 2-ethyl-3-methyl-pyrazine (**10**) were analysed and compared, as shown in table 3-2.

Table 3-2: $\delta^{15}N_{AIR}$, $\delta^{2}H_{V\text{-}SMOW}$ and $\delta^{13}C_{V\text{-}PDB}$ values of educts, ethylendiamine and 2,3-pentanedione, and the product 2-ethyl-3-methylpyrazine (**10**).

Compound	$\delta^{15}N_{AIR}$ value [‰] ± SD	$\delta^{2}H_{V\text{-}SMOW}$ value [‰] ± SD	$\delta^{2}C_{V\text{-}PDB}$ value [‰] ± SD
ethylendiamine	-0.7 ± 0.3	-137 ± 2	-24.9 ± 0.2
2,3-pentanedione	-	-150 ± 4	-17.8 ± 0.2
2-ethyl-3-methylpyrazine (**10**)	-0.5 ± 0.3	-143 ± 2	-22.5 ± 0.2

The stable isotope values of 2-ethyl-3-methylpyrazine (**10**) displayed the expected values with $\delta^{15}N_{AIR}$ = -0.5 ‰, $\delta^{2}H_{V\text{-}SMOW}$ = -143 ‰ and $\delta^{13}C_{V\text{-}PDB}$ = -22.5 ‰ being in between or around the values of the educts.

In comparison to commercially available references, the stable isotope values of the self-synthesised 2-ethyl-3-methylpyrazine (**10**) was, for all values, in the range of the commercial products, with $^{15}N/^{14}N$ ratios varying from 0.7 ‰ to -0.5 ‰, $^{2}H/^{1}H$ ratios from -95 ‰ to -179 ‰ and $^{13}C/^{12}C$ ratios from -22.3 ‰ to -28.4 ‰.

3.3.1.3 Synthesis and $^{15}N/^{14}N$, $^{2}H/^{1}H$ and $^{13}C/^{12}C$ Analyses of 2,3,5-Trimethyl-pyrazine

For the synthesis of 2,3,5-trimethylpyrazine (**11**), 1,2-diaminopropane and 2,3-butanedione were employed. They condensed, as planned, to 2,3,5-trimethyl-5,6-dihydropyrazine. For 2,3,5-trimethyl-5,6-dihydropyrazine no literary references were found for the mass spectra, although Shibamoto et al. (1977) had synthesised and characterised this compound, but the mass spectrometric data was not available. As this intermediate compound could not be purified sufficiently for NMR-analysis, without leading to isotope discrimination, the

fragmentation pattern of the mass spectrum was analysed and the compound subsequently found was the required 2,3,5-trimethyl-5,6-dihydropyrazine - see chapter 4.6.4.1, figure 4-10.

The catalytic dehydration led to 2,3,5-trimethylpyrazine (**11**), with a purity of 89 ‰, and further compounds found were the intermediate products 2,3,5-trimethyl-5,6-dihydropyrazine and 2,3,5,6-tetramethylpyrazine (**14**) - see figure 3-31. After this successful synthesis, the $\delta^{15}N_{AIR}$, $\delta^{2}H_{V\text{-}SMOW}$ and $\delta^{13}C_{V\text{-}PDB}$ values of both of the educts, 1,2-diaminopropane and 2,3-butanedione, plus the product 2,3,5-trimethylpyrazine (**11**) were analysed and compared, as shown in table 3-3.

Table 3-3: $\delta^{15}N_{AIR}$, $\delta^{2}H_{V\text{-}SMOW}$ and $\delta^{13}C_{V\text{-}PDB}$ values of educts, 1,2-diaminopropane and 2,3-butanedione, and the product 2,3,5-trimethylpyrazine (**11**).

Compound	$\delta^{15}N_{AIR}$ value [‰] ± SD	$\delta^{2}H_{V\text{-}SMOW}$ value [‰] ± SD	$\delta^{2}C_{V\text{-}PDB}$ value [‰] ± SD
1,2-diaminopropane	-1.7 ± 0.2	-136 ± 3	-22.5 ± 0.1
2,3-butanedione	-	-179 ± 2	-29.4 ± 0.1
2,3,5-trimethylpyrazine (**11**)	-5.6 ± 0.1	-139 ± 3	-28.7 ± 0.2

The stable isotope values of 2,3,5-trimethylpyrazine displayed a strongly depleted $^{15}N/^{14}N$ ratio of -5.6 ‰, compared to the educt value of -1.7 ‰, whilst the $^{2}H/^{1}H$ ratio of -139 ‰, although positioned between the educt values of -136 ‰ and -179 ‰, was sufficiently enriched to be close to the value of 1,2-diaminopropane. The $^{13}C/^{12}C$ ratio of -28.7 ‰ lay between the educt values, although exhibiting more depletion towards the $\delta^{13}C_{V\text{-}PDB}$ value of -29.4 ‰ for 2,3-butanedione.

It was not possible to determine the isotope discrimination of the first step, regarding the condensation of the α-diketone and α-diamine, but a small study was conducted regarding the second step, the oxidation of the 2,3,5-trimethyl-5,6-dihydropyrazine. Here, the $^{15}N/^{14}N$ and $^{2}H/^{1}H$ ratios of 2,3,5-trimethyl-pyrazine (**11**) were measured at 12 h, 26 h, 39 h and 50 h intervals of oxidation of the intermediate product using Fehling's solution.

As seen in table 3-4, with increasing duration of the oxidation time, the $\delta^{15}N_{AIR}$ values tend to become more depleted, whilst the $\delta^{2}H_{V\text{-}SMOW}$ values tend to become more enriched. These results concur with the results from the self-synthesised alkylpyrazines, with the $\delta^{15}N_{AIR}$ values tending to be more depleted, when not expressing the educt value, and with the $\delta^{2}H_{V\text{-}SMOW}$ values tending to be

more enriched than the average $\delta^2H_{V\text{-}SMOW}$ value of the two educts. An interesting question on the behaviour of the $\delta^{13}C_{V\text{-}PDB}$ value concerns whether any depletion would be noticed, as it is with the $\delta^{15}N_{AIR}$ values, and if so, would this behaviour be seen for all compounds, using this method of synthesised alkylpyrazines.

Table 3-4: $\delta^{15}N_{AIR}$ and $\delta^2H_{V\text{-}SMOW}$ values of 2,3,5-trimethylpyrazine (**11**), after differing durations of oxidation of 2,3,5-trimethyl-5,6-dihydropyrazine, using Fehling's solution.

2,3,5-trimethylpyrazine (**11**) after oxidation in h	$\delta^{15}N_{AIR}$ value [‰] ± SD	$\delta^2H_{V\text{-}SMOW}$ value [‰] ± SD
12	-4.4 ± 0.2	-155 ± 3
26	-4.9 ± 0.1	-149 ± 5
39	-4.9 ± 0.2	-148 ± 3
50	-5.6 ± 0.1	-141 ± 2

In comparison to commercially available references, the stable isotope values of the self-synthesised 2,3,5-trimethylpyrazine (**11**) was more depleted, with $\delta^{15}N_{AIR}$ = -5.6 ‰, than the commercial references, with $^{15}N/^{14}N$ ratios from 0.6 ‰ to -1.5 ‰. The $\delta^2H_{V\text{-}SMOW}$ value of -139 ‰ and the $\delta^{13}C_{V\text{-}PDB}$ value of -28.7 ‰ were within those values derived from the commercial samples, with $^2H/^1H$ ratios of -109 ‰ to -182 ‰ and $^{13}C/^{12}C$ ratios of -20.4 ‰ to -30.2 ‰.

3.3.1.4 Synthesis and $^{15}N/^{14}N$, $^2H/^1H$ and $^{13}C/^{12}C$ Analyses of 2-Ethyl-3,5/6-dimethylpyrazine

For the synthesis of 2-ethyl-3,5/6-dimethylpyrazine (**12**/**13**), 1,2-diamino-propane and 2,3-pentanedione were employed. They condensed into two isomeric compounds, 2-ethyl-3,5- and 2-ethyl-3,6-dimethyl-5,6-dihydropyrazine. For these compounds the mass spectra were compared to literary references (Kurniadi et al., 2003) but, additionally, the fragmentation pattern of the mass spectra were analysed with the resulting compounds, subsequently, found to be the required 2-ethyl-3,5- and 2-ethyl-3,6-dimethyl-5,6-dihydropyrazine - see chapter 4.6.5.1, figure 4-13.

The catalytic dehydration led to 2-ethyl-3,5/6-dimethylpyrazine (**12**/**13**), with a purity of 90 ‰, and further compounds found were the intermediate products, 2-ethyl-3,5- and 2-ethyl-3,6-dimethyl-5,6-dihydropyrazine - see figure 3-31. After this successful synthesis, the $\delta^{15}N_{AIR}$, $\delta^2H_{V\text{-}SMOW}$ and $\delta^{13}C_{V\text{-}PDB}$ values of both of the educts, 1,2-diaminopropane and 2,3-pentanedione, plus the product 2-

ethyl-3,5/6-dimethylpyrazine (**12**/**13**), as combined parameters, were analysed and compared, as shown in table 3-5.

The $\delta^{15}N_{AIR}$ value = -2.9 ‰ of 2-ethyl-3,5/6-dimethylpyrazine (**12**/**13**) was more depleted than the educt value of $\delta^{15}N_{AIR}$ = -1.7‰, otherwise the $\delta^{2}H_{V\text{-}SMOW}$ and $\delta^{13}C_{V\text{-}PDB}$ values of 2-ethyl-3,5/6-dimethylpyrazine (**12**/**13**) (-143 ‰ and -20.6 ‰, respectively) displayed the average between the educt values of -136 ‰ to -150 ‰ and -22.5 ‰ to -17.8 ‰, respectively, as expected.

Table 3-5: $\delta^{15}N_{AIR}$, $\delta^{2}H_{V\text{-}SMOW}$ and $\delta^{13}C_{V\text{-}PDB}$ values of educts, 1,2-diaminopropane and 2,3-pentanedione, and the product 2-ethyl-3,5/6-dimethylpyrazine (**12**/**13**).

Compound	$\delta^{15}N_{AIR}$ value [‰] ± SD	$\delta^{2}H_{V\text{-}SMOW}$ value [‰] ± SD	$\delta^{2}C_{V\text{-}PDB}$ value [‰] ± SD
1,2-diaminopropane	-1.7 ± 0.2	-136 ± 3	-22.5 ± 0.1
2,3-pentanedione	-	-150 ± 4	-17.8 ± 0.2
2-ethyl-3,5/6-dimethylpyrazine (**12**/**13**)	-2.9 ± 0.3	-143 ± 1	-20.6 ± 0.1

Comparing the stable isotope values of self-synthesised 2-ethyl-3,5/6-dimethylpyrazine (**12**/**13**) to commercially available references, the $^{15}N/^{14}N$ ratio of the self-synthesised compounds was more depleted, with -2.9 ‰ compared to that for commercial references of $\delta^{15}N_{AIR}$ = -1.3 ‰ to 3.2 ‰. $\delta^{2}H_{V\text{-}SMOW}$ and $\delta^{13}C_{V\text{-}PDB}$ values of reference (**12**/**13**), with -105 ‰ to -144 ‰ and -18.2 ‰ to -24.6 ‰, respectively, concurred nicely with the obtained self-synthesised values.

3.3.2 Alkylpyrazine Synthesis via Reduction of Methyl pyrazinecarboxylate

According to the synthesis method of Schwaiger et al. (1984), a pyrazine-carboxylate can react, similar to a Grignard reaction, with alkyllithium to produce alkylpyrazineketone, which is then reduced, with hydrazinehydrate, to the required alkylpyrazine. The only obtainable pyrazinecarboxylate was methyl 2-pyrazinecarboxylate, so that the only synthesisable alkylpyrazine was 2-ethyl-pyrazine (**6**).

3.3.2.1 Synthesis and $^{15}N/^{14}N$, $^{2}H/^{1}H$ and $^{13}C/^{12}C$ Analyses of 2-Ethylpyrazine

For the synthesis of 2-ethylpyrazine (**6**), methyl 2-pyrazinecarboxylate reacted, with the help of methyllithium, to produce 2-methylpyrazineketone. For 2-methylpyrazineketone no literary references were found for the mass spectra. As this intermediate compound could not be purified sufficiently for NMR-analysis, without leading to isotope discrimination, the fragmentation pattern of the mass spectrum was analysed, and the compound, subsequently, found was the required 2-methylpyrazineketone - see chapter 4.6.6.1 and figure 4-16.

The reduction with hydrazinehydrate led to 2-ethylpyrazine (**6**), with a purity of 71 ‰, the impurity being unreduced methylpyrazineketone - see figure 3-32. After this successful synthesis, the $\delta^{15}N_{AIR}$, $\delta^{2}H_{V\text{-}SMOW}$ and $\delta^{13}C_{V\text{-}PDB}$ values of both of the educts, methyl 2-pyrazinecarboxylate and hydrazinehydrate, plus the product 2-ethylpyrazine (**6**), were analysed and compared, as shown in table 3-6.

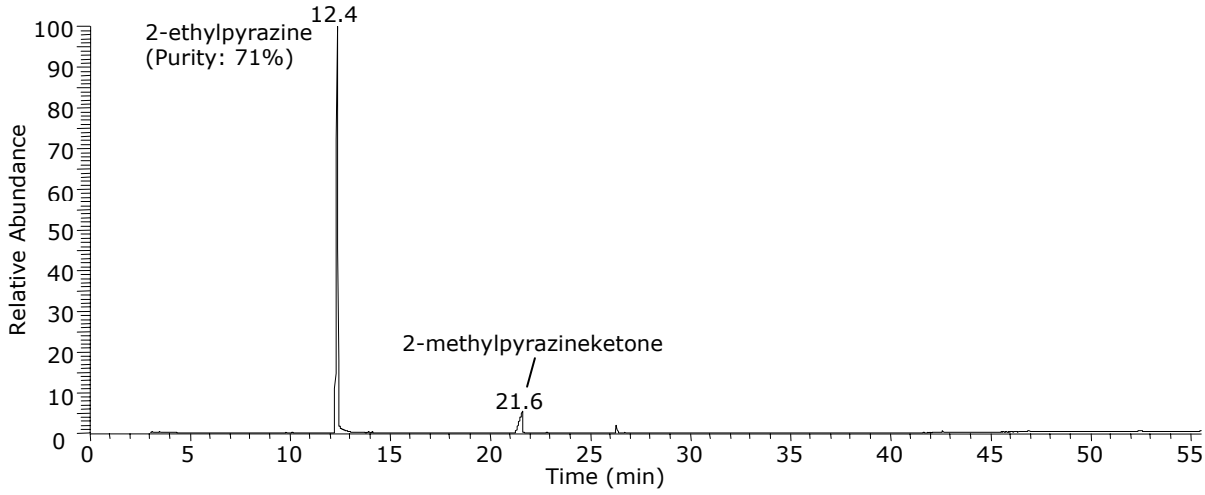

Figure 3-32: Total ion chromatogram of the synthesised alkylpyrazine 2-ethylpyrazine (**6**).

Table 3-6: $\delta^{15}N_{AIR}$, $\delta^{2}H_{V\text{-}SMOW}$ and $\delta^{13}C_{V\text{-}PDB}$ values of educts, methyl 2-pyrazinecarboxylate and hydrazinehydrate, and the product 2-ethylpyrazine (**6**).

Compound	$\delta^{15}N_{AIR}$ value [‰] ± SD	$\delta^{2}H_{V\text{-}SMOW}$ value [‰] ± SD	$\delta^{2}C_{V\text{-}PDB}$ value [‰] ± SD
methyl 2-pyrazinecarboxylate	1.0 ± 0.2	41 ± 2	-23.2 ± 0.1
hydrazinehydrate	-1.8 ± 0.1	-146 ± 4	-
2-ethylpyrazine (**6**)	0.8 ± 0.2	19 ± 1	-24.7 ± 0.2

The stable isotope values for 2-ethylpyrazine (**6**) showed slightly more depleted $\delta^{15}N_{AIR}$, $\delta^{2}H_{V\text{-}SMOW}$ and $\delta^{13}C_{V\text{-}PDB}$ values with 0.8 ‰, 19 ‰ and -24.7 ‰, respectively, than the main educt methyl 2-pyrazinecarboxylate ($\delta^{15}N_{AIR}$ = 1.0 ‰, $\delta^{2}H_{V\text{-}SMOW}$ = 41 ‰ and $\delta^{13}C_{V\text{-}PDB}$ = -23.2 ‰).

In comparison to synthetic references, with $\delta^{15}N_{AIR}$ = -1.4 ‰ to -1.6 ‰, $\delta^{2}H_{V\text{-}SMOW}$ = -59 ‰ to -126 ‰ and $\delta^{13}C_{V\text{-}PDB}$ = -25.1 ‰ to -26.0 ‰, the self-synthesised 2-ethylpyrazine (**6**) displayed more enriched values than the references, in all stable isotopes. This was due to the enriched values of the educt methyl 2-pyrazinecarboxylate. Similar stable isotope values from the commercial references, especially for the $\delta^{2}H_{V\text{-}SMOW}$, were found only for 2-methylpyrazine (**3**).

3.3.3 Syntheses of Alkylpyrazines from Amino Acids

Alkylpyrazines have been generated from amino acids in the past, with or without carbohydrates, in dry or fluid systems, by many groups (Van Praag, 1968; Kort, 1970; Shibamoto et al., 1977; Baltes and Bochmann, 1987 a, b, c, d; Wright, 1991; Reese and Baltes, 1992; Hwang et al., 1993; Sohn and Ho, 1995; Bristow and Isaacs, 1999; Ho and Chen, 1999; Ames et al., 2001). By modifying the synthesis method of Shu (1999), different alkylpyrazines were synthesised, by application of high temperatures to amino acids, in a closed reaction cylinder - see chapter 4.5.6, figure 4-1. This method always resulted in a mixture of alkylpyrazines and other compounds, which were not further purified by silica gel chromatography. Besides the stable isotope values of the compounds, the alkylpyrazine distribution was of interest for comparison with that of other research groups.

3.3.3.1 Synthesis and $^{15}N/^{14}N$, $^{2}H/^{1}H$ and $^{13}C/^{12}C$ Analyses of Alkylpyrazines from L-Serine

Research work on the pyrolysis of L-serine was performed by Kato et al. (1970), Wang and Odell (1973), Shu (1999) and Yaylayan and Keyhani (2001 b). Theoretically, L-serine can react with itself after decarboxylation and dehydration to produce the molecule pyrazine (**2**) (Shu et al., 1999). Without water as solvent no reaction was observed in our reaction system. The reaction of L-serine and water at 300 °C in the reaction cylinder led to many different alkylpyrazines – see figure 3.33, chromatogram A. The main alkylpyrazine found was pyrazine (**2**), as theoretically expected, but also large amounts of 2-ethylpyrazine (**6**) and

2-methylpyrazine (**3**) and lesser amounts of 2,3-dimethylpyrazine (**7**), 2-ethyl-5-, 2-ethyl-6- and 2-ethyl-3-methylpyrazine (**8**/**9**/**10**). No 2,5-, 2,6-dimethylpyrazine (**4**/**5**), 2-ethyl-3,5-dimethylpyrazine (**12**) nor 2,3,5-trimethylpyrazine (**11**) were found. Altogether, only methyl and ethyl substituted alkylpyrazines were found (Yaylayan and Keyhani, 2001 b).

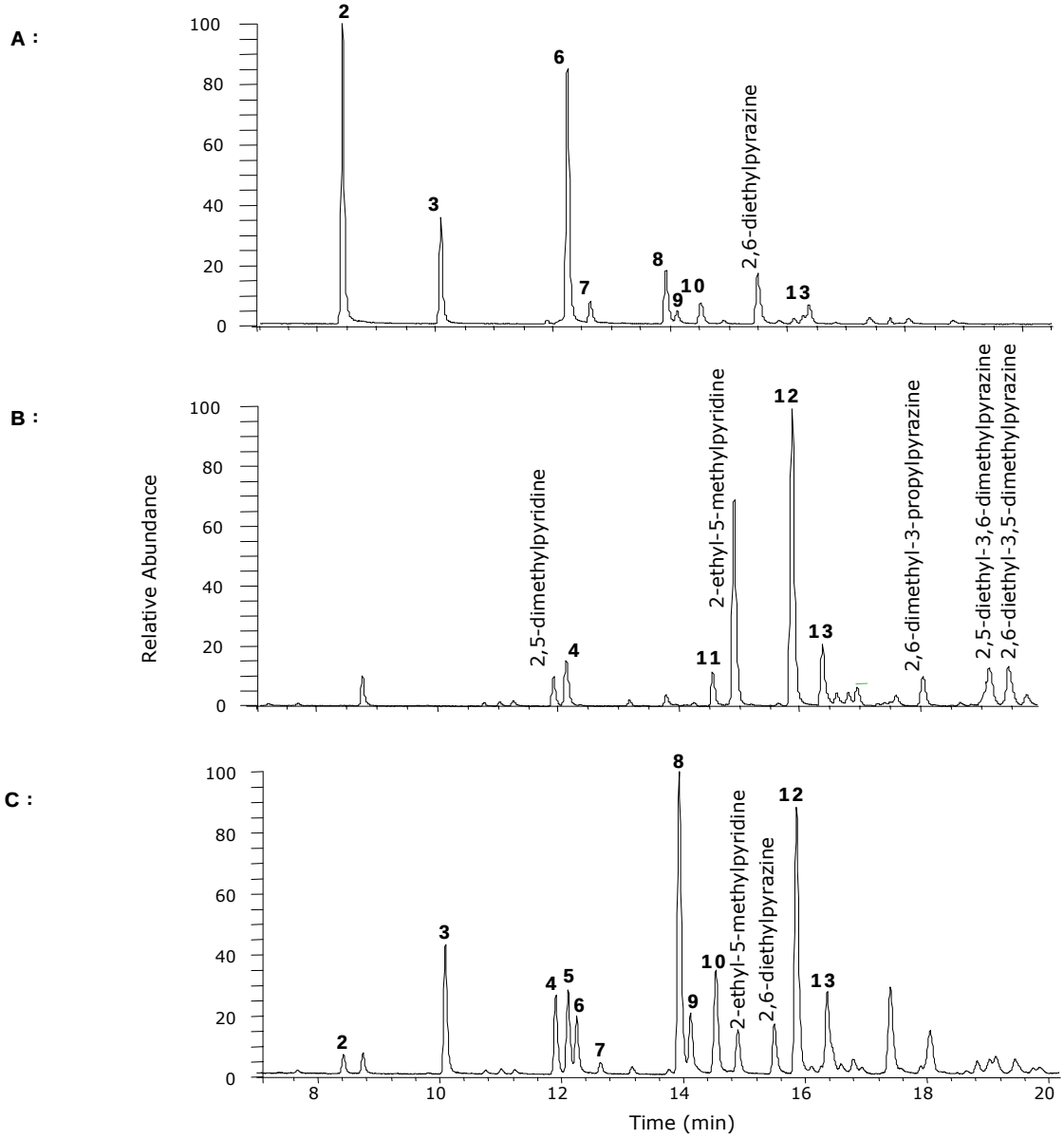

Figure 3-33: Total ion chromatogram of synthesised alkylpyrazines from A: L-serine, B: L-threonine and C: L-serine and L-threonine. The peak numbers indicate the compounds under IRMS study, **2** pyrazine, **3** 2-methylpyrazine, **4** 2,5-dimethylpyrazine, **5** 2,6-dimethylpyrazine, **6** 2-ethylpyrazine, **7** 2,3-dimethylpyrazine, **8** 2-ethyl-5-methylpyrazine, **9** 2-ethyl-6-methylpyrazine, **10** 2-ethyl-3-methylpyrazine, **11** 2,3,5-trimethylpyrazine, **12** 2-ethyl-3,5-dimethylpyrazine and **13** 2-ethyl-3,6-dimethylpyrazine.

Wang and Odell (1973) and Shu (1999) found similar distributions of alkylpyrazines after L-serine pyrolysis, as in this work, and concluded, as no

carbohydrates were involved in the reaction, that decarboxylation and dehydroxylation of L-serine, due to thermal degradation, led to reactive carbonyls and amino carbonyls, which then reacted to produce alkylpyrazines. Yaylayan and Keyhani (2001 b) determined, with labelled L-serine, three degradation pathways of L-serine being: 1. decarboxylation and deamidation to ethanolamine and acetaldehyde, 2. retroaldol pathway to formaldehyde and glycine and 3. dehydration to pyruvic acid and further to alanine or acetaldehyde.

Table 3-7: $\delta^{15}N_{AIR}$, $\delta^{2}H_{V\text{-}SMOW}$ and $\delta^{13}C_{V\text{-}PDB}$ values of the educt, L-serine and the alkylpyrazine products. Compound **8**/**9** was not separated chromatographically, with the results being displayed as combined values.

Compound	$\delta^{15}N_{AIR}$ value [‰] ± SD	$\delta^{2}H_{V\text{-}SMOW}$ value [‰] ± SD	$\delta^{2}C_{V\text{-}PDB}$ value [‰] ± SD
L-serine	3.3 ± 0.3	227 ± 4	-27.5 ± 0.2
pyrazine (**2**)	2.5 ± 0.2	-38 ± 4	-27.8 ± 0.2
2-methylpyrazine (**3**)	2.5 ± 0.2	-22 ± 4	-28.0 ± 0.2
2-ethylpyrazine (**6**)	3.3 ± 0.2	-45 ± 4	-30.7 ± 0.2
2,3-dimethylpyrazine (**7**)	3.1 ± 0.1	-32 ± 5	-31.1 ± 0.2
2-ethyl-5/6-methylpyrazine (**8**/**9**)	3.1 ± 0.3	-29 ± 5	-31.2 ± 0.2
2-ethyl-3-methylpyrazine (**10**)	2.7 ± 0.2	-5 ± 5	-30.4 ± 0.1
2,6-diethylpyrazine	2.4 ± 0.1	-31 ± 4	-32.8 ± 0.2
2-ethyl-3,6-dimethylpyrazine (**13**)	2.6 ± 0.3	-17 ± 3	-30.6 ± 0.1

The $\delta^{15}N_{AIR}$, $\delta^{2}H_{V\text{-}SMOW}$ and $\delta^{13}C_{V\text{-}PDB}$ values of both of the educt, L-serine, plus the alkylpyrazine products, were analysed and compared, as shown in table 3-7. For $\delta^{15}N_{AIR}$ values the educt L-serine showed a stable isotope value of 3.3 ‰, with all from this compound derived products displaying identical to slightly depleted values. For $\delta^{13}C_{V\text{-}PDB}$ values a similar picture was seen with the educt having a value of -27.5 ‰ and the alkylpyrazines having values of -27.8 ‰ to -32.8 ‰. Yaylayan et al. (2000 b) discovered that, for 2-methylpyrazine from L-serine, three formation pathways were found, with especially the C-2 and C-3 atoms of L-serine playing the main role, whereas the C-1 atom was only incorporated in 2-methylpyrazine in 10% of the molecules. For 2-ethylpyrazine only the C-2 and C-3 atoms of L-serine were incorporated. The depletion in $\delta^{13}C_{V\text{-}PDB}$ values of the alkylpyrazines with their size, leads to the assumption, that, the C-2 and C-3 atoms of the used L-serine were more depleted than the C-1 atom. The $\delta^{2}H_{V\text{-}SMOW}$ values showed a surprising depletion in the alkylpyrazines compared to L-serine's value of 227 ‰. All L-serine samples in our laboratory displayed positive

$\delta^2H_{V\text{-}SMOW}$ values. For this reason, the industrial synthesis of L-serine is probably not via microbial or fermentative methods, as these would be expected to have negative values, but via chemical synthesis. Procedures for the chemical synthesis of L-serine involve either a basic reaction with N-acetoamido malonic ester or a pathway via methyl acrylate. After tests, involving the stable isotope behaviour of L-serine in contact with water, it was clear that L-serine took on a value close to that of water ($\delta^2H_{V\text{-}SMOW}$= -59 ‰). This behaviour was found also for sucrose and citric acid, but surprisingly enough not for L-threonine. The $\delta^2H_{V\text{-}SMOW}$ values of the alkylpyrazines ($\delta^2H_{V\text{-}SMOW}$= -5 ‰ to -45 ‰), synthesised from L-serine, did not display the value of L-serine, but rather the value of water.

3.3.3.2 Synthesis and $^{15}N/^{14}N$, $^{2}H/^{1}H$ and $^{13}C/^{12}C$ Analyses of Alkylpyrazines from L-Threonine

Theoretically, L-threonine can react, with itself, after decarboxylation and dehydration to form the molecule 2,5-dimethylpyrazine (**4**) (Shu, 1999). Without water as solvent no reaction was observed. The reaction, in the reaction cylinder, of L-threonine with water at 300 °C led to different alkylpyrazines and alkyl-pyridines of mainly higher substituted forms – see figure 3.33, chromatogram B. 2,5-Dimethylpyrazine was found in small amounts, further alkylpyrazines present were compound **11**, the main component **12** and **13**, as well as smaller quantities of 2,6-dimethyl-3-propylpyrazine, 2,5-diethyl-3,6-dimethylpyrazine and 2,6-diethyl-3,5-dimethylpyrazine. The larger molecule L-threonine led to larger fragments, than L-serine, which in turn led to alkylpyrazines with more side chains. Furthermore, two alkylpyridines, 2,5-dimethylpyridine and 2-ethyl-5-methylpyridine, were found. Shu (1999) found a slightly differing spectrum for the pyrolysis of L-threonine. Both quantities and alkylpyrazines pattern were different, with compound **5** being detected in the work of Shu but no compounds **4**, 2,6-dimethyl-3-propylpyrazine, 2,5-diethyl-3,6-dimethylpyrazine, 2,6-diethyl-3,5-dimethyl-pyrazine.

The $\delta^{15}N_{AIR}$, $\delta^2H_{V\text{-}SMOW}$ and $\delta^{13}C_{V\text{-}PDB}$ values of both of the educt, L-threonine, plus the alkylpyrazine and alkylpyridine products, were analysed and compared, as shown in table 3-8. For $\delta^{15}N_{AIR}$ values the educt L-threonine displayed a stable isotope value of -1.0 ‰, with all derived products showing $\delta^{15}N_{AIR}$ values of -1.2 ‰ to -2.5 ‰, the most depleted value being that of 2-ethyl-5-methylpyridine. The $^{13}C/^{12}C$ ratio of L-threonine showed a value of -25.8 ‰, and the alkylpyrazines displayed $\delta^{13}C_{V\text{-}PDB}$ values of -30.1 ‰ to -19.2 ‰, with the most depleted compound again being 2-ethyl-5-methylpyridine. The $^{2}H/^{1}H$ ratio

of L-threonine with -198 ‰ was, compared to L-serine, hardly affected by the solvent water, where an enrichment of 20 ‰ was measured. The $\delta^2H_{V\text{-}SMOW}$ values of the products ranged from -250 ‰ to -168 ‰.

Table 3-8: $\delta^{15}N_{AIR}$, $\delta^2H_{V\text{-}SMOW}$ and $\delta^{13}C_{V\text{-}PDB}$ values of the educt, L-threonine and the alkylpyrazine products. Compound **4** and 2,5-dimethylpyridine, as well as **12**/**13** were not separated chromatographically, with their results being displayed as combined values.

Compound	$\delta^{15}N_{AIR}$ value [‰] ± SD	$\delta^2H_{V\text{-}SMOW}$ value [‰] ± SD	$\delta^2C_{V\text{-}PDB}$ value [‰] ± SD
L-threonine	-1.0 ± 0.3	-198 ± 1	-25.8 ± 0.1
2,5-dimethylpyrazine (**4**) + 2,5-dimethylpyridine	-1.2 ± 0.3	-218 ± 4	-20.4 ± 0.2
2,3,5-trimethylpyrazine (**11**)	-1.1 ± 0.1	-168 ± 4	-19.2 ± 0.1
2-ethyl-5-methylpyridine	-2.5 ± 0.3	-185 ± 2	-30.1 ± 0.2
2-ethyl-3,5/6-dimethylpyrazine (**12**/**13**)	-1.3 ± 0.3	-170 ± 2	-24.5 ± 0.2
2,6-dimethyl-3-propylpyrazine	-1.5 ± 0.2	-204 ± 5	-25.2 ± 0.2
2,5-diethyl-3,6-dimethylpyrazine	-1.9 ± 0.1	-172 ± 3	-24.7 ± 0.1
2,6-diethyl-3,5-dimethylpyrazine	-1.3 ± 0.2	-250 ± 3	-26.6 ± 0.2

3.3.3.3 Synthesis and $^{15}N/^{14}N$, $^{2}H/^{1}H$ and $^{13}C/^{12}C$ Analyses of Alkylpyrazines from L-Serine and L-Threonine

The reaction of L-threonine and L-serine (in equal amounts) with water at 300 °C, in the reaction cylinder, led to a variation of alkylpyrazines shown in figure 3.33, chromatogram C. Altogether, the compounds **2**-**10**, **12** and **13** were detected, with the chromatogram displaying a strong similarity to the alkylpyrazine distribution of roast coffee - see chromatogram 3-3 in chapter 3.2.1. The main differences between the synthesis composition and that of the roast coffee were the larger quantities of **12** and **13**, and the occurrence of 2-ethyl-5-methylpyridine and 2,6-diethylpyrazine in the synthesis product. Compounds **12**, **13** and 2-ethyl-5-methylpyridine also occurred in the pyrolysis of L-threonine, with 2,6-diethylpyrazine also occurring in the pyrolysis of L-serine. This synthesis was in good agreement with findings from Shu (1999), their highest quantities being for the compounds **13** and **9** and not, as in this research work, with the isomeric compounds **12** and **8**. Particularly interesting was the fact that the combined alkylpyrazine distribution was different to the

individual distributions of the L-serine and L-threonine reactions. Baltes and Bochmann (1987 d) described how an increase in the number of generated alkylpyrazines occurred when L-serine and L-threonine were pyrolysed together as compared to individual reactions - this was also observed in this research work.

In table 3-9 the $\delta^{15}N_{AIR}$, $\delta^{2}H_{V\text{-}SMOW}$ and $\delta^{13}C_{V\text{-}PDB}$ values of the educts, L-serine and L-threonine, and the alkylpyrazine products are displayed. As the educts were mixed in the ratio 1:1, the educt stable isotope values of $\delta^{15}N_{AIR}$ and $\delta^{13}C_{V\text{-}PDB}$ were calculated to be $\delta^{15}N_{AIR}$ = 1.2 ‰, $\delta^{2}H_{V\text{-}SMOW}$ = 15 ‰ and $\delta^{13}C_{V\text{-}PDB}$ = -26.7 ‰. The $\delta^{15}N_{AIR}$ values of the produced alkylpyrazines ranged from 0.2 ‰ to 2.8 ‰. An allocation of single alkylpyrazines to one of the two educt amino acids was not possible, with some ranging around the calculated median value of $\delta^{15}N_{AIR}$ = 1.2 ‰, and others being more enriched or more depleted. For $\delta^{13}C_{V\text{-}PDB}$ the calculated value of the educt mixture lay at -26.7 ‰, and the synthesised alkylpyrazines ranged from -25.1 ‰ to -31.8 ‰. The $\delta^{2}H_{V\text{-}SMOW}$ values of the alkylpyrazines ranged from -49 ‰ to -124 ‰, a large difference between the compounds. Due to the behaviour of L-serine taking on the $^{2}H/^{1}H$ ratios of water, no definite conclusions could be made for the large differences between the $\delta^{2}H_{V\text{-}SMOW}$ values of single alkylpyrazines.

Table 3-9: $\delta^{15}N_{AIR}$, $\delta^{2}H_{V\text{-}SMOW}$ and $\delta^{13}C_{V\text{-}PDB}$ values of the educts, L-serine and L-threonine and the alkylpyrazine products. Compound **4**/**5**/**6** and **8**/**9** were not separated chromatographically, with the results being displayed as combined values.

Compound	$\delta^{15}N_{AIR}$ value [‰] ± SD	$\delta^{2}H_{V\text{-}SMOW}$ value [‰] ± SD	$\delta^{2}C_{V\text{-}PDB}$ value [‰] ± SD
L-threonine	-1.0 ± 0.3	-198 ± 1	-25.8 ± 0.1
L-serine	3.3 ± 0.3	227 ± 4	-27.5 ± 0.2
pyrazine (**2**)	0.2 ± 0.2	-49 ± 3	-27.9 ± 0.1
2-methylpyrazine (**3**)	0.9 ± 0.3	-80 ± 5	-25.4 ± 0.2
2,5/6-dimethylpyrazine + 2-ethylpyrazine (**4**/**5**/**6**)	1.3 ± 0.2	-84 ± 3	-25.1 ± 0.2
2,3-dimethylpyrazine (**7**)	2.8 ± 0.1	-124 ± 5	-26.8 ± 0.2
2-ethyl-5/6-methylpyrazine (**8**/**9**)	1.0 ± 0.2	-87 ± 2	-29.3 ± 0.2
2-ethyl-3-methylpyrazine (**10**)	1.9 ± 0.2	-82 ± 3	-27.0 ± 0.2
2,6-diethylpyrazine	1.3 ± 0.2	-80 ± 2	-31.8 ± 0.2
2-ethyl-3,5/6-dimethylpyrazine (**12**/**13**)	1.4 ± 0.2	-78 ± 3	-27.9 ± 0.2

3.3.4 Synthesis and $^{15}N/^{14}N$, $^{2}H/^{1}H$ and $^{13}C/^{12}C$ Analyses of Alkylpyrazines from Diethylentriamine

Based on the synthesis of pyrazine and piperazine by Anderson et al. (1967), with diethylentriamine as educt, this research work was modified to generate alkylpyrazines in the reaction cylinder – see figure 3.34. Altogether, the compounds pyrazine (**2**), 2-methylpyrazine (**3**), 2-ethylpyrazine (**6**), 2,3-dimethylpyrazine (**7**), 2-ethyl-3-methylpyrazine (**10**), 2,6-diethylpyrazine and 2-ethyl-3,5-dimethylpyrazine (**12**) were detected.

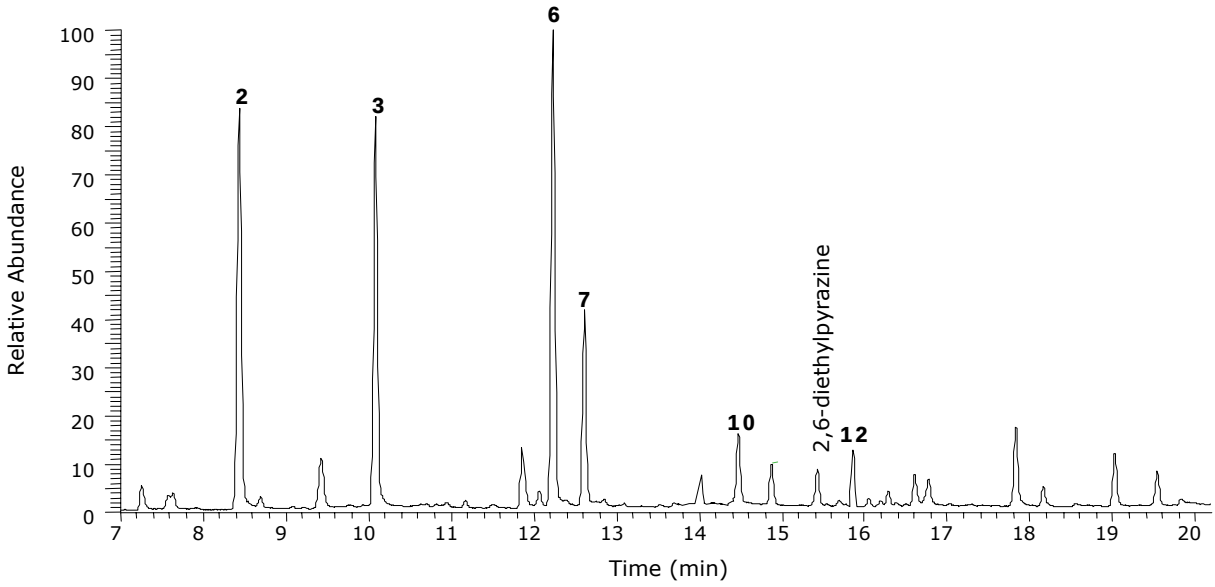

Figure 3-34: Total ion chromatogram of alkylpyrazines synthesised from diethylentriamine. The peak numbers indicate the compounds under IRMS study, **2** pyrazine, **3** 2-methylpyrazine, **6** 2-ethylpyrazine, **7** 2,3-dimethylpyrazine, **10** 2-ethyl-3-methylpyrazine and **12** 2-ethyl-3,5-dimethylpyrazine.

Table 3-10: $\delta^{15}N_{AIR}$, $\delta^{2}H_{V\text{-}SMOW}$ and $\delta^{13}C_{V\text{-}PDB}$ values of the educt, diethylentriamine and the alkylpyrazine products.

Compound	$\delta^{15}N_{AIR}$ value [‰] ± SD	$\delta^{2}H_{V\text{-}SMOW}$ value [‰] ± SD	$\delta^{2}C_{V\text{-}PDB}$ value [‰] ± SD
diethylentriamine	0.4 ± 0.3	31 ± 4	-29.5 ± 0.1
pyrazine (**2**)	0.1 ± 0.1	22 ± 1	-30.7 ± 0.2
2-methylpyrazine (**3**)	2.3 ± 0.2	28 ± 3	-29.2 ± 0.1
2-ethylpyrazine (**6**)	2.2 ± 0.1	28 ± 1	-30.5 ± 0.2
2,3-dimethylpyrazine (**7**)	2.3 ± 0.1	22 ± 1	-31.5 ± 0.2
2-ethyl-3-methylpyrazine (**10**)	2.2 ± 0.1	23 ± 1	-32.2 ± 0.1
2,3-diethylpyrazine	2.4 ± 0.2	23 ± 3	-31.7 ± 0.1
2-ethyl-3,5-dimethylpyrazine (**12**)	2.3 ± 0.2	25 ± 2	-34.2 ± 0.1

In table 3-10 the $\delta^{15}N_{AIR}$, $\delta^{2}H_{V\text{-}SMOW}$ and $\delta^{13}C_{V\text{-}PDB}$ values of the educt, diethylentriamine, and the alkylpyrazine products are displayed. Diethylentriamine showed values of $\delta^{15}N_{AIR}$ = 0.4 ‰, $\delta^{2}H_{V\text{-}SMOW}$ = 31 ‰ and $\delta^{13}C_{V\text{-}PDB}$ = -29.5 ‰. In comparison with these values, the $^{15}N/^{14}N$ ratios for the alkylpyrazine products were, for the most part, more enriched, ranging from 0.1 ‰ for pyrazine to 2.4 ‰ for 2,6-diethylpyrazine. Only the $^{2}H/^{1}H$ ratios differed slightly from the educt, displaying slightly depleted values, ranging from 22 ‰ to 28 ‰. The $^{13}C/^{12}C$ ratios of the synthesised alkylpyrazines displayed the greatest variation, with a range from -34.2 ‰ to -29.2 ‰, nearly all being more depleted than the educt value.

3.3.5 Studies to Pyridine Formation

During the studies on roast coffee aroma, pyridine (**1**) showed an interesting behaviour, both in the formation and quantity of the component and in its stable isotope values. In particular, the $\delta^{15}N_{AIR}$ values of pyridine (**1**) showed extremely depleted values, but its formation remains unclear, with studies on the roasting degree of coffee only showing that the longer the duration of the roast, the more pyridine (**1**) would be found. Unfortunately, no clear-cut correlation of stable isotope values with the roast duration was found. Rizzi and Sanders proposed in 1996 that the formation of pyridine (**1**) was mostly due to degradation of trigonelline, during roasting of the coffee beans. They based their thesis on the fact that only low amounts of trigonelline were left in roast coffee, and that the molecular structure of trigonelline was predestined to result in pyridine. All theories to pyridine formation are found in chapter 2.6.3. For this reason trigonelline was synthesised and the $\delta^{15}N_{AIR}$, $\delta^{2}H_{V\text{-}SMOW}$ and $\delta^{13}C_{V\text{-}PDB}$ values, thereof determined, so that degradation experiments could be performed and the stable isotope values, of the hopefully formed pyridine, measured. Not only trigonelline could contribute to pyridine formation, but also caffeine, amino acids and proteins were considered as possible pyridine precursors in roast coffee and so investigated. Further investigations to pyridine formation, especially the role of proteins, were performed as described in chapter 3.4.3.

3.3.5.1 Synthesis and $^{15}N/^{14}N$, $^{2}H/^{1}H$ and $^{13}C/^{12}C$ Analyses of Trigonelline

Trigonelline was synthesised, using a method from Sarett et al. (1940), via a methylation of nicotinic acid to trigonelline hydro iodide, and a subsequent transformation of this, to trigonelline. Both the intermediate product, trigonelline hydro iodide, and the product, trigonelline, showed virtually identical stable

isotope values (see table 3-11) of $\delta^{15}N_{AIR}$ = -7.5 ‰, $\delta^{2}H_{V\text{-}SMOW}$ = -124 ‰ and $\delta^{13}C_{V\text{-}PDB}$ = -41.6 ‰ (values for trigonelline).

Table 3-11: $\delta^{15}N_{AIR}$, $\delta^{2}H_{V\text{-}SMOW}$ and $\delta^{13}C_{V\text{-}PDB}$ values of synthesised trigonelline hydro iodide and trigonelline.

Compound	$\delta^{15}N_{AIR}$ value [‰] ± SD	$\delta^{2}H_{V\text{-}SMOW}$ value [‰] ± SD	$\delta^{2}C_{V\text{-}PDB}$ value [‰] ± SD
trigonelline hydro iodide	-7.6 ± 0.1	-127 ± 3	-41.3 ± 0.1
trigonelline	-7.5 ± 0.3	-124 ± 5	-41.6 ± 0.2

3.3.5.2 Degradation of Pyridine Precursors

As a next step, the pyridine precursors were degraded by heat, analogous to the green coffee fraction roasting method. The roasting method included the formation of the precursor into small pellets, with the help of Aerosil®, silica gel and water, with the pellets then being roasted, using the coffee roaster. These roasted pellets were then ground and extracted, via SDE, with the aroma extracts then being analysed via GC-MS. The whole procedure is explained in more detail in chapter 3.4.3.

For this study, five different precursors, or combinations of precursors, were roasted: trigonelline, trigonelline with citric acid, caffeine, caffeine and citric acid, as well as employing the amino acids, glycine, L-serine, L-threonine and citric acid.

The roasting of pure trigonelline resulted in no pyridine at all. Considering that the pH value is slightly acidic (pH = 4) in the coffee bean, a mixture of trigonelline and citric acid were roasted, resulting in pyridine traces. Unfortunately, these traces were insufficient for HRGC-C/P-IRMS measurement, so no statements on the isotope ratios were possible. The roasting of caffeine and the mixtures, caffeine and citric acid, as well as the amino acids, glycine, L-serine, L-threonine and citric acid, resulted in no pyridine formation.

3.3.6 Conclusion

The syntheses of alkylpyrazines, via condensation of α-diamines and α-diketones, with subsequent catalytic dehydration as per the process from Flament and Stoll (1967) and Jorré (1897), was performed for 2,3-dimethylpyrazine (**7**), 2-ethyl-3-

methylpyrazine (**10**), 2,3,5-trimethylpyrazine (**11**) and 2-ethyl-3,5/6-dimethyl-pyrazine (**12**/**13**). The $\delta^{15}N_{AIR}$ values of these products displayed, for the greatest part, more depleted values than the educt α-diamine, which resulted from the lengthy catalytic dehydration. Similar tendencies were shown by the $\delta^{13}C_{V\text{-}PDB}$ values, with these being between the educt values, but with a tendency to be nearer to the depleted value. $\delta^{2}H_{V\text{-}SMOW}$ values lay, as expected, between the stable isotope values of the educts, with the tendency to be slightly enriched, also caused by the length of catalytic dehydration. For the methylpyrazines **7** and **11** the by-product 2,3,5,6-tetramethylpyrazine (**14**) was identified despite the basic conditions employed. This by-product was also found by Shibamoto et al. (1977) to be the most abundant by-product when synthesising methyl-pyrazines and they concluded that rearrangement reactions led to **14**. The syntheses of further alkylpyrazines were tried, using this method, but failed, due to non-existent educts or educts of only low purity.

In comparison to commercially available references the $^{15}N/^{14}N$ and $^{13}C/^{12}C$ ratios of self-synthesised 2,3-dimethylpyrazine (**7**) were more depleted, with the $^{2}H/^{1}H$ ratio lying within the range of the commercial products. For 2-ethyl-3-methylpyrazine (**10**) all stable isotope values were in the range of the commercial references. The $^{15}N/^{14}N$ ratios of the self-synthesised 2,3,5-trimethylpyrazine (**11**) and 2-ethyl-3,5/6-dimethylpyrazine (**12**/**13**) were more depleted, with $^{13}C/^{12}C$ and $^{2}H/^{1}H$ ratios lying within the range of the commercial products.

The synthesis of 2-ethylpyrazine (**6**) was conducted, from the educt methyl 2-pyrazinecarboxylate, using a method developed by Schwaiger et al. (1984). The $\delta^{15}N_{AIR}$, $\delta^{13}C_{V\text{-}PDB}$ and $\delta^{2}H_{V\text{-}SMOW}$ values of the product 2-ethylpyrazine (**6**) lay slightly depleted in comparison to the educt values, but still more enriched than the commercially available references.

Modifying a synthesis method from Shu et al. (1999), alkylpyrazines were generated by thermal degradation of amino acids. The degradation of L-serine led to the alkylpyrazines, pyrazine (**2**), 2-methylpyrazine (**3**), 2-ethylpyrazine (**6**), 2,3-dimethylpyrazine (**7**), 2-ethyl-5/6-methylpyrazine (**8**/**9**), 2-ethyl-3-methylpyrazine (**10**), 2,6-diethylpyrazine and 2-ethyl-3,6-dimethylpyrazine (**13**). The stable isotope values of these were, generally, more depleted for $\delta^{15}N_{AIR}$ and $\delta^{13}C_{V\text{-}PDB}$, with $\delta^{2}H_{V\text{-}SMOW}$ displaying the water Würzburg value. The degradation of L-threonine led to the alkylpyrazines, 2,5-dimethylpyrazine (**4**), 2,5-dimethyl-pyridine, 2,3,5-trimethylpyrazine (**11**), 2-ethyl-5-methylpyridine, 2-ethyl-3,5/6-dimethylpyrazine (**12**/**13**), 2,6-dimethyl-3-propylpyrazine, 2,5-diethyl-3,6-di-methylpyrazine and 2,6-diethyl-3,5-dimethylpyrazine. $\delta^{15}N_{AIR}$

values, thereof, were more depleted than the educt, with the $\delta^{2}H_{V\text{-}SMOW}$ and $\delta^{13}C_{V\text{-}PDB}$ values being both enriched and depleted, respectively, in comparison to the educt. The degradation of both L-serine and L-threonine together, led to a similar chromatogram to that of roast coffee with the alkylpyrazines pyrazine (**2**), 2-methylpyrazine (**3**), 2,5/6-dimethylpyrazine (**4**/**5**), 2-ethylpyrazine (**6**), 2,3-dimethylpyrazine (**7**), 2-ethyl-5/6-methylpyrazine (**8**/**9**), 2-ethyl-3-methyl-pyrazine (**10**), 2,6-diethylpyrazine and 2-ethyl-3,5/6-dimethylpyrazine (**12**/**13**). No tendencies were found for the stable isotope values of the generated alkylpyrazines.

Based on the synthesis of pyrazine, by Anderson et al. (1967), the compounds pyrazine (**2**), 2-methylpyrazine (**3**), 2-ethylpyrazine (**6**), 2,3-dimethylpyrazine (**7**), 2-ethyl-3-methylpyrazine (**10**), 2,6-diethylpyrazine and 2-ethyl-3,5-dimethylpyrazine (**12**), were generated by degradation of diethylentriamine with heat. The $^{15}N/^{14}N$ ratios for the alkylpyrazine products were, for the most part, more enriched, with the $^{2}H/^{1}H$ ratios displaying slightly depleted values compared to the educt, whilst the $^{13}C/^{12}C$ ratios of the synthesised alkylpyrazines were all more depleted than the educt value.

Further alkylpyrazine syntheses by Stadel and Rügheimer (1876), Etard (1881) and Stoehr (1890), Tutin (1910), Aston et al. (1934), Krems and Spoerri (1947), Coleman III and Lawson (2000) and Anand et al. (2002) were tried, but due to non-available chemicals, non-obtainable reaction conditions or insufficient yield, these were abandoned.

The studies of pyridine formation, using the roasting of nitrogenous compounds of the coffee bean caffeine, amino acids and trigonelline, with and without citric acid, led to the observation that, the only pyridine formation using this method, derived from the roasting of trigonelline with citric acid.

3.4 Stable Isotope Analysis of Green Coffee Fractions and Roasting, thereof

For a better understanding of the formation of alkylpyrazines and pyridine during the roasting of green coffee beans, the green coffee beans were extracted into different fractions, i.e. amino acids, low molecular carbohydrates, proteins, polysaccharides, and lipids. These fractions were first measured via EA-C/P-IRMS, then roasted using the coffee roaster, and finally, the chromatograms compared and, when possible, the stable isotope values of the resulting alkylpyrazines and pyridine, measured. These values were then compared to other roasted fractions, to each another in the fraction and to the green coffee

fraction values. As a dividing of the green coffee bean into compound classes was wanted, without losses or isotope discrimination, solvents were chosen, which should leave no measurable residue. For this reason many established extraction and isolation techniques could not be applied. The extraction methods often employed water as an extraction solvent, so that the $\delta^2H_{V\text{-}SMOW}$ values had to be analysed with care, especially for fractions with high hydrogen exchange potential, i.e. sugars.

3.4.1 Fractionation Scheme

Fractionation of plant materials into compound classes for stable isotope determination had not been performed often in the past, with records found only for potato tubers (Smith and Jacobsen, 1976) and tobacco leaves (Jamin et al., 1997). According to literary references, green coffee had not been, previously, totally fractioned into compound classes for stable isotope determination. For composition determinations of green coffee, research had been conducted, though (Wolfrom et al., 1960; De Maria et al., 1996 a; Grosch, 2000; Fischer at al., 2001; Oosterfeld et al., 2003), but the extraction methods employed were mostly not suitable for stable isotope analysis, due to residues or non-exhaustive extraction. Therefore, an extraction scheme had to be developed, which separated the green coffee into compound classes, without any losses or discrimination. In figure 3-35 the extraction scheme is displayed in a simplified form, in table 3-12, the extraction percentages are presented.

The green coffee beans were first ground into green coffee powder and then de-fatted, using the method from §64 LFGB, L 01.00-20 with n-hexane, to extract the lipids from the green coffee powder. The n-hexane was evaporated from the lipid fraction and then measured as n-Hexane Soluble Fraction (HSF). The non-lipid n-Hexane Insoluble Fraction (HIF) was then extracted further.

To separate low molecular compounds, such as sugars, amino acids, organic acids and trigonelline, from high molecular compounds, such as polysaccharides and proteins, the fraction HIF was extracted using ethanol/water (80:20, v/v) by the method from De Maria et al. (1996 a) into an Ethanol/water Soluble Fraction (ESF) and an Ethanol/water Insoluble Fraction (EIF).

The Ethanol/water Soluble Fraction (ESF) was then further fractioned, using the method modified from Jamin et al. (1997), via cation exchange chromatography, into a Cationic Fraction, which contained amino acids, caffeine and trigonelline and via anion exchange chromatography, into the Anionic Fraction, containing

organic acids, and directly into the Neutral Fraction, containing sugars. Isotope discriminations, as described by Filer (1999) during cation exchange chromatography, were not observed for $^{15}N/^{14}N$ and $^{13}C/^{12}C$ analysis, but due to hydrogen exchange reactions with the eluents, a discrimination of $^{2}H/^{1}H$ was observed (Schmidt et al., 2003).

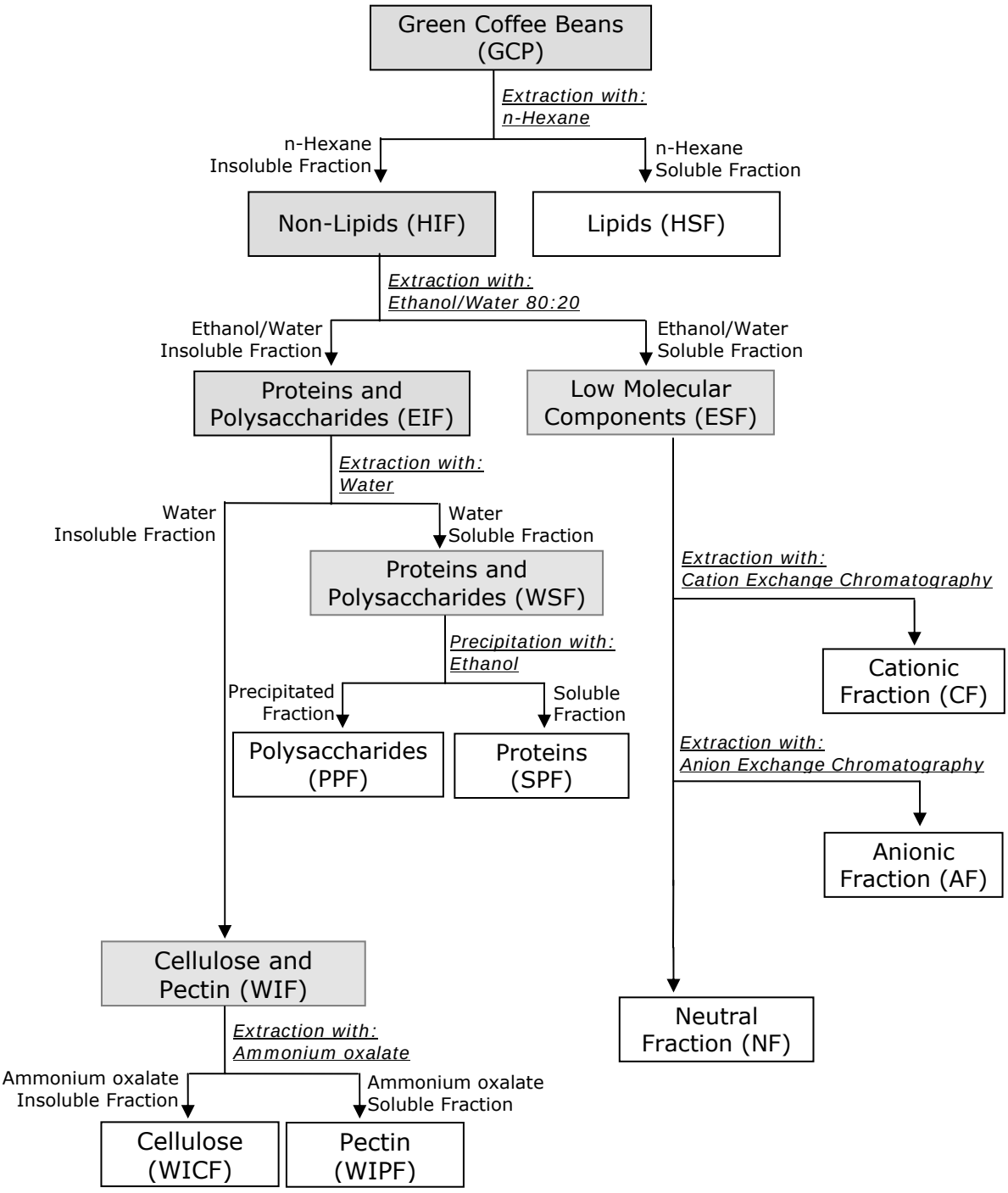

Figure 3-35: Scheme of the fractionation of green coffee beans with the expected compound classes and abbreviations of the fractions.

The Ethanol/water Insoluble Fraction (EIF), containing polysaccharides and proteins, was separated into a Water Soluble Fraction, containing proteins and polysaccharides and a Water Insoluble Fraction, containing cellulose and pectin, using a method by Oosterveld et al. (2003). The separation of cellulose and pectin was performed, via an ammonium oxalate extraction, by Wolfrom et al. (1960), resulting in a Water Insoluble Pectin Fraction and a Water Insoluble Cellulose Fraction. The proteins and polysaccharides from WSF were then separated, by precipitating the polysaccharides with ethanol, by Wolfrom et al. (1960), into a Soluble Protein Fraction and a Precipitated Polysaccharide Fraction.

Table 3-12: Extraction percentages of the green coffee beans.

Fraction	Content in Green Coffee Beans (%)
Lipids	18.9 (HSF)
Free amino acids and trigonelline	2.9 (CF)
Low molecular carbohydrates	11.4 (NF)
Organic acids	7.2 (AF)
Proteins	4.5 (SPF)
Water Soluble polysaccharides	2.6 (PPF)
Cellulose and β-mannan	21.9 (WICF)
Further polysaccharides	30.7 (WIPF)

The desire to separate the compound classes of the green coffee bean for stable isotope analysis, without discrimination, proved to be more difficult than expected. The main problem was finding practical extraction techniques for extracting whole compound classes, whilst leaving no influential residues or rendering part of the green coffee sample useless. The extraction of the EIF, in particular, was not as successful as planned, with the proteins and polysaccharides of the compound classes not being clearly distinguishable, when using these extraction methods. This was seen in the extremely low extraction of protein (SPF), in comparison to literary references (Wolfrom et al, 1960; Belitz, 2001), and in the low amount of cellulose (WICF), suggesting that cellulose was extracted by ammonium oxalate into the WIPF. Similar difficulties were found in other research work by Oosterfeld et al. (2003) and Fischer et al. (2001), producing similar quantities of SPF (yield: 4.8 %) and PPF (yield: 2.8 %), but concluding that most of the polysaccharides were embedded in the cell wall and were, therefore, non-extractable. De Maria et al. (1996 a) detected proteins in their cellulose and pectin fraction (WIF), as did Wolfrom et al. (1960) in their

PPF. Using the simple ninhydrin detection in this work, no proteins were found in polysaccharide fractions, but this does not exclude polysaccharides being in protein fractions, or proteins not reacting with ninhydrin. A reliable separation of proteins and polysaccharides was not achieved with these methods, and the determination of the success of the extraction methods was not possible. Altogether 5 kg of green coffee was fractionated according to the scheme in figure 3-35.

3.4.2 $^{15}N/^{14}N$, $^{2}H/^{1}H$ and $^{13}C/^{12}C$ Analyses of Green Coffee Fractions

The extracted fractions of the green coffee beans, as explained in chapter 3.4.1, were measured via EA-C/P-IRMS and the results displayed in figure 3-36. In the green coffee powder fraction (GCP) and the ethanol/water soluble fraction (ESF), a determination of the $\delta^{15}N_{AIR}$ values was not possible, due to unknown peaks overlapping with the measurement gases. Care must be taken also when analysing the $\delta^{2}H_{V\text{-}SMOW}$ values, as extraction solvents can influence these values towards those of the solvent value.

The influence of the extraction solvents on the isotope values was determined by two different methods: the correlation of $^{2}H/^{1}H$ and $^{13}C/^{12}C$ values (Chiriakashi and Naraoka, 2001) of the 'mother' fraction with the 'daughter' fractions - displayed in figure 3-37. For a successful extraction, without isotopic discrimination, these $\delta^{2}H$ and $\delta^{13}C$ values of the 'mother' and 'daughter' fractions have to lie on a straight line with a good positive correlation ($R^2 > 0.95$) between them. A good correlation was only found for the extraction of GCP into HIF and HSF and the extraction of WIF into WICF and WIPF.

A further possibility to control discrimination of the extraction for each element is by correlating the $^{2}H/^{1}H$ or $^{13}C/^{12}C$ values of the 'daughter' fractions, with their extraction percentages, relative to the 'mother' fraction' (Fry, 2006). An example for this calculation is shown in equation (3-1), with $\delta^{13}C$ determination of the extraction of green coffee powder (GCP) into a n-hexane soluble fraction (HSF) and n-hexane insoluble fraction (HIF).

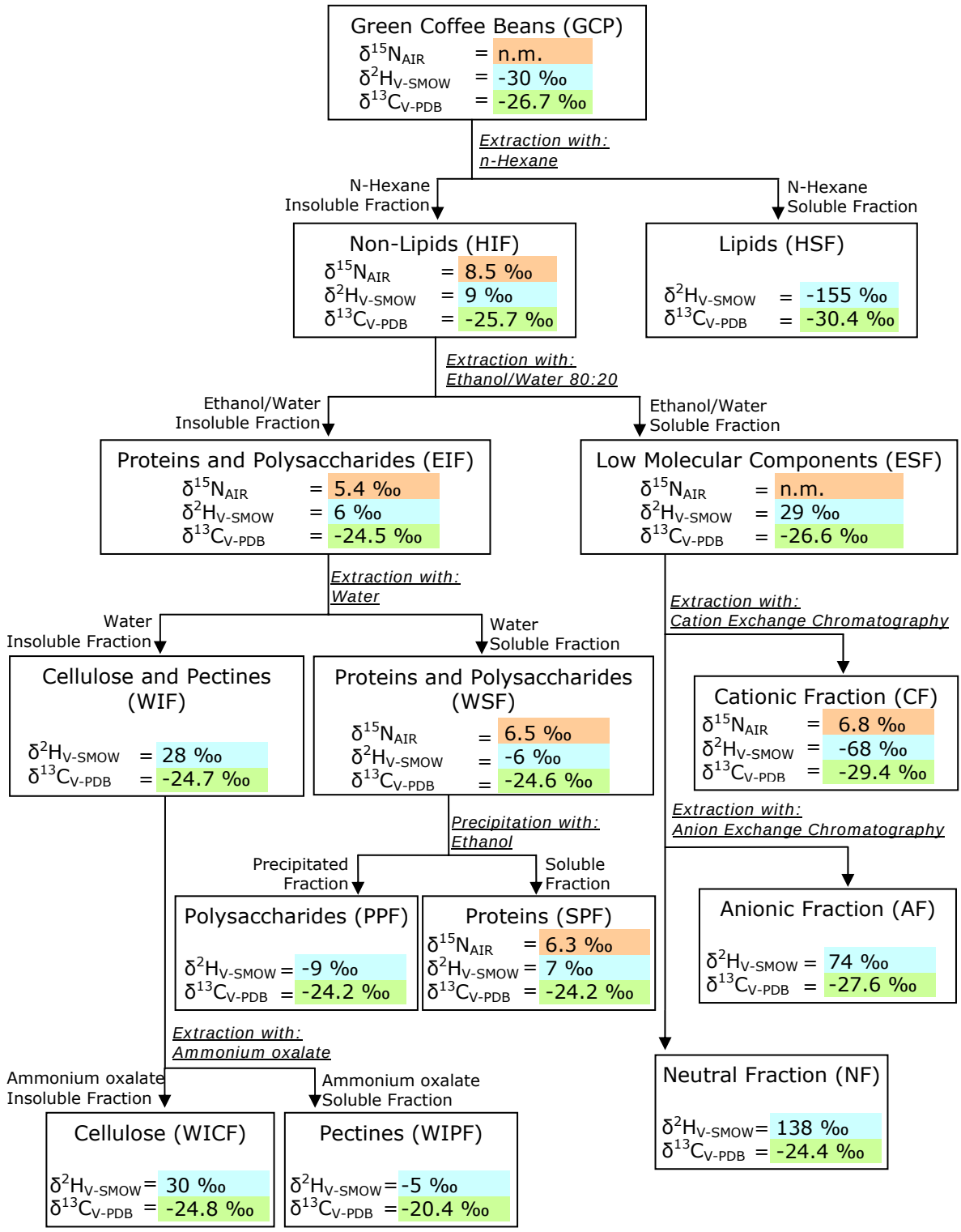

Figure 3-36: $\delta^{15}N_{AIR}$, $\delta^{2}H_{V\text{-}SMOW}$ and $\delta^{13}C_{V\text{-}PDB}$ values [‰] of extracted fractions from the green coffee bean; n.m. = not measured.

(3-1)
$$\delta^{13}C_{V\text{-}PDB\ total} = \frac{(\delta^{13}C_{V\text{-}PDB\ HSF} \times yield_{HSF}) + (\delta^{13}C_{V\text{-}PDB\ HIF} \times yield_{HIF})}{yield_{HSF} + yield_{HIF}}$$

$$= \frac{(-30.4\ ‰ \times 18.9\ \%) + (-25.7\ ‰ \times 81.1\ \%)}{18.9\ \% + 81.1\ \%} = -26.6\ ‰$$

For both 'daughter' fractions, HSF and HIF, the stable isotope value is multiplied by its extraction percentage, and these are then added together, with this total being divided by the sum of the extraction percentages. The resulting value should correspond, within usual tolerances, to the isotope value of the 'mother' fraction (here: GCP: $\delta^{13}C_{V\text{-}PDB}$ = -26.7 ‰). With this method, isotope discriminations in hydrogen values were detected for the fractionation of ESF into CF, AF and NF and of EIF in WSF and WIF.

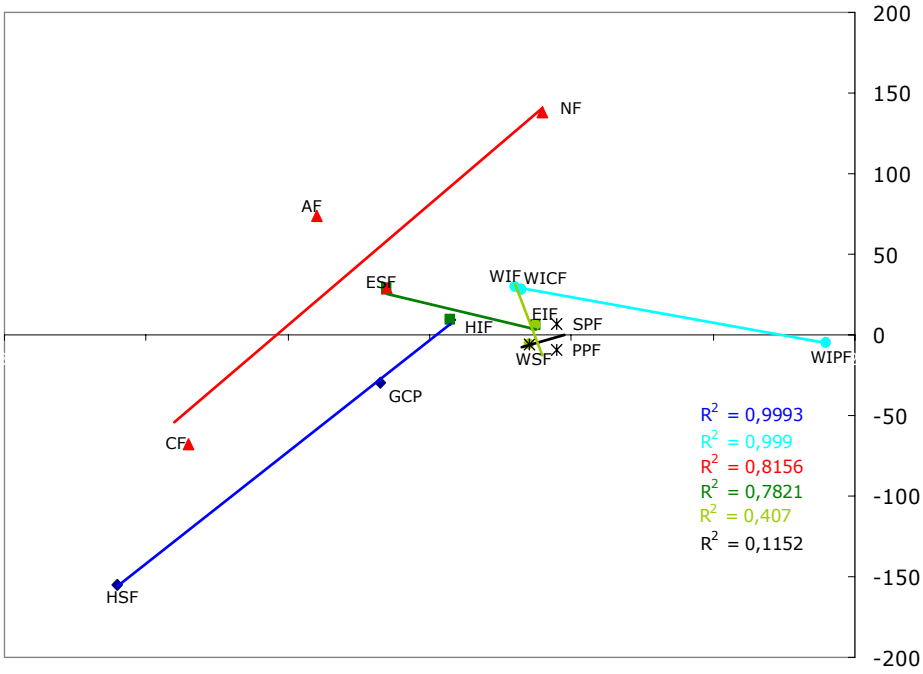

Figure 3-37: Correlation of $^{2}H/^{1}H$ and $^{13}C/^{12}C$ values of the 'mother' fractions with the 'daughter' fractions: ◆ GCP extraction R^2 = 0.9993, ● WIF extraction R^2 = 0.999, ▲ ESF extraction R^2 = 0.8156, ■ HIF extraction R^2 = 0.7821, ● EIF extraction R^2 = 0.407 and ∗ WSF extraction R^2 = 0.1152 (modified from Naraoka and Chikaraishi, 2001).

Regarding the stable isotope data of the isolated green coffee fractions, the fraction green coffee powder (GCP) displayed the bulk isotope values for the green coffee bean with $\delta^{13}C_{V\text{-}PDB}$ = -26.7 ‰ and $\delta^{2}H_{V\text{-}SMOW}$ = -30 ‰. Mean $^{13}C/^{12}C$ isotope ratios of -25.7 ‰ (range: $\delta^{13}C_{V\text{-}PDB}$ = -23.8 ‰ to -28.1 ‰) were found for green coffee beans from Serra et al. (2005). Bulk hydrogen isotope ratios were not found for green coffee in literary references, with these ratios

normally being similar or lower to meteoric hydrogen water (Ziegler et al., 1976; White, 1989). For C_3 plants bulk hydrogen values have been found of $\delta^2H_{V\text{-}SMOW}$ = -44 ‰ to -80 ‰ (Chikaraishi and Naraoka, 2001), and even up to $\delta^2H_{V\text{-}SMOW}$ = -132 ‰ (Smith and Jacobsen, 1976; Ziegler et al., 1976; Estep and Hoerig, 1980). The value of $\delta^2H_{V\text{-}SMOW}$ = -30 ‰ for GCP in this work belongs to the most enriched bulk hydrogen values. Nitrogen values were not measurable, due to overlapping unknown gas peaks during EA-C-IRMS measurement. The subsequent fractionation into n-hexane soluble fraction (HSF) and n-hexane insoluble fraction (HIF) was conducted without isotope discrimination.

The n-hexane soluble fraction (HSF) displayed strongly depleted values for lipids, with $\delta^{13}C_{V\text{-}PDB}$ = -30.4 ‰ and $\delta^2H_{V\text{-}SMOW}$ = -155 ‰, but no $^{15}N/^{14}N$ ratios were measurable, due to the low content of nitrogen. In literary references for lipid fractions of C_3 plants $\delta^{13}C_{V\text{-}PDB}$ values of -30.0 ‰ to -35.9 ‰ and $\delta^2H_{V\text{-}SMOW}$ values of -140 ‰ to -227 ‰ were found (Smith and Jacobsen, 1976; Estep and Hoenig, 1980; Northfelt et al., 1981; Sternberg, 1988; Chikaraishi and Naraoka, 2001; Schmidt et al., 2003). For lipid fractions it was recognised that depletion takes place in both $^{13}C/^{12}C$ and $^{2}H/^{1}H$ ratios (Schmidt et al., 1998) with the $^{13}C/^{12}C$ depletion in the range of 5 ‰ towards the bulk value (Deines, 1980; Kennicutt et al., 1992). Fraction HSF was not fractioned further, as no contribution to the formation of alkylpyrazines during roasting had been expected.

The pendant to the fraction HSF was the n-hexane insoluble fraction (HIF). It contained non-lipids, such as polysaccharides and proteins, as well as other low-molecular constituents, such as caffeine, trigonelline, amino acids and carbohydrates. Following the metabolic balance, the HSF fraction displayed depleted stable isotope values, so the stable isotope values of HIF were expected to be more enriched than GCP fraction. This was the case with $\delta^{13}C_{V\text{-}PDB}$ = -25.7 ‰ and $\delta^2H_{V\text{-}SMOW}$ = 9 ‰. The first measurable nitrogen value, was obtained in this fraction, with $\delta^{15}N_{AIR}$ = 8.5 ‰; this agrees with bulk values in literary references (Werner and Schmidt, 2002). $\delta^{13}C_{V\text{-}PDB}$ and $\delta^2H_{V\text{-}SMOW}$ values of HIF in C_3 plants (leaves and roots) ranged from -25.9 ‰ to -31.9 ‰ and -36 ‰ to -65 ‰, respectively (Chikaraishi and Naraoka, 2001), being more depleted than the values found here.

The fraction HIF was then further extracted by an ethanol/water mixture (80/20, v/v) into an ethanol/water soluble fraction (ESF) and an ethanol/water insoluble fraction (EIF). This extraction process showed, despite the use of water, no significant isotope discrimination in the resulting values. The low molecular components in fraction ESF displayed, in comparison to fraction HSF, enriched

$^{2}H/^{1}H$ ratios and depleted $^{13}C/^{12}C$ ratios, with -26.6 ‰ for $\delta^{13}C_{V\text{-}PDB}$ and 29 ‰ for $\delta^{2}H_{V\text{-}SMOW}$. EIF showed naturally depleted $^{2}H/^{1}H$ ratios and enriched $^{13}C/^{12}C$ ratios, with 6 ‰ for $\delta^{2}H_{V\text{-}SMOW}$ and -24.5 ‰ for $\delta^{13}C_{V\text{-}PDB}$. In this fraction the measurement of the $^{15}N/^{14}N$ ratios were conducted with a depleted value of 5.4 ‰, compared to the HIF value of 8.5 ‰.

The isolation of ESF into a cationic, anionic and neutral fraction (CF, AF and NF) was conducted with no isotope discrimination for $^{13}C/^{12}C$ and $^{15}N/^{14}N$ ratios, but the $^{2}H/^{1}H$ ratios showed a strong discrimination, probably due to the solvents and exchange resins used. $\delta^{15}N_{AIR}$ values were only measurable for the cationic fraction (CF), displaying a value of 6.8 ‰. Fraction CF displayed the most depleted $\delta^{13}C_{V\text{-}PDB}$ value of the three fractions CF, AF and NF with -29.4 ‰, whilst NF showed the most enriched value of -24.4 ‰. The AF displayed a median value of -27.6 ‰. Isotope measurements of CF, AF and NF as bulk fractions had been seldomly performed in the past, with most groups measuring single compound groups, i.e amino acids (Silfer et al., 1991; Yoneyama et al., 1998 a). Bulk values of CF, AF and NF were measured for potato tubers by Smith and Jacobsen (1976), showing for $^{13}C/^{12}C$ ratios the same tendencies, with CF being most depleted, followed by AF and NF (CF: $\delta^{13}C_{V\text{-}PDB}$ = -27.1 ‰; AF: $\delta^{13}C_{V\text{-}PDB}$ = -26.9 ‰; $\delta^{13}C_{V\text{-}PDB}$ = -23.8 ‰). Further $^{2}H/^{1}H$ ratio bulk values of amino acids and carbohydrates were determined to be $\delta^{2}H_{V\text{-}SMOW}$ = -50 ‰ and -110 ‰ (Schmidt et al., 2003). The $\delta^{2}H_{V\text{-}SMOW}$ values were unreliable, due to isotopic hydrogen exchange during the work-up procedure, with only a derivative giving reliable isotope data. This was not performed, due to the complexity and substance inhomogenity of the groups, and so as not to impair the reaction possibilities during roasting. Isotopic determination of single components of the fractions CF, AF and NF, i.e. trigonelline, single amino acids and sucrose, would be interesting for future research projects concerning roast coffee aroma.

EIF was further extracted into a water soluble fraction (WSF) and a water insoluble fraction (WIF) in the hope of dividing proteins from polysaccharides. As expected, no $\delta^{15}N_{AIR}$ values could be measured for WIF, so the content of protein in this fraction was very low, with the majority having gone into the water soluble fraction. As before, no isotope discrimination was found for $^{13}C/^{12}C$ and $^{15}N/^{14}N$ ratios, but due to the use of water as extraction solvent, a minor isotope discrimination in the $^{2}H/^{1}H$ ratios was noticed. WSF showed a value of 6.5 ‰ for $\delta^{15}N_{AIR}$, a slightly depleted $\delta^{2}H_{V\text{-}SMOW}$ value of -6 ‰ compared to EIF, and a $\delta^{13}C_{V\text{-}PDB}$ value of -24.6 ‰, similar to EIF. WIF showed, with $\delta^{13}C_{V\text{-}PDB}$ = -24.7 ‰, a similar value to EIF and WSF, but an enriched $\delta^{2}H_{V\text{-}SMOW}$ value of 28 ‰.

With the precipitation of polysaccharides from the WSF solution using ethanol, fraction WSF was split into a precipitated polysaccharide fraction (PPF) and a soluble protein fraction (SPF). No isotope discrimination was noticed for either of $^{13}C/^{12}C$, $^{15}N/^{14}N$ or $^{2}H/^{1}H$ ratios. Both fractions displayed similar values to one another and to WSF, with the $\delta^{13}C_{V\text{-}PDB}$ values being -24.2 ‰ for PPF and SPF, and the $\delta^{2}H_{V\text{-}SMOW}$ values being -9 ‰ and 7 ‰ for PPF and SPF, respectively. For $\delta^{15}N_{AIR}$ only a value for SPF was measurable, this being 6.3 ‰, which was similar to the value of WSF.

To complete the picture, fraction WIF was extracted further to isolate cellulose from pectin. This step was conducted with ammonium oxalate solution, which guaranteed a complete extraction of pectin, but also (unfortunately) probably extracted a part of the cellulose. Isotope discrimination was seen for both $^{13}C/^{12}C$ and $^{2}H/^{1}H$ ratios, which resulted from the incomplete separation of ammonium oxalate from the extracts. This ammonium oxalate results in $^{13}C/^{12}C$ and $^{2}H/^{1}H$ ratios of -20.4 ‰ and -5 ‰, respectively, for the water insoluble pectin fraction (WIPF). The water insoluble cellulose fraction (WICF) displayed similar values to WIF, with $\delta^{2}H_{V\text{-}SMOW}$ = 30 ‰ and $\delta^{13}C_{V\text{-}PDB}$ = -24.8 ‰. For cellulose, isotope measurements had been conducted in the past, with Weilacher et al. (1996) measuring $\delta^{13}C_{V\text{-}PDB}$ = -27.0 ‰ and Sternberg et al. (1988) finding values of $\delta^{2}H_{V\text{-}SMOW}$ = -25 ‰ to -40 ‰ for nitrated cellulose. The nitration of cellulose was not conducted in this work, so as not to impair the reaction possibilities during roasting.

3.4.3 Aroma Profile of Roasted Green Coffee Fractions

After extraction of the substance classes into fractions, the roasting of these fractions and the stable isotope analysis of the developed aroma compounds were expected to give information on the formation of the alkylpyrazines and pyridines.

As the fractions are powders, a roasting technique had to be developed. For this reason, the powders were converted into pills utilizing the pharmaceutical classic method of a pill machine made of wood and brass. Pictures of the pill-making machine can be found in chapter 4.6.3.9, figure 4-2. Classical auxiliary substances used for transforming powders to dough by this method, were usually yeast extract and sugar syrup or Aerosil®, glycerine and lycopodium combined, which, when mixed with the pharmaceutical drug, formed a plastic mass for pill-making. As yeast extract, sugar syrup, glycerine and lycopodium would adulterate the alkylpyrazine composition and stable isotope values, these were

substituted with water, Aerosil® and for some fractions, silica gel. These compounds were found to be neutral for the alkylpyrazine formation. The scheme for roasting and extraction of the green coffee fraction is displayed in figure 3-38.

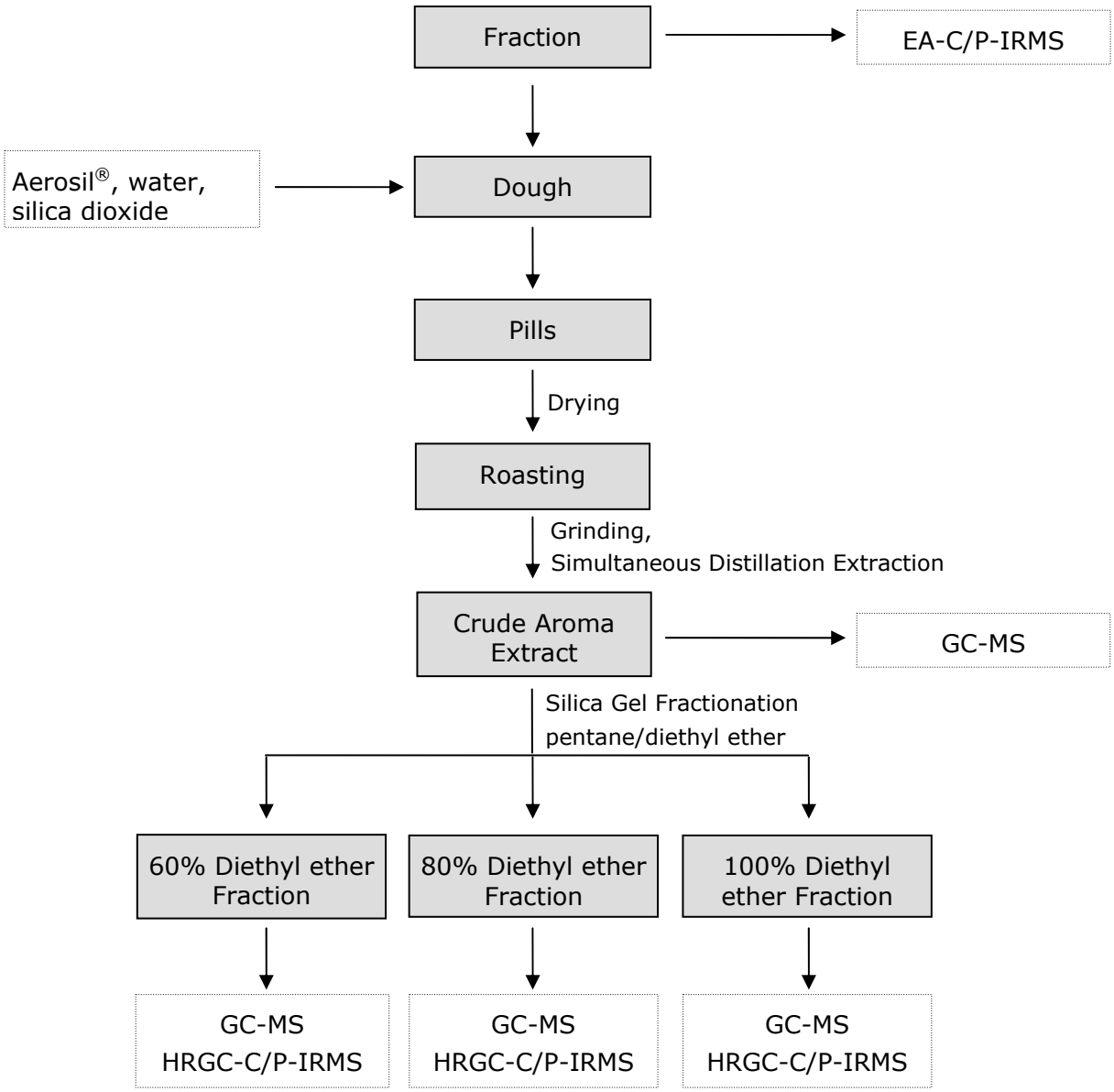

Figure 3-39: Simplified preparation scheme for the roasting and extraction of green coffee fractions.

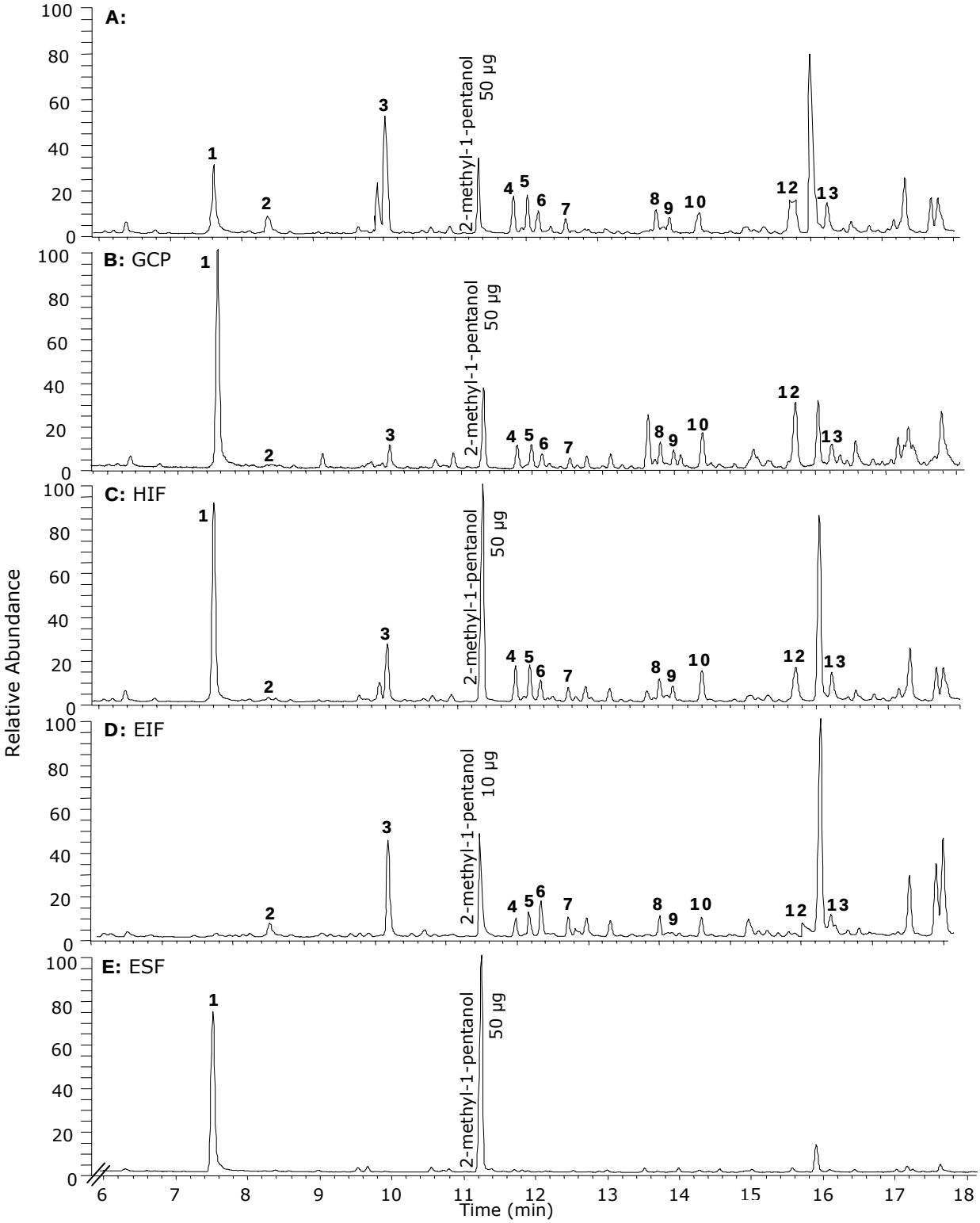

Figure 3-39: Representative HRGC-MS total ion chromatogram (sector) of roasted green coffee fraction volatiles of A: whole green coffee bean, B: ground green coffee bean, C: n-hexane insoluble fraction (HIF), D: ethanol/water insoluble fraction (EIF) and E: ethanol/water soluble fraction (ESF). The compound 2-methyl-1-pentanol was added as a standard in different amounts. The peak numbers indicate the compounds under IRMS study, as shown in chapter 5.

For determining the success of the new roasting technique, the chromatograms and the stable isotope values of both the roasted green coffee powder (GCP) and the roasted whole green beans were compared with each other, as shown in figure 3-39 A and B. The most predominant difference in the two chromatograms is the strong increase of pyridine (**1**) and decrease of pyrazine (**2**) and 2-methylpyrazine (**3**) in the roasted GCP fraction, compared to whole roasted coffee beans. This might be due to the breaking up of cell compartments and the liberation of more pyridine precursors, when grinding green coffee beans to powder, or due to Aerosil® and silica dioxide having a catalytic influence on pyridine formation. Otherwise, the two chromatograms displayed great similarities concerning the alkylpyrazines. A comparison of GCP with whole roasted green coffee beans was not practicable with this method, but a comparison of the other roasted fractions with roasted GCP was possible.

GCP was then fractioned into a non-lipid fraction (HIF) and a lipid fraction (HSF), as explained earlier. The non-lipid fraction (HIF) was roasted and the chromatogram, hereof, displayed in figure 3-39 C. The roasted HIF displayed a near-identical chromatogram to GCP, with a dominant pyridine peak. Altogether, although the amount of roasted HIF equaled the extraction percentile of roasted GCP, the amount of alkylpyrazines and pyridine (**1**) produced in HIF was somewhat lower than the amount in the fraction GCP. As the two chromatograms HIF and GCP were near-identical and the contribution of coffee lipids in alkylpyrazine and pyridine (**1**) formation was considered negligable, a roasting of the lipid fraction (HSF) was renounced (De Maria et al., 1995).

The roasting of the ethanol/water insoluble fraction (EIF), containing polysaccharides and proteins, and the roasting of the ethanol/water soluble fraction (ESF), containing low-molecular amino and sugar components, both deriving from the non-lipid fraction (HIF), proved to give the most interesting results of all. In previous chapters, 3.2.4 and 3.3.5, an explanation for pyridine (**1**) formation was investigated and the first tentative results, concerning the roast degree and also the influence of trigonelline, were postulated. The fractionation of green coffee beans, until now, had shown that grinding the beans also led to an increased pyridine (**1**) formation. A separation of low-molecular from high-molecular substances had been expected to give information on the importance of these compound groups in the formation of pyridine (**1**). When comparing the chromatogram of EIF, with the ‘mother’ fraction HIF, in figure 3-39 D and C, two differences were especially seen. Firstly, the amounts of produced alkylpyrazines in EIF were again less than in HIF (note: standard amount of 2-methyl-1-pentanol is only 10 µg in chromatogram D) and secondly, no pyridine (**1**) was found. In all conducted roastings of the fraction EIF, pyridine

(**1**) was not found except in traces. On the other hand ESF, containing amino acids, trigonelline, saccharides, caffeine and organic acids, displayed, as in figure 3-39 E, pyridine (**1**) and only minute traces of alkylpyrazines. This was a surprising result, as model syntheses, as performed and described in chapter 3.3.3, and also found in literary references (Shu, 1999; Hwang et al., 1994 and 1993), showed that alkylpyrazines were generated from amino acids and in mixtures with saccharides, all being contained in the fraction ESF. These model systems always employed basic conditions to generate the highest yield, which are not found, as such, in coffee beans. Another theory brought forward by Wang (2000) described the inhibition of alkylpyrazine and pyridine (**1**) formation by phenolic compounds. De Maria et al. (1996 a) obtained the same results, when roasting their EIF and ESF fractions and concluded, that for alkylpyrazine generation in ESF the content of amino acids was too low compared to sucrose, and the relevant precursors, proteins and polysaccharides, were not available. De Maria et al.'s high amounts of pyridine (**1**) after roasting ESF, occurred hand in hand with a high loss of trigonelline. The influence of silica dioxide in the alkylpyrazine formation, which was used for the formation of the pills in this fraction only, cannot be excluded, but the conclusion favours the formation of pyridine (**1**) from trigonelline and the alkylpyrazine formation from proteins and polysaccharides.

The next two fractions, water insoluble fraction (WIF) and water soluble fraction (WSF), which derive from EIF, were also roasted and their alkylpyrazine chromatograms compared with each other. In this case, no differences could be seen in the alkylpyrazine formation and its content, with the content being too low for IRMS measurement, so that no further fractions were considered for roasting. A roasting of the cationic fraction (CF) was also abandoned, due to a lack of sufficient content.

3.4.4 $^{15}N/^{14}N$, $^{2}H/^{1}H$ and $^{13}C/^{12}C$ Analyses of Roasted Green Coffee Fractions

Not only had the chromatograms of the alkylpyrazines and pyridine (**1**) displayed significant differences between the single fractions, but also the measurement of the stable isotope values had produced differences, see figure 3-40.

Generally speaking, for all fractions roasted and measured (figure 3-40), the most depleted $\delta^{15}N_{AIR}$ values found were those for pyridine (**1**), with these values becoming more enriched the larger the substitution on the pyrazine ring (albeit with exceptions). A similar tendency was found for $\delta^{13}C_{V\text{-}PDB}$ values, with pyridine (**1**) having the most depleted values in all fractions and pyrazine (**2**) having the

second most depleted values. Otherwise, all other alkylpyrazines displayed $\delta^{13}C_{V\text{-}PDB}$ values between -25 ‰ and -27 ‰.

Compound	**1**	**2**	**3**	**4/5/6**	**7**	**8/9**	**10**	**12/13**	
Whole Green Coffee Beans									
$\delta^{15}N_{AIR}$ =	-2.7 ‰	-1.6 ‰	2.6 ‰	4.1 ‰	4.7 ‰	2.8 ‰	3.7 ‰	4.4 ‰	
$\delta^{2}H_{V\text{-}SMOW}$ =	-115 ‰	-84 ‰	-106 ‰	-103 ‰	-114 ‰	-75 ‰	-116 ‰	-97 ‰	
$\delta^{13}C_{V\text{-}PDB}$ =	-39.3 ‰	-36.3 ‰	-30.4 ‰	-26.4 ‰	-28.8 ‰	-25.6 ‰	-27.1 ‰	-27.0 ‰	
Green Coffee Powder (GCP)									GCP Fraction
$\delta^{15}N_{AIR}$ =	0.5 ‰	1.0 ‰	2.7 ‰	4.0 ‰	4.4 ‰	3.1 ‰	5.7 ‰	7.4 ‰	n.m.
$\delta^{2}H_{V\text{-}SMOW}$ =	-64 ‰	n.m.	-9 ‰	-59 ‰	-46 ‰	-60 ‰	-98 ‰	-90 ‰	-30 ‰
$\delta^{13}C_{V\text{-}PDB}$ =	-34.8 ‰	-29.1 ‰	-26.9 ‰	-25.8 ‰	-26.7 ‰	-25.7 ‰	-27.1 ‰	-27.3 ‰	-26.7 ‰
N-Hexane Insoluble Fraction (HIF)									HIF Fraction
$\delta^{15}N_{AIR}$ =	0.2 ‰	3.1 ‰	1.3 ‰	4.6 ‰	5.1 ‰	4.6 ‰	6.2 ‰	6.1 ‰	8.5 ‰
$\delta^{2}H_{V\text{-}SMOW}$ =	-74 ‰	n.m.	-9 ‰	-68 ‰	-54 ‰	-62 ‰	-113 ‰	-87 ‰	9 ‰
$\delta^{13}C_{V\text{-}PDB}$ =	-35.4 ‰	-28.4 ‰	-26.5 ‰	-25.6 ‰	-24.7 ‰	-27.1 ‰	-26.9 ‰	-26.5 ‰	-25.7 ‰
Ethanol/Water Insoluble Fraction (EIF)									EIF Fraction
$\delta^{15}N_{AIR}$ =	n.m.	-0.5 ‰	3.4 ‰	4.8 ‰	4.9 ‰	5.7 ‰	6.4 ‰	6.1 ‰	5.4 ‰
$\delta^{2}H_{V\text{-}SMOW}$ =	n.m.	45 ‰	25 ‰	-2 ‰	-48 ‰	-38 ‰	-39 ‰	-136 ‰	6 ‰
$\delta^{13}C_{V\text{-}PDB}$ =	n.m.	-25.1 ‰	-26.5 ‰	-25.6 ‰	-24.7 ‰	-27.1 ‰	-26.9 ‰	-26.5 ‰	-24.5 ‰

Figure 3-40: $\delta^{15}N_{AIR}$, $\delta^{2}H_{V\text{-}SMOW}$ and $\delta^{13}C_{V\text{-}PDB}$ values [‰] of alkylpyrazines and pyridine from roasted green coffee fractions and the $\delta^{15}N_{AIR}$, $\delta^{2}H_{V\text{-}SMOW}$ and $\delta^{13}C_{V\text{-}PDB}$ values [‰] of the unroasted fraction. The numbers indicate the compounds under IRMS study, **1** pyridine, **2** pyrazine, **3** 2-methylpyrazine, **4** 2,5-dimethylpyrazine, **5** 2,6-dimethylpyrazine, **6** 2-ethylpyrazine, **7** 2,3-dimethylpyrazine, **8** 2-ethyl-5-methylpyrazine, **9** 2-ethyl-6-methylpyrazine, **10** 2-ethyl-3-methylpyrazine, **12** 2-ethyl-3,5-dimethylpyrazine and **13** 2-ethyl-3,6-dimethylpyrazine.

Roasted whole green coffee beans showed, as in figure 3-40, with -2.7 ‰ ($\delta^{15}N_{AIR}$), the most depleted $\delta^{15}N_{AIR}$ value for the compound pyridine (**1**), with the most enriched $\delta^{15}N_{AIR}$ value = 4.7 ‰ being found for 2,3-dimethylpyrazine (**7**). The $\delta^{2}H_{V\text{-}SMOW}$ values lay in a constant region between -75 ‰ and -116 ‰. Once again the most depleted value for $\delta^{13}C_{V\text{-}PDB}$ was pyridine (**1**) with -39.3 ‰, and the most enriched -25.6 ‰ for 2-ethyl-5/6-methylpyrazine (**8**/**9**).

Comparing roasted ground green coffee beans (GCP) to roasted whole green coffee beans, the first noticeable difference in the $\delta^{15}N_{AIR}$ values was seen to be a general enrichment of these values for compounds **1**, **2**, **10** and **12**/**13** from 2 ‰ to 3.2 ‰, whilst compounds **3**, **4**/**5**/**6**, **7** and **8**/**9** displayed the same

values as roasted whole green coffee beans. $\delta^2H_{V\text{-}SMOW}$ values of roasted ground green coffee beans, on the other hand, showed similar values when compared to whole roasted green coffee beans in compounds **12**/**13**, with compounds **9** and **10** showing a 15 ‰ to 18 ‰ enrichment. All other alkylpyrazines and pyridine displayed highly enriched $\delta^2H_{V\text{-}SMOW}$ values, with the most enriched value being -9 ‰ for 2-methylpyrazine (**3**), when compared to the whole beans. $\delta^{13}C_{V\text{-}PDB}$ values were, for compounds **8**/**9**, **10** and **12**/**13,** constant with roasted whole bean samples, whilst compounds **1**, **2**, **3**, **4**/**5**/**6** and **7** of the roasted GCP displayed more enriched values than the whole beans. The non-roasted GCP with $\delta^{13}C_{V\text{-}PDB}$= -26.7 ‰ showed this value in all the compounds **3**, **7**, **10** and **12**/**13**, with compounds **4**/**5**/**6** and **8**/**9** being more enriched and compound **1** and **2** being more depleted. The differences between roasted ground green coffee beans (GCP) and roasted whole green coffee beans were astounding, seeing that there is no difference between the two, apart from the grinding and the pill-making for roasting for GCP. A comparison of the stable isotope values of the isolated fractions with whole coffee beans is, therefore, difficult, but a comparison, with ground green coffee beans, is possible.

The roasted n-hexane insoluble fraction (HIF) displayed, in figure 3-40, very similar stable isotope values to roasted GCP, with a few exceptions. The compounds pyrazine (**2**), 2-methylpyrazine (**3**), 2-ethyl-5/6-methylpyrazine (**8**/**9**) and 2-ethyl-3,5/6-dimethylpyrazine (**12**/**13**) showed discrepancies to GCP, for $\delta^{15}N_{AIR}$, with compounds **2** and **8**/**9** being more enriched ($\delta^{15}N_{AIR}$ = 3.1 ‰ and 4.6 ‰, respectively), and compounds **3** and **12**/**13** more depleted ($\delta^{15}N_{AIR}$ = 1.3 ‰ and 6.1 ‰, respectively). For HIF the $\delta^2H_{V\text{-}SMOW}$ values showed no strong discrepancies to GCP, with compound **10** displaying a 15 ‰ depletion in the HIF compared to GCP, this being the largest difference. Compounds **7** ($\delta^{13}C_{V\text{-}PDB}$ = -24.7‰) and **8**/**9** ($\delta^{13}C_{V\text{-}PDB}$ = -27.1 ‰) in HIF, showed differences of ca. 2 ‰ towards GCP, these being the only differences. Compared to the non-roasted n-hexane insoluble fraction (HIF; $\delta^{15}N_{AIR}$ = 8.5 ‰; $\delta^2H_{V\text{-}SMOW}$ = 9 ‰; $\delta^{13}C_{V\text{-}PDB}$ = -25.7 ‰), the roasted HIF displayed far more depleted $\delta^{15}N_{AIR}$ and $\delta^2H_{V\text{-}SMOW}$ values and also, mostly more depleted $\delta^{13}C_{V\text{-}PDB}$ values, with compounds **4**/**5**/**6** having the same value and **7** being more enriched.

For the stable isotope determination of the ethanol/water insoluble fraction (EIF), in figure 3-40, a difference to HIF was expected, as the precursors of the alkylpyrazines in this fraction consisted of polysaccharides and proteins, without low-molecular amino acids and sugars. Nearly identical to the previous fraction HIF, were compounds **7** and **12**/**13**. Compounds **12**/**13** displayed only a further depletion in the $\delta^2H_{V\text{-}SMOW}$ value ($\delta^2H_{V\text{-}SMOW}$ = -136 ‰), but had otherwise similar $\delta^{13}C_{V\text{-}PDB}$ and $\delta^{15}N_{AIR}$ values. No differences in $\delta^{13}C_{V\text{-}PDB}$ and $\delta^{15}N_{AIR}$ values towards

HIF were found. Furthermore, for compounds **4**/**5**/**6** and **10**, the $^{2}H/^{1}H$ ratios were found to be enriched by ca. 70 ‰, compared to previous fractions. Pyridine (**1**) was not found or only in traces, so that no stable isotope values were measurable. Pyrazine (**2**) displayed its most enriched values of all fractions for $^{2}H/^{1}H$ ratio = 45 ‰ and $^{13}C/^{12}C$ ratio = -25.1 ‰, with the $^{15}N/^{14}N$ ratio being depleted at -0.5 ‰. 2-Methylpyrazine (**3**) and 2-ethyl-5/6-methylpyrazine (**8**/**9**) showed no differences in their $^{13}C/^{12}C$ ratios to the previous fraction HIF but displayed enriched $\delta^{2}H_{V\text{-}SMOW}$ and $\delta^{15}N_{AIR}$ values (**3**: $\delta^{2}H_{V\text{-}SMOW}$ = 25 ‰ and $\delta^{15}N_{AIR}$ = 3.4 ‰; **8**/**9**: $\delta^{2}H_{V\text{-}SMOW}$ = -38 ‰ and $\delta^{15}N_{AIR}$ = 5.7 ‰). The influence of the stable isotope values of the non-roasted EIF fraction could not be directly seen in the product alkylpyrazines, where the $\delta^{2}H_{V\text{-}SMOW}$ values showed especially remarkable enrichments.

3.4.5 Conclusion

The fractionation of green coffee in its compound classes, the measurement of these via EA-C/P-IRMS and the subsequent roasting and GC-C/P-IRMS measurement of the produced alkylpyrazines and pyridine gave insight into the until now never performed stable isotope characterisation of green coffee.

The fractionation into compound classes was partly successful, with the n-hexane and ethanol/water extractions, as well as the exchange chromatography, which satisfactorily separated the compound classes without isotope discrimination (the exception being the $\delta^{2}H_{V\text{-}SMOW}$ values of exchange chromatography). Further separation of polysaccharides and proteins was attempted, but not performed with satisfactory results. A separation of polysaccharides and proteins could not be confirmed.

The stable isotope analysis of the thus extracted fractions was not always without isotope discrimination for $\delta^{2}H_{V\text{-}SMOW}$, due to proton exchange of low-molecular substances with water, for fractions deriving both from ethanol/water soluble fraction (ESF) and for fractions extracted with water (WSF and WIF). $\delta^{2}H_{V\text{-}SMOW}$ and $\delta^{13}C_{V\text{-}PDB}$ values were also affected isotopically, due to residues of extraction solvents in the fraction, as with the water insoluble pectin fraction (WIPF). Otherwise, the stable isotope values concurred with references, providing bulk values of $\delta^{2}H_{V\text{-}SMOW}$ = -30 ‰ and $\delta^{13}C_{V\text{-}PDB}$ = -26.7 ‰, with the lipids showing more depleted values and polysaccharides and proteins more enriched ones. $\delta^{15}N_{AIR}$ values for the fractions ranged between 8.5 ‰ and 5.4 ‰

The subsequent roasting of some of the fractions provided a connection between the isotope values of the fractions and the produced alkylpyrazines and pyridine, as well as to mark differences in the roast aroma profiles. The produced alkylpyrazines, on the whole, represented the $\delta^{13}C_{V\text{-}PDB}$ values for C_3 plants. A strong difference was seen both in the aroma profile and the stable isotope values of the roasted ground green coffee bean (GCP), compared to roasted whole green beans. The main differences were significantly more pyridine and less alkylpyrazines, as well as, generally, more enriched $\delta^{15}N_{AIR}$, $\delta^{2}H_{V\text{-}SMOW}$ and $\delta^{13}C_{V\text{-}PDB}$ values. The reason for these differences could not be determined, but two theories were put forward: firstly, the grinding led to cell compartment degrading, which set free more of certain precursors or led to different reaction possibilities and, secondly, the adding of Aerosil® acted as a catalyst, changing the reaction mechanisms of alkylpyrazines during roasting. The n-hexane insoluble fraction (HIF) displayed, on the whole, a similar chromatogram and stable isotope values, compared to GCP. As a conclusion, the n-hexane soluble fraction (HSF) was considered not to be important for alkylpyrazine and pyridine formation. The first large difference was seen after the extraction of HIF with an ethanol/water solution. The fraction containing low-molecular substances (ESF), which was thought to be the main fraction for alkylpyrazine formation, displayed next to no alkylpyrazines but mostly pyridine. The high-molecular substances (EIF), on the other hand, displayed the alkylpyrazine aroma profile after roasting, which was typical for roast coffee, but without pyridine (**1**). Summarising this, the formation of pyridine in roast coffee aroma derives from trigonelline and/or other low molecular substance degradation whilst the formation of alkylpyrazines derives from polysaccharides and proteins. In the fraction EIF, for most of the substances under study, the $\delta^{2}H_{V\text{-}SMOW}$ values were especially strongly enriched. Altogether, the alkylpyrazines, with ethyl-rests, were the most consistent stable isotope values. Furthermore, it was noticed that the amount of alkylpyrazines found, after roasting the fractions, decreased from the whole coffee beans over GCP, HIF to EIF. Grosch (2000), who had been analysing the formation of 2-furfurylthiol from green coffee fractions, also noticed a decrease in the yield of 2-furfurylthiol after defatting the samples. This observation seems to be less a consequence of the roasting technique, but more an indicator that it is the combination of the fractions, which leads to the greatest yield of coffee aroma, despite the importance that single fractions may have.

4 Materials and Methods

4.1 Coffee Bean Samples

Green coffee beans (*Coffea arabica* L. and *Coffea canephora var. robusta*) of different origins, that is, India, Brazil, Ethiopia, Malawi, Costa Rica, Hawaii, Indonesia, and Malabar (n = 9) were obtained from RONA Inc. (Kingston Court, U.K.) and Illycafé (Trieste, Italy). Roasted coffee beans from commercial German trademarks (n = 8) were purchased from a local supermarket. Unspecified roast coffee samples (n = 7), coffee products, as coffee drinks and instant coffees, (n = 12), coffee flavours (n = 4) and cocoa (n = 1) were supplied from Dr. König (Givaudan, formerly Quest, Naarden, The Netherlands). For green coffee bean fractionation and roasting experiments *Coffea arabica* L. beans from Porto de Santos, Brasil, were used.

4.2 Chemicals

As references, synthetic and those 'declared to be natural', that is pyridine (**1**), pyrazine (**2**), 2-methylpyrazine (**3**), 2,5-dimethylpyrazine (**4**), 2,6-dimethylpyrazine (**5**), 2-ethylpyrazine (**6**), 2,3-dimethylpyrazine (**7**), 2-ethyl-5-methylpyrazine (**8**), 2-ethyl-6-methylpyrazine (**9**), 2-ethyl-3-methylpyrazine (**10**), 2,3,5-trimethylpyrazine (**11**), 2-ethyl-3,5/6-dimethylpyrazine (**12**/**13**), 2,3,5,6-tetramethylpyrazine (**14**), and 2,3-diethylpyrazine were employed. They were obtained from Fluka (Deisenhofen, Germany), Treatt (Suffolk, U.K.), Sigma-Aldrich (Steinheim, Germany), Givaudan (formerly Quest, Naarden, The Netherlands), Bedoukian (Dunbury, USA), and Oxford (Duisburg, Germany). All other chemicals were purchased in p.a. quality, if not mentioned otherwise, from Sigma-Aldrich (Steinheim, Germany), Fluka (Deisenhofen, Germany), Degussa (Frankfurt/M, Germany) as well as from Roth (Karlsruhe, Germany). Educts for synthesis were also purchased from the above named companies. Solvents were redistilled before use.

Ethanol absolute was of p.a. quality (Riedel de Haen, Seelze, Germany); the water was of Millipore quality, unless noted otherwise.

Pure gases were from Linde (Unterschleißheim, Germany) and Messer Griesheim (Frankfurt, Germany), and liquid nitrogen from Air Liquide (Düsseldorf, Germany). As carrier gas, helium (purity 5.3), was used; for $\delta^{13}C_{V\text{-}PDB}$ and $\delta^{15}N_{AIR}$ analyses oxygen (purity 5.0), as oxidation gas, was used (both from Linde, Unterschleißheim, Germany). Certified CO_2 gas, with defined isotope values

($\delta^{13}C_{V\text{-}PDB}$ value = -25.9 ‰ and -24.9 ‰), as well as H_2 gas (purity 6.0), with defined isotope values of $\delta^2H_{V\text{-}SMOW}$ = -149.4 ‰, -280.0 ‰ and -255.0‰, were purchased from Messer Griesheim (Unterschleißheim, Germany). For $^{15}N/^{14}N$ determination, the mass spectrometer was calibrated against reference N_2 gas (Messer Griesheim, Frankfurt, Germany) with a defined $\delta^{15}N_{AIR}$ value = -10 ‰. For routine measurements, calibrated laboratory N_2 gas (purity 5.3; $\delta^{15}N_{AIR}$ = -5.5 ‰ calibrated with IAEA-N-1 and IAEA-N-2 standards) was used.

International isotope standards came from the International Atomic Energy Agency (IAEA, Vienna, Austria) and the former National Bureau of Standards (NBS, Gaithersburg, Maryland, USA) now named N.I.S.T (National Institute of Standards and Technology).

4.3 Consumables for Isotope Ratio - Mass Spectrometry

The material needed, for measuring with the elemental analysers, was obtained from HEKATech (Wegberg, Germany). For $\delta^2H_{V\text{-}SMOW}$ measurements nickel wool, glass carbon slivers, nickel-coated carbon, silver capsules (2 mm x 5 mm) and silver cartridges (3.5 mm x 5 mm) were used. For $\delta^{13}C_{V\text{-}PDB}$ measurements tin capsules (2 mm x 5 mm) and tin cartridges (3.5 mm x 5 mm), as well as packed CNS reactors were used.

The water separators for both elemental analysers were filled with quartz wool and magnesium perchlorate. For $\delta^2H_{V\text{-}SMOW}$ and $\delta^{15}N_{AIR}$ measurements additional carbosorb (adsorption for CO_2) was needed.

All expendable materials for the mass spectrometer were obtained from Thermo Electron GmbH (Bremen, Germany); material for the gas chromatography-combustion/pyrolysis was obtained from Thermo Electron GmbH (Bremen, Germany) and CZT Chromatographie Zubehör Trott (Kriftel, Germany).

4.4 Chromatography

4.4.1 Column Chromatography

4.4.1.1 Silica Gel Chromatography

Silica gel column chromatography was performed with a glass column, 2 cm × 30 cm, filled with silica gel 60 (Merck), particle size 0.2 mm - 0.5 mm. Elution

was performed, using a pentane - diethyl ether mixture from 0 % to 100 % diethyl ether in 20 % steps, each 150 ml, with a flow rate of 3 ml/min.

4.4.1.2 Cation Exchange Chromatography

Cation exchange chromatography was performed with a glass column, 2 cm x 30 cm, filled with Dowex® 50 WX 8-400 resin (Sigma-Aldrich). The resin in the column was conditioned before use as follows:

- 300 ml dest. water
- 300 ml 1N NaOH
- 300 ml dest. water
- 300 ml 1N HCl
- 300 ml dest. water

For all elutions a flow rate of 2 ml/min was generated with pressure.

4.4.1.3 Anion Exchange Chromatography

Anion exchange chromatography was performed with a glass column, 2 cm x 30 cm, filled with Dowex® 1 x 8 200-400 resin (Sigma-Aldrich). The resin in the column was conditioned before use as follows:

- 300 ml dest. water
- 300 ml 1N NaOH
- 300 ml dest. water
- 300 ml 1N HCl
- 300 ml dest. water

For all elutions a flow rate of 2 ml/min generated with pressure was applied.

4.4.2 Thin Layer Chromatography (TLC)

4.4.2.1 Detection of Sucrose via TLC

Plate: TLC aluminium foil ready plates silica gel Polygram® SIL G/UV_{254} (5 cm x 10 cm), layer thickness 0.2 mm (Merck, Darmstadt, Germany).

Mobile phase:	n-Butanol, acetic acid conc., water (8:3:3, v/v/v)
Detection agent:	Vanillin-sulfuric acid; 1 g vanillin dissolved in 100 ml ethanol + 1 ml conc. sulfuric acid
Processing:	Drying oven at 110 °C for 5 min

The identification of sucrose was carried out by comparison of R_f values with references.

4.4.2.2 Detection of Amino Acids via TLC

Plate:	TLC aluminium foil ready plates silica gel Polygram® SIL G/UV_{254} (5 cm x 10 cm), layer thickness 0.2 mm (Merck, Darmstadt, Germany).
Mobile phase:	n-Butanol, acetic acid conc., water (8:3:3, v/v/v)
Detection agent:	0.3 % Ninhydrin solution in ethanol/acetic acid conc. (93:3, v/v)
Processing:	Drying oven at 110 °C for 5 min

The identification of amino acids was carried out by comparison of R_f values with references.

4.4.2.3 Detection of Trigonelline via TLC

Plate:	TLC aluminium foil ready plates aluminium oxide (20 cm x 20 cm), layer thickness 0.2 mm (Merck, Darmstadt, Germany).
Mobile phase:	Methanol, acetic acid conc., water (95:5, v/v)
Detection agent:	UV light, 254 nm

The identification of trigonelline was carried out by comparison of R_f values with references.

4.4.2.4 Detection of Citric Acid via TLC

Plate:	TLC aluminium foil ready plates aluminium oxide (20 cm x 20 cm), layer thickness 0.2 mm (Merck, Darmstadt, Germany).
Mobile phase:	n-Propanol, ammoniak conc., water (6:3:1, v/v/v)
Detection agent:	0.1 % Bromothymolblue solution in water/KOH (99:1, m/m)
Processing:	Drying oven at 110 °C for 5 min

The identification of citric acid was carried out by comparison of R_f values with references.

4.5 Instruments

4.5.1 Capillary Gas Chromatography - Mass Spectrometry (HRGC-MS)

GC 1: Agilent 6890 GC System (Agilent Technologies, Wilmington, USA)

Injection:	Split/splitless injection (1:20), temperature 220 °C
Autosampler:	Agilent 7683 Series Injector
Chromatography:	J&W DB-Wax (30 m x 0.25 mm, df = 0.25 µm)
Temperature program:	50 °C, 3 min isothermal, 4 °C/min, 250 °C, 10 min isothermal
Carrier gas:	2.0 ml/min, helium 5.0, constant flow

MS 1: Agilent 5973 Mass Selective Detector MSD (Agilent Technologies, Wilmington, USA)

Ionisation:	Electron impact ionisation (EI), 70 eV
Temperature:	Ion source 150 °C, transfer line 250 °C
Source pressure:	1×10^{-5} mbar
Cathode current:	1.5 mA
Multiplier:	1300 V
Mass spectrum:	38-450 u

Data recording via HP Chem Station, after conversion with file converter data evaluation via Xcalibur.

4.5.2 Isotope Ratio Mass Spectrometry (IRMS)

4.5.2.1 Capillary Gas Chromatography

GC 2: Agilent 6890 GC System (Agilent Technologies, Wilmington, USA)

Injection:	1 µL splitless injection, temperature 250 °C
Autosampler:	CTC A 200 S (Zwingen, Switzerland)
Column:	J&W DB-Wax (60 m x 0.32 mm, df = 0.25 µm)

Temperature program:	50 °C to 220 °C at 5 °C/min, 10 min isothermal
Carrier gas:	2.0 ml/min, helium 5.3, constant flow

4.5.2.2 HRGC-'Interfaces'

'Interface 1': Combustion for $^{13}C/^{12}C$ determination

Combustion reactor:	Al_2O_3, 0.5 mm i.d., 1.5 mm o.d., 320 mm with Cu, Ni, Pt wires (each 240 mm × 0.125 mm), 960 °C
Oven:	Heated Al_2O_3 oven 260 mm x 1.6 mm i.d., 32 Ω cold resistance
Thermoelement:	Pt/Rh/Pt-
Reduction reactor:	Al_2O_3, 0.5 mm i.d., 1.5 mm o.d., 320 mm, Cu, 600 °C
Reoxidation:	2 Hours at 960 °C, oxygen 5.0, 5 ml/min

'Interface 2': Combustion for $^{15}N/^{14}N$ determination

Combustion reactor:	Al_2O_3, 0.5 mm i.d., 1.5 mm o.d., 320 mm with Cu, Ni, Pt wires (each 240 mm × 0.125 mm), 960 °C
Oven:	Heated Al_2O_3 oven 260 mm x 1.6 mm i.d., 32 Ω cold resistance
Thermoelement:	Pt/Rh/Pt-
Reduction reactor:	Al_2O_3, 0.5 mm i.d., 1.5 mm o.d., 320 mm, Cu, 600 °C
Reoxidation:	From 600 °C to 960 °C, 1 min isothermal

'Interface 3': Pyrolysis for $^{2}H/^{1}H$ determination

Pyrolysis reactor:	Ceramic tube, Al_2O_3; 0.5 mm i.d., 320 mm, 1440 °C
Oven:	Heated Al_2O_3 oven 260 mm x 1.6 mm i.d., 32 Ω cold resistance
Thermoelement:	Silicon carbide
Water separation:	Nafion® membrane Permapure (Toms River, New York) 200 mm x 0.8 mm, 0.6 mm i.d. coaxial in a glass liner 4 mm i.d., 6 mm o.d.
Coupling:	Open coupling via 'open-split'

4.5.2.3 Elemental Analysers

EA 1: Combustion ($^{15}N/^{14}N$ and $^{13}C/^{12}C$) Euro Vector EA 3000 (Milan, Italy)

Reactor:	Quarz tube filled with tungsten oxide, quartz wool, copper; temperature 1000 °C
Oxygen volume:	Oxygen 5.0, 7 seconds
Oxygen pressure:	15 kPa
Water separator:	Glass tube (10 cm x 2 cm) filled with magnesium perchlorate ($^{13}C/^{12}C$)/ 30 % magnesium perchlorate and 70 % carbosorb ($^{15}N/^{14}N$)
Column:	Porapak® QS (2 m x 5 mm i.d.)
Oven temperature:	95 °C
Autosampler:	Eurocap
Carrier gas:	Helium 5.3, 90 kPa (flow 80 ml/min)

EA 2: Pyrolysis ($^{2}H/^{1}H$) HT Sauerstoff Analysator (HEKATech, Wegberg, Germany)

Reactor:	Ceramic tube (outside) with a quartz glass tube filled with nickel wool, glass carbon slivers and nickel-coated carbon
Water separator:	Glass tube (10 cm x 2 cm) filled with 70 % magnesium perchlorate and 30 % carbosorb
Column:	Molecular sieve 5ª (1 m x 5 mm i.d.)
Oven temperature:	95 °C
Autosampler:	Eurocap
Carrier gas:	Helium 5.3, 90 kPa (flow 80 ml/min)
Detector:	Thermal conduction detector (TCD)
Coupling:	Open coupling via “open-split”

4.5.2.4 Isotope Ratio – Mass Spectrometer

MS 2:	Finnigan MAT DELTA^{plus} XL (ThermoQuest, Egelsbach, Germany)
Ionisation:	Electron impact Ionisation (EI), 70 eV
Temperature:	Ion source ca. 70 °C (2 halogen lamps 12 V, 10 W), cathode voltage 3 kV

Transfer capillaries:	Unheated 1.5 m x 0.1 mm (sample), 1.5 m x 0.005 mm (reference gas)
Mass spectrum:	1-70 Dalton
Detector:	Collector system (Faraday cups) for m/z 2 and 3 ($\delta^2H_{V\text{-}SMOW}$ analysis); H_2 m/z 28, 29 and 30 ($\delta^{15}N_{AIR}$ analysis); N_2 m/z 44, 45 and 46 ($\delta^{13}C_{V\text{-}PDB}$ analysis); CO_2

Data recording and evaluation via Isodat NT for Real 32 (Thermoquest, Egelsbach, Germany)

4.5.3 Nuclear Magnetic Resonance Spectroscopy (NMR)

Maschine:	Bruker NMR (400/100 Hz)
Solvent:	D_2O (Merck, Darmstadt, Germany)

4.5.4 Other Instruments

pH electrode:	WTW pH 330 Wissenschaftliche Technische Werkstätten (Weilheim, Germany)
Scales:	Mettler PL 300 and Mettler P 1200 N, Mettler Waagen GmbH (Gießen, Germany) Sartorius BP 210 S and Sartorius BP 2105, Sartorius AG (Göttingen, Germany)
Rotary evaporator:	Büchi Rotavapor with Büchi vacuum system B-173 and Büchi vacuum controller B-720, Büchi, (Konstanz, Germany)
Mixer:	Mixi 700
Coffee roaster:	40201 Precision Coffee Roaster™ (Hearthware Home Products, Inc.)
Coffee grinder:	Bodum Antigua (Bodum, Triengen, Switzerland)
Reaction cylinder:	Stainless steel, 18 cm x 3 cm i.d., with threaded top onto which a stainless steel lid with inner Teflon seal fits (see figure 4-1)
Centrifuge:	Universal 16, Hettich Zentrifugen
Shaker:	GFL 3033 and GFL 3031 (GFL, Burgwedel, Germany)
Freeze dryer:	Christ Alpha 1-4, 0.1 mbar (Christ, Osterode, Germany)

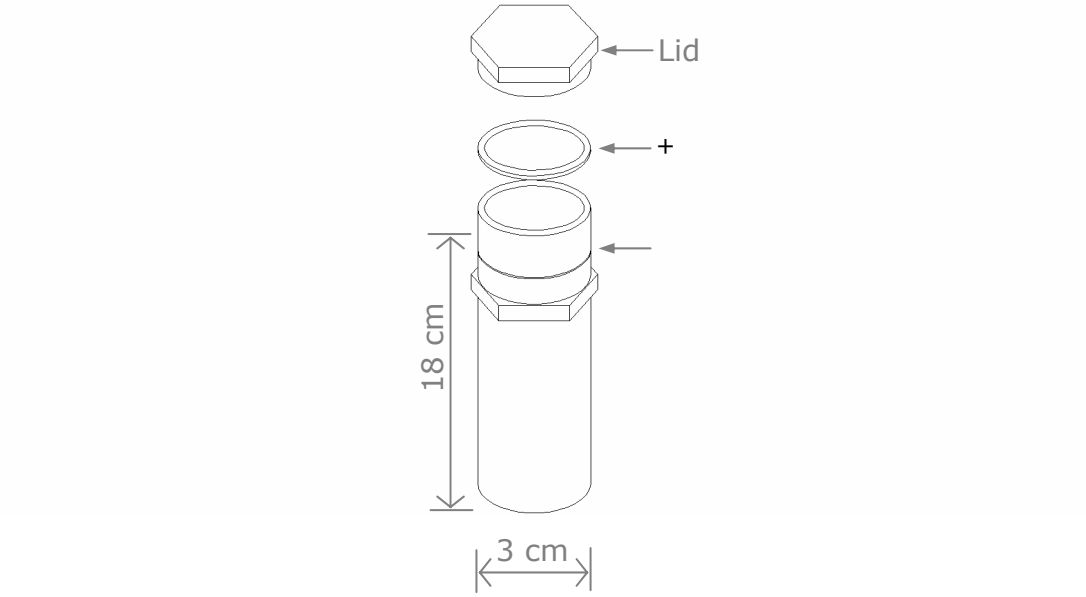

Figure 4-1: Schematic drawing of the reaction cylinder

4.6 Methods

4.6.1 Stability of Alkylpyrazines in Water and Ethanol

The correct pH value of the solvents (pH = 3, 5 or 7) was obtained by addition of 0.1 mol/L hydrochloric acid to the solvent, with continuous control via pH-meter.

For the storage studies in ethanol, 2 mg of each: pyrazine (**2**), 2-methylpyrazine (**3**), 2-ethylpyrazine (**6**), 2,3,5-trimethylpyrazine (**11**), 2-ethyl-3,5/6-dimethylpyrazine (**12**/**13**) and 2,3,5,6-tetramethylpyrazine (**14**) were dissolved in 1 ml of ethanol of each appropriate pH value (3, 5, 7). These were measured directly, without sample preparation, on day 0 (directly after addition of the alkylpyrazines), 1, 3, 6, 10, 20 and 30, via HRGC-P-IRMS.

Milipore water (each 100 ml) was adjusted to pH = 3, 5 and 7, respectively, and 20 mg of each of the above named alkylpyrazines were added. On the specific days 0, 1, 3, 6, 10, 20 and 30, 10 ml of solution were removed from the flasks and the alkylpyrazines extracted with 3 x 30 ml of diethyl ether. The extracts obtained were combined and dried over anhydrous sodium sulphate, filtered, and carefully concentrated to approximately 1.5 ml on a Vigreux column (45 °C). This extract was then submitted to HRGC-P-IRMS.

4.6.2 Sample Preparation

4.6.2.1 References

Synthetic and ‘declared to be natural’ references were dissolved (1 mg/ml) in diethyl ether and the solutions were analysed by HRGC-MS and HRGC-C/P-IRMS. References were also directly measured by EA-C/P-IRMS.

4.6.2.2 Coffee Samples

4.6.2.2.1 Roasting of Green Coffee Beans

The roasting of green coffee beans (in portions of 80 g) was performed using the coffee roaster, with the setting at position 5 (corresponding to 6 min at 210 °C). For studying the influence of roasting time on the aroma composition of green coffee beans, the positions 4 (corresponding to 4 min 30 s at 210 °C), 6 (corresponding to 8 min 50 s at 210 °C) and 9 (corresponding to 15 min at 210 °C) were employed.

4.6.2.2.2 Simultaneous Distillation Extraction (SDE)

Commercially available and self-roasted coffee beans (each 350 g), roast cocoa beans and solid coffee products (each 350 g) and aqueous coffee products (1000 g), were ground if needed and, after addition of 2 litres of distilled water, subjected to simultaneous distillation extraction (SDE with a modified Likens-Nickerson apparatus) for 2 h with pentane-diethyl ether mixture (1:1 v/v). The extract obtained by SDE was dried over anhydrous sodium sulfate, filtered, and carefully concentrated to approximately 5 ml on a Vigreux column (45 °C).

4.6.2.2.3 Silica Gel Fractionation

For the HRGC-C/P-IRMS analysis, roast coffee aroma extracts from SDE were purified by liquid chromatography on silica gel, see chapter 4.4.1.1. The fraction eluted with 60 % diethyl ether contained 2-ethylpyrazine (**6**), 2-ethyl-5/6-methylpyrazine (**8**/**9**), 2-ethyl-3-methylpyrazine (**10**) and 2-ethyl-3,5/6-methylpyrazine (**12**/**13**). 2-Methylpyrazine (**3**), 2,5-dimethylpyrazine (**4**), 2,6-dimethylpyrazine (**5**), 2,3-dimethylpyrazine (**7**), and 2,3,5-trimethylpyrazine (**11**) were recovered in the 80 % diethyl ether fraction. Pyridine (**1**) and pyrazine

(**2**) were eluted in the 100 % diethyl ether fraction. After evaporation of the solvent, all fractions were applied to HRGC-C/P-IRMS analysis. Because of insufficient separation of components **8** and **9** as well as **12** and **13** during HRGC-C/P-IRMS analysis, the isotope ratios were measured for the mixtures of **8**/**9** and **12**/**13**, respectively.

The influence of sample preparation on the $^{2}H/^{1}H$, $^{15}N/^{14}N$ and $^{13}C/^{12}C$ isotope ratios was checked for compounds **1** to **14** by model SDE and subsequent silica gel column separation. No significant isotope discrimination effects were observed by the applied workup procedure, if the compounds were eluted in one fraction. When a compound was found to have eluted in two fractions, these were combined to exclude isotope discrimination.

4.6.2.2.4 Coffee Aroma

Coffee aroma samples were diluted by a factor of 10 and then measured directly via HRGC-MS and HRGC-C/P-IRMS.

4.6.3 Fractionation of Green Coffee Beans

4.6.3.1 Grinding of Green Coffee Beans

Green coffee beans (*Coffea arabica* L., Porto de Santos, Brasil) were ground with the mixer Mixi 700, and subsequently sieved (metal sieve; mesh size 1 mm) with the green coffee powder then being separated from the larger coffee pieces. This procedure was repeated until all the green coffee beans had been finely ground to powder (abbr. GCP, Green Coffee Powder).

4.6.3.2 Extraction of Green Coffee Powder with n-Hexane

The lipid soluble fraction of green coffee beans was isolated, via Soxhlet extraction, with n-hexane using the method from §64 LFGB, L 01.00-20. Green coffee powder (GCP) was filled in either small Soxhlet (diameter 3.5 cm, length 10 cm, 20 g to 40 g of GCP) or large Soxhlet hulls (diameter 5 cm, length 15 cm, 80 g to 130 g). The hulls were closed by cotton wool and extracted with n-hexane for 8 h or 24 h, respectively.

Subsequently, the n-hexane was evaporated carefully at 45 °C, under pressure, and the excess solvent was removed carefully with nitrogen gas. The resulting oily, orange-brown n-hexane soluble coffee fraction was stored at -20 °C until EA-C/P-GCMS measurement (abbr. HSF, n-Hexane Soluble Fraction; yield: 18.9 %) was conducted.

After solvent evaporation, the Soxhlet hull was freeze-dried and homogenised and the resulting n-hexane insoluble coffee powder (abbr. HIF, n-Hexane Insoluble Fraction; yield: 81.1 %) was stored at -20 °C until conducting EA-C/P-GCMS measurement, roasting of the fraction, or further extraction, see 4.6.3.3.

4.6.3.3 Extraction of n-Hexane Insoluble Fraction with Ethanol/Water (80:20, v/v)

To separate polysaccharides and proteins from lower molecular components, the n-hexane insoluble fraction was extracted, with an ethanol/water (80:20, v/v) solvent (De Maria et al., 1996 a). For the extraction, 20 g - 25 g of HIF was weighed into an Erlenmeyer flask, 50 ml – 60 ml of solvent was added and, after closing the flask with Parafilm®, the flask was placed in the shaker (frequency 120 min^{-1}) for 24 h at 20 °C. The flask content was centrifuged at 4000 rpm for 4 min; the supernatant was then filtered to remove small amounts of solids. The residue was again extracted as above. The extraction was repeated until no saccharides, amino acids, organic acids or trigonelline were detected in the supernatant (ca. 20 times), see chapter 4.4.2.1, 4.4.2.2, 4.4.2.3 and 4.4.2.4.

The filtered supernatant was concentrated carefully under pressure until no ethanol was present anymore and was then freeze-dried and homogenised. The resulting ethanol/water soluble coffee powder (abbr. ESF, Ethanol/water Soluble Fraction; yield (whole green bean): 21.4 %) was stored at -20 °C until conducting EA-C/P-GCMS measurement, roasting of the fraction, or further extraction, see 4.6.3.4, was conducted.

The residue was freeze-dried and homogenised and the resulting ethanol/water insoluble coffee powder (abbr. EIF, Ethanol/water Insoluble Fraction; yield (whole green bean): 59.7 %) was stored at -20 °C until the conducting of EA-C/P-GCMS measurement, roasting of the fraction, or further extraction, see 4.6.3.6.

4.6.3.4 Isolation of Amino Acids from the Ethanol/Water Soluble Fraction via Cation Exchange Chromatography

To isolate amino acids and other cationic substances (at pH = 3) from ESF, cation exchange chromatography, as in chapter 4.4.1.2, was employed with the method modified from Jamin et al. (1997).

6 g ESF was dissolved in 150 ml water and, after homogenising, the pH value of the mixture was lowered to pH = 2, using concentrated hydrochloric acid. The solution was applied to the conditioned cation exchange resin, being allowed to infiltrate the resin, and then neutral and anionic substances, such as sucrose and organic acids, were eluted in 100 ml steps with water pH = 2 (adjusted with hydrochloric acid conc.). When the eluate was free of sucrose, the column was washed with 300 ml of water (pH = 7) to neutralise the resin. All water fractions, pH = 2 and neutral, were combined, neutralised, carefully concentrated under pressure and freeze-dried. The resulting anionic/neutral fraction (abbr. ANF, anionic/neutral fraction; yield (whole green bean): 18.6 %) was stored at -20 °C until EA-C/P-GCMS measurement or further extraction, see 4.6.3.5, was conducted.

Subsequently, the amino acids and other cationic substances were eluted with 0.25 N sodium hydroxide solution in 100 ml steps until no amino acids were detected. The fractions were combined, neutralised, carefully concentrated under pressure and freeze-dried. The resulting cationic fraction (abbr. CF, Cationic Fraction; yield (whole green bean): 2.9 %) was stored at -20 °C until conducting EA-C/P-GCMS measurement. After all elution steps, the column was conditioned with 300 ml water and stored.

After application of ESF, all eluted fractions were tested for amino acids, sucrose, trigonelline and citric acid by TLC (see chapter 4.4.2.1, 4.4.2.2, 4.4.2.3 and 4.4.2.4), after neutralising.

The influence of sample preparation on the $^{2}H/^{1}H$, $^{15}N/^{14}N$ and $^{13}C/^{12}C$ isotope ratios was checked for L-serine, L-threonine, sucrose and citric acid, as representatives of the groups amino acids, saccharides and acids, by model cation exchange separation. No significant isotope discrimination effects were observed by the applied workup procedure for $^{15}N/^{14}N$ and $^{13}C/^{12}C$ stable isotope ratios, with $^{2}H/^{1}H$ ratios displaying isotopic discrimination.

4.6.3.5 Isolation of Organic Acids from the Anionic/Neutral Fraction via Anion Exchange Chromatography

To isolate organic acids and other anionic substances (at pH = 7) from ANF, anion exchange chromatography was employed by the method modified from Jamin et al. (1997), see chapter 4.4.1.3.

6 g ANF was dissolved in 150 ml water and, after homogenising, the pH value of the mixture was neutralised to pH = 7, with 40 % sodium hydroxide. This mixture was applied to the conditioned anion exchange resin and allowed to infiltrate the resin, and then neutral substances, such as sucrose, were eluted in 100 ml steps, using water pH = 7. When the eluate was free of sucrose, the column was washed with a further 300 ml water (pH = 7). All water fractions were combined, neutralised, carefully concentrated under pressure and freeze-dried. The resulting neutral fraction (abbr. NF, Neutral Fraction; yield (whole green bean): 11.4 %) was stored at -20 °C until EA-C/P-IRMS measurement was conducted.

Subsequently, the organic acids and other anionic substances were eluted with 0.05 N hydrochloric acid in 100 ml steps, until no citric acid was detected. The fractions were combined, neutralised, carefully concentrated under pressure and freeze-dried. The resulting anionic fraction (abbr. AF, Anionic Fraction; yield (whole green bean): 7.2 %) was stored at -20 °C until EA-C/P-IRMS measurement. After all elution steps the column was conditioned with 300 ml 1 N sodium hydroxide and, subsequently, 300 ml water and stored.

After application of ANF all fractions were tested for sucrose and citric acid by TLC (see 4.4.2.1 and 4.4.2.4), after neutralising.

No significant isotope discrimination effects were observed by the applied workup procedure for $^{15}N/^{14}N$ and $^{13}C/^{12}C$ stable isotope ratios, but $^{2}H/^{1}H$ ratios did display isotopic discrimination.

4.6.3.6 Extraction of Ethanol/Water Insoluble Fraction with Water

10 g of EIF was mixed with 100 ml water and heated to 90 °C, whilst stirring using a method from Oosterveld et al. (2003). After 1 h at 90 °C it was centrifuged, with the procedure being repeated again twice. The combined supernatants were carefully concentrated under pressure and freeze-dried. The resulting water soluble fraction (abbr. WSF, Water Soluble Fraction; yield (whole

green bean): 7.1 %) was stored at -20 °C until EA-C/P-IRMS measurement, roasting or further extraction, see 4.6.3.7.

The residue was freeze-dried and the resulting water insoluble fraction (abbr. WIF, Water Insoluble Fraction; yield (whole green bean): 52.6 %) was stored at -20 °C until EA-C/P-IRMS measurement, roasting or further extraction, see 4.6.3.8.

4.6.3.7 Precipitation of Polysaccharides of the Water Soluble Fraction with Ethanol

To separate water soluble proteins and polysaccharides from each other, 1 g of WSF was dissolved in 50 ml water and then 150 ml ethanol was added, to give a final solution containing 70 % ethanol (Wolfrom et al., 1960). The suspension was centrifuged and the residue freeze-dried. The residue resulted in the precipitated polysaccharide fraction (abbr. PPF, Precipitated Polysaccharide Fraction; yield (whole green bean): 2.6 %); this was stored at -20 °C until EA-C/P-IRMS measurement was conducted.

The supernatant was carefully concentrated under pressure and freeze-dried. The resulting soluble protein fraction (abbr. SPF, Soluble Protein Fraction; yield (whole green bean): 4.5 %) was stored at -20 °C until EA-C/P-IRMS measurement was conducted.

4.6.3.8 Extraction of Pectin of the Water Insoluble Fraction with Ammonium Oxalate

For separating cellulose and pectin, 3 g of WIF was extracted using 150 ml 0.5 % ammonium oxalate solution (in water) at 90 °C for 1 h (Wolfrom et al. 1960). The suspension was then centrifuged and the procedure repeated with the residue. The supernatants were combined, freeze-dried and the pectin fraction (abbr. WIPF, Water Insoluble Pectin Fraction; yield (whole green bean): 30.7 %) stored at -20 °C until EA-C/P-IRMS measurement.

The residue was freeze-dried and the cellulose fraction (abbr. WICF, Water Insoluble Cellulose Fraction; yield (whole green bean): 21.9 %) stored at -20 °C until EA-C/P-IRMS measurement was conducted.

4.6.3.9 Roasting of Green Coffee Fractions

To be able to roast the green coffee fractions with the coffee roaster, simulated coffee bean pellets had to be produced from the powders. To produce these pellets, a homogeneous dough was formed individually for each extraction powder, according to the following recipes, as shown in table 4-1. As the powder and water alone could not form a stable dough, Aerosil® 200 (Degussa, Frankfurt/M., Germany) and silica gel 60, 0.04 mm – 0.063 mm (Merck, Darmstadt, Germany), were added in the following amounts:

Table 4-1: Mixtures for homogeneous doughs from green coffee fractions

Fraction	Quantity Fraction	Quantity Aerosil	Quantity Water	Quantity silica gel
Green coffee powder (GCP)	4.0 g	0.5 g	5.0 g	
Hexane insoluble fraction (HIF)	3.0 g	0.3 g	4.5 g	
Ethanol insoluble fraction (EIF)	2.5 g	0.8 g	7.2 g	
Ethanol soluble fraction (ESF)	2.0 g	0.6 g	2.0 g	1.0 g
Water soluble fraction (WSF)	1.0 g	1.5 g	7.0 g	
Water insoluble fraction (WIF)	1.0 g	1.0 g	8.0 g	

To form the pellets, a pill making machine was used, see figure 4-2. The dough was rolled into a strand of 5 mm diameter and divided, with the strand, cutter into single pills of 5 mm diameter. The pills were, subsequently, shaped in to a round form and then dried in the drying oven, at 50 °C for 6 - 8 h, until they could not be crushed between the fingers.

In portions of 20 g the pills were roasted in the coffee roaster, with a setting at position 4 (corresponding to 4 min 30 s at 210 °C). The amount of each fraction to be roasted, for HRGC-C/P-IRMS measurement, was equivalent to the extraction percentile of 1000 g of green coffee bean powder. The extraction percentages are shown for each fraction in chapter 4.3.

Figure 4-2: Formation of pills with the pill maker (picture 1). The dough is rolled to a thread and divided with the thread cutter (picture 2 and 3). The pills are dried in the drying oven at 50 °C (picture 4 and 5) and roasted in the coffee roaster (picture 6).

4.6.4 Roasting of Model Mixtures for Pyridine Formation Studies

For roasting of model mixtures with the coffee roaster, simulated coffee bean pellets were produced from the compound mixtures. To produce these pellets a homogeneous dough was formed individually for each extraction powder, according to the following recipes, as shown in table 4-2. As the powder and water alone could not form a stable dough, Aerosil® 200 (Degussa, Frankfurt/M., Germany) was added in the following amounts:

Table 4-2: Mixtures for homogeneous doughs from trigonelline, amino acids and caffeine.

Substance	Quantity Substance	Quantity Aerosil	Quantity Water	Quantity Citric Acid
Trigonelline	1.0 g	1.4 g	5.0 g	-
Trigonelline	1.0 g	1.2 g	5.0 g	0.6 g
Caffeine	1.7 g	1.2 g	7.0 g	-
Caffeine	1.7 g	1.0 g	7.0 g	0.8 g
Glycin, L-Serine, L-Threonine	1.8 g	1.5 g	5.5 g	-
Glycin, L-Serine, L-Threonine	1.8 g	1.3 g	5.5 g	0.6 g

To form the pellets, the pill making machine was used as in chapter 4.6.3.9 and figure 4-2.

In portions of 10 g the pills were roasted in the coffee roaster with a setting at position 4 (corresponding to 4 min 30 s at 210 °C). After roasting they were ground and subjected to SDE and analysed via GC-MS.

4.7 Syntheses

4.7.1 Syntheses of Alkylpyrazines via Cyclocondensation and Catalytic Dehydration

The synthesis reactions of alkylpyrazines, according to *Flament* and *Stoll* (1967) and Jorré (1897), involved a cyclocondensation of α-diketones and α-diamines to alkyl-5,6-dihydropyrazines, with a subsequent dehydration to alkylpyrazines.

4.7.1.1 General Synthesis of Cyclocondensation of α-Diketones and α-Diamines to Alkyl-5,6-dihydropyrazines

This synthesis reaction was according to *Flament* and *Stoll* (1967). In a 250 ml three neck flask with stirrer, reflux condenser and dropping funnel, 50 mmol α-diamine in 50 ml diethyl ether was cooled on an ice bath to 0 °C. Afterwards, 50 mmol α-diketone in 50 ml diethyl ether, was added slowly, dropwise. The solution was stirred further, between 0 °C and 10 °C, until white crystals precipitated (ca. 30 min).

Subsequently, the ice bath was removed and the solution stirred, at room temperature, until the white crystals dissolved and the solution became slightly yellow and clear. The solution was allowed to stand for 1 h at room temperature. For controlling the intermediate product, a sample (1 ml) was measured by HRGC-MS to define the amount and purity of the alkyl-5,6-dihydropyrazine.

4.7.1.2 General Synthesis of Catalytic Dehydration of Alkyl-5,6-dihydropyrazines to Alykylpyrazines

This synthesis reaction was according to *Jorre* (1897). The solution of alkyl-5,6-dihydropyrazine (4.7.1.1) was heated under reflux at 140 °C, with 20 ml of Fehling's solution (10 ml Fehling I and 10 ml Fehling II), 0.89 g potassium hydroxide in 20 ml ethanol and 0.3 g iron (III) oxide. In hourly intervals, further amounts of 4 x 20 ml of Fehling's solution were introduced into the solution, to complete the dehydration (altogether 5 x 20 ml Fehling, 5 h heating).

The obtained solution was purified, via extraction, using simultaneous distillation extraction (SDE). The extract obtained was combined and dried over anhydrous sodium sulphate, filtered, and carefully concentrated to, approximately, 5 ml on a Vigreux column (45 °C). Excess diethyl ether was carefully removed with nitrogen gas at 45 °C. The extract was then diluted, as needed, and submitted to HRGC-MS and HRGC-C/P-IRMS for determination of purity and measurement.

4.7.1.3 Synthesis of 2,3-Dimethylpyrazine

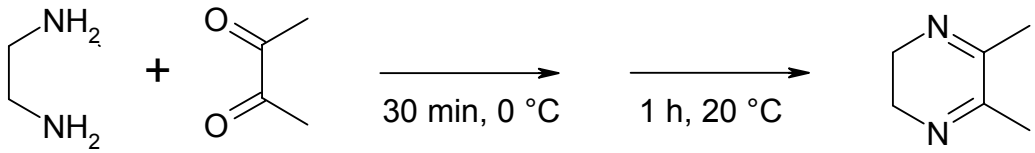

Figure 4-3: Synthesis sequence for 2,3-dimethyl-5,6-dihydropyrazine

For the synthesis of 2,3-dimethyl-5,6-dihydropyrazine, 3.2 g ethylendiamine (50 mmol) and 4.4 g (50 mmol) 2,3-butanedione were employed, as in chapter 4.7.1.1.

HRGC-EI-MS (70 eV) of 2,3-dimethyl-5,6-dihydropyrazine
R_t (Carbowax) = 14.67 min
m/z (%) = 42 (100), 110 (90), 69 (73), 109 (26), 54 (19), 41 (14)

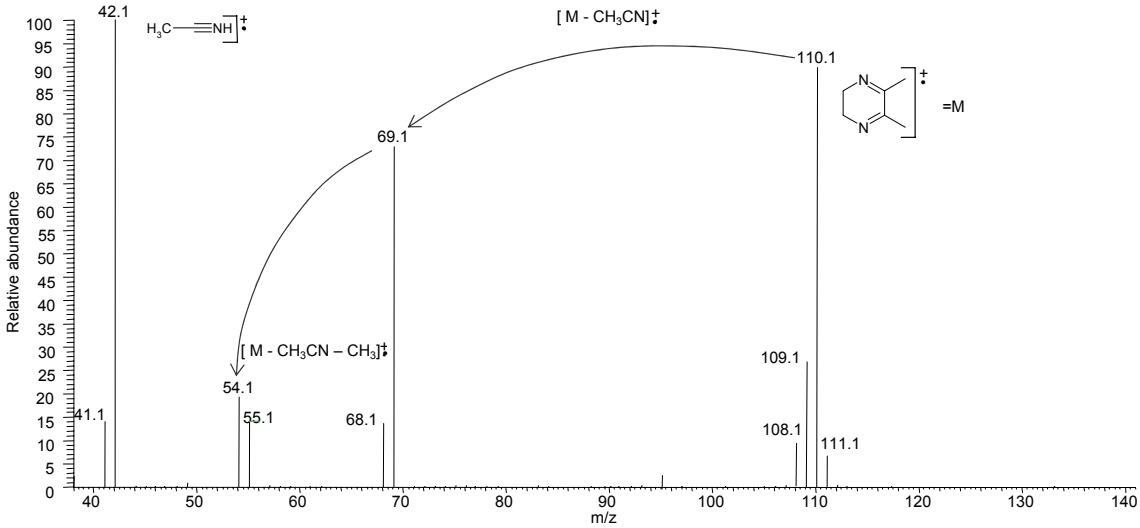

Figure 4-4: Mass spectrum of 2,3-dimethyl-5,6-dihydropyrazine with fragmentation pattern explained according to Brophy and Cavill, 1980.

As seen in figure 4-4 the mass peak of 2,3-dimethyl-5,6-dihydropyrazine is m/z = 110; through the loss of acetonitril and the subsequent loss of yet again acetonitril with a methyl group, the masses m/z = 69 and m/z = 54 are achieved, respectively. This data is in good agreement to the information in the institute's database.

The further conversion to 2,3-dimethylpyrazine was performed, as in chapter 4.7.1.2 and figure 4-5.

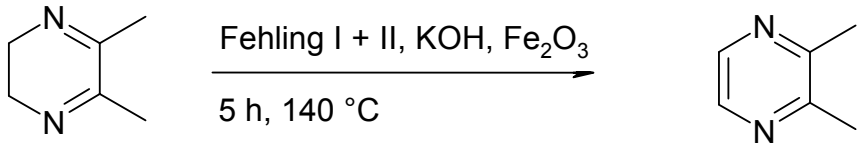

Figure 4-5: Synthesis sequence for 2,3-dimethylpyrazine

Yield: 26 %, purity of 2,3-dimethylpyrazine 66 % (HRGC-MS), secondary components: 2,3-dimethyl-5,6-dihydropyrazine, 2,3,5,6-tetramethylpyrazine. Due to the low purity, NMR data was not obtained for the component; only mass spectra data was available. Retention time and mass data were in agreement with literature and reference compounds.

HRGC-EI-MS (70 eV) of 2,3-dimethylpyrazine
R_t (Carbowax) = 13.1 min
m/z (%) = 67 (100), 108 (96), 42 (28), 41 (21), 66 (17), 52 (7)

4.7.1.4 Synthesis of 2-Ethyl-3-methylpyrazine

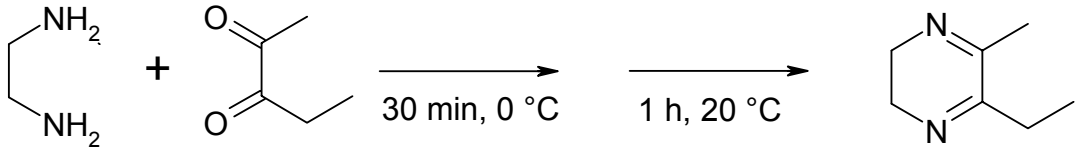

Figure 4-6: Synthesis sequence for 2-ethyl-3-methyl-5,6-dihydropyrazine

For the synthesis of 2-ethyl-3-methyl-5,6-dihydropyrazine, 3.2 g ethylendiamine (50 mmol) and 5.0 g (50 mmol) 2,3-pentanedione were employed, as in chapter 4.7.1.1.

HRGC-EI-MS (70 eV) of 2-ethyl-3-methyl-5,6-dihydropyrazine
R_t (Carbowax) = 16.27 min
m/z (%) = 56 (100), 124 (79), 123 (59), 42 (59), 83 (38), 109 (19), 94 (4)

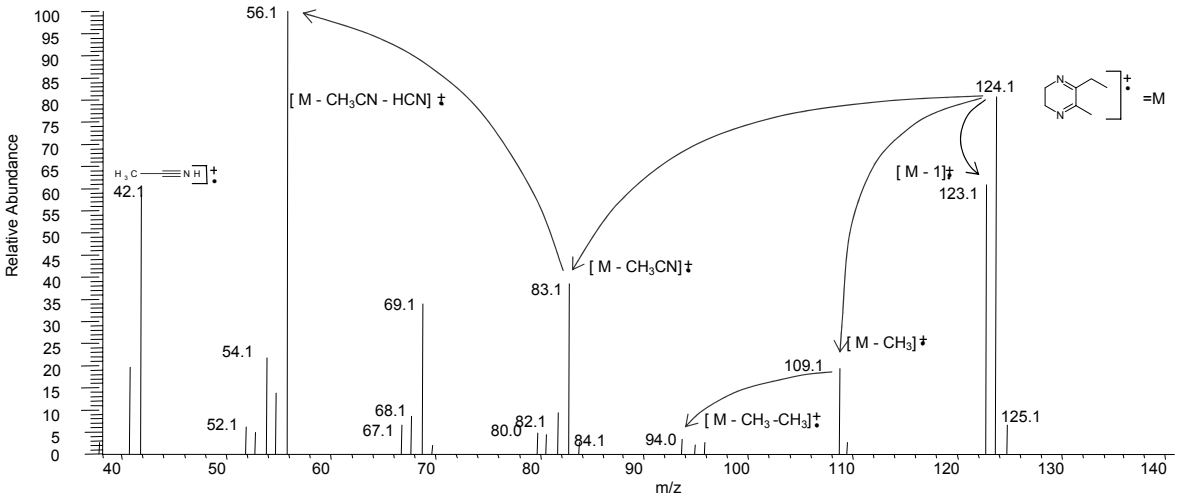

Figure 4-7: Mass spectrum of 2-ethyl-3-methyl-5,6-dihydropyrazine with fragmentation explained according to Brophy and Cavill (1980).

As seen in figure 4-7 the mass peak of 2-ethyl-3-methyl-5,6-dihydropyrazine is m/z = 124; through the loss of acetonitrile, a methyl group and a proton the masses m/z = 83, m/z = 109 and m/z = 123 are achieved, respectively. Through the loss of two methyl groups from the mass peak m/z = 124 the mass m/z = 94 is achieved. The subsequent loss of HCN from m/z = 83 results in the m/z = 56, which is the base peak. The m/z = 42 is protonated acetonitrile.

The further conversion to 2-ethyl-3-methylpyrazine was performed, as in chapter 4.7.1.2 and figure 4-8.

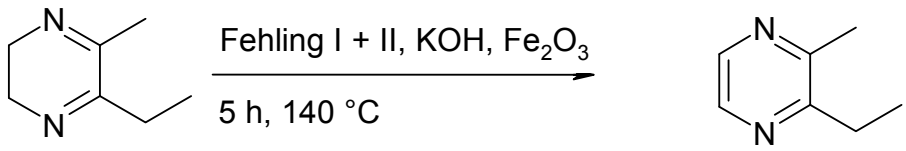

Figure 4-8: Synthesis sequence for 2-ethyl-3-methylpyrazine

Yield: 60 %, purity of 2-ethyl-3-methylpyrazine 66 % (HRGC-MS), secondary component: 2-ethyl-3-methyl-5,6-dihydropyrazine. Due to the low purity, NMR data was not obtained for the component; only mass spectra data was available. Retention time and mass data were in agreement with literature and reference compounds.

HRGC-EI-MS (70 eV) of 2-ethyl-3-methylpyrazine
R_t (Carbowax) = 15.04 min
m/z (%) = 121 (100), 122 (79), 67 (14), 80 (14), 94 (13), 93 (8), 42 (7)

4.7.1.5 Synthesis of 2,3,5-Trimethylpyrazine

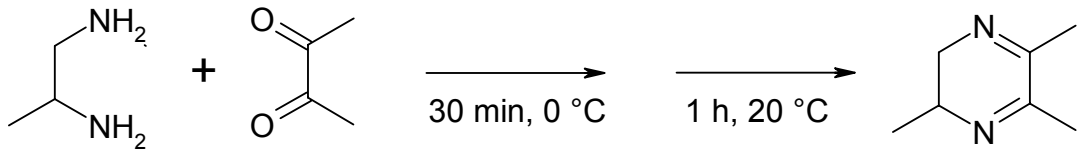

Figure 4-9: Synthesis sequence for 2,3,5-trimethyl-5,6-dihydropyrazine

For the synthesis of 2,3,5-trimethyl-5,6-dihydropyrazine, 3.7 g 1,2-diaminopropane (50 mmol) and 4.4 g (50 mmol) 2,3-butanedione were employed, as in chapter 4.7.1.1.

HRGC-EI-MS (70 eV) of 2,3,5-trimethyl-5,6-dihydropyrazine
R_t (Carbowax) = 14.26 min
m/z (%) = 42 (100), 124 (60), 109 (36), 123 (29), 68 (14), 96 (10), 54 (9)

As seen in figure 4-10 the mass peak of 2,3,5-trimethyl-5,6-dihydropyrazine is m/z = 124; subsequent losses of a proton, a methyl group, a H_2CN group and acetonitrile lead to the masses m/z = 123, m/z = 109, m/z = 96 and m/z = 82, respectively. The mass peak m/z = 42 is protonated acetonitrile, as with the previous mass spectra of other alkyl-5,6-dihydropyrazines. The ions at m/z = 68 and m/z = 54 are C_4H_8 and C_4H_6.

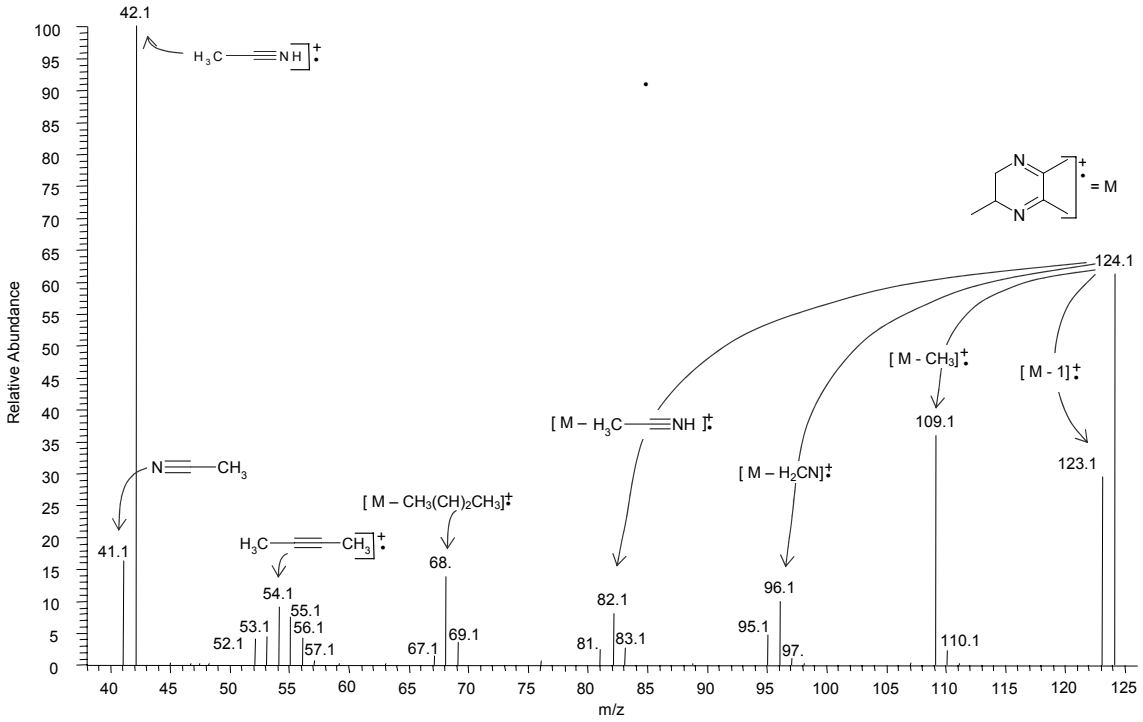

Figure 4-10: Mass spectrum of 2,3,5-trimethyl-5,6-dihydropyrazine with fragmentation pattern explained according to Brophy and Cavill, 1980.

The further conversion to 2,3,5-trimethylpyrazine was performed, as in chapter 4.7.1.2 and figure 4-11.

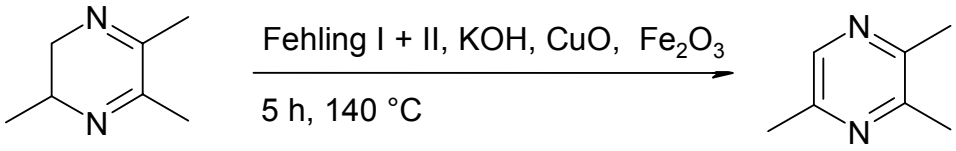

Figure 4-11: Synthesis sequence for 2,3,5-trimethylpyrazine

Yield: 16 %, purity of 2,3,5-trimethylpyrazine 89 % (HRGC-MS), secondary components: 2,3,5-trimethyl-5,6-dihydropyrazine and 2,3,5,6-tetramethyl-pyrazine. Due to the low purity, NMR data was not obtained for the component; only mass spectra data was available. Retention time and mass data were in agreement with literature and reference compounds.

HRGC-EI-MS (70 eV) of 2,3,5-trimethylpyrazine
R_t (Carbowax) = 15.26 min
m/z (%) = 42 (100), 122 (95), 81 (39), 54 (16), 107 (6)

4.7.1.6 Synthesis of 2-Ethyl-3,5/6-dimethylpyrazine

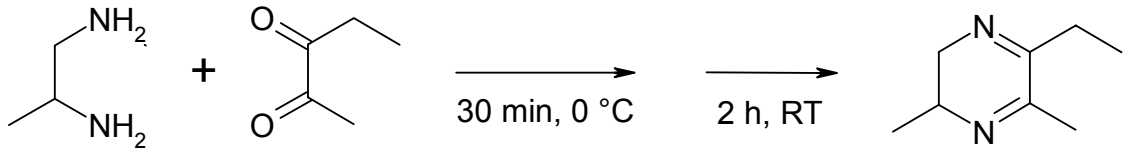

Figure 4-12: Synthesis sequence for 2-ethyl-3,5/6-dimethyl-5,6-dihydropyrazine

For the synthesis of 2-ethyl-3,5/6-dimethyl-5,6-dihydropyrazine, 3.7 g 1,2-diaminopropane (50 mmol) and 5.0 g (50 mmol) 2,3-pentanedione were employed, as in chapter 4.7.1.1.

HRGC-EI-MS (70 eV) of 2-ethyl-3,5/6-dimethyl-5,6-dihydropyrazine
R_t (Carbowax) = 15.16 min and 15.80 min
m/z (%) = 56 (100), 42 (94), 138 (92), 123 (77), 137 (46), 82 (18), 110 (17)

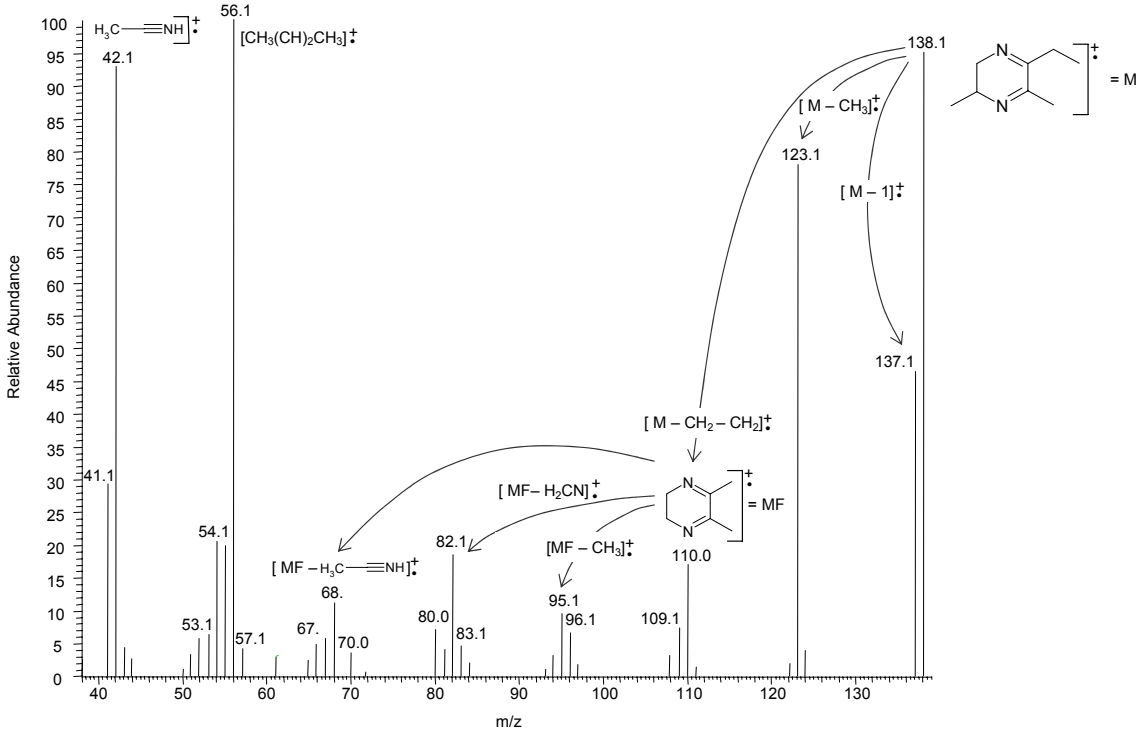

Figure 4-13: Mass spectrum of 2-ethyl-3,5-dimethyl-5,6-dihydropyrazine with fragmentation pattern explained according to Brophy and Cavill, 1980.

As seen in figure 4-13 the mass peak of 2-ethyl-3,5-dimethyl-5,6-dihydropyrazine is m/z = 138; also the dominant mass peaks of m/z = 137 and m/z = 123 are achieved through loss of a proton and a methyl group, respectively. The loss of two methylen groups from the molecule peak leads to m/z = 110 (molecule fragment, MF). The subsequent loss of a methyl group, H_2CN and H_3C-CNH from MF lead to the mass peaks m/z = 95, m/z = 82 and

m/z = 68, respectively. The base peak m/z = 56 results from a C_4H_8 fragment, the m/z = 42 is protonated acetonitrile. The fragmentation pattern for 2-ethyl-3,6-dimethyl-5,6-dihydropyrazine is analogous. The mass spectrum is in good accordance to data from Kurniadi et al. (2003).

The further conversion to 2-ethyl-3,5/6-dimethylpyrazine was performed as in chapter 4.7.1.2 and figure 4-14.

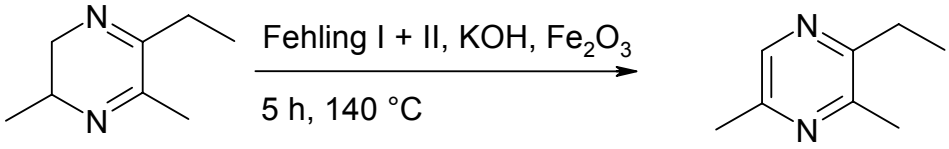

Figure 4-14: Synthesis sequence for 2-ethyl-3,5/6-dimethylpyrazine

Yield: 23 %, purity of 2-ethyl-3,5/6-dimethylpyrazine 90 % (HRGC-MS), secondary component: 2-ethyl-3,5/6-dimethyl-5,6-dihydropyrazine. Due to the low purity, NMR data was not obtained for the components; only mass spectra data was available. The mass spectrum of both components was identical.

HRGC-EI-MS (70 eV) of 2-ethyl-3,5/6-dimethylpyrazine
R_t (Carbowax) = 16.36 and 16.88 min
m/z (%) = 135 (100), 136 (75), 56 (21), 42 (15), 108 (13)

4.7.2 Synthesis of 2-Ethylpyrazine with Methyl 2-pyrazinecarboxylate

4.7.2.1 Synthesis of Methylpyrazineketone

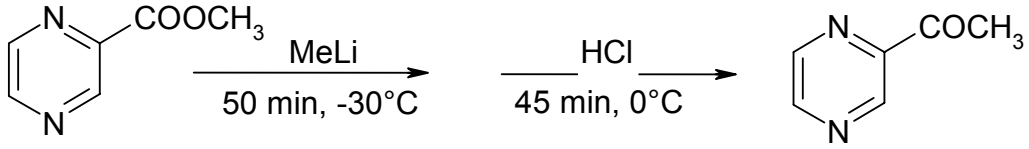

Figure 4-15: Synthesis sequence for methylpyrazineketone

The synthesis reaction was according to *Schwaiger et al.* (1984). In a 250 ml three neck flask with stirrer, reflux condenser and dropping funnel 1 g methylpyrazinecarboxylate (7.25 mmol), in 60 ml diethyl ether (Beyer et al., 1998), was cooled on a dry ice/acetone bath to -30 °C. 4.5 ml methyllithium (1.6 mol) was added slowly, dropwise, over 20 min, with dark yellow crystals precipitating. The solution was stirred further at -30 °C for 30 min and then the temperature allowed to rise to 0 °C, during the next 45 min, whilst adding 7.5 ml 1 molar hydrochloric acid (7.5 mmol). The precipitate was washed three times

with 50 ml diethyl ether, and the combined extracts dried over anhydrous sodium sulfate, filtered, and carefully, concentrated to approximately 5 mL on a Vigreux column (45 °C). Excess diethyl ether was carefully removed with nitrogen gas at 45 °C. The extract was then submitted to HRGC for determination of purity.

HRGC-EI-MS (70 eV) of methylpyrazineketone
R_t (Carbowax) = 21.25 min
m/z (%) = 122 (100), 80 (85), 43 (82), 52 (52), 79 (48), 94 (46), 53 (43)

As seen in figure 4-16 the base mass peak of the spectra is 2-methlpyrazineketone (M) with m/z = 122; the second dominant mass peak of m/z = 80 is a pyrazine fragment (molecule fragment, MF). The loss of alternately a methyl group, a carbonyl group, the ketone side arm and the ketone side arm with a further HCN group from the base peak leads to m/z = 107, m/z = 94, m/z = 79 and m/z = 52, respectively. The loss of HCN from MF results in a m/z = 53.

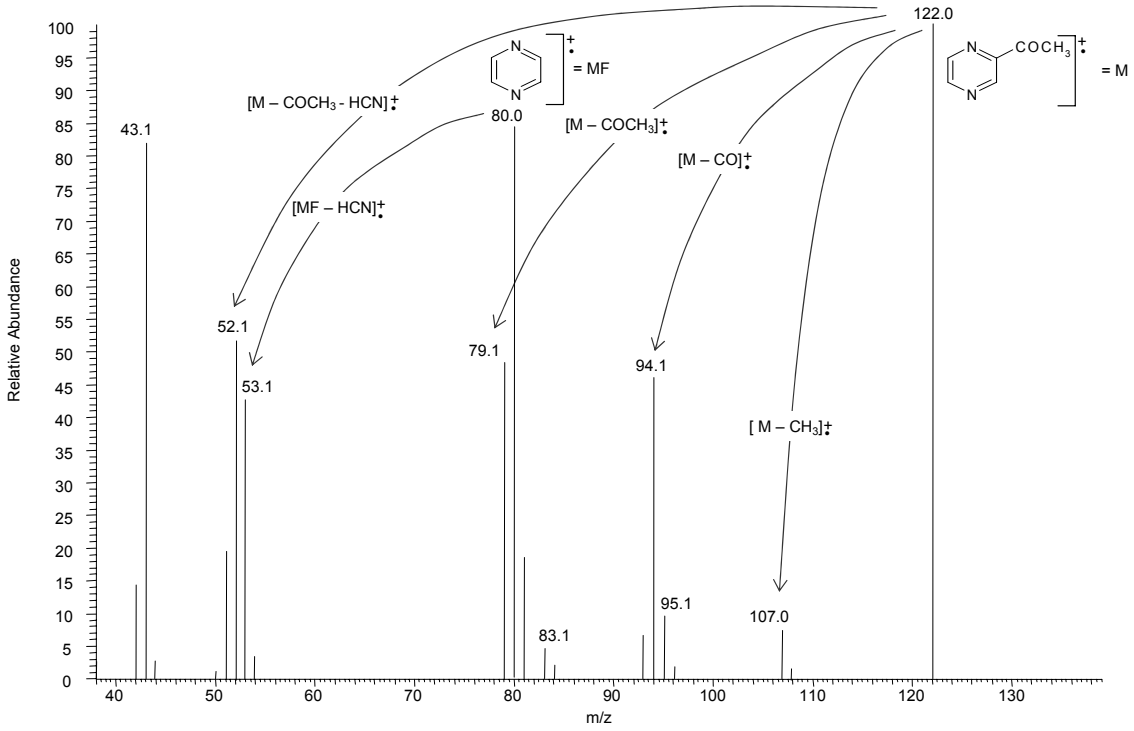

Figure 4-16: Mass spectrum of 2-methlpyrazineketone with fragmentation pattern explained according to Brophy and Cavill, 1980.

4.7.2.2 Reduction of Methylpyrazineketone to 2-Ethylpyrazine

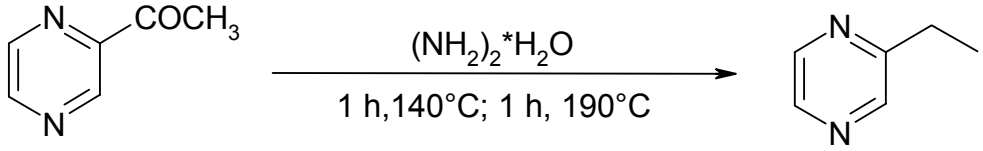

Figure 4-17: Synthesis sequence for methylpyrazineketone

The solution of methylpyrazineketone (4.7.2.1) was heated with 2.2 g potassiumhydroxide (0.04 mol), 2.4 ml hydrazine hydrate (0.05 mmol) and 36 ml ethylenglycol (0.65 mmol) under reflux at 140 °C for 1 h and then at 190 °C for another hour. The solution was then extracted by SDE. The extract obtained was combined and dried over anhydrous sodium sulfate, filtered, and carefully concentrated to approximately 5 ml on a Vigreux column (45 °C). Excess diethyl ether was carefully removed with nitrogen gas at 45 °C. The extract was then diluted, as needed, and submitted to HRGC and HRGC-IRMS for determination of purity and measurement.

Yield: 55 %, purity of 2-ethylpyrazine 71 % (HRGC-MS), secondary component: methylpyrazineketone. Due to the low purity, NMR data was not obtained for the component; only mass spectra data was available.

HRGC-EI-MS (70 eV) of 2-ethylpyrazine
R_t (Carbowax) = 12.41 min
m/z (%) = 107 (100), 108 (62), 80 (20), 53 (11), 52 (10), 39 (7), 81 (6)

4.7.3 Syntheses of Alkylpyrazines via Reaction Cylinder

The syntheses reaction was modified from *Shu et al.* (1999). In the reaction cylinder, see figure 4-1, the educts and catalysts were mixed, filled into the reaction cylinder and placed in a muffle furnace. After cooling to room temperature, the cylinder was opened and the reaction products extracted with water and subjected to SDE. The extract obtained was combined and dried over anhydrous sodium sulfate, filtered, and carefully concentrated to approximately 5 ml on a Vigreux column (45 °C). Excess diethyl ether was carefully removed with nitrogen gas at 45 °C. The extract was then diluted as needed and submitted to HRGC and HRGC-IRMS for determination of purity and measurement.

4.7.3.1 Synthesis of Alkylpyrazines from L-Serine

4 g L-serine and 3 ml water were mixed and, after closing the cylinder, the mixture was placed in a muffle furnace at 300 °C for 45 min, and then further treated as in 4.7.3.

Distribution: Pyrazine 24.8 %, 2-methylpyrazine 9.1 %, 2-ethylpyrazine 23.0 %, 2,3-dimethylpyrazine 1.9 %, 2-ethyl-5-methylpyrazine 5.3 %, 2-ethyl-6-methylpyrazine 1.2 %, 2-ethyl-3-methylpyrazine 2.2 %, 2,6-diethylpyrazine 5.6 %, 2-ethyl-3,5-dimethylpyrazine 1.4 % (HRGC-MS). As the product was a mixture of components NMR data was not obtained; only mass spectra data was available. Retention time and mass data were in agreement with literature and reference compounds.

4.7.3.2 Synthesis of Alkylpyrazines from L-Threonine

In the reaction cylinder 4 g L-threonine and 3 ml water were mixed and, after closing the cylinder, the mixture was placed in a muffle furnace at 300 °C for 45 min and then further treated as in 4.7.3.

Distribution: 2,5-dimethylpyridine 1.7 %, 2,5-dimethylpyrazine 2.8 %, 2,3,5-trimethylpyrazine 2.0 %, 2-ethyl-5-methylpyridine 12.7 %, 2-ethyl-3,5-dimethylpyrazine 19.3 %, 2-ethyl-3,6-dimethylpyrazine 4.1 %, 2,6-dimethyl-3-propylpyrazine 2.4 %, 2,5-diethyl-3,6-dimethylpyrazine 3.8 %, 2,6-diethyl-3,5-dimethylpyrazine 3.3 % (HRGC-MS). As the product was a mixture of components NMR data was not obtained; only mass spectra data was available. Retention time and mass data were in agreement with literature and reference compounds.

4.7.3.3 Synthesis of Alkylpyrazines from L-Serine and L-Threonine

In a reaction cylinder 2 g serine, 2 g threonine and 3 ml water were mixed and after closing the cylinder it was placed in a muffle furnace at 300 °C for 45 min and then further treated as in 4.7.3.

Distribution: pyrazine 1.3 %, 2-methylpyrazine 4.5 %, 2,5-dimethylpyrazine 2.6 %, 2,6-dimethylpyrazine 2.0 %, 2-ethylpyrazine 2.4 %, 2,3-dimethylpyrazine 0.9 %, 2-ethyl-5-methylpyrazine 7.0 %, 2-ethyl-6-methylpyrazine 2.1 %, 2-ethyl-3-methylpyrazine 4.1 %, 2,6-diethylpyrazine 2.0 %, 2-ethyl-3,5-dimethylpyrazine 6.6 %, 2-ethyl-3,6-dimethylpyrazine 3.6 %. As the product

was a mixture of components NMR data was not obtained; only mass spectra data was available. Retention time and mass data were in agreement with literature and reference compounds.

4.7.3.4 Synthesis of Alkylpyrazines from Diethylentriamine

The synthesis reaction was modified according to Anderson et al. (1967). In the reaction cylinder 4 g diethylentriamine, 0.5 g molybdatophosphoric acid and 1 g aluminium oxide (Al_2O_3) were mixed and heated to 350 °C for 2 h and then further treated as in 4.7.3.

Distribution: pyrazine 11.0 %, 2-methylpyrazine 10.0 %, 2-ethylpyrazine 12.0 %, 2,3-dimethylpyrazine 4.9 %, 2-ethyl-3-methylpyrazine 1.7 %, 2-ethyl-3,5-dimethylpyrazine 1.0 %, 2,6-diethylpyrazine 1.5 %. As the product was a mixture of components NMR data was not obtained; only mass spectra data was available. Retention time and mass data were in agreement with literature and reference compounds.

4.7.4 Synthesis of Trigonelline

4.7.4.1 Synthesis of N-Methylnicotinic Acid – Hydroiodide via Nicotinic Acid

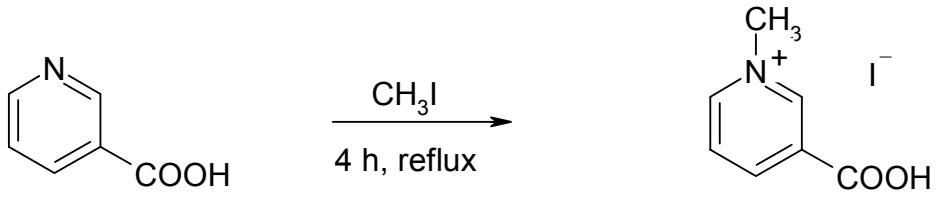

Figure 4-18: Synthesis sequence for N-methylnicotinic acid – hydroiodide

The synthesis of trigonelline was modified from Sarett et al. (1940). In 250 ml Ethanol (95 %) 12.3 g nicotinic acid (0.1 mol) and 17 g iodomethane (0.12 mol) were heated under reflux for 4 hours. The yellow precipitate (N-methyl nicotinic acid – hydro iodide) was then filtered and recrystallised in 95 % ethanol.

Yield: 80 %, mp: 218 °C
^{1}H-NMR: δ [ppm]= 9.22 (s, 1H), 8.90 (d, 2H), 8.12 (t, 1H), 4.46 (s, 3H)
^{13}C-NMR: δ [ppm]= 168.4, 149.0, 148.4, 147.3, 136.6, 130.0, 50.6

4.7.4.2 Synthesis of Trigonelline from N-Methylnicotinic Acid – Hydroiodide

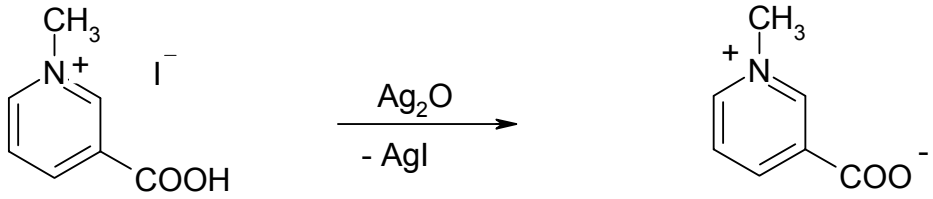

Figure 4-19: Synthesis sequence for trigonelline

25 g silver (I) oxide (Ag_2O) was added to an aqueous solution of 10 g N-methyl nicotinic acid – hydro iodide (0.04 mol) in 50 ml water. The precipitate was filtered and discarded, with the filtrate being lyophilised. The residue was recrystallised in ethanol absolute with a yield of 30 %.

Yield: 30 %, mp: 136 °C
^{1}H-NMR: δ [ppm] = 9.12 (s, 1H), 8.85 (d, 2H), 8.10 (t, 1H), 4.46 (s, 3H)
^{13}C-NMR: δ [ppm] = 167.7, 145.9, 145.8, 144.7, 135.9, 127.6, 48.2

5 Structure Matrix

Structures of selected coffee aroma components chronologically numbered after retention time in the chromatograms.

1 pyridine
2 pyrazine
3 2-methylpyrazine
4 2,5-dimethylpyrazine
5 2,6-dimethylpyrazine
6 2-ethylpyrazine
7 2,3-dimethylpyrazine
8 2-ethyl-5-methylpyrazine
9 2-ethyl-6-methylpyrazine
10 2-ethyl-3-methylpyrazine
11 2,3,5-trimethylpyrazine
12 2-ethyl-3,5-dimethylpyrazine
13 2-ethyl-3,6-dimethylpyrazine
14 2,3,4,5-tetramethylpyrazine

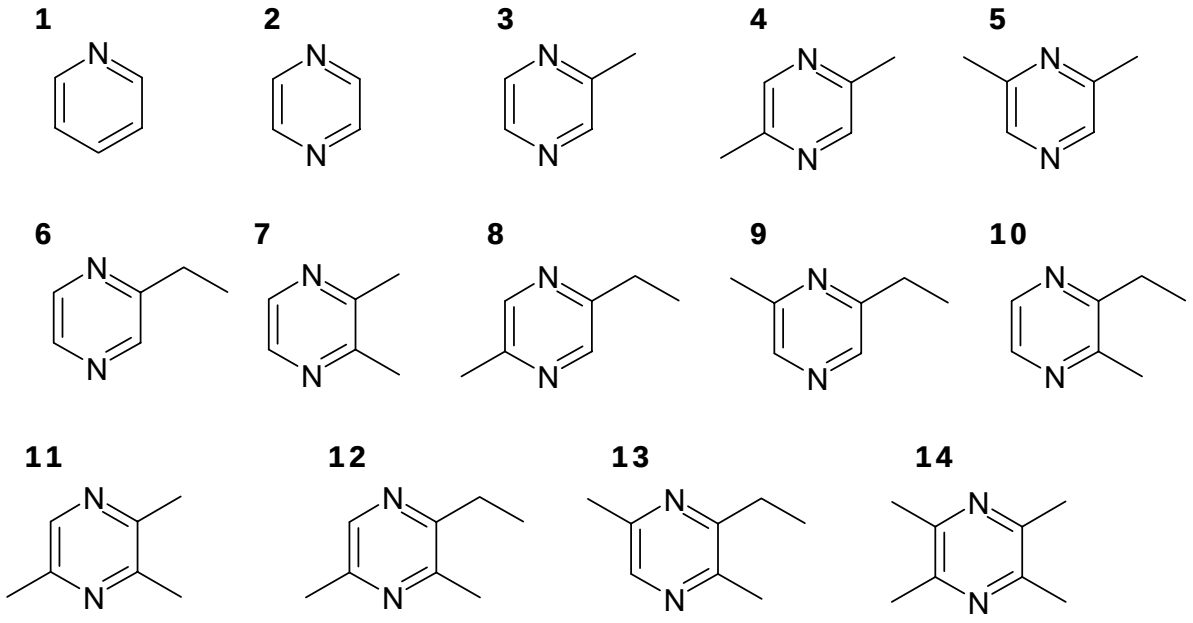

6 Bibliography

Abell, L. M.; O'Leary, M. H. Nitrogen isotope effects on glutamate decarboxylase from *Escherichia coli*. *Biochemistry*, **1988**, *27*, 3325-3330.

Allaway, D.; Lodwig, E. M.; Crompton, L. A.; Wood, M.; Parsons, R.; Wheeler, T. R.; Poole, P. S. Identification of alanine dehydrogenase and its role in mixed secretion of ammonium and alanine by pea bacteroids. *Mol. Microbiol.*, **2000**, *36*, 508-515.

Altabet, M. A.; Francois, R. Sedimentary nitrogen isotopic ratio as a recorder for surface ocean nitrate utilization. *Global Biogeochem. Cy.*, **1994**, *8*, 103-116.

Alvarez, F. J.; Ermer, J.; Hübner, G.; Schellenberger, A.; Schowen, R. L. Catalytic power of pyruvate decarboxylase. Rate-limiting events and microscopic rate constants from primary carbon and secondary hydrogen isotope effects. *J. Am. Chem. Soc.*, **1991**, *113*, 8402-8409.

Ames, J. M.; Guy, R. C. E.; Kipping, G. J. Effect of pH, temperature on the formation of volatile compounds in cysteine/reducing sugar/starch mixtures during extrusion cooking. *J. Agric. Food Chem.*, **2001 a**, *49*, 1885-1894.

Ames, J. M.; Guy, R. C. E.; Kipping, G. J. Effect of pH, temperature, and moisture on the formation of volatile compounds in glycine/glucose model systems. *J. Agric. Food Chem.*, **2001 b**, *49*, 4315-4323.

Anand, R.; Hegde, S. G.; Rao, B. S.; Gopinath, C. S. Catalytic synthesis of 2-methyl pyrazine over Zn-modified zeolites. *Catal. Lett.*, **2002**, *84*, 265-272.

Anderson, A. A.; Yurel, S. P.; Shimanskaya, M. V. Catalytic synthesis of pyrazine, piperazine and 1,4-diaza[2,2,2]-bicyclooctane. *Chem. Heterocycl. Comp.*, **1967**, *3*, No. 2, 346-359.

Arnold, U.; Ludwig, E.; Kühn, R.; Möschwitzer, U. Analysis of free amino acids in green coffee beans. Part I. determination of amino acids after precolumn derivatization using 9-fluorenyl methyl chloro formate. *Z. Lebensm. Unters. Forsch.*, **1994**, *199*, 22-25.

Arnold, U.; Ludwig, E. Analysis of free amino acids in green coffee beans. Part II. Changes of the amino acid content in arabica coffees in connection with post-harvest model treatment. *Z. Lebensm. Unters. Forsch.*, **1996**, *203*, 379-384.

Aston, J. G.; Peterson, T. E.; Holowchak, J. The synthesis of pyrazine by the catalytic dehydration of ethanolamine. *J. Am. Chem. Soc.*, **1934**, *56*, No. 1, 153-154.

Baltes, W. Vorstufen und Entstehung von Farbe und Geschmack des Kaffees. *7th Int. Colloq. Chem. Coffee* (Hamburg 09-14.06.1975), **1976**, 91-107.

Baltes, W. Influence of roasting on the composition of coffee. *8th Int. Colloq. Chem. Coffee* (Abidjan 28.11-03.12.1977), **1979**, 85-96.

Baltes, W.; Bochmann, G. Model reactions on roast aroma formation – The reaction of serine and threonine with sucrose. *3rd Int. Symp. Maillard React.* (Tokyo, July 1985), **1986**, 245-255.

Baltes, W.; Bochmann, G. II. MS identification of furans and furanones from the reaction of serine and threonine with sucrose under the conditions of coffee roasting. *Z. Lebensm. Unters. Forsch.*, **1987 a**, *184*, 179-186.

Baltes, W.; Bochmann, G. III. MS identification of pyrrroles from the reaction of serine and threonine with sucrose under the conditions of coffee roasting. *Z. Lebensm. Unters. Forsch.*, **1987 b**, *184*, 478-484.

Baltes, W.; Bochmann, G. IV. MS identification of pyrazines from the reaction of serine and threonine with sucrose under the conditions of coffee roasting. *Z. Lebensm. Unters. Forsch.*, **1987 c**, *184*, 485-493.

Baltes, W.; Bochmann, G. V. MS identification of pyridines, oxazoles, and carbocyclic compounds from the reaction of serine and threonine with sucrose under the conditions of coffee roasting. *Z. Lebensm. Unters. Forsch.*, **1987 d**, *185*, 5-9.

Barrie, A.; Bricout, J.; Koziet, J. Gas chromatography-stable isotope ratio analysis at natural abundance levels. *Biomed. Mass Spectrom.*, **1984**, *11*, 583-588.

Bauer-Christoph, C.; Wachter, H.; Christoph, N.; Roßmann, A.; Adam, L. Assignment of raw material and authentication of spirits by gas chromatography, hydrogen- and carbon-isotope ratio measurements. I. Analytical methods and results of a study of commercial products. *Z. Lebensm. Unters. Forsch. A*, **1997**, *204*, 445-452.

Belitz, H.-D.; Grosch, W.; Schieberle, A. *Lehrbuch der Lebensmittelchemie*, **2001**, 5. edition, Springer, Berlin, Heidelberg, New York.

Bigeleisen, J. Chemistry of isotopes. *Science* **1965**, *147*, 463-471.

Bilke, S.; Mosandl, A. Authenticity assessment of lavender oils using GC-P-IRMS: $^{2}H/^{1}H$ isotope ratios of linalool and linalyl acetate. *Eur. Food Res. Technol.*, **2002**, *214*, 532-535.

Boner, M.; Förstel, H. Stable isotope variation as a tool to trace the authenticity of beef. *Anal. Bioanal. Chem.*, **2004**, *378*, 301-310.

Braunsdorf, R.; Hener, U.; Stein, S.; Mosandl, A. Comprehensive GC-IRMS analysis in the authenticity control of flavours and essential oils. Part I: Lemon Oil. *Z. Lebensm. Unters. Forsch.*, **1993**, *197*, 137-141.

Bréas, O.; Fourel, F.; Martin, G. J. ^{13}C Analysis of aromas and perfumes by a coupled GC-IRMS technique. The case of vanillin and leaf alcohol extracts. *Analysis*, **1994**, *22*, 268-272.

Bricout, J. Recherches sur le fractionnement des isotopes stables de l'hydrogéne et de l'oxygée dans quelques végétaux. *Rev. Cytol. Biol. Végét.-Bot.*, **1978**, *1*, 133-209.

Bristow, M.; Isaacs, N. S. The effect of high pressure on the formation of volatile products in a model Maillard reaction. *J. Chem. Soc., Perkin Trans. 2*, **1999**, 2213-2218.

Brophy, J. J.; Cavill, G. W. K. Naturally occurring pyrazines and their mass spectrometric characterisation. *Heterocycles*, **1980**, *14* (4), 477-504.

Buffo, R. A.; Cardelli-Freire, C. Coffee flavor: An overview. *Flavour Frag. J.* **2004**, *19*, 99-104.

Burgoyne, T. W.; Hayes, J. M. Quantitative production of H_2 by pyrolysis of gas chromatographic effluents. *Anal. Chem.*, **1998**, *70*, 5136-5141.

Buttery, R. G.; Ling, L. C. 2-Ethyl-3,5-dimethylpyrazine and 2-ethyl-3,6-dimethylpyrazine: odor thresholds in water solution. *Lebensm. Wiss. Technol.*, **1997**, *30*, 109-110.

Cabañero, A. I.; Recio, J. L.; Rupérez, M. Liquid chromatography coupled to isotope ratio mass spectrometry: a new perspective on honey adulteration detection. *J. Agric. Food Chem.*, **2006**, *54*, 9719-9727.

Camin, F.; Wietzerbin, K.; Blanch Cortes, A.; Haberhauer, G.; Lees, M.; Versinit, G. Application of multielement stable isotope ratio analysis to the characterization of French, Italian, and Spanish cheese. *J. Agric. Food Chem.*, **2004**, *52*, 6592-6601.

Carisano, A.; Gariboldi, L. Gas chromatographic examination of the fatty acids of coffee. *J. Sci. Food Agric.*, **1964**, *15*, 619-622.

Casal, S.; Rui Alves, M.; Mendes, E.; Oliveira, M. B. P. P.; Ferreira, M. A. Discrimination between arabica and robusta coffee species on the basis of their amino acid enantiomers. *J. Agric. Food Chem.*, **2003**, *51*, 6495-6501.

Casal, S.; Mendes, E.; Oliveira, M. B. P. P.; Ferreira, M. A. Roast effects on coffee amino acid enantiomers. *Food Chem.*, **2005**, *89*, 333-340.

Chen, J.; Ho, C.-T. Volatile compounds generated in serine–monosaccaride model systems. *J. Agric. Food Chem.*, **1998**, *46*, 1518-1522.

Chikaraishi, Y.; Naraoka, H. Organic hydrogen-carbon isotope signatures of terrestrial higher plants during biosynthesis for distinctive photosynthetic pathways. *Geochem. J.*, **2001**, *35*, 451-458.

Chikaraishi, Y.; Naraoka, H.; Poulson, S. R. Carbon and hydrogen isotopic fractionation during lipid biosynthesis in a higher plant (*Cryptomeria japonica*), *Phytochemistry*, **2004**, *65*, 323-330.

Christeller, J. T.; Laing, W. A.; Troughton, J. H. Isotope discrimination by ribulose-1,5-diphosphat carboxylase, *Plant Physiol.*, **1976**, *57*, 580-582.

Clarke, R. J. The flavour of coffee, In Morton, I. D.; Macleod, A. J. (editors): *Food Flavours Part B. The Flavour of Beverages*, **1986**, Elsevier, Amsterdam, Oxford, New York, Tokyo, 1-47.

Clements, R. L.; Deatherage, F. E. A chromatographic study of some of the compounds in roasted coffee. *Food Res.*, **1957**, *22*, 222-232.

Clifford, M. N. The composition of green and roasted coffee beans. *Process Biochem.*, **1975 a**, *10* (2), 20-23.

Clifford, M. N. The composition of green and roasted coffee beans. *Process Biochem.*, **1975 b**, *10* (4), 13-16.

Clifford, M. N. Chlorogenic acids, In Clarke, R. J.; Macrae, R. (editors): *Coffee, Chemistry*, **1985 a**, Elsevier Applied Science Publishers, Amsterdam, 153-202.

Clifford, M. N. Chemical and physical aspects of green coffee and coffee products, In Clifford, M. N.; Wilson, K. C. (Editors): *Coffee, Botany, biochemistry and production of beans and beverage*, **1985 b**, Croom Helm AVI, London, 305-374.

Clifford, M. N.; Kazi, T. The influence of coffee bean maturity on the content of chlorogenic acids, caffeine and trigonelline. *Food Chem.*, **1987**, *26*, 59-69.

Coleman III, W. M.; Lawson; S. N. Synthesis of materials rich in pyrazines employing no sugar. *J. Agric. Food Chem.*, **2000**, *80* (8), 1262-1270.

Collister, J. W.; Rieley, G.; Stern, B.; Eglinton, G.; Fry, B. Compound-specific $\delta^{13}C$ analyses of leaf lipids from plants with differing carbon dioxide metabolisms. *Org. Geochem.*, **1994**, *21*, 619-627.

Conte, M. H.; Weber, J. C.; Carlson, P. J.; Flanagen, L. B. Molecular and carbon isotope composition of leaf wax in vegetation and aerosols in a northern prairie ecosystem. *Oecologia*, **2003**, *135*, 67-77.

Cooper, T. G.; Wood, H. G. The carboxylation of phosphoenolpyruvate and pyruvate. *J. Biol. Chem.*, **1971**, *246*, 5488-5490.

Craig, H. Isotopic variations in meteoric waters. *Science*, **1961**, *133*, 1702-1703.

Culp, R. A.; Noakes, J. E. Identification of isotopically manipulated cinnamic aldehyde and benzaldehyde. *J. Agric. Food Chem.*, **1990**, *38*, 1249-1255.

Czerny, M.; Wagner, R.; Grosch, W. Detection of odor-active ethenylalkyl-pyrazines in roasted coffee. *J. Agric. Food Chem.*, **1996**, *44*, 3268-3272.

Danho, D.; Naulet, N.; Martin, G. J. Deuterium, carbon and nitrogen isotopic analysis of natural and synthetic caffeines. Authentification of coffees and coffee extracts. *Analusis*, **1992**, *20*, 179-184.

Dansgaard, W. Stable isotopes in precipitation, *Tellus*, **1964**, *16*, 436-468.

Deines, P. The isotopic composition of reduced organic carbon. In Fritz, P; Fontes, J. C. (editors): *Handbook of Environmental Isotope Geochemistry Vol. 1, The Terrestrial Environment, A*, Chapter 9, **1980**, Elsevier Scientific Publishing Company, Amsterdam, 329-406.

De Maria, C. A. B.; Trugo, L. C.; Moreira, R. F. A.; Petracco, M. Simultaneous determination of total chlorogenic acid, trigonelline and caffeine in green coffee samples by high performance gel filtration chromatography. *Food Chem.*, **1995**, *52*, 447-449.

De Maria, C. A. B.; Trugo, L. C.; Aquino Neto F. R.; Moreira, R. F. A.; Alviano, C. S. Composition of green coffee water-soluble fractions and identification of volatiles formed during roasting. *Food Chem.*, **1996 a**, *55*, 203-207.

De Maria, C. A. B.; Trugo, L. C.; Cora, G. Application of HPSE chromatography with a refractive index detector to green coffee analysis. *Quim. Nova, Sociedade Brasileira de Quimica*, **1996 b**, *19* (4), 350-352.

DeNiro, M. J.; Epstein, S. Mechanism of carbon isotope fractionation associated with lipid synthesis. *Science*, **1977**, *197*, 261-263.

Derbesy, M.;Venot, C.; Corte dos Santos, A.; Benfredj, A.; Busson, F. Green coffees of Angola. Chemical study. *Qual. Plant. Mater. Veg.*, **1969**, *18*, 367-375.

Deuser, W. G.; Degens, E. T. Carbon isotope fractionation in the system CO_2 (gas) – CO_2 (aqueous). *Nature*, **1967**, *215*, 1033-1035.

Downton, W. J. S.; Grant, W. J. R.; Robinson, S. P. Photosynthetic and stomatal response of spinach leaves to salt stress. *Plant Physiol.*, **1985**, *77*, 85-88.

Dunbar, J.; Wilson, A. T. Determination of geographic origin of caffeine by stable isotope analysis. *Anal. Chem.*, **1982**, *54*, 592-594.

Ehleringer, J. R.; Field, C. B.; Lin, Z.; Kuo, C. Leaf carbon isotope and mineral composition in subtropical plants along an irradiance cline. *Oecologia*, **1986**, *70*, 520-526.

Elss, S.; Preston, C.; Appel, M.; Heckel, F.; Schreier, P. Influence of technological processing on apple aroma analysed by high resolution gas chromatography mass spectrometry (HRGC-MS) and on-line gas chromatography combustion/pyrolysis isotope ratio mass spectrometry (HRGC-C/P-IRMS). *Food Chem.*, **2006**, *98* (2), 269-276.

Epstein, S.; Mayeda, T. Variations of ^{18}O content of waters from natural sources. *Geochim Cosmochim. Acta*, **1953**, *4*, 213-224.

Estep, M. F.; Hoerig, T. C. Biogeochemistry of the stable hydrogen isotopes. *Geochim Cosmochim. Acta*, **1980**, *44*, 1197-1206.

Estep, M. F.; Tabita, F. R.; Parker, P. L.; Van Baalen, C. Carbon isotope fractionation by ribulose-1,5-bisphosphate carboxylase from various organisms. *Plant Physiol.*, **1978**, *61*, 680-687.

Etard, A. *Ann. Chim. Phys.*, **1881**, *22*, 218.

Evans, J. R.; Sharkey, T. D.; Berry, J. A.; Farquhar, G. D. Carbon isotope discrimination measured concurrently with gas exchange to investigate CO_2 diffusion in leaves of higher plants. *Aust. J. Plant Physiol.*, **1986**, *13*, 281-292.

Evans, R. D.; Physiological mechanisms influencing plant nitrogen isotope composition. *Trends Plant Sci.*, **2001**, *6*, 121-126.

Evans, R. D.; Bloom, A. J.; Sukrapanna, S. S.; Ehleringer, J. R. Nitrogen isotope composition of tomato (*Lycopersicon esculentum* Mill. cv. T-5) grown under ammonium or nitrate nutrition. *Plant, Cell and Environ.*, **1996**, *19*, 1317-1323.

Farouk, A.; Pudil, F.; Janda, V.; Pokorný, J. Effect of amino acids on the composition and properties of extruded mixtures of wheat flour and glucose. *Nahrung*, **2000**, *44* (3), 188-192.

Farquhar, G. D.; O'Leary, M. H.; Berry, J. A. On the relationship between carbon isotope discrimination and the intercellular carbon dioxide concentration in leaves. *Aust. J. Plant Physiol.*, **1982**, *9*, 121-137.

Faulhaber, S.; Hener, U.; Mosandl, A. GC/IRMS analysis of mandarin essential oils. 1. $\delta^{13}C_{PDB}$ and $\delta^{15}N_{AIR}$ values of methyl N-methylanthranilate. *J. Agric. Food Chem.*, **1997**, 45, 2579-2583.

Feldman, J. R.; Ryder, W. S.; Kund, J. T. Importance of nonvolatile compounds in the flavor of coffee. *J. Agric. Food Chem.*, **1969**, *17*, 733-739.

Filer, C. N. Isotopic fractionation of organic compounds in chromatography. *J. Labelled Cpd. Radiopharm.*, **1999**, *42*, 169-197.

Fink, K.; Richling, E.; Heckel, F.; Schreier, P. Determination of $^{2}H/^{1}H$ and $^{13}C/^{12}C$ isotope ratios of (E)-methyl cinnamate from different sources using isotope ratio mass spectrometry. *J. Agric. Food Chem.*, **2004**, *52*, 3065-3068.

Fischer, M.; Reimann, S.; Trovato, V.; Redghwell, R. J. Structural aspects of polysaccharides from arabica coffee, *18th Int. Colloq. Chem. Coffee* (Helsinki 02-06.08.1999). **2000**, 91-94.

Fischer, M.; Reimann, S.; Trovato, V.; Redgwell, R. J. Polysaccharides of green arabica and robusta coffee. *Carbohyd. Res.*, **2001**, *330*, 93-101.

Flament, I.; Stoll, M. Synthése de methyl-2-pyrazines alcoylées en 3, par condensation de l'éthylènediamine avec les dioxo-2,3-alcanes. *Helv. Chim. Acta*, **1967**, *50* (7), 1754-1758.

Flament, I.; *Coffee Flavor Chemistry*. Wiley: West Sussex, U.K., **2002**.

Flanangan, L. B.; Bain, J. F.; Ehleringer, J. R. Stable oxygen and hydrogen isotope composition of leaf water in C_3 and C_4 plant species under field conditions. *Oecologia*, **1991**, *88*, 394-400.

Fogel, M. J.; Cifuentes, L. A. Isotope fractionation during during primary production. In: Engel, M. H. and Macko, S. (Editors) *Organic*

Geochemistry, Principles and Application, **1993**, Plenum Press, New York, 73-98.

Folstar, P.; Lipids, In Clarke, R. J.; Macrae, R. (editors): *Coffee, Chemistry*, **1985**, Elsevier Applied Science Publishers, Amsterdam, Vol. 1, 203-222.

Folstar, P.; Pilnik, W.; de Heus, J. G.; van der Plas, H. C. The composition of the fatty acids in coffee oil and coffee wax, *7th Int. Colloq. Chem. Coffee* (Hamburg 09-14.06.1975), **1975**, 253-258.

Freyer, H. D. On the ^{13}C record in tree rings II, Registration of microenviromental CO_2 and anomalous pollution effects. *Tellus*, **1979**, *31*, 308-312.

Friedmann, I. Deuterium content of natural waters and other substances. *Geochim. Cosmochim. Acta*, **1953**, *4*, 89-103.

Fry, B. *Stable isotope ecology*. Springer: Berlin, Heidelberg, New York, **2006**.

Gani, D.; Archer, C. H.; Botting, N. P.; Pollard, J. R. The 3-methylaspartase reaction probed using ^{2}H- and ^{15}N-isotope effects for three substrates: a flip from a concerted to a carbocationic amino-enzyme elimination mechanism upon changing the C-3 stereochemistry in the substrate from *R* to *S*. *Bioorgan. Med. Chem.*, **1999**, *7*, 977-990.

Gaebler, O. H.; Choitz, H. C.; Vitti, T. G.; Vukmirovich, R. Significance of N^{15} excess in nitrogenous compounds of biological origin. *Can. J. Biochem. Physiol.*, **1963**, *41*, 1089-1097.

García-Martin, M. L.; Ballesteros, P.; Cerdón, S. The metabolism of water in cells and tissues detected by NMR methods. *Progr. Nucl. Magn. Res. Spectros.*, **2001**, *39*, 41-47.

Gat, J. R. Comments on the stable isotope method in the regional groundwater investigations. *Water Resour. Res.*, **1971**, *7*, 980-993.

Georgi, M.; Voerkelius, S.; Roßmann, A.; Graßmann, J.; Schnitzler, W. H. Multielement isotope ratios of vegetables from integrated and organic production. *Plant Soil*, **2005**, *275*, 93-100.

Gleixner, G.; Schmidt, H.-L. Carbon isotope effects on the fructose-1,6-bisphosphate aldolase reaction, Origin for non-statistical ^{13}C-distributions in carbohydrates. *J. Biol. Chem.*, **1997**, *272* (9), 5382-5387.

Gonzáles-Prieto, S. J.; Domenach, A. M.; Beaupied, H.; Moiroud, A.; Jocteur-Monrozier, L. Composition of organic-N and ^{15}N-labelling uniformity in alder leaves. *Soil Biol. Biochem.*, **1995**, *27*, 925-929.

González, J.; Remaud, G.; Jamin, E.; Naulet, N. ; Martin, G. G. Specific natural isotope profile studied by isotope ratio mass spectrometry (SNIP-IRMS): $^{13}C/^{12}C$ ratios of fructose, glucose, and sucrose for improved detection of sugar addition to pineapple juices and concentrates. *J. Agric. Food Chem.*, **2000**, *47*, 2316-2321.

Gorter, K. Beiträge zur Kenntniss des Kaffees. I., *Liebigs Ann. Chem.*, **1908 a**, *358*, 327-348.

Grosch, W. Flavour of coffee. *Nahrung*, **1998**, *42* (6), 344-350.

Grosch, W. Key odorants of roasted coffee: evaluation, release, formation. In *Int. Colloq. Chem. Coffee* (Helsinki 02-06.08.1999), **2000**, 17-26.

Grosch, W.; Czerny, M.; Wagner, R.; Mayer, F. Studies on the aroma of roasted coffee. *Spec. Publ.-R. Soc. Chem.* **1996**, *197*, 200-205.

Guyot, B.; Petnga, E.; Vincent, J. C. Analyse qualitative d'un café Coffea canephora var. Robusta en fonction de la maturité. *Café, Cacao, Thé*, **1988 a**, *32*, 127-139.

Habfast, K. Advanced isotope ratio mass spectrometry I: Magnetic isotope ratio mass spectrometers. In Platzner, I. T. (Editor): Modern isotope ratio mass spectrometry, band 145, In Winefordner, J. D. (Editor): *Chemical Analysis* (A series of monographs on analytical chemistry and its application), **1997**, Wiley Verlag, Weinheim, 11-82.

Handley, L. L.; Raven, J. A. The use of natural abundance of nitrogen isotopes in plant physiology and ecology. *Plant, Cell Environ.*, **1992**, *15*, 965-985.

Hanneguelle, S. Etude de la biosynthese des monoterpenes par la mesure du fractionnement isotopique naturel specifique en resonance magnetique

nucleaire et spectrometrie de masse. Applications au contrôle d'origine et de qualite d'huiles essentielles. *Dissertation*, **1991**, University of Nantes.

Harper, L. A.; Sharpe, R. R. Atmospheric ammonia: issues on transport and nitrogen isotope measurement. *Atmos. Environ.*, **1998**, *32*, 273-277.

Hayes, J. M. Fractionation of the isotopes of carbon and hydrogen in biosynthetic processes. In: Valley, J. W. and Cole, D. R. (Editors) *Stable Isotope Geochemistry, Reviews in Mineralogy and Geochemistry*, **2001**, *43*, Mineralogical Society of America, Washington DC, USA, 225-277.

Heaton, T. H. E. $^{15}N/^{14}N$ ratios of nitrate and ammonium in rain at Pretoria, South Africa. *Atmos. Environ.*, **1987**, *21*, 843-852.

Hener, U.; Brand, W. A.; Hilkert, A. W.; Juchelka, D.; Mosandl, A.; Podebrad, F. Simultaneous on-line analysis of $^{18}O/^{16}O$ and $^{13}C/^{12}C$ isotope ratios of organic compounds using GC-pyrolysis-IRMS. *Z. Lebensm. Unters. Forsch.*, **1998**, *206*, 230-232.

Hermes, J. D.; Weiss, P. M.; Cleland, W. W. Use of nitrogen-15 and deuterium isotope effects to determine the chemical mechanism of phenylalanine ammonia-lyase. *Biochem.*, **1985**, *24*, 2959-2967.

Hilkert, A. W.; Douthitt, C. B.; Schlüter, H. J.; Brandt, W. A. Isotope ratio monitoring gas chromatography/mass spectrometry of D/H by high temperature conversion isotope ratio mass spectrometry. *Rapid Commun. Mass Spectrom.*, **1999**, *13*, 1226-1230.

Ho, C. T.; Hwang, H. I.; Yu, T. H.; Zhang, J. An overview of the Maillard reactions related to aroma generation in coffee. *15th Int. Colloq. Chem. Café* (Montpellier 06-11.06.1993), **1993**, *2*, 519-527.

Ho, C. T.; Chen, J. Generation of volatile compounds from Maillard reaction of serine, threonine, and glutamine with monosaccharides. In Teranishi, R.; Wick, E. L.; Hornstein, I. (editors): *Flavor Chemistry. Thirty Years of Progress*, **1999**, Kluwer Academic/Plenum, New York, 327-333.

Hobbie, E. A.; Macko, S. A.; Shugart, H. H. Patterns in N dynamics and N isotopes during primary succession in Glacier Bay. Alaska, *Chem. Geol.*, **1998**, *152*, 3-11.

Hobbie, E. A.; Macko, S. A.; Shugart, H. H. Insights into nitrogen and carbon dynamics of ectomycorrhizal and saprotrophic fungi from isotopic evidence. *Oecologia*, **1999 a**, *118*, 353-360.

Hobbie, E. A.; Werner, R. A. Intramolecular, compound-specific, and bulk carbon isotope patterns in C_3 and C_4 plants: a review and synthesis. *New Phytol.*, **2004**, *161*, 371-385.

Hoch, M. P.; Fogel, M. L.; Kirchman, D. L. Isotope fractionation associated with ammonium uptake by a marine bacterium. *Limnol. Oceanogr.*, **1992**, *37*, 1447-1459.

Hoefs, J. Stable Isotope Geochemistry, Springer: Berlin, Heidelberg, New York, **1973**.

Högberg, P.; Högberg, M. N.; Quist, M. E.; Ekblad, A.; Näsholm, T. Nitrogen isotope fractionation during nitrogen uptake by ectomycorrhizal and non-mycorrhizal *Pinus sylvestris*. *New Phytol.*, **1999**, *142*, 569-576.

Hör, K. Authentizitätskontrolle von Aromastoffen: $^2H/^1H$-Analytik mittels on-line Gaschromatographie – Isotopenverhältnis – Massenspektrometrie (HRGC-IRMS) als Baustein einer Multielement-Isotopenverhältnisanalyse. *Dissertation*, **2001**, Julius-Maximilians-Universität Würzburg.

Hör, K.; Ruff, C.; Weckerle, B.; König, T.; Schreier, P. Flavor authenticity studies by $^2H/^1H$ ratio determination using on-line gas chromatography pyrolysis isotope ratio mass spectrometry. *J. Agric. Food Chem.*, **2001 a**, *49*, 21-25.

Hör, K.; Ruff, C.; Weckerle, B.; König, T.; Schreier, P. $^2H/^1H$ Ratio analysis of flavor compounds by on-line gas chromatography-pyrolysis-isotope ratio mass spectrometry (HRGC-P-IRMS): Citral. *Flav. Fragr. J.*, **2001 b**, *16*, 344-348.

Hughes, E. B; Smith, R. F. The nicotinic acid content of coffee. *J. Soc. Chem. Ind.*, **1946**, *65*, 284-286.

Hwang, H.-I.; Hartman, T. G.; Rosen, R. T.; Ho, C.-T. Formation of pyrazines from the maillard reaction of glucose and glutamine-amide-^{15}N. *J. Agric. Food Chem.*, **1993**, *41*, 2112-2115.

Hwang, H.-I.; Hartman, T. G.; Rosen, R. T.; Lech, J.; Ho, C.-T. Formation of pyrazines from the maillard reaction of glucose and lysine-α-amine-^{15}N. *J. Agric. Food Chem.*, **1994**, *42*, 1000-1004.

Hwang, H.-I.; Hartman, T. G.; Ho, C.-T. Relative reactivities of amino acids in the formation of pyridines, pyrroles, and oxazoles. *J. Agric. Food Chem.*, **1995**, *43*, 2917-2921.

Ivlev, A. A. Carbon isotope effects (^{13}C/^{12}C) in biological systems. *Separ. Sci. Techn.*, **2001**, *36* (8 & 9), 1819-1914.

Jamin, E.; Martin, F.; Santamaria-Fernandez, R.; Lees, M. Detection of exogenous citric acid in fruit juices by stable isotope ratio analysis. *J. Agric. Food Chem.*, **2005**, *53*, 5130-5133.

Jamin, E.; Naulet, N.; Martin, G. J. Stable istotope analysis of components from tobacco leaves. *Phytochem. Analysis*, **1997**, *8*, 105-109.

Jones, D. L.; Edwards, A. C.; Donachie, K.; Darrah, P. R. Role of proteinaceous amino acids released in root exudates in nutrient acquisition from the rhizosphere. *Plant Soil*, **1994**, *158*, 183-192.

Jorré. Dissertation, **1897**, Kiel.

Jung, J.; Sewenig, S.; Hener, U.; Mosandl, A Comprehensive authenticity assessment of lavender oils using multielement/multicomponent isotope ratio mass spectrometry analysis and enantioselective multidimensional gas chromatography-mass spectrometry. *Eur. Food Res. Technol.*, **2005**, *220*, 232-237.

Kahle, K.; Preston, C.; Richling, E.; Heckel, F.; Schreier, P. On-line gas chromatography combustion/pyrolysis isotope ratio mass spectrometry (HRGC-C/P-IRMS) of major volatiles from pear fruit (*Pyrus communis*) and pear products. *Food Chem.*, **2005,** *91*, 449-455.

Kappeler, A. W.; Baumann, T. W. Purine alkaloid pattern in coffee beans. *11th Int. Colloq. Chem. Coffee* (Lomé 11-15.02.1985), **1986**, 273-279.

Kato, S.; Kurata, T.; Ishitsuka, R.; Fujimaki, M. Pyrolysis of β-hydroxy amino acids, especially L-serine. *Agric. Biol. Chem.*, **1970**, *34*, 1826-1832.

Kato, S.; Kurata, T.; Ishiguro, S.; Fujimaki, M. Additional volatile compounds produced by pyrolysis of sulfur containing amino acids. *Agric. Biol. Chem.*, **1973**, *37*, 1759-1761.

Kaufmann, H. P.; Hamsagar, R. S. Zur Kenntnis der Lipoide der Kaffeebohne. I. Über Fettsäure-Ester der Cafestols. *Fette, Seifen, Anstrichm.*, **1962**, *64*, 206-213.

Kaunzinger, A.; Juchelka, D.; Mosandl, A. Progress in the authenticity assessment of vanilla. 1. Initiation of authenticity profiles. *J. Agric. Food Chem.*, **1997**, *45*, 1752-1757.

Keeling, C. D.; Mook, W. G.; Tans, P. P. Recent trends in the $^{13}C/^{12}C$ ratio of atmospheric carbon dioxide. *Nature*, **1979**, *277*, 121-123.

Kennicutt, M. C.; Bidigare, R. R.; Macko, S. R.; Keeney-Kennicutt, W. L. The stable isotopic composition of photosynthetic pigments and related biochemicals. *Chem. Geol.* (Isotope Geoscience Section), **1992**, *101*, 235-245.

Kim, S. C.; Raushel, F. M. Isotopic probes of the argininosuccinate lyase reaction. *Biochem.*, **1986**, *25*, 4744-4749.

Kluge, M.; Brulfert, J.; Rauh, W.; Ravelomanana, D.; Ziegler H. Ecophysiological studies on the vegetation of Madagaskar: A $\delta^{13}C$ and δD survey for incidence of crassulacean acid metabolism (CAM) among orchids from montane forests and succulents from the xerophytic thorn-bush. *Isotopes Environ. Helath Stud.*, **1995**, *31*, 191-210.

Koehler, P. E.; Mason, M. E.; Newell, J. A. Formation of pyrazine compounds in sugar-amino acid model systems. *J. Agric. Food Chem.*, **1969**, *17*, 393-396.

Kornexl, B. E.; Werner, T.; Roßmann, A.; Schmidt, H.-L. Measurement of stable isotope abundances in milk and milk ingredients-a possible tool for origin assignment and quality. *Z. Lebens. Unters. Forsch. A*, **1997**, *205*, 19-24.

Kort, M J. Reactions of free sugars with aqueous ammonia. *Adv. Carbohyd. Chem. Bi.*, **1970**, *25*, 311-349.

Kozhu, A.; Tateishi, T.; Yamada, A.; Koba, K.; Wada, E. Nitrogen isotope fractionation during nitrogen transport from ectomycorrhizal fungi, *Suillus granulatus*, to the host plant, *Pinus densiflora*. *Soil Sci. Plant Nutr.*, **2000**, *46*, 733-739.

Krems, I. J.; Spoerri, P. E. The pyrazines. *Chem. Rev.*, **1947**, *40*, 328.

Kurniadi, T. H.; Rhlid, R. B.; Laurent-Bernard, F.; Juillerat, M. A.; Berger, R. G. Chemoenzymatic synthesis of aroma active 5,6-dihydro- and tetrahydropyrazines from aliphatic acyloins produces by baker's yeast. *J. Agric. Food Chem.*, **2003**, *51*, 3103-3107.

Lentner, C.; Deatherage, F. E. Organic acids in coffee in relation to the degree of roast. *Food Res.*, **1959**, *24*, 483-492.

Lesaint, C.; Merlivat, L.; Bricout, J.; Fontes, J. C.; Gatheret, R. Sur la composition en isotopes stables de l'eau de la tomate et du mais. *C. R. Acad. Sci., Paris, Ser. D*, **1974**, *278*, 2925-2930.

Liu, K. K. ; Kaplan, I. R. The Eastern tropical Pacific as a source of ^{15}N-enriched nitrate in seawater off southern California. *Limnol. Oceanogr.*, **1989**, *34*, 820-830.

Ludwig, E.; Lipke, U.; Raczek, U. Investigations of peptides and proteases in green coffee beans. *Eur. Food Res. Technol.*, **2000**, *211*, 111-116.

Luo, Y.; Sternberg, L.; Suda, S.; Kumazawa, S.; Mitsui, A. Extremely low D/H ratios of photoproduced hydrogen by cyanobacteria. *Plant Cell Physiol.*, **1991**, *32*, 897-900.

Macdonald, I. A.; Macrae, R. The determination of amino acids in coffee products. In: *11th Int. Colloq. Chem. Coffee* (Lomé 11-15.02.1985), **1986**, 333-340.

Macko, S. A.; Fogel Estep, M. L.; Engel, M. H.; Hare, P. E. Kinetic fractionation of stable nitrogen isotopes during amino acid transamination. *Geochim. Cosmochim. Acta*, **1986**, *50*, 2143-2146.

Macko, S. A.; Fogel Estep, M. L.; Hare, P. E.; Hoering, T. C. Isotopic fractionation of nitrogen and carbon in the synthesis of amino acids by microorganisms. *Chem. Geol.* (Isotope Geoscience Section), **1987**, *65*, 79-92.

Macko, S. A.; Helleur, R.; Hartley, G.; Jackmann, P. Diagenesis of organic matter – a study using stable isotopes of individual carbohydrates, *Org. Geochem.*, **1990**, *16*, 1129-1137.

Macrae, R. Nitrogenous components. In Clarke, R. J.; Macrae, R. (editors): *Coffee, Chemistry*, **1985**, *1*, Elsevier Applied Science Publishers, 115-152.

Maier, H. G. *Kaffee*, **1981**, Verlag Paul Parey, Berlin, Hamburg, Series: Grundlagen und Fortschritte der Lebensm. Unters. und Lebensm. Technol. Vol. *18*, 199 pp.

Mar Caja, M.; Preston, C.; Kempf, M. and Schreier, P. Flavor authentication studies of α-ionone, β-ionone and α-ionol from various sources. *J. Agric. Food Chem.*, **2007**, *55*, 6700-6704.

Mariotti, A.; Germon, J. C.; Hubert, P.; Kaiser, R.; Letolle, A.;Tardieux, A.; Tardieux, P. Experimental determination of nitrogen kinetic isotope fractions : Some principles ; illustration for the denitrification and nitrification processes. *Plant Soil*, **1981**, *62*, 413-430.

Mariotti, A. Atmospheric nitrogen is a reliable standard for natural ^{15}N abundance measurements. *Nature*, **1983**, *303*, 685-687.

Marlier, J. F.; O'Leary, M. H. Carbon kinetic isotope effects on the hydration of carbon dioxide and the dehydration of bicarbonate ion. *J. Am. Chem. Soc.*, **1984**, *106*, 5054-5057.

Martin, B.; Sutherland, E. K. Air pollution in the past recorded in width and stable carbon isotope composition of annual growth rings of Douglas-fir. *Plant Cell Environ.*, **1990**, *13*, 839-844.

Martin, G. J.; Martin, M.L. Deuterium labelling at the natural abundance level as studied by high field quantative ^{2}H NMR. *Tetrahed. Lett.*, **1981**, *22*, 3525-3528.

Martin, G. J.; Zhang, B. L.; Naulet, N.; Martin, M. L. Deuterium transfer in the bioconversion of glucose to ethanol studied by specific labeling at the natural abundance level. *J. Am. Chem. Soc.*, **1986**, *108*, 5122-5126.

Martin, G. J.; Martin, M.L. Climate significance of isotope ratios. *Phytochemistry Reviews*, **2003**, *2*, 179-190.

Martin, M. J.; Pablos, F.; Gonzalez, A. G. Discrimination between arabica and robusta green coffee varieties according to their chemical composition. *Talanta*, **1998**, *46* (6), 1259-1264.

Matsubara, M.; Koji, T.; Nakajima, T. Preparation of 2,6-disubstituted pyrazines, *Japanese patent*, JP 2000-367668 20001201, **2002**.

Matthews, D. E.; Hayes, J. M. Isotope ratio monitoring gas chromatography mass spectrometry. *Anal. Chem.*, **1978**, *50*, 1465-1473.

Mazzafera, P. Trigonelline in coffee. *Phytochemistry*, **1991**, *30* (7), 2309-2310.

McKinney, C. R.; McCrea, J. M.; Epstein S.; Allen, H. A.; Urey, H. C. Improvements in mass spectrometers for the measurement of small differences in isotope abundance ratios. *Rev. Sci. Instrum.* **1950**, *21*, 724-730.

Medina, R.; Schmidt, H.-L. Nitrogen isotope ratio variations in biological material, indicator for metabolic correlations? In Schmidt, H.-L.; Förstel, H.; Heinzinger, K. (editors): *Stable Isotopes, Proceedings of the 4th International Conference*, **1982**, Elsevier Scientific Publishing Company, Amsterdam, 465-473.

Melzer, E.; Schmidt, H.-L. Carbon isotope effects on the pyruvate-dehydrogenase reaction and their importance for relative C-13 depletion in lipids. *J. Biol. Chem.*, **1987**, *262*, 8159-8164.

Merkler, D. J.; Kline, P. C.; Weiss, P.; Schramm, V. L. Transition state analysis of AMP-deaminase. *Biochemistry*, **1993**, *32*, 12993-13001.

Merrit, C. Jr.; Robertson, D. H.; McAdoo, D. J. The relationship of volatile compounds in roasted coffee beans to their precursors. *4th Int. Colloq. Chem. Coffee* (Amsterdam, 02-06.06.1969), **1970**, 144-148.

Mook, W. G.; Bommerson, J. C.; Staverman, W. H. Carbon isotope fractionation between dissolved bicarbonate and gaseous carbon dioxide. *Earth Planet. Sci. Letters*, **1974**, *22*, 169-176.

Moran, E. J.; Easterday, O. D.; Oser, B. L. Acute oral toxicity of selected flavour chemicals. *Drug Chem. Toxicol.*, **1980**, *3* (3), 249-258.

Mosandl, A.; Braunsdorf, R.; Dietrich, A.; Faber, B.; Karl, V.; Köpke, T.; Lehmann, D.; Maas, B. Recent development in the authenticity control of flavours and fragrances. In Maarse, H.; van der Heij, D. G. (Editors): *Trends in Flavour Research*, **1994**, Elsevier Science B. V., Amsterdam, 89-98.

Mosandl, A. Enantioselective capillary gas chromatography and stable isotope ratio mass spectrometry in the authenticity control of flavors and essential oils. *Food Rev. Int.*, **1995**, *11*, 597-664.

Mosandl, A. Authenticity assessment: A permanent challenge in food flavor and essential oil analysis. *J. Chromatogr. Sci.*, **2004**, *42*, 440-449.

Mottram, D. S. Meat volatile compounds. In Maarse, H. (Editor): *Food and Beverages*, **1991**, Marcel Dekker, New York, 107-177.

Nakabayashi, T.; Masano, M. Changes of the trigonelline and caffeine contents in coffee beans during roasting. *Nippon Shokuhin Kogyo Gakkaishi*, **1986**, *33* (10), 725-728.

Nakatani, Y.; Yanatori, Y. Simple synthesis of 2,3-disubstituted pyrazines. *Agric. Biol. Chem.*, **1973**, *37*, 1509.

Naraoka, H.; Chikaraishi, Y. Organic hydrogen-carbon isotope signatures of terrestrial higher plants during biosynthesis for distinctive photosynthetic pathways. *Geochem. J.*, **2001**, *35*, 451-458.

Navellier, P. Composition moyenne du café vert. In Coste, R. (Editor): *Les caféiers et les cafés dans le monde*, **1961**, *2*, 163-220.

Nhu-Trang, T.-T.; Casabianca, H.; Grenier-Loustalot, M.-F. Authenticity control of essential oils containing citronellal and citral by chiral and stable-isotope gas-chromatographic analysis. *Anal. Bioanal. Chem.*, **2006**, *386*, 2141-2152.

Northfelt, D. W.; DeNiro, M. J.; Epstein, S. Hydrogen and carbon isotopic ratios of the cellulose nitrate and saponifiable lipid fractions prepared from

annual growth rings of a califormia redwood. *Geochim. Cosmochim. Acta*, **1981**, *45* (10), 1895-1898.

Odell, G. V. The role of pyrazine compounds in the flavor of coffee. *6th Int. Colloq. Chem. Coffee* (Bogota 04-09.06.1973), **1973**, 312-318.

O'Leary, M. H.; Urberg, M.; Young, A. P. Nitrogen isotope effects on the papain-catalyzed hydrolysis of N-benzoyl-L-argininamide. *Biochemistry*, **1974**, *13*, 2077-2081.

O'Leary, M. H. Carbon isotope fractionation in plants. *Phytochemistry*, **1981**, *20*(4), 553-567.

Oosterfeld, A.; Harmsen, J. S.; Voragen, A. G. J.; Schols, H. A. Extraction and characterization of polysaccharides from green and roasted *Coffea arabica* beans. *Carbohyd. Polym.*, **2003**, *52*, 285-296.

Park, R.; Epstein, S. Carbon isotope fractionation during photosynthesis. *Geochim. Cosmochim. Acta*, **1960**, *21*, 110-126.

Parkin, D. W.; Mentch, F.; Banks, G. A.; Horenstein, B. A.; Schramm, V. L. Transition-state analysis of a V_{max} mutant of AMP nucleosidase by the application of heavy-atom kinetic isotope effects. *Biochemistry*, **1991**, *30*, 4586-4594.

Payen. Mémoire sur le café. Deuxième partie. *Compt. Rend. Acad. Sci. Paris*, **1846 a**, *23*, 8-15.

Payen. Untersuchung des Kaffees. *Ann. Chem. Pharm.*, **1846 b**, Wöhler & Liebig, Heidelberg, *60*, 286-294.

Penuelas, J.; Azcón-Bieto, J., Changes in leaf $\Delta^{13}C$ of herbarium plant species during the last 3 centuries of CO_2 increase. *Plant cell Environ.*, **1992**, *15*, 485-489.

Peterson, B. J.; Fry, B. Stable isotopes in ecosystem studies. *Annu. Rev. Ecol. Sys.*, **1987**, *18*, 293-320.

Preston, C.; Richling, E.; Elss, S.; Appel, M.; Heckel, F.; Hartlieb, A.; Schreier, P. On-line gas chromatography combustion/pyrolysis isotope ratio mass

spectrometry (HRGC-C/P-IRMS) of pineapple (*Ananas comosus*) volatiles. *J. Agric. Food Chem*., **2003**, *51*, 8027-8031.

Preston, C.; Richling, E.; Kahle, K.; Kraus, M.; Hümmer, W.; Appel, M.; Heckel, F.; Schreier, P. Ester Synthesis: Authenticity assessment by stable isotope analysis. In Hofmann, T.; Rothe, M.; Schieberle, P. (Editors): *State-of-the-Art in Flavour Chemistry and Biology*, Proceedings of the 7th Wartburg Symposium, **2004**, 358-362.

Preston, C.; Elss, S.; Kohlhepp, S.; Appel, M.; Heckel, F.; Schreier, P. Stabil-isotopenanalytik: Erfassung und Bewertung von technologiebedingten Isotopeneffekten von Aromastoffen. *Poster* - 34. Deutscher Lebensmittel-chemikertag, Hamburg, 19.-21, September **2005**.

Procida, G.; de Palo, D.; Bogoni, P. Analysis of the volatile constituents of green coffee by headspace GC-MS. *Riv. Ital. EPPOS*, **1997**, 251-261.

Prodolliet, J.; Baumgartner, M.; Martin, Y. L.; Remaud, G. Determination of the geographic origin of green coffee by stable isotope techniques. *17th Int. Colloq. Chem. Coffee* (Nairobi 20-25.07.1997), **1998**, 197-200.

Prodolliet, J.; Zbinden, P.; Andrey, D.; Baumgartner, D. Determination of the geographical origin of green coffee by inductively coupled plasma mass spectrometry (ICP-MS). *19th Int. Colloq. Chem. Coffee* (Turrialba 06-11.06.2001), **2001**, 344-349.

Reese, G.; Baltes, W. Model reactions on roast aroma formation XI. Heating of serine with selected sugars and sugar degradation products in an autoclave. *Z. Lebensm. Unters. Forsch.*, **1992**, *194*, 417-421.

Rehm, S.; Espig, G. *Die Kulturpflanzen der Tropen und Subtropen: Anbau, wirtschaftliche Bedeutung, Verwertung*, **1996**, 3. edition, Ulmer, Stuttgart.

Reibach, P. H.; Benedict, C. R. Fractionation of stable carbon isotopes by phosphoenolpyruvate carboxylase from C_4 plants. *Plant Physiol.*, **1977**, *59*, 564-568.

Reichstein, T.; Staudinger, H. Improvements in a method for isolating the aromatic principle contained in roasted coffee. *British Patent* 246454, **1926**.

Richards, N. G. J.; Schuster, S. M. Mechanistic issues in asparagine synthase catalysis. In Purich, D. L. (Editor): *Adv. Enzym.*, **1998**, *72*, John Wiley & Sons Inc, New York, 145-198.

Richling, E.; Höhn, C.; Weckerle, B.; Heckel, F.; Schreier, P. Authentication analysis of caffeine-containing foods via elemental analysis combustion/pyrolysis isotope ratio mass spectrometry (EA-C/P-IRMS). *Eur. Food Res. Technol.*, **2003**, *216*, 544-548.

Richling, E.; Preston, C.; Kavvadias, D.; Kahle, K.; Heppel, C.; Hummel, S.; König, T.; Schreier, P. Determination of the $^{2}H/^{1}H$ and $^{15}N/^{14}N$ ratios of alkylpyrazines from coffee beans (*Coffea arabica* L. and *Coffea robusta* L.) by isotope ratio mass spectrometry. *J. Agric. Food Chem.*, **2005,** *53*, 7925-7930.

Richling, E.; Appel, M.; Heckel, F.; Kahle, K.; Kraus, M.; Preston, C.; Hümmer, W.; Schreier, P. Flavor authenticity studies by isotope ratio mass spectrometry: perspective and limits. In Ebeler, S. E.; Takeoka, G. R.; Winterhalter, P. (Editors): Authentication of Food and Wine, *ACS Symposium Series*, **2007**, *952*, 75-86.

Richter, G. *Biochemie der Pflanzen*, **1996**, Georg Thieme Verlag, Stuttgart, New York, 127, 134-137, 140-145, 171, 476-479.

Rishavy, M. A.; Cleland, W. W. ^{13}C and ^{15}N Kinetic isotope effects on the reaction of aspartate aminotransferase and the tyrosine-225 to phenylalanine mutant. *Biochemistry*, **2000**, *39*, 7546-7551.

Rizzi, G. P. Heat-induced flavor formation from peptides. In: Patliment, T. W.; Megorin, R. J.; Ho, C.-T. (editors): *Thermal generation of Aromas*, Chapter 16, **1989**, 172-181, Oxford University Press, USA.

Rizzi, G. P.; Sanders, R. A. Mechanism of pyridine formation from trigonelline under coffee roasting conditions. *Spec. Publ. R. Soc. Chem.*, **1996**, *197*, 206-210.

Rodriguez, D. B.; Frank, H. A.; Yamamoto, H. Y. Acetaldehyde as a possible indicator of spoilage in green kona (Hawaiian) coffee. *J. Sci. Food Agric.*, **1969**, *20*, 15-17.

Roempp CD Lexikon Chemie, Thieme Verlag, Stuttgart, **2006**.

Roffi, J.; Corte dos Santos, A.; Mexia, J. T.; Busson, F.; Miagrot, M. Cafés verts et torréfiés de l'Angola. Etude chimique. *5th Int. Colloq. Chem. Coffee* (Lisbon, 14-19.06.1971), **1973**, 179-200.

Rossmann, A; Butzenlecher, M.; Schmidt, H.-L. Evidence for a nonstatistical carbon isotope distribution in natural glucose. *Plant Physiol.*, **1991**, *96* (2), 609-614.

Ruff, C.; Hör, K.; Weckerle, B.; Schreier, P. $^{2}H/^{1}H$ Ratio analysis of flavor compounds by on-line gas chromatography pyrolysis isotope ratio mass spectrometry (HRGC-P-IRMS): Benzaldehyde. *J. High Resol. Chromatogr.*, **2000**, *23*, 357-359.

Ruff, C. Authentizitätskontrolle von Aromastoffen: $^{18}O/^{16}O$-Analytik mittels on-line Gaschromatographie-Isotopenverhältnis-Massenspektrometrie (HRGC-IRMS) als Baustein einer Multielement-Isotopenverhältnisanalyse. *Dissertation*, **2001**, Julius-Maximilians-Universität Würzburg.

Russwurm, H. Jr. Fractionation and analysis of aroma precursors in green coffee. *4th Int. Colloq. Chem. Coffee* (Amsterdam, 02-06.06.1969), **1970**, 103-107.

Sarett, H. P.; Perlzweig, W. A.; Levy, E. D. Synthesis and excretion of trigonelline. *J. Biol. Chem.*, **1940**, *135*, 483-485.

Sayed, O. H. Crassulacean acid metabolism 1975-2000, a check list. *Phytosynthetica*, **2001**, *39* (3), 339-352.

Scharrer, A.; Mosandl, A. Progress in the authenticity assessment of vanilla. 2. $\delta^{13}C_{V\text{-}PDB}$ correlations and methodical optimisations. *Dtsch. Lebensm.-Rundsch.*, **2002**, *98*, 117-121.

Schimmelmann, A.; Wintsch, R. P.; Lewan, M. D.; DeNiro, M. J. Chitin: 'forgotten' source of nitrogen. From modern chitin to thermally mature kerogen: lessons from nitrogen isotope ratios. In Stankiewicz, B. A.; van Bergen, P. F. (Editors): *Nitrogen-Containing Macromolecules in the Bio- and Geosphere*, ACS Symposium Series, **1998**, *707*, American Chemical Society, Washington, 226-242.

Schleucher, J.; Vanderveer, P.; Markley, J. L.; Sharkey, T. D. Intramolecular deuterium distributions reveal disequilibrium of chloroplast phosphoglucose isomerase. *Plant, Cell Environ.*, **1999**, *22* (5), 525-533.

Schmidt, H.-L.; Fundamentals and systematics of the non-statistical distributions of isotopes in natural compounds. *Naturwissenschaften*, **2003**, *90*, 537-552.

Schmidt, H.-L. Analyse von stabil-isotop markierten Verbindungen. In Simon, H. (Editor): *Messung von radioaktiven und stabilen Isotopen*, Band 2, **1974**, Springer Verlag, Berlin, 291-400.

Schmidt, H.-L.; Winkler, F. J.; Latzko, E.; Wirth, E. Photosynthetic carboxylation reactions and delta-C-13-values of plant material. *Isr. J. Chem.*, **1978**, *17*, 223-224.

Schmidt, H.-L.; Roßmann, A; Werner, R. A. Stable isotope ratio analysis in quality control of flavourings. In Ziegler, H.; Ziegler, E. (editors): *Flavourings*, **1998**, Wiley-VCH, Weinheim, 539-594.

Schmidt, H.-L.; Werner, R. A.; Eisenreich, W.; Systematics in ^{2}H patterns in natural compounds and ist importance for the elucidation of biosynthetic pathways. *Phytochemistry Reviews*, **2003**, *2*, 61-85.

Schmidt, H.-L.; Roßmann, A; Stöckigt, D.; Christoph, N. Stabilisotopenanalytik – Herkunft und Authentizität von Lebensmitteln. *Chem. Unserer Zeit*, **2005 a**, *39*, 90-99.

Schmidt, H.-L.; Roßmann, A; Voerkelius, S.; Schnitzler, W. H.; Georgi, M.; Graßmann, J.; Zimmermann, G.; Winkler, R. Isotope characteristics of vegetables and wheat from conventional and organic production. *Isotopes in Environmental and Health Studies*, **2005 b**, *41*, 223-228.

Schmidt, H.-L.; Werner, R. A.; Roßmann, A; Mosandl, A.; Schreier, P. Stable isotope ratio analysis in quality control of flavourings. In Ziegler, H. (editor): *Flavourings*, **2007**, Wiley-VCH, Weinheim, 602-663.

Schwaiger, W.; Cornelissen, J. M.; Ward, J. P. A convenient synthesis of alkyl- and arylpyrazinyl ketones. *J. Agric. Food Chem.*, **1984**, *13*, 225-234.

Serra, F.; Guillou, C. G.; Reniero, F.; Ballarin, L.; Cantagallo, M. I.; Wieser, M.; Lyer, S. S.; Héberger, K.; Vanhaecke, F. Determination of the geographical origin of green coffee by principal component analysis of carbon, nitrogen and boron stable isotope ratios. *Rapid Commun. Mass Spectrom.*, **2005**, *19*, 2111-2115.

Serra, F.; Janeiro, A.; Calderone, G.; Rojas, J. M.; Rhodes, C.; Gonthier, L. A.; Martin, F.; Lees, M; Mosandl, A.; Sewenig, S.; Hener, U.; Henriques, B.; Ramalho, L.; Reniero, F.; Teixeira, A. J.; Guillou, C. Inter-laboratory comparison of elemental analysis and gas chromatography combustion isotope ratio mass spectrometry (GC-C-IRMS). Part I: delta13C measurements of selected compounds for the development of an isotopic Grob-test. *J. Mass Spectrom.*, **2007**, *42*, 361-369.

Sewenig, S.; Hener, U.; Mosandl, A. Online determination of $^{2}H/^{1}H$ and $^{13}C/^{12}C$ isotope ratios of cinnamaldehyde from different sources using gas chromatography isotope ratio mass spectrometry. *Eur. Food Res. Technol.*, **2003**, *217*, 444-448.

Sewenig, S.; Bullinger, D.; Hener, U.; Mosandl, A. Comprehensive authentication of (E)-α(β)-ionone from raspberries, using constant flow MDGC-C/P-IRMS and Enantio-MDGC-MS. *J. Agric. Food Chem.*, **2005**, *53*, 838-844.

Shepard, A. T.; Danielson, N. D.; Pauls, R. E.; Mahle, N. H.; Taylor, P.J.; Rogers, L. B. Gas-chromatographic fractionations of stable isotopes of carbon and oxygen in carbon dioxide. *Separ. Sci.*, **1976**, *11*, 279-292.

Shibamoto, T.; Bernhard, R. A. Investigation of pyrazine formation pathways in sugar-ammonia model systems. *J. Agric. Food Chem.*, **1977**, *25*, No. 3, 609-614.

Shu, C. Pyrazine formation from serine and threonine. *J. Agric. Food Chem*., **1999**, *47*, 4332-4335.

Silfer, J. A.; Engel, M. H.; Macko, S. A.; Jumeau, E. J. Stable carbon isotope analysis of amino acid enantiomers by conventional isotope ratio mass spectrometry and combined gas chromatography/isotope ratio mass spectrometry. *Anal. Chem.*, **1991**, *63*, 370-374.

Smith, B. N.; Jacobsen, B. S. $^{2}H/^{1}H$ and $^{13}C/^{12}C$ ratios for classes of compounds isolated from potato tuber. *Plant Cell Physiol.*, **1976**, *17*, 1089-1092.

Smith, B. N.; Ziegler, H. Isotopic fractionation of hydrogen in plants. *Bot. Acta*, **1990**, *103*, 335-342.

Smith, R. F. The determination of caffeine in coffee and in coffee mixtures. 1st Int. Coll. Chem. Coffee (Paris, 20-22.05-1963), *Café, Cacao, Thé*, **1963 a**, *3*, 223-230.

Smith, S. E.; Read, D. J. *Mycorrhizal Symbiosis*, **1997**, 2nd ed. Academic Press, San Diego, 147-151, 255-275, 402-405.

Sohn, M.; Ho, C.-T. Ammonia generation during thermal degradation of amino acids. *J. Agric. Food Chem.*, **1995**, 43 (12), 3001-3003.

Souci, Fachmann, Kraut. *Die Zusammensetzung der Lebensmittel Nährwert-Tabellen*. **2000**, 6. edition, Medpharm, Stuttgart.

Speer, K. 16-*O*-Methylcafestol – ein neues Diterpen im Kaffee. *Z. Lebensm. Unters. Forsch.*, **1989**, *189*, 326-330.

Speer, K.; Tewis, R.; Montag, A. 16-*O*-Methylcafestol a quality indicator in coffee. *14th Int. Colloq. Chem. Café* (San Francisco 14-19.07.1991), **1992 a**, 237-244.

Speer, K.; Tewis, R.; Montag, A. A new roasting component in coffee. *14th Int. Colloq. Chem. Café* (San Francisco 14-19.07.1991), **1992 b**, 615-621.

Stadel, W.; Rugheimer, L. Ueber die Einwirkung von Ammoniak auf Chloracetylbenzol. *Ber. Deut. Chem. Ges.*, **1876**, *9* (1), 563-564.

Steinhart, H.; Luger, A. Amino acid pattern of steam treated coffee. *16th Int. Colloq. Chem. Coffee* (Kyoto 09-14.04.1995), **1995**, 278-285.

Stennert, A.; Maier, H. G. Trigonelline in coffee. III. Calculation of the degree of roast by the trigonelline/nicotinic acid ratio. New GC method for nicotinic acid. *Z. Lebensm. Unters. Forsch.*, **1996**, *202*, 45-47.

Sternberg, L. D/H ratios of environmental water recorded by D/H ratios of plant lipids. *Nature*, **1988**, *333*, 59-61.

Sternberg, L.; DeNiro, M. J. Isotopic composition of cellulose from C_3, C_4 and CAM plants growing near one another. *Science*, **1983**, *220*, 947-949.

Sternberg, L.; DeNiro, M. J.; Ajie, H. Stable hydrogen isotope ratios of saponifiable lipids and cellulose nitrate from CAM, C_3 and C_4 plants. *Phytochemistry*, **1984 a**, *23*, No. 11, 2475-2477.

Sternberg, L.; DeNiro, M. J.; Johnson, H. B. Isotope ratios of cellulose from plants having different photosynthetic pathways. *Plant Physiol.*,**1984 b**, *74*, 557-561.

Sternberg, L.; DeNiro, M. J.; Ting, I. P. Carbon, hydrogen, and oxygen isotope ratios of cellulose from plants having intermediary photosynthetic modes. *Plant Physiol.*, **1984 c**, *74*, 104-107.

Sternberg, L.; DeNiro, M. J.; Johnson, H. B. Oxygen and hydrogen isotope ratios of water from photosynthetic tissues of CAM and C_3 plants. *Plant Physiol.*, **1986**, *82*, 428-431.

Stetter, H. Über neue Reaktionsprodukte des Diacetyls mit Äthylendiamin und Polyaminen. *Chem. Ber.*, **1953**, *86*, 69-74.

Stoehr, C. Ueber eine neue Classe von organischen Basen. *Journal f. prakt. Chemie*, **1890**, *42*, 156-160.

Sun, S.; Duggleby, R. G.; Schowen, R. L. Linkage of catalysis and regulation in enzyme action. Carbon isotope effects, solvent isotope effects, and proton inventories for the unregulated pyruvate decarboxylase of *Zymomonas mobilis*. *J. Am. Chem.. Soc.*, **1995**, *117*, 7317-7322.

Tamura, H.; Appel, M.; Richling, E.; Schreier, P. Authenticity assessment of γ- and δ-decalactone from Prunus fruits by gas chromatography combustion/pyrolysis isotope ratio mass spectrometry (GC-C/P-IRMS). *J. Agric. Food Chem.*, **2005**, *53*, 5397-5401.

Taylor, A. F. S.; Högbom, L.; Högberg, M.; Lyon, A. J. E.; Näsholm, T.; Högberg, P. Natural ^{15}N abundance in fruit bodies of ectomychorrizal fungi from boreal forests. *New Phytologist*, **1997**, *136*, 713-720.

Thaler, H. Makromolekulare Strukturen in Kaffee. *7th Int. Colloq. Chem. Café* (Hamburg 09-14.06.1975), **1976**, 175-187.

Thaler, H.; Gaigl, R. Untersuchungen an Kaffee und Kaffee-ersatz. VII. Die Zusammensetzung des Eiweisses des Rohkaffees. *Z. Lebensm. Unters. Forsch.*, **1962**, *119* (1), 10-25.

Tjepkema, J. D.; Schwintzer, C. R.; Burris, R. H.; Johnson, G. V.; Silvester, W. B. Natural abundance of ^{15}N in actinorhizal plants and nodules. *Plant Soil*, **2000**, *219*, 285-289.

Totlani, V. M.; Peterson, D. G. Reactivity of epicatechin in aqueous glicine and glucose Maillard reaction models: quenching of C_2, C_3, and C_4 sugar fragments. *J. Agric. Food Chem.*, **2005**, *53*, 4130-4135.

Tremblay, P.; Paquin, R. Improved detection of sugar addition to maple syrup using malic acid as internal standard and in ^{13}C isotope ratio mass spectrometry (IRMS). *J. Agric. Food Chem.*, **2006**, *55*, 197-203.

Tressl, R. Formation of aroma compounds by Maillard reaction. *9th Int. Colloq. Chem. Café* (London 16-20.06.1980), **1981**, 55-76.

Tressl, R.; Holzer, M.; Kamperschroer, H. Bildung von Aromastoffen in Röstkaffee in Abhängigkeit vom Gehalt an freien Aminosäuren und reduzierenden Zuckern. *10th Int. Colloq. Chem. Café* (Salvador, Bahia 11-14.10.1982), **1983**, 279-292.

Trugo, L. C.; Macrae, R. The determination of carbohydrates in coffee products using high performance liquid chromatography. *10th Int. Colloq. Chem. Café* (Salvador, Bahia 11-14.10.1982), **1983**, 187-192.

Trugo, L. C.; Macrae, R. A study of the effect of roasting on the chlorogenic acid composition of coffee using HPLC. *Food Chem.*, **1984**, *15*, 219-227.

Tutin, F. Synthesis in the epinephrine series. Part II. The formation and properties of some 2,5- and 2,6-substituted pyrazines and their conversion into amino-ketones and imino-diketones. *J. Chem. Soc.*, **1910**, *97*, 2495.

Tyerman, S. D.; Whitehead, L. F.; Day, D. A. A channel-like transporter for NH_4^+ on the symbiotic interface of N_2-fixing plants. *Nature*, **1995**, *378*, 629-632.

Van Praag, M.; Stein, H. S.; Tibbetts, M. S. Steam volatile aroma constituents of roasted cocoa beans. *J. Agric. Food Chem.*, **1968**, *16* (6), 1005-1008.

Vitzhum, O. G.; Werkhoff, P.; Ablanque, E. Flüchtige Inhaltsstoffe des Rohkaffee. *7th Int. Colloq. Chem. Café* (Hamburg 09-14.06.1975), **1976**, 115-123.

Wagner, R.; Czerny, M.; Biehlohradsky, J.; Grosch, Werner. Structure-odour activity relationship of alkylpyrazines. *Eur. Food Res. Technol.* **1999**, *208*, 308-316.

Walter, W.; Grigal, H. G.; Heukershoven, J. Ueber freie Aminosäuren in grünen Kaffee. *Naturwissenschaften*, **1970**, *57*, 246-247.

Wang, Y. Effects of naturally occurring phenolic compounds on the formation of Maillard aromas. *Dissertation*, **2000**, Rutgers State University.

Wang, P. S.; Odell, G. V. Formation of pyrazines from thermal treatment of some amino-hydroxy compounds. *J. Agric. Food Chem.*, **1973**, *21*, 868-870.

Waters, J. K.; Hughes II, B. L.; Purcell, L. C.; Gerhardt, K. O.; Mawhinney, T. P.; Emerich, D. W. Alanine, not ammonia, is excreted from N_2-fixing soybean nodule bacteroids. *Proceedings of the National Academy of Sciences of the United States of America*, **1998**, *95*, 12038-12042.

Werner, R. A.; Kornexl, B. A.; Roßmann, A.; Schmidt, H.-L. On-line determination and $\delta^{18}O$ values of organic substances. *Anal. Chim. Acta*, **1996**, *319*, 159-164.

Werner, R. A.; Schmidt, H.-L. The in vivo nitrogen isotope discrimination among organic plant compounds. *Phytochemistry*, **2002**, *61*, 465-484.

Whelan, T.; Sackett, W. M.; Benedict, C. R. Carbon isotope discrimination in a plant possessing the C_4 dicarboxylate acid pathway. *Biochem. Biophys. Res. Com.*, **1970**, *41*, 1205-1210.

Whelan, T.; Sackett, W. M.; Benedict, C. R. Enzymatic fractionation of carbon isotopes by phosphoenolpyruvate carboxylase from C_4 plants. *Plant Physiol.*, **1973**, *51*, 1051-1054.

White, J. W. C. Stable hydrogen isotope ratios in plants: a review of current theory and some potential applications. In Rundel, P.; Ehleringer, J. R.; Nagy, K. A. (editors): *Stable Isotopes in Ecological Research*, **1989**, Springer, 142-162.

Winkler, F. J.; Kexel, H.; Kranz, C.; Schmidt, H.-L. Parameters affecting the $^{13}CO_2/^{12}CO_2$ isotope discrimination of the ribulose-1,5-bisphosphate carboxylase reaction. In: Schmidt, H.-L.; Förstel, H.; Heinzinger, K. (Editors): *Stable Isotopes*, **1982**, Elsevier, Amsterdam, 83-89.

Winkler, F. J. Applicationof natural abundance stable isotope mass spectrometry in food control. In Frigerio, A.; Milon, H. (Editors): *Chromatography and Mass Spectrometry in Nutrition Science and Food Safety*, **1984**, Elsevier, Amsterdam, 173-190.

Winter, K.; Holtum, A. M. How closely do the $\delta^{13}C$ values of crassulacean acid metabolism plants reflect the proportion of CO_2 fixed during day and night? *Plant Physiol.*, **2002**, *129*, 1843-1851.

Wirén, N. von; Gazzarrini, S.; Frommer, W. B. Regulation of mineral nitrogen uptake in plants. *Plant Soil*, **1997**, *196*, 191-199.

Wolfrom, M. L.; Patin, D. L. Isolation and characterization of cellulose in the coffee bean. *J. Agric. Food Chem.*, **1964**, *12*, 376-377.

Wolfrom, M. L.; Patin, D. L. Carbohydrates of the coffee bean. IV. An arabinogalactan. *J. Org. Chem.*, **1965**, *30*, 4060-4063.

Wolfrom, M. L.; Plunkett, R. A.; Laver, M. L. Carbohydrates of the coffee bean. *J. Agric. Food Chem.*, **1960**, *8* (1), 58-65.

Wolfrom, M. L.; Laver, M. L.; Patin, D. L. Carbohydrates of the coffee bean. II. Isolation and characterization of a mannan. *J. Org. Chem.*, **1961**, *26*, 4533-4535.

Wright, T. H. Nonenzymatic deamidation of asparaginyl and glutaminyl residues in proteins. *CRC Crit. Rev. Biochem. Mol. Biol.*, **1991**, *26*, 1-52.

Yakir, D.; DeNiro, M. J. Oxygen and hydrogen isotope fractionation during cellulose metabolism in *Lemma gibba L., Plant Physiol.*, **1990**, *93*, 325-332.

Yaylayan, V. A.; Keyhani, A. Carbohydrate and amino acid degradation pathways in L-Methionine/D-[^{13}C] glucose model systems. *J. Agric. Food Chem.*, **2001 a**, *49*, 800-803.

Yaylayan, V. A.; Keyhani, A. Elucidation of the mechanism of pyrrole formation durino thermal degradation of ^{13}C-labeled L-serines. *Food Chem.*, **2001 b**, *74*, 1-9.

Yeretzian, C.; Jordan, A.; Badoud, R.; Lindinger, W. From the green bean to the cup of coffee: investigating coffee roasting by on-line monitoring of volatiles. *Eur. Food Res. Technol.*, **2002**, *214*, 92-104.

Yoneyama, T. Uptake, assimilation and translocation of nitrogen by crops. *JARQ – Japan Agricultural Research Quarterly*, **1991**, *25*, 75-82.

Yoneyama, T. Nitrogen metabolism and fractionation of nitrogen isotopes in plants. In Wada, E.; Yoneyama, T.; Minagawa, M.; Ando, T; Fry, B. D. (Editors): *Stable Isotopes in the Biosphere*, **1995**, Kyoto University Press, Kyoto, Japan, 92-102.

Yoneyama, T.; Fujiwara, H.; Wilson, J. W. Variations in fractionation of carbon and nitrogen isotopes in higher plants: N-metabolism and partitioning in phloem and xylem exudates. In: Griffiths, H. (Editor): *Stable Isotopes, Integration in Biological, Ecological and Geochemical Processes*, **1998 a**, BIOS Scientific Publishers Ltd, Oxford, 99-109.

Yoneyama, T.; Tanaka, F. Natural abundance of ^{15}N in nitrate, ureides, and amino acids from plant tissues. *Soil Sci. Plant Nutr.*, **1999**, *45*, 751-755.

Yoneyama, T.; Matsumaru, T.; Usui, K.; Engelaar, W. M. H. G. Discrimination of nitrogen isotopes during absorption of ammonium and nitrate at different nitrogen concentrations by rice (Oryza sativa L.) plants. *Plant, Cell Environ.*, **2001**, *24*, 133-139.

Zhang, B.-L.; Billaut, I.; Li, X.; Mabon, F.; Remaud, G.; Martin, M. L. Hydrogen isotopic profile in the characterisation of sugars. Influence of the metabolic pathway. *J. Agric. Food Chem.*, **2002**, *50*, 1574-1580.

Ziegler, H.; Osmond C. B.; Stichler, W.; Trimborn, B. Hydrogen isotope discrimination in higher plants: Correlations with photosynthetic pathway and environment. *Planta*, **1976**, *128*, 85-92.

Ziegler, H. Carbon- and hydrogen-isotope discrimination in Crassulacean acid metabolism. In: Winter, Smith (Editors): Ecological Studies Vol. 114,

Crassulacean Acid Metabolism, **1996**, Springer, Berlin Heidelberg, 336-348.

Zlatkis, A.; Sivetz, M.; Analysis of coffee volatiles by gas chromatography. *Food Res.*, **1960**, *25*, 395-398.

Appendix

Tables A1-A12: Linearity regions for the HRGC-P-IRMS-analysis ($^2H/^1H$) of relevant aroma components. Due to impure references and chromatographic non-separation, the compounds **8**/**9** and **12**/**13** are measured as combined parameters.

Table A-1: pyridine (**1**)

Quantity [µg on column]	Amplitude [V]	Peak Area [Vs]	$\delta^2H_{V\text{-}SMOW}$ value [‰] ± SD
0.5	0.4	4	-10 ± 3
1.2	1.0	11	-19 ± 5
2.4	2.2	24	-20 ± 1
3.6	3.4	36	-21 ± 2
4.8	4.5	46	-22 ± 3

Table A-2: pyrazine (**2**)

Quantity [µg on column]	Amplitude [V]	Peak Area [Vs]	$\delta^2H_{V\text{-}SMOW}$ value [‰] ± SD
0.5	0.1	1	-110 ± 21
1.1	0.3	4	-115 ± 3
2.2	0.7	8	-110 ± 1
3.4	0.9	10	-113 ± 4
4.6	1.2	14	-111 ± 1
6.8	1.9	22	-113 ± 2
10.0	2.8	34	-112 ± 3

Table A-3: 2-methylpyrazine (**3**)

Quantity [µg on column]	Amplitude [V]	Peak Area [Vs]	$\delta^2H_{V\text{-}SMOW}$ value [‰] ± SD
0.5	0.3	2	50 ± 24
1.2	0.6	6	28 ± 1
2.4	1.4	13	28 ± 1
3.5	2.1	20	29 ± 3
4.7	3.5	24	32 ± 2
6.8	5.4	50	33 ± 1

Table A-4: 2,5-dimethylpyrazine (**4**)

Quantity [µg on column]	Amplitude [V]	Peak Area [Vs]	$\delta^2H_{V\text{-}SMOW}$ value [‰] ± SD
0.5	0.3	3	-68 ± 12
1.2	0.9	7	-78 ± 11
2.3	1.7	14	-72 ± 2
3.4	2.3	21	-67 ± 1
4.6	2.8	27	-66 ± 3
5.5	3.1	33	-66 ± 2
6.8	3.4	42	-69 ± 2
8.5	3.8	52	-70 ± 3

Table A-5: 2,6-dimethylpyrazine (**5**)

Quantity [µg on column]	Amplitude [V]	Peak Area [Vs]	$\delta^2H_{V\text{-}SMOW}$ value [‰] ± SD
0.4	0.3	3	-78 ± 3
1.1	0.8	7	-90 ± 1
2.2	1.8	15	-88 ± 1
3.3	2.6	23	-82 ± 1
4.4	3.0	29	-82 ± 1
6.5	3.8	44	-85 ± 2

Table A-6: 2-ethylpyrazine (**6**)

Quantity [µg on column]	Amplitude [V]	Peak Area [Vs]	$\delta^2H_{V\text{-}SMOW}$ value [‰] ± SD
0.5	0.4	4	-56 ± 1
1.3	1.3	11	-68 ± 3
2.5	2.0	16	-66 ± 3
3.7	2.8	25	-63 ± 1
5.0	3.3	33	-61 ± 2
6.5	3.9	46	-65 ± 1

Table A-7: 2,3-dimethylpyrazine (**7**)

Quantity [µg on column]	Amplitude [V]	Peak Area [Vs]	$\delta^2H_{V\text{-}SMOW}$ value [‰] ± SD
0.5	0.4	3	-94 ± 7
1.1	1.1	9	-96 ± 4
2.4	2.0	16	-95 ± 1
3.6	2.7	24	-91 ± 1
4.8	3.2	30	-87 ± 2
6.0	3.7	36	-91 ± 2

Table A-8: 2-ethyl-5/6-methylpyrazine (**8**/**9**)

Quantity [µg on column]	Amplitude [V]	Peak Area [Vs]	$\delta^2H_{V\text{-}SMOW}$ value [‰] ± SD
0.4	0.4	3	-62 ± 2
1.1	1.0	8	-66 ± 1
2.2	2.2	16	-63 ± 1
3.2	3.0	24	-64 ± 2
4.3	3.6	31	-60 ± 1
6.7	5.4	73	-66 ± 1
10.1	5.8	112	-65 ± 1
13.4	6.1	149	-60 ± 2

Table A-9: 2-ethyl-3-methylpyrazine (**10**)

Quantity [µg on column]	Amplitude [V]	Peak Area [Vs]	$\delta^2H_{V\text{-}SMOW}$ value [‰] ± SD
0.5	0.5	4	-172 ± 2
1.2	1.6	12	-180 ± 1
2.4	2.2	19	-181 ± 1
3.7	3.0	29	-180 ± 1
4.9	3.6	38	-178 ± 1
6.2	4.1	49	-179 ± 2

Table A-10: 2,3,5-trimethylpyrazine (**11**)

Quantity [µg on column]	Amplitude [V]	Peak Area [Vs]	$\delta^2H_{V\text{-}SMOW}$ value [‰] ± SD
0.5	0.4	3	-147 ± 7
1.2	1.1	8	-160 ± 1
2.3	2.1	17	-158 ± 2
3.4	2.9	27	-156 ± 1
4.6	3.3	34	-155 ± 2
5.8	3.7	42	-156 ± 2

Table A-11: 2-ethyl-3,5/6-dimethylpyrazine (**12**/**13**)

Quantity [µg on column]	Amplitude [V]	Peak Area [Vs]	$\delta^2H_{V\text{-}SMOW}$ value [‰] ± SD
0.5	0.6	4	-88 ± 8
1.1	1.6	10	-109 ± 2
2.2	2.8	20	-114 ± 2
3.3	3.8	30	-112 ± 1
4.5	4.6	41	-112 ± 2
5.7	5.3	54	-113 ± 2

Table A-12: 2,3,4,5-tetramethylpyrazine (**14**)

Quantity [µg on column]	Amplitude [V]	Peak Area [Vs]	$\delta^2H_{V\text{-}SMOW}$ value [‰] ± SD
0.5	0.3	2	-151 ± 8
1.1	0.9	7	-154 ± 1
2.2	1.7	14	-153 ± 1
3.4	2.2	20	-155 ± 1
4.5	2.6	26	-154 ± 1
5.6	3.0	33	-152 ± 2

Tables A-13 to A-18 display hydrogen values of alkylpyrazines **2**, **3**, **6**, **11**, **12**/**13**, **14** stored in ethanol and water at 25 °C, with pH values 3, 5 and 7 for 0 to 20 days.

Table A-13: pyrazine (**2**)

Pyrazine ($\delta^2H_{V\text{-}SMOW}$= -112 ‰ ± 3 ‰) in ethanol at 25 °C			
	pH=3	pH=5	pH=7
	$\delta^2H_{V\text{-}SMOW}$ value [‰] ± SD	$\delta^2H_{V\text{-}SMOW}$ value [‰] ± SD	$\delta^2H_{V\text{-}SMOW}$ value [‰] ± SD
Solvent	-204 ± 3	-204 ± 5	-224 ± 2
Day 0	-103 ± 3	-102 ± 3	-105 ± 1
Day 1	-105 ± 1	-112 ± 2	-109 ± 2
Day 3	-106 ± 4	-109 ± 6	-107 ± 1
Day 6	-103 ± 5	-111 ± 5	-111 ± 1
Day 10	-107 ± 6	-108 ± 6	-115 ± 3
Day 20	-104 ± 4	-103 ± 5	-108 ± 1

Pyrazine ($\delta^2H_{V\text{-}SMOW}$= -112 ‰ ± 3 ‰) in water at 25 °C			
	pH=3	pH=5	pH=7
	$\delta^2H_{V\text{-}SMOW}$ value [‰] ± SD	$\delta^2H_{V\text{-}SMOW}$ value [‰] ± SD	$\delta^2H_{V\text{-}SMOW}$ value [‰] ± SD
Solvent	-52 ± 1	-56 ± 1	-57 ± 1
Day 0	-108 ± 2	-107 ± 2	-105 ± 4
Day 1	-106 ± 2	-109 ± 1	n.m.
Day 3	-108 ± 2	-109 ± 1	-109 ± 1
Day 6	-100 ± 1	-104 ± 1	-100 ± 3
Day 10	-103 ± 1	-104 ± 1	-102 ± 2
Day 20	-107 ± 1	-101 ± 1	-104 ± 2

Table A-14: 2-methylpyrazine (**3**)

2-methylpyrazine ($\delta^2H_{V\text{-}SMOW}$= 40 ‰ ± 3 ‰) in ethanol at 25 °C			
	pH=3	pH=5	pH=7
	$\delta^2H_{V\text{-}SMOW}$ value [‰] ± SD	$\delta^2H_{V\text{-}SMOW}$ value [‰] ± SD	$\delta^2H_{V\text{-}SMOW}$ value [‰] ± SD
Solvent	-204 ± 3	-204 ± 5	-224 ± 2
Day 0	43 ± 4	49 ± 4	51 ± 5
Day 1	45 ± 2	47 ± 4	54 ± 3

Day 3	47 ± 3	55 ± 2	59 ± 1
Day 6	48 ± 7	53 ± 3	52 ± 2
Day 10	49 ± 2	48 ± 4	55 ± 1
Day 20	56 ± 3	57 ± 1	55 ± 1

2-methylpyrazine ($\delta^2H_{V\text{-}SMOW}$= 40 ‰ ± 3 ‰) in water at 25 °C			
	pH=3	pH=5	pH=7
	$\delta^2H_{V\text{-}SMOW}$ value [‰] ± SD	$\delta^2H_{V\text{-}SMOW}$ value [‰] ± SD	$\delta^2H_{V\text{-}SMOW}$ value [‰] ± SD
Solvent	-52 ± 1	-56 ± 1	-57 ± 1
Day 0	36 ± 1	41 ± 1	33 ± 5
Day 1	36 ± 1	42 ± 1	30 ± 3
Day 3	43 ± 1	42 ± 1	42 ± 1
Day 6	34 ± 1	35 ± 1	36 ± 2
Day 10	36 ± 2	37 ± 1	38 ± 1
Day 20	36 ± 2	36 ± 1	35 ± 1

Table A-15: 2-ethylpyrazine (**6**)

2-ethylpyrazine ($\delta^2H_{V\text{-}SMOW}$= -59 ‰ ± 1 ‰) in ethanol at 25 °C			
	pH=3	pH=5	pH=7
	$\delta^2H_{V\text{-}SMOW}$ value [‰] ± SD	$\delta^2H_{V\text{-}SMOW}$ value [‰] ± SD	$\delta^2H_{V\text{-}SMOW}$ value [‰] ± SD
Solvent	-204 ± 3	-204 ± 5	-224 ± 2
Day 0	-54 ± 2	-45 ± 2	-45 ± 2
Day 1	-54 ± 1	-40 ± 1	-32 ± 1
Day 3	-52 ± 4	-46 ± 4	-38 ± 4
Day 6	-51 ± 1	-46 ± 1	-44 ± 1
Day 10	-52 ± 1	-49 ± 1	-47 ± 1
Day 20	-47 ± 2	-46 ± 2	-46 ± 2

2-ethylpyrazine ($\delta^2H_{V\text{-}SMOW}$= -59 ‰ ± 1 ‰) in water at 25 °C			
	pH=3	pH=5	pH=7
	$\delta^2H_{V\text{-}SMOW}$ value [‰] ± SD	$\delta^2H_{V\text{-}SMOW}$ value [‰] ± SD	$\delta^2H_{V\text{-}SMOW}$ value [‰] ± SD
Solvent	-52 ± 1	-56 ± 1	-57 ± 1
Day 0	-60 ± 2	-60 ± 2	-61 ± 2
Day 1	-57 ± 1	-55 ± 1	-60 ± 1
Day 3	-64 ± 4	-62 ± 4	-65 ± 4

Day 6	-60 ± 1	-61 ± 1	-60 ± 1
Day 10	-61 ± 1	-61 ± 1	-61 ± 1
Day 20	-62 ± 2	-59 ± 2	-62 ± 2

Table A-16: 2,3,5-trimethylpyrazine (**11**)

2,3,5-trimethylpyrazine ($\delta^2H_{V\text{-}SMOW}$= -157 ‰ ± 2 ‰) in ethanol at 25 °C			
	pH=3	pH=5	pH=7
	$\delta^2H_{V\text{-}SMOW}$ value [‰] ± SD	$\delta^2H_{V\text{-}SMOW}$ value [‰] ± SD	$\delta^2H_{V\text{-}SMOW}$ value [‰] ± SD
Solvent	-204 ± 3	-204 ± 5	-224 ± 2
Day 0	-151 ±3	-136 ± 3	-134 ± 1
Day 1	-148 ± 2	-137 ± 1	-131 ± 2
Day 3	-149 ± 3	-141 ± 3	-136 ± 2
Day 6	-147 ± 4	-135 ± 2	-138 ± 1
Day 10	-151 ± 2	-148 ± 1	-149 ± 1
Day 20	-145 ± 1	-144 ± 1	-145 ± 1

2,3,5-trimethylpyrazine ($\delta^2H_{V\text{-}SMOW}$= -157 ‰ ± 2 ‰) in water at 25 °C			
	pH=3	pH=5	pH=7
	$\delta^2H_{V\text{-}SMOW}$ value [‰] ± SD	$\delta^2H_{V\text{-}SMOW}$ value [‰] ± SD	$\delta^2H_{V\text{-}SMOW}$ value [‰] ± SD
Solvent	-52 ± 1	-56 ± 1	-57 ± 1
Day 0	-156 ± 2	-155 ± 3	-153 ± 2
Day 1	-155 ± 1	-151 ± 4	-147 ± 1
Day 3	n.m.	n.m.	n.m.
Day 6	-162 ± 1	-161 ± 1	-158 ± 1
Day 10	-162 ± 1	-161 ± 1	-160 ± 1
Day 20	-161 ± 2	-156 ± 2	-164 ± 1

Table A-17: 2-ethyl-3,5/6-dimethylpyrazine (**12**/**13**)

2-ethyl-3,5-dimethylpyrazine ($\delta^2H_{V\text{-}SMOW}$= -105 ‰ ± 3 ‰) in ethanol at 25 °C			
	pH=3	pH=5	pH=7
	$\delta^2H_{V\text{-}SMOW}$ value [‰] ± SD	$\delta^2H_{V\text{-}SMOW}$ value [‰] ± SD	$\delta^2H_{V\text{-}SMOW}$ value [‰] ± SD
Solvent	-204 ± 3	-204 ± 5	-224 ± 2
Day 0	-102 ± 3	-100 ± 3	-98 ± 3

Day 1	-102 ± 2	-100 ± 2	-98 ± 1
Day 3	-102 ± 1	-104 ± 1	-106 ± 1
Day 6	-104 ± 3	-106 ± 3	-100 ± 1
Day 10	-104 ± 1	-105 ± 1	-109 ± 1
Day 20	-98 ± 1	-97 ± 1	-98 ± 1

2-ethyl-3,5-dimethylpyrazine ($\delta^2H_{V\text{-}SMOW}$= -105 ‰ ± 3 ‰) in water at 25 °C			
	pH=3	pH=5	pH=7
	$\delta^2H_{V\text{-}SMOW}$ value [‰] ± SD	$\delta^2H_{V\text{-}SMOW}$ value [‰] ± SD	$\delta^2H_{V\text{-}SMOW}$ value [‰] ± SD
Solvent	-52 ± 1	-56 ± 1	-57 ± 1
Day 0	-102 ± 4	-98 ± 2	-101 ± 1
Day 1	-103 ± 2	-101 ± 1	-99 ± 4
Day 3	-110 ± 1	-110 ± 1	-112 ± 1
Day 6	-102 ± 1	-102 ± 1	-105 ± 1
Day 10	-103 ± 1	-99 ± 1	-99 ± 1
Day 20	-100 ± 1	-98 ± 3	-106 ± 1

Table A-18: 2,3,5,6-tetramethylpyrazine (**14**)

2,3,5,6-tetramethylpyrazine ($\delta^2H_{V\text{-}SMOW}$= -154 ‰ ± 1 ‰) in ethanol at 25 °C			
	pH=3	pH=5	pH=7
	$\delta^2H_{V\text{-}SMOW}$ value [‰] ± SD	$\delta^2H_{V\text{-}SMOW}$ value [‰] ± SD	$\delta^2H_{V\text{-}SMOW}$ value [‰] ± SD
Solvent	-204 ± 3	-204 ± 5	-224 ± 2
Day 0	-155 ± 6	-161 ± 3	-154 ± 1
Day 1	-156 ± 2	-159 ± 1	-155 ± 3
Day 3	-159 ± 1	-161 ± 1	-158 ± 2
Day 6	-161 ± 2	-162 ± 1	-161 ± 1
Day 10	-159 ± 1	-160 ± 3	-160 ± 3
Day 20	-153 ± 2	-152 ± 1	-153 ± 1

2,3,5,6-tetramethylpyrazine ($\delta^2H_{V\text{-}SMOW}$= -154 ‰ ± 1 ‰) in water at 25 °C			
	pH=3	pH=5	pH=7
	$\delta^2H_{V\text{-}SMOW}$ value [‰] ± SD	$\delta^2H_{V\text{-}SMOW}$ value [‰] ± SD	$\delta^2H_{V\text{-}SMOW}$ value [‰] ± SD
Solvent	-52 ± 1	-56 ± 1	-57 ± 1
Day 0	-174 ± 4	-165 ± 3	-166 ± 3
Day 1	-168 ± 3	-167 ± 1	-165 ± 1

Day 3	n.m.	n.m.	n.m.
Day 6	-168 ± 3	-162 ± 2	-165 ± 1
Day 10	-168 ± 1	-157 ± 1	-158 ± 2
Day 20	-161 ± 3	-153 ± 3	-159 ± 2

Tables A-19 to A-30 display nitrogen, hydrogen and carbon values of compounds **1**-**14** from different origins. Natural references are declared by the company to be natural. In table A-22 only references for **4** were measured. Table A-23 displays references of **5** and the combined parameters of **4**/**5** of different origins.

Table A-19: pyridine (**1**)

Sample	$\delta^{15}N_{AIR}$ value [‰] ± SD	$\delta^{2}H_{V\text{-}SMOW}$ value [‰] ± SD	$\delta^{2}C_{V\text{-}PDB}$ value [‰] ± SD
References			
a-synthetic	0.0 ± 0.1	-10 ± 1	-29.4 ± 0.2
b-synthetic	0.0 ± 0.2	-21 ± 3	-33.9 ± 0.2
Self-roasted arabica coffee			
a-Brasil	-22.1 ± 0.2	-83 ± 1	n.m.
b-Ethiopia	-13.1 ± 0.1	-75 ± 1	n.m.
c-Malawi	-8.8 ± 0.2	-57 ± 1	n.m.
d-India	-12.6 ± 0.1	-83 ± 1	n.m.
e-Hawaii	-3.7 ± 0.1	-60 ± 1	n.m.
Self-roasted robusta coffee			
a-India	-7.0 ± 0.1	-72 ± 1	n.m.
b-India	-11.9 ± 0.1	-63 ± 2	n.m.
c-Indonesia	-9.1 ± 0.1	-72 ± 1	n.m.
d-Malabar	-1.7 ± 0.1	-43 ± 1	n.m.
Commercial roast coffee beans			
a-commercial	-32.0 ± 0.1	-117 ± 1	n.m.
b-commercial	-20.7 ± 0.2	-89 ± 1	n.m.
c-commercial	-29.1 ± 0.2	-87 ± 4	n.m.
d-commercial	-17.5 ± 0.1	-96 ± 1	n.m.
e-commercial	-6.2 ± 0.2	-53 ± 1	n.m.
f-commercial	-29.2 ± 0.2	-114 ± 2	n.m.

g-commercial	-28.5 ± 0.2	-111 ± 1	n.m.
Unspecified origin roast coffee beans			
b-unspecified	-1.6 ± 0.2	-71 ± 1	n.m.
d-unspecified	-23.1 ± 0.3	-77 ± 2	n.m.
e-unspecified	-23.6 ± 0.2	-105 ± 1	n.m.
g-unspecified	-35,7 ± 0.1	-112 ± 1	n.m.
Coffee products			
c-products	-27.4 ± 0.2	-92 ± 2	n.m.
d-products	-16.4 ± 0.3	-74 ± 1	n.m.
e-products	-8.9 ± 0.3	-60 ± 2	n.m.
f-products	-5.3 ± 0.1	-59 ± 2	n.m.
g-products	-8.4 ± 0.3	-77 ± 1	n.m.
h-products	-3.2 ± 0.2	-56 ± 1	n.m.
i-products	-8.6 ± 0.1	-68 ± 1	n.m.
k-products	-14.2 ± 0.1	-93 ± 1	n.m.
l-products	-1.7 ± 0.1	-85 ± 1	n.m.

Table A-20: pyrazine (**2**)

Sample	$\delta^{15}N_{AIR}$ value [‰] ± SD	$\delta^{2}H_{V\text{-}SMOW}$ value [‰] ± SD	$\delta^{2}C_{V\text{-}PDB}$ value [‰] ± SD
References			
a-synthetic	-1.2 ± 0.2	-112 ± 3	-28.1 ± 0.2
Self-roasted arabica coffee			
a-Brasil	-3.7 ± 0.2	-4 ± 1	n.m.
b-Ethiopia	-1.8 ± 0.1	-59 ± 3	n.m.
Commercial roast coffee beans			
c-commercial	0.2 ± 0.3	-34 ± 5	n.m.
d-commercial	-7.5 ± 0.3	-72 ± 1	n.m.
Unspecified origin roast coffee beans			
b-unspecified	0.9 ± 0.3	3 ± 5	n.m.
Coffee products			
h-products	-0.5 ± 0.3	-25 ± 5	n.m.

Table A-21: 2-methylpyrazine (**3**)

Sample	$\delta^{15}N_{AIR}$ value [‰] ± SD	$\delta^{2}H_{V\text{-}SMOW}$ value [‰] ± SD	$\delta^{2}C_{V\text{-}PDB}$ value [‰] ± SD
References			
a-synthetic	-0.5 ± 0.2	30 ± 3	-27.2 ± 0.2
b-synthetic	-1.2 ± 0.3	15 ± 2	-26.1 ± 0.1
c-synthetic	0.1 ± 0.3	40 ± 3	-26.9 ± 0.2
d-natural	-2.4 ± 0.2	-102 ± 1	-26.4 ± 0.2
e-natural	-0.9 ± 0.2	-117 ± 1	-25.0 ± 0.1
Self-roasted arabica coffee			
a-Brasil	1.5 ± 0.1	-16 ± 1	n.m.
b-Ethiopia	2.6 ± 0.1	-58 ± 1	n.m.
c-Malawi	3 ± 0.2	-5 ± 2	n.m.
d-India	-4.6 ± 0.1	-40 ± 2	n.m.
e-Hawaii	-2.5 ± 0.1	-47 ± 1	n.m.
Self-roasted robusta coffee			
a-India	1.3 ± 0.1	-21 ± 1	n.m.
b-India	-9.1 ± 0.1	-67 ± 1	n.m.
c-Indonesia	-3.6 ± 0.1	-45 ± 1	n.m.
d-Malabar	-10.2 ± 0.1	-72 ± 1	n.m.
Commercial roast coffee beans			
a-commercial	-1.8 ± 0.2	-77 ± 2	n.m.
b-commercial	-0.6 ± 0.2	-50 ± 1	n.m.
c-commercial	2.3 ± 0.2	-35 ± 3	n.m.
d-commercial	-1.2 ± 0.1	-39 ± 1	n.m.
e-commercial	2.5 ± 0.3	-13 ± 2	n.m.
f-commercial	-2.8 ± 0.1	-50 ± 1	n.m.
g-commercial	1.3 ± 0.3	-39 ± 1	n.m.
h-commercial	0.1 ± 0.1	-57 ± 1	n.m.
Unspecified origin roast coffee beans			
a-unspecified	2.9 ± 0.2	-20 ± 2	n.m.
b-unspecified	2.4 ± 0.2	-31 ± 1	n.m.
c-unspecified	-0.9 ± 0.1	-36 ± 1	n.m.
d-unspecified	-2.3 ± 0.2	-37 ± 5	n.m.
e-unspecified	-0.2 ± 0.2	-47 ± 1	n.m.
g-unspecified	-1.1 ± 0.1	-37 ± 1	n.m.

Coffee products			
a-products	-1.1 ± 0.1	-83 ± 1	n.m.
c-products	-0.8 ± 0.2	-49 ± 1	n.m.
d-products	6.3 ± 0.1	-37 ± 1	n.m.
e-products	0.3 ± 0.3	-43 ± 1	n.m.
f-products	0.7 ± 0.2	-37 ± 1	n.m.
g-products	-1.0 ± 0.3	-67 ± 1	n.m.
h-products	1.3 ± 0.1	-49 ± 1	n.m.
i-products	-2.4 ± 0.1	-25 ± 4	n.m.
k-products	-3.1 ± 0.1	-49 ± 1	n.m.
l-products	-2.2 ± 0.1	-49 ± 1	n.m.
Roasted cocoa beans			
a-cocoa	0.8 ± 0.1	-30 ± 1	n.m.

Table A-22: 2,5-dimethylpyrazine (**4**)

Sample	$\delta^{15}N_{AIR}$ value [‰] ± SD	$\delta^{2}H_{V\text{-}SMOW}$ value [‰] ± SD	$\delta^{2}C_{V\text{-}PDB}$ value [‰] ± SD
References			
a-synthetic	-5.3 ± 0.1	-68 ± 3	-25.1 ± 0.1
b-synthetic	-5.5 ± 0.2	-74 ± 2	-28.3 ± 0.1
c-synthetic	-1.6 ± 0.2	-59 ± 1	-23.4 ± 0.1
d-synthetic	-4.8 ± 0.1	-80 ± 1	-26.2 ± 0.1
e-natural	0.5 ± 0.1	-149 ± 1	-30.6 ± 0.2
f-natural	-0.5 ± 0.3	-50 ± 2	-23.3 ± 0.1

Table A-23: 2,6-dimethylpyrazine (**5**) and 2,5/6-dimethylpyrazine (**4**/**5**)

Sample	$\delta^{15}N_{AIR}$ value [‰] ± SD	$\delta^{2}H_{V\text{-}SMOW}$ value [‰] ± SD	$\delta^{2}C_{V\text{-}PDB}$ value [‰] ± SD
References (**5**)			
a-synthetic	-0.6 ± 0.1	-86 ± 4	-26.0 ± 0.1
b-synthetic	-1.0 ± 0.2	-133 ± 1	-29.7 ± 0.1
c-natural	-0.1 ± 0.2	-151 ± 2	-27.8 ± 0.2
Self-roasted arabica coffee (**4**/**5**)			

a-Brasil	3.1 ± 0.1	-40 ± 1	n.m.
b-Ethiopia	3.4 ± 0.3	-75 ± 1	n.m.
Commercial roast coffee beans (**4**/**5**)			
a-commercial	-0.3 ± 0.1	-85 ± 2	n.m.
b-commercial	8.3 ± 0.1	-43 ± 1	n.m.
c-commercial	3.1 ± 0.1	-68 ± 3	n.m.
d-commercial	2.8 ± 0.2	-60 ± 1	n.m.
f-commercial	-1.1 ± 0.1	-47 ± 4	n.m.
g-commercial	-0.9 ± 0.1	-40 ± 1	n.m.
Unspecified origin roast coffee beans (**4**/**5**)			
a-unspecified	4.0 ± 0.3	-32 ± 4	n.m.
b-unspecified	4.7 ± 0.1	-32 ± 2	n.m.
c-unspecified	1.2 ± 0.1	-18 ± 1	n.m.
e-unspecified	7.0 ± 0.2	-59 ± 1	n.m.
Coffee products (**4**/**5**)			
a-products	1.4 ± 0.1	-61 ± 1	n.m.
c-products	1.9 ± 0.3	-50 ± 1	n.m.
d-products	6.1 ± 0.2	-46 ± 3	n.m.
e-products	2.5 ± 0.2	-45 ± 1	n.m.
f-products	1.2 ± 0.3	-42 ± 1	n.m.
g-products	1.5 ± 0.3	-58 ± 1	n.m.
k-products	2.7 ± 0.1	-31 ± 2	n.m.
l-products	-0.1 ± 0.1	-49 ± 1	n.m.
m-products	2.1 ± 0.3	-15 ± 1	n.m.
n-products	-1.7 ± 0.3	-102 ± 3	n.m.
Roasted cocoa beans (**4**/**5**)			
a-cocoa	7.6 ± 0.1	-68 ± 4	n.m.

Table A-24: 2-ethylpyrazine (**6**)

Sample	$\delta^{15}N_{AIR}$ value [‰] ± SD	$\delta^{2}H_{V\text{-}SMOW}$ value [‰] ± SD	$\delta^{2}C_{V\text{-}PDB}$ value [‰] ± SD
References			
a-synthetic	-1.6 ± 0.1	-59 ± 1	-25.1 ± 0.1
b-synthetic	-1.4 ± 0.1	-126 ± 1	-26.0 ± 0.1

Self-roasted arabica coffee			
a-Brasil	-0.2 ± 0.1	-93 ± 1	n.m.
b-Ethiopia	2.5 ± 0.2	-111 ± 1	n.m.
Commercial roast coffee beans			
a-commercial	0.1 ± 0.3	-134 ± 4	n.m.
c-commercial	1.3 ± 0.1	-105 ± 2	n.m.
d-commercial	-4.0 ± 0.1	-122 ± 2	n.m.
Unspecified origin roast coffee beans			
a-unspecified	-6.2 ± 0.2	-132 ± 6	n.m.
b-unspecified	-7.0 ± 0.1	-115 ± 1	n.m.
Coffee products			
a-products	-1.7 ± 0.3	-124 ± 2	n.m.
c-products	-3.4 ± 0.1	-134 ± 1	n.m.
e-products	-0.4 ± 0.1	-107 ± 1	n.m.
f-products	-0.6 ± 0.3	-106 ± 1	n.m.
g-products	-1.5 ± 0.2	-120 ± 2	n.m.
h-products	1.4 ± 0.1	-110 ± 6	n.m.
Roasted cocoa beans			
a-cocoa	-5.9 ± 0.1	-177 ± 1	n.m.

Table A-25: 2,3-dimethylpyrazine (**7**)

Sample	$\delta^{15}N_{AIR}$ value [‰] ± SD	$\delta^{2}H_{V\text{-}SMOW}$ value [‰] ± SD	$\delta^{2}C_{V\text{-}PDB}$ value [‰] ± SD
References			
a-synthetic	-1.4 ± 0.1	-92 ± 2	-23.0 ± 0.1
b-synthetic	-0.5 ± 0.3	-177 ± 1	-26.6 ± 0.2
c-synthetic	-1.3 ± 0.3	-175 ± 1	-30.4 ± 0.1
d-synthetic	-2.2 ± 0.2	-129 ± 2	-24.9 ± 0.1
Self-roasted arabica coffee			
b-Ethiopia	4.7 ± 0.3	-54 ± 5	n.m.
c-Malawi	2.0 ± 0.2	-21 ± 5	n.m.
d-India	4.4 ± 0.2	-25 ± 3	n.m.
e-Hawaii	5.2 ± 0.3	-25 ± 3	n.m.

Self-roasted robusta coffee			
a-India	-0.5 ± 0.1	-23 ± 1	n.m.
b-India	-10.2 ± 0.3	-63 ± 5	n.m.
c-Indonesia	-6.9 ± 0.3	-69 ± 5	n.m.
d-Malabar	-20.0 ± 0.3	-114 ± 5	n.m.
Commercial roast coffee beans			
b-commercial	8.0 ± 0.1	-52 ± 3	n.m.
c-commercial	4.1 ± 0.3	-80 ± 3	n.m.
d-commercial	6.6 ± 0.3	-45 ± 1	n.m.
g-commercial	4.3 ± 0.1	-48 ± 2	n.m.
h-commercial	4.3 ± 0.3	-59 ± 4	n.m.
Unspecified origin roast coffee beans			
b-unspecified	6.7 ± 0.2	-32 ± 2	n.m.
c-unspecified	2.1 ± 0.2	-28 ± 2	n.m.
d-unspecified	6.5 ± 0.3	-46 ± 5	n.m.
e-unspecified	4.2 ± 0.3	-62 ± 2	n.m.
g-unspecified	1.6 ± 0.3	-34 ± 4	n.m.
Coffee products			
c-products	3.4 ± 0.3	-59 ± 2	n.m.
d-products	9.9 ± 0.3	-30 ± 5	n.m.
i-products	2.1 ± 0.2	-39 ± 4	n.m.
k-products	2.2 ± 0.3	-58 ± 3	n.m.
l-products	-0.4 ± 0.3	-79 ± 2	n.m.
m-products	4.3 ± 0.3	89 ± 2	n.m.

Table A-26: 2-ethyl-5/6-methylpyrazine (**8**/**9**)

Sample	$\delta^{15}N_{AIR}$ value [‰] ± SD	$\delta^{2}H_{V\text{-}SMOW}$ value [‰] ± SD	$\delta^{2}C_{V\text{-}PDB}$ value [‰] ± SD
References			
a-synthetic	0.0 ± 0.1	-49 ± 2	-24.1 ± 0.1
b-synthetic	0.3 ± 0.1	-63 ± 2	-24.7 ± 0.2
Self-roasted arabica coffee			
a-Brasil	3.1 ± 0.1	-64 ± 1	n.m.

b-Ethiopia	2.8 ± 0.1	-96 ± 1	n.m.
Self-roasted robusta coffee			
a-India	-0.4 ± 0.1	-98 ± 1	n.m.
b-India	-2.0 ± 0.2	-80 ± 2	n.m.
c-Indonesia	-1.4 ± 0.1	-95 ± 3	n.m.
d-Malabar	-1.6 ± 0.2	-91 ± 1	n.m.
Commercial roast coffee beans			
a-commercial	1.2 ± 0.3	-127 ± 5	n.m.
b-commercial	-0.9 ± 0.3	-108 ± 1	n.m.
d-commercial	1.4 ± 0.3	-101 ± 2	n.m.
e-commercial	6.5 ± 0.2	-26 ± 2	n.m.
g-commercial	0.6 ± 0.2	-101 ± 1	n.m.
h-commercial	1.0 ± 0.1	-112 ± 1	n.m.
Unspecified origin roast coffee beans			
a-unspecified	1.5 ± 0.1	-82 ± 2	n.m.
b-unspecified	2.3 ± 0.1	-85 ± 1	n.m.
c-unspecified	2.1 ± 0.1	-75 ± 5	n.m.
d-unspecified	3.1 ± 0.2	-109 ± 1	n.m.
e-unspecified	2.9 ± 0.1	-111 ± 1	n.m.
f-unspecified	4.7 ± 0.1	-91 ± 1	n.m.
g-unspecified	0.0 ± 0.1	-91 ± 1	n.m.
Coffee products			
a-products	1.7 ± 0.3	-99 ± 2	n.m.
c-products	0.7 ± 0.1	-103 ± 1	n.m.
e-products	2.3 ± 0.1	-84 ± 1	n.m.
f-products	-0.1 ± 0.2	-98 ± 1	n.m.
g-products	2.4 ± 0.1	-94 ± 1	n.m.
h-products	2.5 ± 0.1	-97 ± 4	n.m.
k-products	2.9 ± 0.1	-92 ± 1	n.m.
n-products	9.5 ± 0.2	-95 ± 1	n.m.
Roasted cocoa beans			
a-cocoa	-0.3 ± 0.2	-126 ± 1	n.m.

Table A-27: 2-ethyl-3-methylpyrazine (**10**)

Sample	$\delta^{15}N_{AIR}$ value [‰] ± SD	$\delta^{2}H_{V\text{-}SMOW}$ value [‰] ± SD	$\delta^{2}C_{V\text{-}PDB}$ value [‰] ± SD
References			
a-synthetic	0.1 ± 0.3	-179 ± 1	-22.3 ± 0.1
b-synthetic	0.0 ± 0.4	-144 ± 1	-25.7 ± 0.1
c-synthetic	-0.4 ± 0.4	-95 ± 1	-28.4 ± 0.1
d-synthetic	-0.3 ± 0.3	-121 ± 1	-28.2 ± 0.1
e-synthetic	0.7 ± 0.3	-122 ± 1	-24.5 ± 0.2
f-natural	-0.5 ± 0.2	-117 ± 1	-27.6 ± 0.1
Self-roasted arabica coffee			
a-Brasil	3.4 ± 0.1	-55 ± 1	n.m.
b-Ethiopia	3.7 ± 0.1	-119 ± 2	n.m.
e-Hawaii	-5.5 ± 0.1	-85 ± 1	n.m.
Self-roasted robusta coffee			
a-India	-4.5 ± 0.1	-83 ± 2	n.m.
b-India	-3.2 ± 0.2	-49 ± 5	n.m.
c-Indonesia	-2.7 ± 0.3	-83 ± 3	n.m.
d-Malabar	2.4 ± 0.1	-62 ± 5	n.m.
Commercial roast coffee beans			
d-commercial	1.0 ± 0.2	-79 ± 3	n.m.
f-commercial	-1.4 ± 0.1	-91 ± 1	n.m.
g-commercial	-1.4 ± 0.1	-62 ± 4	n.m.
h-commercial	-4.7 ± 0.1	-92 ± 1	n.m.
Unspecified origin roast coffee beans			
a-unspecified	-7.1 ± 0.1	-107 ± 2	n.m.
c-unspecified	1.6 ± 0.2	-87 ± 5	n.m.
e-unspecified	-0.6 ± 0.3	-89 ± 1	n.m.
f-unspecified	-0.6 ± 0.1	-89 ± 3	n.m.
Coffee products			
a-products	-2.2 ± 0.3	-91 ± 5	n.m.
c-products	-4.4 ± 0.2	-100 ± 4	n.m.
e-products	-2.1 ± 0.2	-76 ± 2	n.m.
f-products	-0.8 ± 0.1	-92 ± 3	n.m.
g-products	-2.0 ± 0.3	-95 ± 5	n.m.

h-products	2.2 ± 0.2	-76 ± 5	n.m.
i-products	-2.8 ± 0.1	-81 ± 2	n.m.
k-products	-0.4 ± 0.1	-88 ± 4	n.m.
l-products	-1.4 ± 0.2	-87 ± 2	n.m.
n-products	-2.5 ± 0.3	-125 ± 3	n.m.
Coffee aroma			
a-aroma	-1.5 ± 0.1	-138 ± 2	n.m.
b-aroma	0.9 ± 0.1	-130 ± 4	n.m.
c-aroma	-0.9 ± 0.1	-105 ± 1	n.m.
d-aroma	-1.5 ± 0.3	-138 ± 2	n.m.

Table A-28: 2,3,5-trimethylpyrazine (**11**)

Sample	$\delta^{15}N_{AIR}$ value [‰] ± SD	$\delta^{2}H_{V\text{-}SMOW}$ value [‰] ± SD	$\delta^{2}C_{V\text{-}PDB}$ value [‰] ± SD
References			
a-synthetic	-1.5 ± 0.1	-157 ± 2	-27.4 ± 0.1
b-synthetic	-0.8 ± 0.1	-113 ± 1	-20.4 ± 0.1
c-synthetic	-1.0 ± 0.1	-177 ± 2	-25.5 ± 0.1
d-synthetic	-1.4 ± 0.1	-182 ± 1	-29.2 ± 0.1
e-natural	0.2 ± 0.2	-143 ± 1	-30.2 ± 0.1
f-natural	0.6 ± 0.1	-109 ± 2	-27.7 ± 0.1
Self-roasted arabica coffee			
a-Brasil	3.7 ± 0.3	-42 ± 4	n.m.
b-Ethiopia	4.3 ± 0.1	-98 ± 3	n.m.
Self-roasted robusta coffee			
d-Malabar	0.3 ± 0.1	-52 ± 4	n.m.
Commercial roast coffee beans			
c-commercial	2.2 ± 0.1	-82 ± 5	n.m.
Unspecified origin roast coffee beans			
b-unspecified	4.1 ± 0.3	-25 ± 5	n.m.
c-unspecified	1.6 ± 0.3	2 ± 3	n.m.
Coffee products			

n-products	4.1 ± 0.3	-116 ± 2	n.m.
Roasted cocoa beans			
a-cocoa	7.8 ± 0.2	-95 ± 2	n.m.

Table A-29: 2-ethyl-3,5/6-dimethylpyrazine (**12**/**13**)

Sample	$\delta^{15}N_{AIR}$ value [‰] ± SD	$\delta^{2}H_{V\text{-}SMOW}$ value [‰] ± SD	$\delta^{2}C_{V\text{-}PDB}$ value [‰] ± SD
References			
a-synthetic	-1.3 ± 0.1	-105 ± 3	-18.2 ± 0.2
b-synthetic	1.2 ± 0.1	-117 ± 2	-24.6 ± 0.2
c-synthetic	3.2 ± 0.1	-144 ± 1	-22.7 ± 0.1
Self-roasted arabica coffee			
a-Brasil	4.3 ± 0.1	-57 ± 1	n.m.
b-Ethiopia	4.4 ± 0.2	-66 ± 2	n.m.
Commercial roast coffee beans			
c-commercial	3.3 ± 0.3	-65 ± 5	n.m.
Unspecified origin roast coffee beans			
a-unspecified	2.7 ± 0.2	-63 ± 1	n.m.
b-unspecified	2.9 ± 0.3	-31 ± 3	n.m.
Coffee products			
a-products	2.2 ± 0.3	-63 ± 2	n.m.
c-products	2.2 ± 0.3	-82 ± 2	n.m.
e-products	3.1 ± 0.3	-40 ± 5	n.m.
f-products	2.1 ± 0.2	-51 ± 2	n.m.
h-products	3.3 ± 0.2	-58 ± 5	n.m.
m-products	0.2 ± 0.3	10 ± 1	n.m.
n-products	11.1 ± 0.3	-58 ± 1	n.m.
Coffee aroma			
a-aroma	0.0 ± 0.1	-129 ± 5	n.m.
c-aroma	0.8 ± 0.1	-142 ± 5	n.m.
d-aroma	-0.7 ± 0.3	-108 ± 4	n.m.

Roasted cocoa beans			
a-cocoa	8.4 ± 0.2	-115 ± 1	n.m.

Table A-30: 2,3,4,5-tetramethylpyrazine (**14**)

Sample	$\delta^{15}N_{AIR}$ value [‰] ± SD	$\delta^{2}H_{V\text{-}SMOW}$ value [‰] ± SD	$\delta^{2}C_{V\text{-}PDB}$ value [‰] ± SD
References			
a-synthetic	-0.7 ± 0.1	-128 ± 1	-25.5 ± 0.1
b-synthetic	-0.6 ± 0.2	-138 ± 1	-24.6 ± 0.1
c-synthetic	0.8 ± 0.3	-179 ± 1	-26.1 ± 0.1
d-synthetic	-60.8 ± 0.2	-115 ± 2	-24.2 ± 0.2
e-natural	-2.7 ± 0.3	-168 ± 1	-19.6 ± 0.1
f-natural	-1.9 ± 0.2	-140 ± 2	-23.2 ± 0.1
g-natural	-2.2 ± 0.1	-154 ± 1	-18.8 ± 0.1
Roasted cocoa beans			
a-cocoa	8.5 ± 0.3	-84 ± 5	n.m.

Table A-31: Nitrogen, hydrogen and carbon stable isotope values of compounds **1**-**10** after 'light' roasting. Compounds **4**/**5**/**6** and **8**/**9** were not separated chromatographically, the results are displayed as combined values.

Compound	$\delta^{15}N_{AIR}$ value [‰] ± SD	$\delta^{2}H_{V\text{-}SMOW}$ value [‰] ± SD	$\delta^{2}C_{V\text{-}PDB}$ value [‰] ± SD
1	-2.7 ± 0.1	-109 ± 2	-39.6 ± 0.2
2	-0.5 ± 0.1	-75 ± 2	-32.7 ± 0.1
3	1.1 ± 0.2	-82 ± 2	-28.9 ± 0.2
4/**5**/**6**	4.8 ± 0.2	-94 ± 1	-28.6 ± 0.1
7	4.0 ± 0.1	-94 ± 2	-29.2 ± 0.3
8/**9**	9.2 ± 0.3	-108 ± 2	-25.1 ± 0.2
10	6.4 ± 0.2	-101 ± 1	-28.7 ± 0.1

Table A-32: Nitrogen, hydrogen and carbon stable isotope values of compounds **1**-**10** after 'medium' roasting. Compounds **4**/**5**/**6** and **8**/**9** were not separated chromatographically, the results are displayed as combined values.

Compound	$\delta^{15}N_{AIR}$ value [‰] ± SD	$\delta^{2}H_{V\text{-}SMOW}$ value [‰] ± SD	$\delta^{2}C_{V\text{-}PDB}$ value [‰] ± SD
1	-7.5 ± 0.3	-45 ± 3	-33.1 ± 0.3
2	-1.6 ± 0.2	-3 ± 5	-31.5 ± 0.3
3	1.2 ± 0.1	-35 ± 4	-26.3 ± 0.2
4/**5**/**6**	3.9 ± 0.2	-63 ± 2	-26.7 ± 0.1
7	3.8 ± 0.2	-103 ± 5	-27.6 ± 0.1
8/**9**	0.7 ± 0.3	-79 ± 5	-29.7 ± 0.1
10	7.3 ± 0.3	-55 ± 5	-30.6 ± 0.2

Table A-33: Nitrogen, hydrogen and carbon stable isotope values of compounds **1**-**10** after 'dark' roasting. Compounds **4**/**5**/**6** and **8**/**9** were not separated chromatographically, the results are displayed as combined values.

Compound	$\delta^{15}N_{AIR}$ value [‰] ± SD	$\delta^{2}H_{V\text{-}SMOW}$ value [‰] ± SD	$\delta^{2}C_{V\text{-}PDB}$ value [‰] ± SD
1	-1.0 ± 0.3	-19 ± 1	-31.1 ± 0.1
2	-0.8 ± 0.3	-25 ± 1	-27.2 ± 0.2
3	1.0 ± 0.3	-6 ± 5	-26.0 ± 0.3
4/**5**/**6**	4.1 ± 0.2	-22 ± 4	-22.6 ± 0.3
7	4.3 ± 0.1	-88 ± 1	-25.5 ± 0.3
8/**9**	0.4 ± 0.3	-55 ± 3	-29.7 ± 0.3
10	6.7 ± 0.3	-83 ± 5	-28.6 ± 0.1

Table A-34: Nitrogen, hydrogen and carbon stable isotope values of synthesised trigonelline hydro iodide and trigonelline.

Compound	$\delta^{15}N_{AIR}$ value [‰] ± SD	$\delta^{2}H_{V\text{-}SMOW}$ value [‰] ± SD	$\delta^{2}C_{V\text{-}PDB}$ value [‰] ± SD
Trigonelline hydro iodide	-7.6 ± 0.1	-127 ± 3	-41.3 ± 0.1
Trigonelline	-7.5 ± 0.3	-124 ± 5	-41.6 ± 0.2

Table A-35: Nitrogen, hydrogen and carbon stable isotope values of educts for alkylpyrazine synthesis and synthesised alkylpyrazines. Compounds **12**/**13** were not separated chromatographically; the results are displayed as combined values. The allocation of the educts to the product alkylpyrazines is found in chapter 4.7 and 3.3.

Compound	$\delta^{15}N_{AIR}$ value [‰] ± SD	$\delta^{2}H_{V\text{-}SMOW}$ value [‰] ± SD	$\delta^{2}C_{V\text{-}PDB}$ value [‰] ± SD
Educts			
Ethylendiamine	-0.7 ± 0.3	-137 ± 2	-24.9 ± 0.2
2,3-Butanedione	-	-179 ± 2	-29.4 ± 0.1
2,3-Pentanedione	-	-150 ± 4	-17.8 ± 0.2
1,2-Diaminopropane	-1.7 ± 0.2	-136 ± 3	-22.5 ± 0.1
2-Methylpyrazine-carboxylate	1.0 ± 0.2	41 ± 2	-23.2 ± 0.1
Hydrazinhydrate	-1.8 ± 0.1	-146 ± 4	-
Alkylpyrazines			
6	0.8 ± 0.2	19 ± 1	-24.7 ± 0.2
7	-2.9 ± 0.1	-164 ± 1	-35.1 ± 0.1
10	-0.5 ± 0.3	-143 ± 2	-22.5 ± 0.2
11	-5.6 ± 0.1	-139 ± 3	-28.7 ± 0.2
12/**13**	-2.9 ± 0.3	-143 ± 1	-20.6 ± 0.1

Table A-36: Nitrogen, hydrogen and carbon stable isotope values of L-serine and thereof synthesised alkylpyrazines. Compounds **8**/**9** were not separated chromatographically, the results are displayed as combined values.

Compound	$\delta^{15}N_{AIR}$ value [‰] ± SD	$\delta^{2}H_{V\text{-}SMOW}$ value [‰] ± SD	$\delta^{2}C_{V\text{-}PDB}$ value [‰] ± SD
L-Serine	3.3 ± 0.3	227 ± 4	-27.5 ± 0.2
2	2.5 ± 0.2	-38 ± 4	-27.8 ± 0.2
3	2.5 ± 0.2	-22 ± 4	-28.0 ± 0.2
6	3.3 ± 0.2	-45 ± 4	-30.7 ± 0.2
7	3.1 ± 0.1	-32 ± 5	-31.1 ± 0.2
8/**9**	3.1 ± 0.3	-29 ± 5	-31.2 ± 0.2
10	2.7 ± 0.2	-5 ± 5	-30.4 ± 0.1
2,6-Diethylpyrazine	2.4 ± 0.1	-31 ± 4	-32.8 ± 0.2
13	2.6 ± 0.3	-17 ± 3	-30.6 ± 0.1

Table A-37: Nitrogen, hydrogen and carbon stable isotope values of L-threonine and thereof synthesised alkylpyrazines and alkylpyridines. Compounds **12**/**13** were not separated chromatographically, the results are displayed as combined values.

Compound	$\delta^{15}N_{AIR}$ value [‰] ± SD	$\delta^{2}H_{V\text{-}SMOW}$ value [‰] ± SD	$\delta^{2}C_{V\text{-}PDB}$ value [‰] ± SD
L-Threonine	-1.0 ± 0.3	-198 ± 1	-25.8 ± 0.1
4/2,5-Dimethylpyridine	-1.2 ± 0.3	-218 ± 4	-20.4 ± 0.2
11	-1.1 ± 0.1	-168 ± 4	-19.2 ± 0.1
2-Ethyl-5-methylpyridine	-2.5 ± 0.3	-185 ± 2	-30.1 ± 0.2
12/**13**	-1.3 ± 0.3	-170 ± 2	-24.5 ± 0.2
2,6-Dimethyl-3-propylpyrazine	-1.5 ± 0.2	-204 ± 5	-25.2 ± 0.2
2,5-Diethyl-3,6-dimethylpyrazine	-1.9 ± 0.1	-172 ± 3	-24.7 ± 0.1
2,6-Diethyl-3,5-dimethylpyrazine	-1.3 ± 0.2	-250 ± 3	-26.6 ± 0.2

Table A-38: Nitrogen, hydrogen and carbon stable isotope values of synthesised alkylpyrazines from L-serine (stable isotope values see table A-36) and L-threonine (stable isotope values see table A-37). Compounds **4**/**5**/**6** and **8**/**9** were not separated chromatographically, the results are displayed as combined values.

Compound	$\delta^{15}N_{AIR}$ value [‰] ± SD	$\delta^{2}H_{V\text{-}SMOW}$ value [‰] ± SD	$\delta^{2}C_{V\text{-}PDB}$ value [‰] ± SD
2	0.2 ± 0.2	-49 ± 3	-27.9 ± 0.1
3	0.9 ± 0.3	-80 ± 5	-25.4 ± 0.2
4/**5**/**6**	1.3 ± 0.2	-84 ± 3	-25.1 ± 0.2
7	2.8 ± 0.1	-124 ± 5	-26.8 ± 0.2
8/**9**	1.0 ± 0.2	-87 ± 2	-29.3 ± 0.2
10	1.9 ± 0.2	-82 ± 3	-27.0 ± 0.2
2,6-Diethylpyrazine	1.3 ± 0.2	-80 ± 2	-31.8 ± 0.2
12/**13**	1.4 ± 0.2	-78 ± 3	-27.9 ± 0.2

Table A-39: Nitrogen, hydrogen and carbon stable isotope values of diethylentriamine and synthesised alkylpyrazines, thereof.

Compound	$\delta^{15}N_{AIR}$ value [‰] ± SD	$\delta^{2}H_{V\text{-}SMOW}$ value [‰] ± SD	$\delta^{2}C_{V\text{-}PDB}$ value [‰] ± SD
Diethylentriamine	0.4 ± 0.3	31 ± 4	-29.5 ± 0.1
2	0.1 ± 0.1	22 ± 1	-30.7 ± 0.2
3	2.3 ± 0.2	28 ± 3	-29.2 ± 0.1
6	2.2 ± 0.1	28 ± 1	-30.5 ± 0.2
7	2.3 ± 0.1	22 ± 1	-31.5 ± 0.2
10	2.2 ± 0.1	23 ± 1	-32.2 ± 0.1
2,6-Diethylpyrazine	2.4 ± 0.2	23 ± 3	-31.7 ± 0.1
12	2.3 ± 0.2	25 ± 2	-34.2 ± 0.1

Table A-40: Nitrogen, hydrogen and carbon stable isotope values of green coffee fractions.

Fraction	$\delta^{15}N_{AIR}$ value [‰] ± SD	$\delta^{2}H_{V\text{-}SMOW}$ value [‰] ± SD	$\delta^{2}C_{V\text{-}PDB}$ value [‰] ± SD
Green Coffee Powder (GCP)	n.m.	-30 ± 2	-26.7 ± 0.2
n-Hexane Insoluble (HIF)	8.5 ± 0.3	9 ± 3	-25.7 ± 0.1
n-Hexane Soluble (HSF)	-	-155 ± 2	-30.4 ± 0.1
Ethanol/Water Insoluble (EIF)	5.4 ± 0.1	6 ± 3	-24.5 ± 0.2
Ethanol/Water Soluble (ESF)	n.m.	29 ± 2	-26.6 ± 0.1
Cationic (CF)	6.8 ± 0.3	-68 ± 2	-29.4 ± 0.1
Anionic (AF)	-	74 ± 1	-27.6 ± 0.1
Neutral (NF)	-	138 ± 3	-24.4 ± 0.1
Water Soluble (WSF)	6.5 ± 0.3	-6 ± 4	-24.6 ± 0.1
Soluble Protein (SPF)	6.3 ± 0.3	7 ± 5	-24.2 ± 0.2
Precipitated Polysaccharid (PPF)	-	-9 ± 4	-24.8 ± 0.1
Water Insoluble (WIF)	-	28 ± 5	-24.7 ± 0.2
Water Insoluble Cellulose (WICF)	-	30 ± 5	-24.8 ± 0.1
Water Insoluble Pectine (WIPF)	-	-5 ± 6	-20.4 ± 0.1

Table A-41: Nitrogen, hydrogen and carbon stable isotope values of alkylpyrazines and pyridine of roasted whole green coffee beans. Compounds **4**/**5**/**6**, **8**/**9** and **12**/**13** were not separated chromatographically, the results are displayed as combined values.

Compound	$\delta^{15}N_{AIR}$ value [‰] ± SD	$\delta^{2}H_{V\text{-}SMOW}$ value [‰] ± SD	$\delta^{2}C_{V\text{-}PDB}$ value [‰] ± SD
1	-2.7 ± 0.1	-115 ± 1	-39.3 ± 0.2
2	-1.6 ± 0.1	-84 ± 1	-36.3 ± 0.2
3	2.6 ± 0.1	-106 ± 2	-30.4 ± 0.2
4/**5**/**6**	4.1 ± 0.2	-103 ± 1	-26.4 ± 0.1
7	4.7 ± 0.3	-114 ± 1	-28.8 ± 0.2
8/**9**	2.8 ± 0.1	-75 ± 1	-25.6 ± 0.1
10	3.7 ± 0.1	-116 ± 1	-27.1 ± 0.2
12/**13**	4.4 ± 0.2	-97 ± 3	-27.0 ± 0.1

Table A-42: Nitrogen, hydrogen and carbon stable isotope values of alkylpyrazines and pyridine of roasted ground green coffee powder (GCP). Compounds **4**/**5**/**6**, **8**/**9** and **12**/**13** were not separated chromatographically, the results are displayed as combined values.

Compound	$\delta^{15}N_{AIR}$ value [‰] ± SD	$\delta^{2}H_{V\text{-}SMOW}$ value [‰] ± SD	$\delta^{2}C_{V\text{-}PDB}$ value [‰] ± SD
1	0.5 ± 0.2	-64 ± 1	-34.8 ± 0.1
2	1.0 ± 0.2	n.m.	-29.1 ± 0.1
3	2.7 ± 0.2	-9 ± 2	-26.9 ± 0.1
4/**5**/**6**	4.0 ± 0.3	-59 ± 1	-25.8 ± 0.2
7	4.4 ± 0.3	-46 ± 3	-26.7 ± 0.2
8/**9**	3.1 ± 0.2	-60 ± 2	-25.7 ± 0.2
10	5.7 ± 0.2	-98 ± 3	-27.1 ± 0.2
12/**13**	7.4 ± 0.1	-90 ± 2	-27.3 ± 0.2

Table A-43: Nitrogen, hydrogen and carbon stable isotope values of alkylpyrazines and pyridine of roasted n-hexane insoluble fraction (HIF). Compounds **4**/**5**/**6**, **8**/**9** and **12**/**13** were not separated chromatographically, the results are displayed as combined values.

Compound	$\delta^{15}N_{AIR}$ value [‰] ± SD	$\delta^{2}H_{V\text{-}SMOW}$ value [‰] ± SD	$\delta^{2}C_{V\text{-}PDB}$ value [‰] ± SD
1	0.2 ± 0.1	-74 ± 1	-35.4 ± 0.2
2	3.1 ± 0.1	n.m.	-28.4 ± 0.2
3	1.3 ± 0.3	-9 ± 2	-26.5 ± 0.3
4/**5**/**6**	4.6 ± 0.3	-68 ± 3	-25.6 ± 0.2
7	5.1 ± 0.3	-54 ± 3	-24.7 ± 0.2
8/**9**	4.6 ± 0.3	-62 ± 5	-27.1 ± 0.2
10	6.2 ± 0.3	-113 ± 5	-26.9 ± 0.2
12/**13**	6.1 ± 0.3	-87 ± 2	-26.5 ± 0.2

Table A-44: Nitrogen, hydrogen and carbon stable isotope values of alkylpyrazines and pyridine of roasted ethanol/water insoluble fraction (EIF). Compounds **4**/**5**/**6**, **8**/**9** and **12**/**13** were not separated chromatographically, the results are displayed as combined values.

Compound	$\delta^{15}N_{AIR}$ value [‰] ± SD	$\delta^{2}H_{V\text{-}SMOW}$ value [‰] ± SD	$\delta^{2}C_{V\text{-}PDB}$ value [‰] ± SD
2	-0.5 ± 0.3	45 ± 5	-28.4 ± 0.2
3	3.4 ± 0.3	25 ± 5	-26.5 ± 0.3
4/**5**/**6**	4.8 ± 0.2	-2 ± 5	-25.6 ± 0.2
7	4.9 ± 0.1	-48 ± 5	-24.7 ± 0.2
8/**9**	5.7 ± 0.3	-38 ± 5	-27.1 ± 0.2
10	6.4 ± 0.3	-39 ± 6	-26.9 ± 0.2
12/**13**	6.1 ± 0.3	-136 ± 6	-26.5 ± 0.2

Erklärung

Hiermit erkläre ich an Eides statt, dass ich die Dissertation "Multi-element Stable Isotope Analysis of Alkylpyrazines and Pyridine from Roast Coffee" selbständig angefrtigt und keine anderen als die von mir angegebenen Quellen und Hilfsmittel benutzt habe.

Ich erkläre außerdem, dass diese Dissertation weder in gleicher oder anderer Form bereits in einem anderen Prüfungsverfahren vorgelegen hat.

Ich habe früher außer den mit dem Zulassungsgesuch urkundlich vorgelegten Graden keine weiteren akademischenGrade erworben oder zu erwerben versucht.

Aalen, den Christina Preston